NTNU

Norwegian University of
Science and Technology

Offshore Wind Farm Layouts

Performance Comparison for a 540 MW Offshore Wind Farm

Thomas Haugsten Hansen

Master of Science in Energy and Environment

Submission date: July 2009

Supervisor: Terje Gjengedal, ELKRAFT

Norwegian University of Science and Technology
Department of Electric Power Engineering

Problem Description

With the recently accepted goals set by the European Union, stating that 20 % of all energy production shall come from renewable energy sources in 2020, and the Norwegian government's ambitious goal of no net CO2 emission in 2050, the development of wind power production is a more current issue than ever. Especially large scale offshore wind power will require attention to new focus areas. The wind may be more stable offshore, but there will be less geographical smoothing effect, so wind variations will still be a key issue. Power transmission, grid connection and the internal grid structure represent other main challenges for realization of large scale wind power, and especially for offshore wind farms.

Off the Norwegian coastline, the large water depths of the Norwegian trench make it impossible to utilize today's technology, where the wind turbines are mounted to the seabed. To reach shallow enough areas, the wind turbines must be placed at a minimum distance of approximately 100 km from shore. At these distances, AC cable connection to shore is challenging, due to the high capacitance of the cables, and HVDC technology may be a competitive option.

Presently, there is also a debate among the offshore wind community regarding the value of redundancy required in the offshore grid to maximize the energy yield, and the impact it may impose on the capital costs of the wind farm. The major concern is related to the cost of supplementary subsea cabling, either in terms of extra length or higher ratings, versus the value of the decreased losses during normal operation and contingency operation due to the redundancy provided to the wind farm. For small wind farms, the power loss due to a fault is relatively small, and redundancy has not been considered a profitable option. With planned wind farms in the 1GW range, the power and, in consequence, income lost due to a fault may be large enough for redundancy to be profitable.

With this as the background, this thesis will focus on the effect of the offshore wind farm layout on the wind farm's performance. Different options for the design of the offshore grid and the transmission to shore will be studied. The wind farm investigated will have an installed capacity of 540 MW, and will be modeled in detail, meaning that all turbines are modeled separately.

Assignment given: 15. January 2009
Supervisor: Terje Gjengedal, ELKRAFT

Preface

This master thesis has been written for the department of Electric Power Engineering at the Norwegian university of technology and science, NTNU, in cooperation with Statkraft. As I have chosen to spend the last year of my studies abroad, the work has been carried out at the Royal Institute of Technology, KTH, in Stockholm, Sweden.

Being abroad has given certain challenges that I would not have experienced if I would have stayed in Trondheim. Nobody at the department at KTH knew how to use the simulation program PSS/E, which has been used in this thesis. Also, when it became clear that the version of the program did not function correctly, I could not just go to the computer engineer at the department to get a new version, since I had to get it from NTNU. This was eventually solved by having Kurt Salmi from NTNU logging on to my computer via remote desktop control. Thank you for reading and answering the large amount of mails I sent you, and for installing the right version of PSS/E on my computer.

Even though they could not help me with the use of PSS/E, I would like to thank the people at the division of electric power systems at KTH for helping me with other, more technical, issues in relations to my thesis work. A special thanks to Katherine Elkington for lending me her licentiate thesis, where the dynamics of the doubly fed induction generator is well explained.

I would especially like to thank Knut Magnus Sommerfelt at Norconsult for acting as the de facto supervisor of this master thesis. He helped me getting started with PSS/E, and has spent considerable time helping me get past the rookie mistakes and unexplainable bugs in PSS/E, discussing the results that were hard to understand and giving me good advice during the six months I have worked on this thesis. He made me realize that I needed to use the ABB model for HVDC Light, as the VSC HVDC model that comes with PSS/E does not represent HVDC Light in a good matter when it comes to dynamic simulations. Also, the VSC HVDC model gave dynamic simulations that did not converged, making PSS/E crash when I tried to run dynamic simulations.

I would also like to thank Magnus Gustafsson at Statnett for valuable comments, Leif Warland at Sintef for helping me with the troubleshooting related to PSS/E, and of course Professor Terje Gjengedal for being the supervisor of the thesis from NTNU and Statkraft.

Finally, to Cecilie, I send the biggest thanks of all for all the support and encouragement!

Thomas Haugsten Hansen
July 19, 2009

Abstract

This master thesis has been written at the Department of Electric Power Engineering at the Norwegian University of Science and Technology. The work has been carried out at the Royal Institute of Technology in Stockholm, where the author spent the last year of his studies as an exchange student.

In the thesis, six different designs of the electrical grid of a 540 MW offshore wind farm, placed 100km off the Norwegian coast, have been studied and compared. At this distance, AC cable transmission might be difficult because of the reactive power production in the cables. Taking this into consideration, two options for the transmission system to shore have been studied. In addition to the AC cable transmission, voltage source converter based HVDC transmission, in the form of HVDC Light, has been studied, giving a total of 12 models.

The main scope of the thesis was to study the load flow situation and power system performance of the different offshore wind farm layouts. Two load flow cases were run for each model; the first studying the model when the active power transmission to shore was maximized, the second studying the model under a contingency situation. The reliability of the six designs was compared by calculating the expected number of cable failures during the life time of the wind farm for each design, and what consequence the disconnection of any cable would have on the power losses. In order to study the effect of the offshore grid design and transmission system design on the offshore power system stability, dynamic simulations have also been executed, and the voltage response and rotor speed response following a fault have been studied.

All simulations have been executed in version 31 of the program PSS/E. The wind farm was modeled full scale, consisting of 108 wind turbines rated at 5MW. The wind turbines were modeled as doubly fed induction generators, using the generic wind model that comes with the program.

The load flow simulations showed that an AC cable connection to shore gave lower total system losses than a DC connection for all designs. The lowest losses were found at the *n*-sided ring design in the AC/AC system, and the highest losses were found for the star design in the AC/DC system. These losses were 2.33% and 8.19% of the total installed capacity, respectively.

In the dynamic simulations, a three phase short circuit fault, lasting 150ms, was applied at three different places in the system. The simulations showed that except from at the wind turbines that were islanded as a result of a fault, all dynamic responses were stable. The HVDC Light transmission to shore gave the highest voltage drops and the lowest voltage peaks offshore. Also, the maximum speed deviation was found to be larger when using HVDC Light transmission compared to using AC cables, with two exceptions; the radial and star designs when a fault was applied to the transmission system. A comparison of the six different grid designs showed that the results were varying. Based on the results in this thesis it has not been concluded that one of the offshore designs have better dynamic qualities than the other. The simulation results indicated that this is case specific, and more dependent on where in the offshore grid the fault occurs rather than the design of the offshore grid.

Table of contents

Table of figures

Table of tables

1 Introduction

With the recently accepted goals set by the European Union, stating that 20 % of all energy production shall come from renewable energy sources in 2020, and the Norwegian government's ambitious goal of no net CO_2 emission in 2050, the development of offshore wind power production is a more current issue than ever. For Norway, Enova has estimated the physical potential for offshore wind power production to 14 000 TWh.

The wind industry is, together with the solar power industry, the fastest growing energy technology in the world today. Wind strengths are higher offshore, and the wind turbines are moved away from the visible surroundings of humans. Nevertheless, outside of the Norwegian coastline, the large water depths of the Norwegian trench make it impossible to utilize today's technology, where the wind turbines are mounted to the seabed. This technology can only be used at maximum depths of approximately 60 meters. To reach areas with water depths not exceeding 60 meters, the turbines must be placed at a minimum distance of approximately 100 km from the coastline. At these distances, long AC cable connections to shore can lead to the need of very large and expensive reactive power compensators due to the high capacitance of the cables. HVDC technology may be utilized instead.

Presently, there is also a debate among the offshore wind community regarding the value of redundancy required in the offshore grid to maximize the energy yield, and the impact it may impose on the capital costs of the wind farm. The major concern is related to the cost of supplementary subsea cabling, either in terms of extra length or higher ratings, versus the value of the decreased losses during normal operation and contingency operation due to the redundancy provided to the wind farm. For small wind farms, the power loss due to a fault is relatively small, and redundancy has not been considered a profitable option. With planned wind farms in the 1GW range, the issue is more current, as the amount of power and, in consequence, income lost due to a fault may be large enough for redundancy to be profitable.

With this as the background, this thesis will focus on the effect of the offshore wind farm layout on total power system performance. Different options for the design of the offshore grid shall be compared by looking at the difference in power losses and ability to provide redundancy. Also, the dynamic behavior of selected generators in the different grids shall be studied in order to compare the dynamic characteristics of each design. Two transmission options to shore will be studied. Both of the transmission options use two parallel connections to shore in order to provide redundancy. The first option is to have two parallel AC cable connections to shore. The second option is to have two parallel HVDC Light connections. The difference in power losses and effect of the transmission choice on the dynamic behavior offshore shall be studied.

All simulations will be executed in the program PSS/E (*Power System Simulator for Engineering*), version 31. Twelve wind farm models, one for each grid design and transmission choice, shall be developed in this program. The wind farm will have a total installed power capacity of 540 MW, and will consist of 108 wind turbines, rated at 5MW. The wind farm is modeled in detail, meaning that all wind turbines will be modeled separately in the model. Realistic parameters for all elements of the wind farm will be chosen. The HVDC Light model is developed and provided by ABB, while cable data will be gathered from cable manufacturers. The generator will be modeled as a doubly fed induction generator, using the generic wind model that comes with PSS/E.

2 Wind energy conversion systems

Figure 1 shows the contents of a Vestas V90 3.0 MW wind turbine. The energy conversion process in the wind turbine is as follows: When the air mass enters the blades (1) of the turbine, the kinetic energy in the wind makes the blades rotate. The blades are connected to the blade hub (2) which again is coupled to a rotational shaft, rotating at the same speed as the blades. This shaft is connected to a gear (3) where the rotational speed of the shaft is increased to suit the generator (4), which operates at a much higher rotational speed than the hub. In the generator, the rotating kinetic energy of the shaft is converted to electric energy. The electric energy is transferred to a high voltage transformer (5) and from the transformer it is sent down the tower (6) and to the grid.

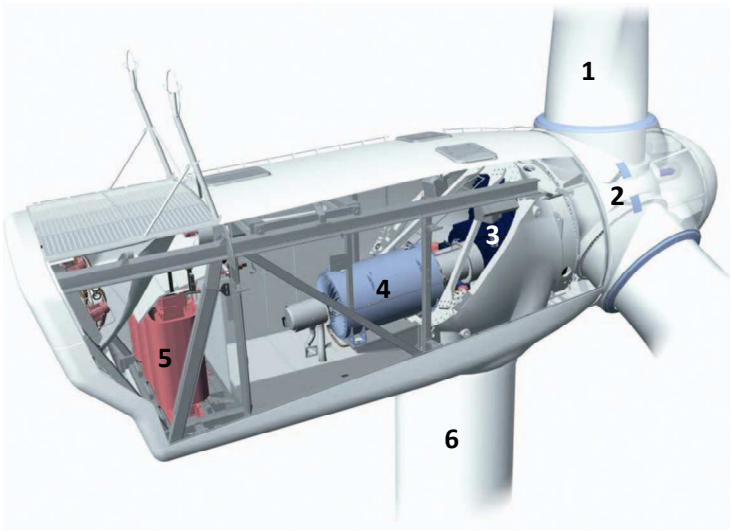

Figure 1 - Vestas V90 3.0 MW wind turbine (Vestas Wind systems AS)

There are several ways to construct the wind energy conversion system (WECS) of a wind turbine. This chapter gives an introduction to the physical laws describing the conversion from wind energy to electrical energy, and it also presents concepts for turbine technology. The standard, state-of-the-art wind turbine types are presented, along with a DC turbine that may be used in future DC wind farms.

2.1 Betz' law

The power contained by an air mass with the air density ρ [kg/m^3] flowing at a wind speed v [m/s] through an area A [m^2] can be calculated as:

$$P_{wind} = \frac{1}{2}\rho A v^3 \qquad \textbf{2-1}$$

The air density ρ is a function of the height above sea level, and can be expressed as:

$$\rho(h) = \frac{P_0}{RT} e^{\frac{-gh}{RT}} \qquad \textbf{2-2}$$

, where

$\rho(h)$	=	air density as a function of altitude	[kg/m^3]
P_0	=	standard sea level atmospheric density = 1.225	[kg/m^3]
R	=	specific gas constant for air = 287.05	[J/kg·K]

T	=	temperature	[K]
g	=	gravity constant = 9,81	[m/s^2]
h	=	altitude above sea level	[m]

In a wind turbine, the power in the wind is converted to rotational energy in the rotor of the wind turbine. This results in a decreased wind speed after the air mass has passed the wind turbine. The wind turbine cannot utilize all of the power contained by the air mass passing through the rotor area, as the speed of this air mass then would be equal to zero at the downwind side of the rotor, thus resulting in an accumulation of air in this area. The theoretical optimum for the utilization of the power in the wind was deduced by Albert Betz in 1919

$$P_{opt,wind} = \frac{16}{27}\frac{1}{2}\rho A v^3 \approx 0{,}59 \cdot \frac{1}{2}\rho A v^3 = 0{,}59 \cdot P_{wind} \quad \textbf{2-3}$$

Hence, if it was possible to extract power without any power losses, it would be possible to utilize approximately 59% of the available wind power in a wind turbine.

2.2 Turbine efficiency factor

Practically, depending on the efficiency factor of the wind turbine, the extracted electric power from the wind is in the range of 35 – 45 %. The efficiency factor of the turbine depends on several factors such as blade profiles, pitch angle, tip speed ratio and air density.

Considering the losses in the conversion system, the electric power that is extracted from the wind turbine is often expressed as:

$$P_e = C_p(\beta, \lambda) \cdot P_{opt,wind} \quad \textbf{2-4}$$

, where $C_p(\beta,\lambda)$ is the turbine efficiency factor. β is the pitch angle (the angle of the blades towards the rotational plane). If the pitch angle is low, the blades are almost perpendicular to the wind and if the pitch angle is high (near 90 degrees) the blades are almost parallel with the hub direction.
λ is the tip speed ratio; the ratio between the tip speed of the blades and the wind speed, and can be expressed:

$$\lambda = \frac{\omega_T R_{rotor}}{v} \quad \textbf{2-5}$$

, where

R_{rotor}	=	the turbine rotor diameter	[m]
ω_T	=	the turbine rotor speed	[rad/s]
v	=	the wind speed	[m/s]

Figure 2 shows the mechanical output as a function of the wind speed v and the pitch angle β, and the turbine efficiency factor C_p as a function of tip speed ratio λ and the pitch angle β for a defined blade profile. The maximum extracted electric power from the wind is slightly below 45%, peaking at a tip speed ratio at between eight and nine for a pitch angle at 0º, as shown in the right plot.

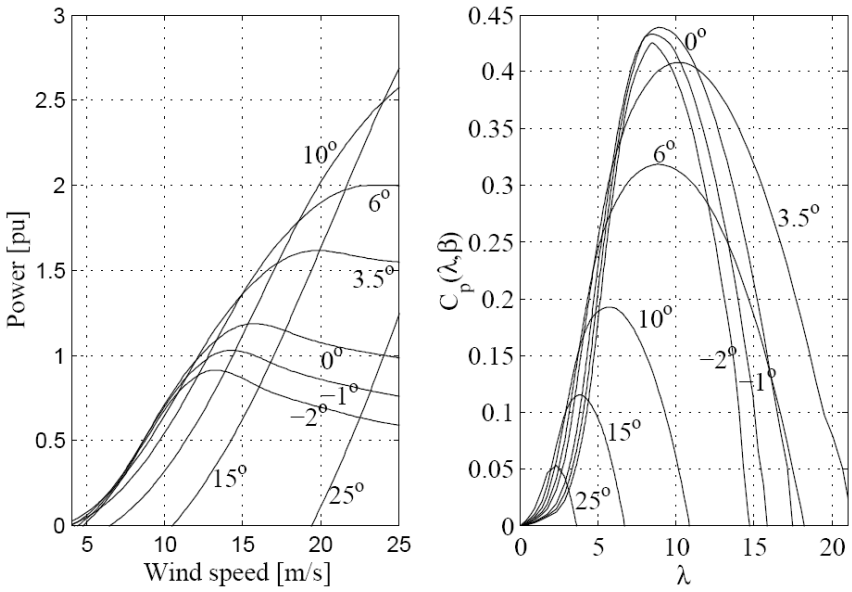

Figure 2 - Power output as a function of wind speed and pitch angle (left) and turbine efficiency factor as a function of tip speed ratio and pitch angle (right) (Lundberg, 2006)

2.3 Wind turbines

Wind turbines can operate at either fixed speed or at variable speed. There are also several concepts for power control in wind turbines. This section will describe the different concepts used for speed- and power control, and present the standard AC based wind turbine types. Applying speed control as the criterion, there are four dominating types of wind turbines. Further on, wind turbines can be classified by considering the power control method used. Taking both of these classification criterions into consideration, Table 1 indicates the different types of AC wind turbine configurations:

Speed control		**Power control**		
		Stall	*Pitch*	*Active stall*
Fixed speed	Type A	Type A0	Type A1	Type A2
Variable speed	Type B	Type B0	Type B1	Type B2
	Type C	Type C0	Type C1	Type C2
	Type D	Type D0	Type D1	Type D2

Table 1 – AC wind turbine concepts. The grey zones indicate combinations that are not used in the wind turbine industry today (Ackermann, 2005).

2.3.1 Fixed speed wind turbines

In fixed speed wind turbines, the speed of the rotor is fixed and determined by the frequency of the supply grid, the gear ratio and the generator design. A fixed speed wind turbine is characteristically equipped with an induction generator (wound rotor or squirrel cage). To ensure a smoother grid connection it is equipped with a soft starter. The soft starter is a simple power electronic component used to decrease the in-rush current, and thereby limiting the disturbances to the grid. Its topology is shown in Figure 7. The generator is directly connected to the grid. Since induction generators always draw reactive power from the grid, a capacitor bank for this type of configuration is used to provide reactive power compensation. The concept of the type A turbine is shown in Figure 3: The generator is a squirrel cage induction machine (SCIG).

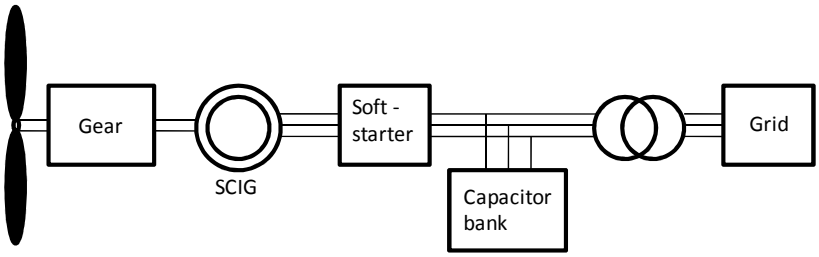

Figure 3 – Type A configuration: Fixed speed control.

The advantages of fixed speed wind turbines are that they are simple, robust and reliable. Also, the technology is well-proven and the cost of parts is low. Its disadvantages are that the reactive power consumption is uncontrollable, and the power quality control is limited. Also, the turbine is exposed to rather large mechanical stresses. Since the wind turbine operates at fixed speed, all fluctuations in the wind speed is transmitted as torque fluctuations and thus also as fluctuations in the electrical power delivered to the grid. In the case of weak grids, these fluctuations might lead to voltage fluctuations which eventually can result in significant line losses. It therefore requires a stiff grid.

To control the power output of a type A wind turbine, there are mainly three concepts that are used; *stall (passive) control, pitch (active) control* and *active stall control*.

Type A0: stall control
The simplest concept is the *stall control*, where the blades are bolted to the hub at a fixed angle. The design of the rotor aerodynamics causes the rotor to lose power (stall) when the wind speed exceeds a predefined level. The advantages of this control method are that it is simple, robust and cheap. Disadvantages are that it contributes to lower efficiency at low wind speed, there is no assisted startup and there are variations in the maximum steady-state power due to variations in air density and grid frequency.

Type A1: pitch control
The *pitch control* allows the blades to be turned out of or into the wind as the power output is too high or too low. The advantages of this type of control are that it provides good power control, assisted startup and emergency stop. From an electrical point of view, good power control means that at high wind speeds the mean output is kept close to the rated power of the generator. The main disadvantage of this method is that there are higher power fluctuations at high wind speeds. Due to the slow nature of the pitch speed, the instantaneous power will fluctuate around the rated power output as the turbine is subject to wind gusts.

Type A2: Active stall control
The *active stall control* controls the stall of the blade actively by pitching the blades. At low wind speeds, the blades are pitched just like a pitch controlled wind turbine, in order to achieve maximum efficiency. At high wind speeds, the blades go into a deeper stall by being by being pitched slightly in the opposite direction of the one the blades of a pitch controlled wind turbine would go into. The advantages of this method is that it provides a smoother limited power without the high power fluctuations that the pitch-controlled wind turbines experience, and it is able to compensate variations in air density. The combination with the pitch mechanism makes it easier to carry out emergency stops and to start up the wind turbine.

2.3.2 Variable speed wind turbines

Variable speed wind turbines operate at a speed that keeps the tip speed ratio λ constant at a predefined value that corresponds to the maximum power coefficient. This is done by adjusting the rotational speed

of the wind turbine as the wind speed varies. Variable speed wind turbines are designed to achieve maximum aerodynamic efficiency over a wide spectrum of wind speeds. Contrary to the fixed-speed turbines, the variable speed system provides a generator torque that is almost constant. The power fluctuations due to variations in the wind strength are absorbed by changes in the generator speed. The electrical system is more complicated than for fixed speed turbines. Variable wind speed turbines are typically equipped with an induction or synchronous generator and connected to the grid through a power converter. The advantages of variable speed wind turbines are an increased energy capture, improved power quality and reduced mechanical stress on the turbine. The disadvantages are that the more complicated electrical system leads to losses in the power electronics, the use of more components and increased cost of equipment.

Due to power limitation considerations, the variable speed concept is only used in combination with a fast pitch control mechanism, as indicated in Table 1. Variable speed- or active stall controlled wind turbines are not included here as they potentially lack the capability of fast power reduction which might lead to a critically high aerodynamic torque. This again might lead to a runaway situation. Underneath the variable speed concepts that are used today are described:

Type B: Limited variable speed:
This configuration consists of a wound rotor induction generator (WRIG) with a variable rotor resistance. This additional variable rotor resistance is known as OptiSlip and is a registered trademark of the Danish manufacturer Vestas. It changes by an optically controlled converter which is mounted on the rotor shaft. The generator is directly connected to the grid through a transformer, with a capacitor bank and a soft-starter.

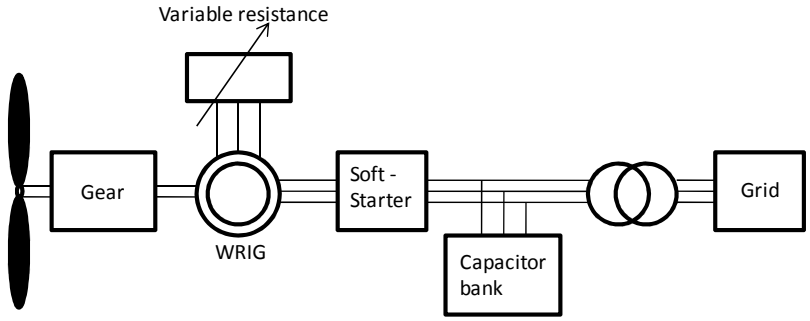

Figure 4 - Type B configuration: Limited variable speed control

The advantage of this configuration is that when the rotor resistance is controlled, the slip is controlled, and thus the power output is controlled. The circuit topology is quite simple, and the optical coupling eliminates the need for slip rings that need brushes and maintenance. Compared to the SCIG the speed range is improved. The disadvantages are that the speed range is typically limited to 0-10% above the synchronous speed as it is dependent on the variable rotor resistance, that the power control is quite poor and that the slip power is dissipated in the variable resistances as losses.

Type C: Variable speed with partial scale frequency converter:
This configuration is widely known as the doubly fed induction generator (DFIG) concept. It consists of a WRIG which is connected to the grid via a transformer. A partial scale frequency converter is used on the rotor circuit. This provides smoother grid connection and performs the reactive power compensation that was provided by the soft-starter and capacitor bank respectively.

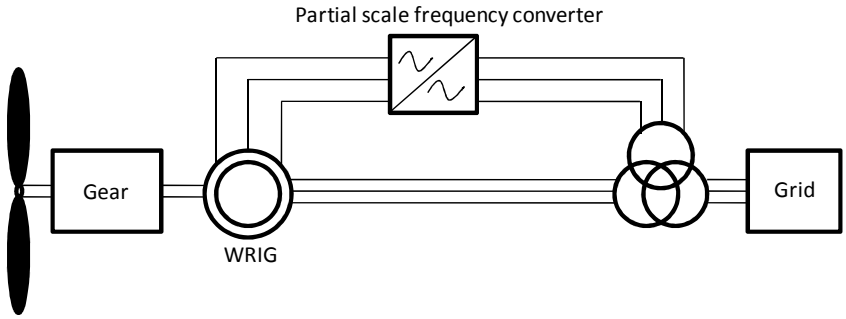

Figure 5 - Type C configuration: Variable speed control with partial scale converter.

This configuration has several advantages. It provides a wide range of dynamic speed control; typically the speed range comprises synchronous speed -40% to +30%. The DFIG can provide a decoupled active and reactive power control, and the generator does not necessarily need to be magnetized from the grid. The smaller frequency converter makes the concept economically desirable. Its main disadvantages are the use of slip rings that need brushes and maintenance, and that it is poorly protected in the case of grid faults.

Type D: Variable speed with full scale frequency converter:
In this configuration, the generator can be excited either by a permanent magnet (Permanent magnet synchronous generator (PMSG)), or electrically (Wound rotor synchronous generator (WRSG) or WRIG). It is connected to the grid via a full scale frequency converter which performs the reactive power compensation and the smoother grid connection. The gearbox can be left out for some full-variable speed wind turbine systems, and in these cases a direct driven multipole generator with relatively large diameter is used.

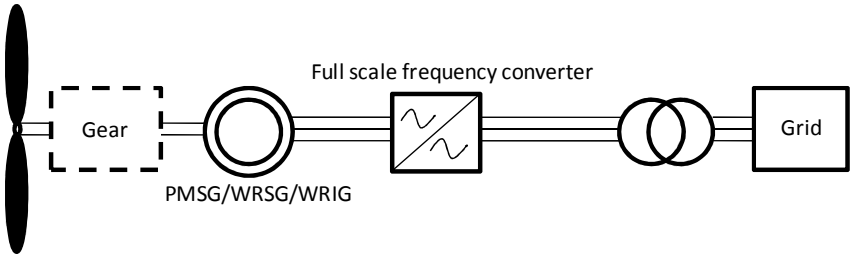

Figure 6 - Type D configuration: Variable speed control with full scale frequency converter.

The advantage of this configuration is the full range speed control and that the gearbox can be omitted. For the permanent magnet generator, the efficiency is higher than in the induction machine as no energy supply is needed for the excitation. The disadvantage is that to omit the gearbox, a large and heavy generator is needed, and a full scale power converter that has to handle the full power of the system is needed. PMSGs may cause problems during startup, synchronization and voltage regulation. The synchronous operation causes a stiff performance during an external short circuit and if the wind speed is unsteady. Also, PMSGs are sensitive to temperature, and therefore the rotor temperature must be supervised and a cooling system is required.

2.3.3 Power electronics in wind turbines

This chapter will give a brief explanation of why power electronics are important in wind turbine systems, and presents the most commonly used power electronics devises in wind turbine systems. The details of the operation of the power electronics are beyond the scope of this project, and interested readers are

referred to (Mohan & Undeland, 2006). The two main features of power electronics is that they make it possible to control the frequency, which is important for the wind turbine.

Power electronic equipment also provides the possibility for wind farms to become active elements in the power grid, i.e. they can have power plant characteristics. This is important for the grid. The disadvantages of using power electronics are from the wind turbine perspective the additional power losses and the increased price of equipment. Concerning the grid side, the power electronics generate high harmonics. Table 2 lists the advantages and disadvantages of using power electronics in wind turbine systems:

Power electronics properties	Advantages	Disadvantages
Controllable frequency (important for the wind turbine)	• Energy optimal operation • Soft drive train • Load control • Gearless option • Reduced noise	• Extra costs • Additional losses
Power plant characteristics (important for the grid)	• Controllable active and reactive power • Local reactive power source • Improved voltage stability • Improved power quality - Reduced flicker level - Filters out low harmonics - Limited short circuit power	• High harmonics

Table 2 - Advantages and disadvantages of using power electronics in wind turbine systems

The two main power electronic devices are the soft starter and the frequency converter, as indicated in Figure 3to Figure 6. The topology of the soft starter is shown in Figure 7:

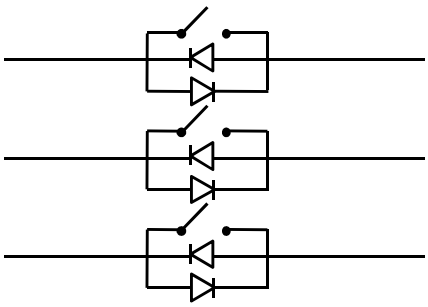

Figure 7 – Three phase soft starter topology

As shown, it consists of two thyristors connected in antiparallel for each phase. The in-rush current is controlled by adjusting the firing angle of the thyristors. After the in-rush, the thyristors are bypassed in order to reduce the power losses.

There are several frequency converter topologies present, but only the most commonly used is described in this chapter. This is the back-to-back converter, whose topology is shown in Figure 8

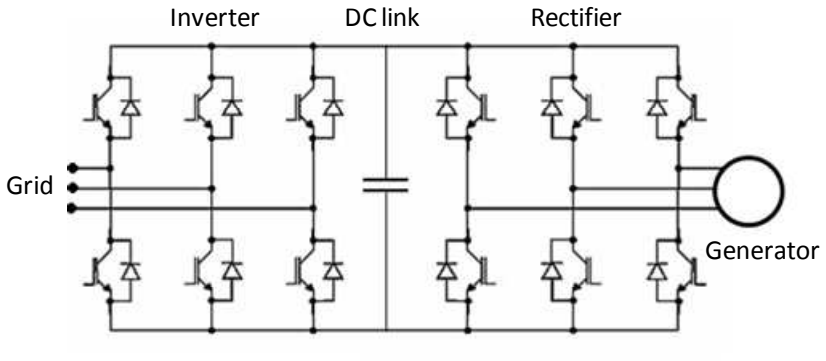

Figure 8 - Back to back converter topology

Due to the increasing amount of, and sizes of, wind farms, the wind farms will have to have power plant characteristics, that is, they have to be able to work as active controllable components in the power system. The wind farms will have to perform frequency and voltage control, to regulate active and reactive power and to provide quick responses during transient and dynamic disturbances in the power system. Without power electronics, there are no solutions as of today that can meet these high demands. Power electronic devices will therefore play a significant part in large wind farms.

2.3.4 The dynamics of a DFIG

In this thesis, it is chosen to use a model of the DFIG for the simulations. The DFIG is widely used in wind farms, for instance in the 160 MW Horns rev offshore wind farm (www.hornsrev.dk) where the VestasV80 turbine is used. A wind power plant consisting of DFIGs can improve the angular behavior of the power system, but may decrease voltage stability under larger disturbances. DFIGs with power system stabilizers (PSS) may be used as a positive contribution to power system damping (Elkington, 2009). The electrical scheme of a DFIG is shown in Figure 9. It resembles the traditional circuit for the induction machine (Hubert, 2002). The only difference in the electrical scheme is that since the rotor of the DFIG is also excited, the rotor side is open-circuit instead of being short circuit as in the standard induction machine model.

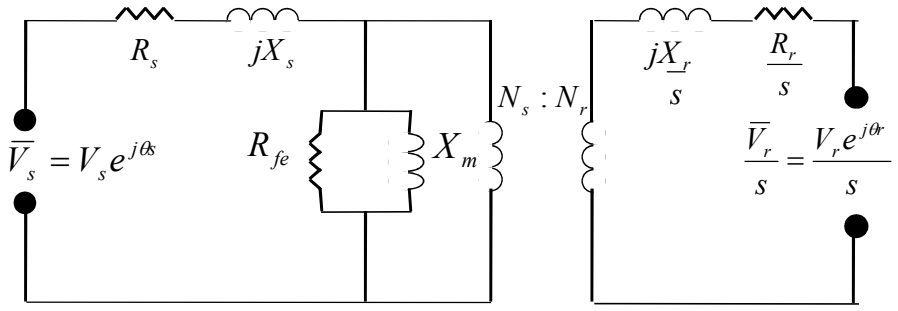

Figure 9 - Electrical scheme of DFIG

In the figure, values with the subscript *s* are located on the stator side of the generator and values with the subscript *r* are located on the rotor side. The nomenclature otherwise is as follows:

V	=	voltage	[V]
θs	=	network voltage phase angle	[º]
θs	=	angular displacement between stator and rotor voltage	[º]
R	=	resistance	[Ω]
X	=	reactance	[H]
N	=	number of windings	

R_{fe} and X_m are the iron resistance and magnetic reactance respectively. k s is the slip, which is given by:

$$s = 1 - \frac{\omega_r}{\omega_s} \quad \textbf{2-6}$$

, where

ω_r = rotational speed of the rotor [rad/s]
ω_s = rotational speed of the stator [rad/s]

Using the third order, two-axis model, neglecting the stator resistance, the equations describing the dynamics of a doubly-fed induction machine without any compensation in the form of voltage regulation or a PSS are (Elkington, 2009):

$$\dot{\delta} = \frac{1}{E'T_0}(-T_0(\omega_s - \omega_r)E' - \frac{X_s - X'}{X'}V_s \sin(\delta - \theta_s) + T_0\omega_s V_r \sin(\delta - \theta_r) \quad \textbf{2-7}$$

$$\dot{\omega}_r = \frac{1}{M}(P_m \frac{\omega_s}{\omega_r} - P_e) \quad \textbf{2-8}$$

$$\dot{E}_q = \frac{1}{T_0}(T_0\omega_s V_{dr} - T_0(\omega_s - \omega_r)E'_d - \frac{X_s}{X'}E'_q + \frac{X_s - X'}{X'}V_q) \quad \textbf{2-9}$$

$$\dot{E}_d = \frac{1}{T_0}(-T_0\omega_s V_{qr} + T_0(\omega_s - \omega_r)E'_q - \frac{X_s}{X'}E'_d + \frac{X_s - X'}{X'}V_d) \quad \textbf{2-10}$$

$$P_e = \frac{E'V}{X'}\sin(\delta - \theta_s) = v_{ds}i_{ds} + v_{qs}i_{qs} = P_s \quad \textbf{2-11}$$

$$X' = X_s - \frac{X_m^2}{X_r} \quad \textbf{2-12}$$

$$T_0 = \frac{X_r}{\omega_s R_r} \quad \textbf{2-13}$$

$$M = \frac{2HS_n}{\omega_s} \quad \textbf{2-14}$$

, where the subscripts q and d denotes the q and d axis value of the symbols they are attached to. The subscripts r and s denote that the value in question is connected to the rotor and stator respectively. The parameter symbols not already accounted for in relation to Figure 9 are:

δ	=	angle between transient emf and stator (output) voltage	[º]
E'	=	transient emf	[V]
T_0	=	open circuit time constant	[s]
ω	=	rotational speed	[rpm]
X'	=	transient reactance	[H]
M	=	inertia coefficient	[MVA·s^2]
P_m	=	mechanical output power	[W]
P_e	=	electrical output power	[W
P_s	=	stator power	[W]
H	=	inertia constant of turbine shaft and generator	[s]
S_n	=	transient reactance	[MVA]

For the background for these equations and further details regarding the modeling of DFIGs, see (Elkington, 2009).

The simulation tool PSS/E®, which is used for the simulations in this thesis, contains a generic wind model using this type of generator. The model is described in chapter 6.3.

3 Wind farm layouts

Depending on how transformers and power electronics are utilized, there are several possibilities for the layout of a wind farm. This chapter presents and discusses these. The contents of the chapter is based on (Ackermann, 2005), (Martander, 2002) and (Lundberg, 2006), where several solutions for wind farm layouts are presented.

3.1 General wind farm layout

The wind farms investigated in this thesis can be represented by the general sketch presented in Figure 10.

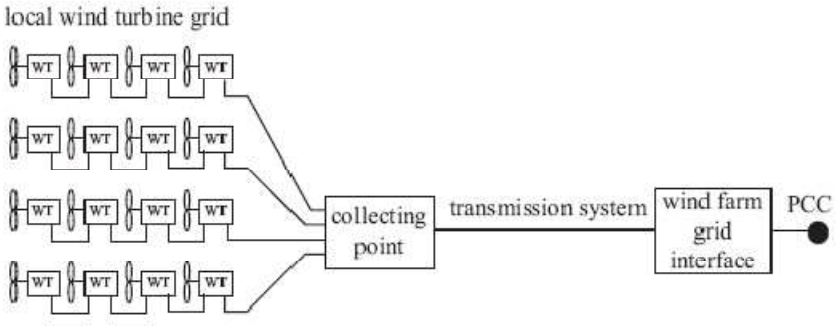

Figure 10 - General wind farm layout

Even though the offshore grid in the figure is connected in radials, there are several ways of constructing the local wind turbine grid (see chapter 3.5). As indicated in the figure, a wind farm consists of the following elements:

- Wind turbines
- Local wind turbine grid
- Collecting point
- Transmission system
- Wind farm interface to the point of common coupling (PCC)

The wind turbines include generators, power electronics and a voltage adjusting unit in the form of an AC or DC transformer, as discussed in chapter 2. The local wind turbine grid can be AC or DC and is the grid connecting the wind turbines together and to the collecting point. The collecting point is an offshore substation, including the transformer and power electronics used for the respective transmission technology that is chosen. The transmission system is the connection to shore, where the power is transmitted to the wind farm grid interface Transmission technologies are further discussed in chapter 4. The wind farm grid interface adapts the voltage, frequency and reactive power to suit the voltage, frequency and reactive power demand of the grid in the PCC.

3.2 AC layouts for wind farms

All present wind farms are built using AC technology for the grid and transmission system. In this thesis, two AC concepts are presented, the small AC wind farm and the large AC wind farm.

3.2.1 Small AC wind farm

In the small AC wind farm, the grid is used not only to connect the wind turbines together, but also to transfer power from the wind farm to the grid interface. This solution is the most feasible for small wind farms quite close to shore. The topology is presented in Figure 11

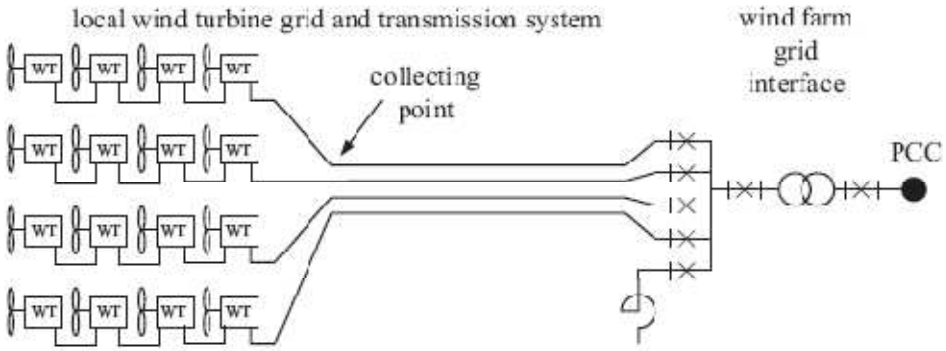

Figure 11 - Small AC wind farm layout

As shown, the local wind farm grid is used both for connecting the wind turbines together and to shore. The voltage level of such wind farms will mainly depend on the distance to shore and the power rating of the wind farm. At the Swedish offshore wind warm Utgrunden 1, the voltage level is 22 kV, and at Bockstigen it is 10,5 kV.

3.2.2 Large AC wind farm

In the large AC wind farm the wind turbines are connected to an offshore substation, where the voltage is adjusted to minimize transmission losses and reactive power compensation devices are placed. Voltage levels are dependent on the distance to shore and the power rating of the wind farm. At Horns rev (www.hornsrev.dk), the offshore grid voltage is 36 kV, while the transmission voltage is 150 kV. The topology is presented in Figure 12

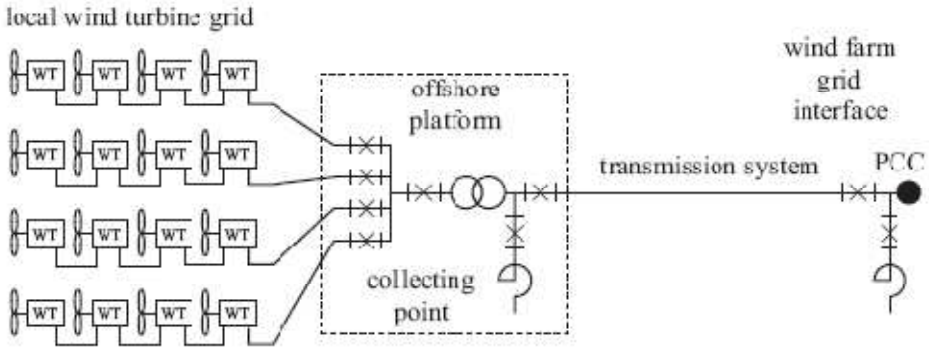

Figure 12 - Large AC wind farm layout

This solution is suitable for relatively large wind farms that are placed at a considerable distance from shore. The transfer limit of the AC transmission system is dependent on the distance from shore and is therefore physically limited by this.

A solution to this could be to decrease the offshore frequency and use an offshore low frequency AC network, as suggested by for instance (Schütte, Gustavsson, & Ström, 2001) . Low frequency systems are

used in electrified railway systems, where the frequency ranges from 16.67 Hz to 25 Hz. There are mainly two advantages of a low frequency AC network:
Firstly, the lowered frequency would increase the transfer capability of the transmission system, as the capacitive charging current of the cable is significantly reduced when the frequency drops. The disadvantage of this concept is that transformer sizes would increase, and hence, transformer costs would increase. Secondly, the low frequency network would allow a simpler design of the offshore wind turbines. The aerodynamic rotor of a large wind turbine operates at maximum revolutions at 15-20 rpm, and the lower frequency would therefore allow a smaller gear ratio for turbines with a gearbox, or decrease the number of poles for wind turbines with direct driven generators. This would lead to lighter and probably also cheaper turbines.

3.3 AC/DC mixed layouts for wind farms

The mixed AC/DC system consists of wind turbines connected in an offshore AC grid, which is collected at an offshore station. At this station, the AC power is rectified and transmitted to shore using an HVDC solution. Onshore, the power is inverted to AC again and fed to the grid. This is shown in Figure 13:

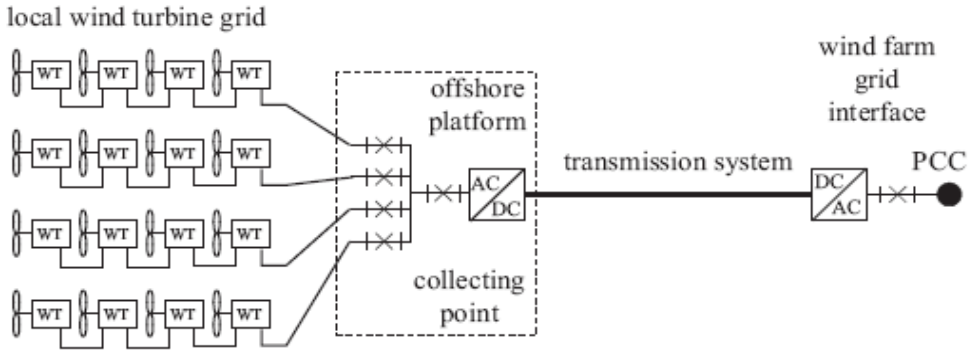

Figure 13 - AC/DC wind farm layout

The DC connection separates the offshore grid from the onshore grid, which makes this type of connection suitable for wind farms where the distance to the PCC is long or if the AC grid that it is connected to is weak. The voltage and frequency of the offshore grid are fully controllable from the offshore converter station, which can be utilized for a collective variable speed system of all the wind turbines in the farm.

An option is, as for the AC layouts, to use a low frequency AC grid on the offshore side. The turbine advantages described in the previous chapter are still valid, but the AC transmission system is replaced by a DC system, which removes the need for large and expensive transformers.

3.4 DC layouts for wind farms

When it comes to DC layouts for wind farms, three layouts are presented in this thesis, the small DC wind farm, the large DC wind farm and the series DC wind farm. The main disadvantages of using DC wind turbines are that all turbines connected to the same DC/DC transformer will operate at the same speed. One solution to this challenge is to supply every wind turbine with a variable speed design to have optimal aerodynamic efficiency of every wind turbine. Another solution is to connect the wind turbines in clusters to a common converter to save the costs of supplying each wind turbine with a variable speed design. Finding the best solution is a matter of economical optimization. The best solution is found where the benefits of reducing the losses by increasing aerodynamic efficiency is equal to the extra costs of

supplying separate variable speed systems for the next turbine. This is a complicated matter, since there is a need to predict the price of electrical power for the entire lifetime of the wind turbines to be able to find the optimal decision. In this chapter, the large DC wind farm denotes the solution where several turbines are collected at a common DC\DC transformer, and the series DC wind farm denotes a solution where all wind turbines have a separate variable speed design.

3.4.1 Small DC wind farm

The small DC wind farm has the same electrical system as the small AC wind farm. Each wind turbine is equipped with a rectifier and the power is sent as DC to the grid interface where it is inverted and fed into the grid. Figure 14 shows the system topology:

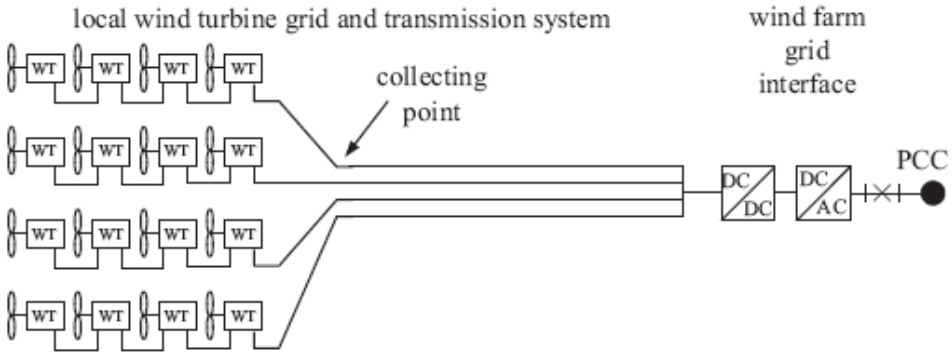

Figure 14 - Small DC wind farm layout

The only difference from the small AC wind farm is that the transformer in the grid interface is replaced with a DC\DC transformer and an inverter. The advantage of the small DC wind farm versus the large DC wind farm is that it does not require an offshore substation, the same advantage as the small AC wind farm has versus the large AC wind farm.

3.4.2 Large parallel DC wind farm

Figure 15 shows the layout of the large DC wind farm. Several wind turbines are connected in clusters to the first DC\DC transformer step. The power is then sent to the main collecting point, where the DC voltage is boosted in the second DC\DC transformer and sent to shore. Onshore, the power is rectified and fed into the grid.

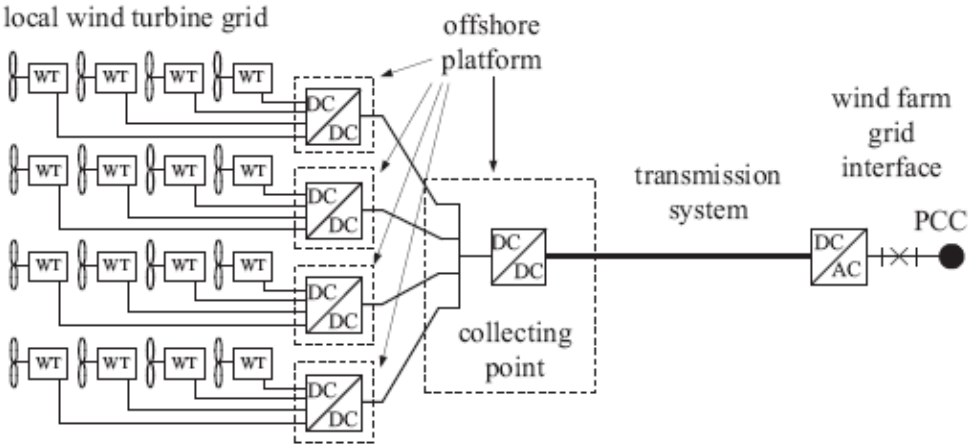

Figure 15 - Large DC wind farm layout

The difference from the large AC wind farm is that the transformers on and offshore are replaced by DC/DC converters, and that the wind turbines are connected in parallel to the first offshore converter step.

3.4.3 Series DC wind farm

Figure 16 shows the layout of the series DC wind farm: In this system layout, the wind turbines are connected in series in order to obtain a voltage suitable for transmission directly. The advantage of this layout is that it does not require offshore DC-transformers and offshore platforms.

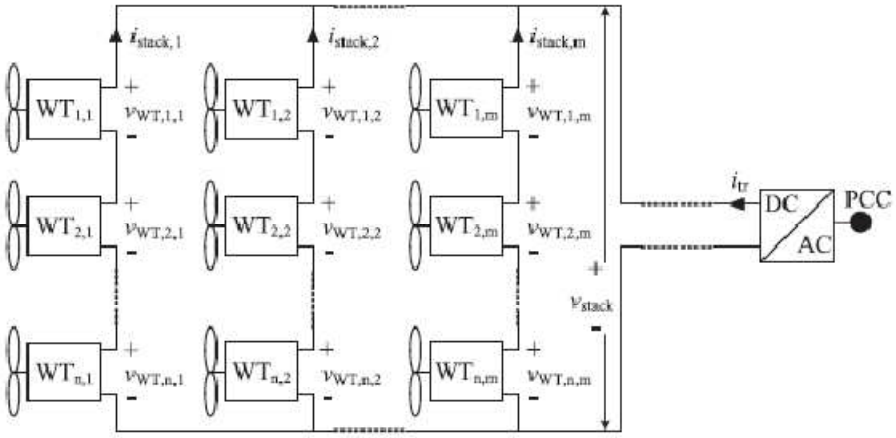

Figure 16 - Series DC wind farm layout based on DC generators

In the topology, *n* wind turbines are series connected to obtain a voltage suitable for transmission, and *m* series-connections are coupled in parallel to obtain the desired power level. The *n* series-connected turbines are referred to as "stacks". The power is transferred to shore where it is inverted and fed into the grid at the PCC.

The main drawback is that the DC\DC converters in the wind turbines must have the ability to operate at high voltage levels The nominal output voltage $v_{WT,x,y}$ of a wind turbine can be expressed by:

$$v_{WT,nom} = \frac{v_{stack}}{n} \qquad \textbf{3-1}$$

$$P_{s,y} = \frac{1}{n}\sum_{x=1}^{n} P_{out,x,y} \quad \textbf{3-2}$$

$$i_{stack,y} = \frac{\sum_{x=1}^{n} P_{out,x,y}}{v_{stack}} = \frac{P_{s,y}}{v_{WT,nom}} \quad \textbf{3-3}$$

$$v_{WT,x,y} = v_{WT,nom}\frac{P_{out,x,y}}{P_{s,y}} \quad \textbf{3-4}$$

, where:

x	=	$1 \ldots n$	
y	=	$1 \ldots m$	
$v_{WT,nom}$	=	Nominal output voltage of one wind turbine	[V]
$i_{stack,y}$	=	Current in stack y	[A]
$P_{out,x,y}$	=	Power output of wind turbine x in stack y	[W]
$P_{s,y}$	=	Mean power production of stack y	[A]

Thus, if one or more wind turbines are disconnected, the voltage level of the remaining turbines increases. Due to this, the wind turbines must be overrated. An overvoltage rating of 1.35 pu is suitable (Lundberg, 2006).

3.5 Offshore grid design options

In this thesis, only an AC offshore grid is studied. The offshore grid denotes the electrical system from the wind turbines to the (first) offshore substation of the wind farm. Only cable faults are addressed.

The offshore grid can be designed in several ways, depending on the wind farm size and the desired level of redundancy. Up until today, providing redundancy has not been considered for existing wind farms since the expected loss of income due to a fault has been assumed to be lower than the costs of the extra equipment needed to provide redundancy. Nevertheless, as wind farm sizes increase, the amount of energy (and income) lost during a fault might be high enough for redundancy to become profitable. As a part of the EU sponsored DOWNVInD (**D**istant **O**ffshore **W**ind farms with **N**o **V**isual **I**mpact i**n** **D**eepwater) project, a project group studied and evaluated the offshore grid of offshore wind farms. The content of this chapter is mainly based on the findings of this project group (Quinonez-Varela, Ault, Anaya-Lara, & McDonald, 2007). The group found that there are mainly three different conceptual designs that can be utilized:

- Radial design, where all wind turbines are connected to a single series circuit (radial). This has been used in several small offshore wind farms.
- Looped design, where redundancy is provided by the establishment of a looped circuit between the wind turbines
- Star design, where the wind turbines are distributed over several feeders, allowing the use of lower rated equipment.

The options may all be utilized for both AC and DC solutions. The following chapters present six designs for the offshore grid in an offshore wind farm, five of which have been suggested by the DOWNVInD group, while the last one is proposed as a part of this thesis.

3.5.1 Radial design

Figure 17shows the layout of the radial offshore grid. *m* wind turbines are connected in series to one feeder and collected at the collector hub. The maximum number of wind turbines that can connect to one feeder is determined by the cable rating and the generator rating. In practice, this will be case specific as the geographical constraints will influence on the choice. The main advantage of this design is that it is inexpensive as the total cable length is smaller than for the other options. Also, it is simple to control, and it provides the possibility to taper the cable capacity as the distance from the hub increases, since the amount of power transmitted is smaller further out in each feeder. A stepwise tapering of the feeder might be an option for long feeders with high total power rating but after conferring with professor Terje Gjengedal at NTNU (Gjengedal, 2009), this option is not considered here as the extra costs during the cable installation is considered too high for this to be feasible. The major disadvantage with this design is the poor reliability provided. Cable or switchgear faults at the hub side of the feeder will lead to the loss of power from all downstream turbines in the feeder.

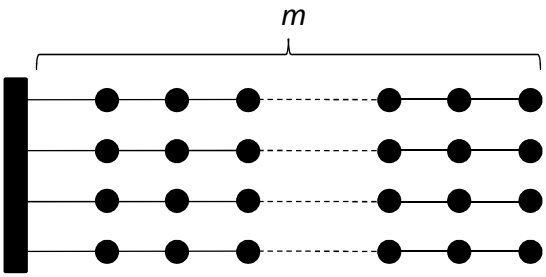

Figure 17 - Radial offshore grid

3.5.2 Single-sided ring

Figure 18 shows the single sided ring design. This is a version of the looped design, which addresses some of the reliability issues of the radial design by providing a redundant path for the power flow within a feeder. In the single-sided ring design, this additional security comes at the expense of higher cable costs as the cable length will double. A cable is installed from the outermost turbine in the feeder to the collector hub. This cable must be able to carry the entire power flow of the feeder in the case of a fault occurring at a point between the first turbine and the hub, and must therefore have the same power rating as the original cable. Even though the cable costs increase compared to the radial system, an initial feasibility study(Quinonez-Varela, Ault, Anaya-Lara, & McDonald, 2007) commissioned by the DOWNVInD consortium recommended and utilized this design for the 1000 MW wind farm offshore grid studied.

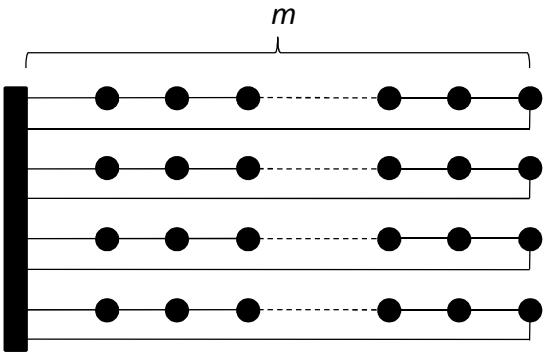

Figure 18 - Single sided ring offshore grid

3.5.3 Double-sided ring

Figure 19shows the single sided ring, which is another version of the looped design. Two feeders are connected in parallel to provide redundancy. This means that for two feeders, the cable length will only increase by the distance between the turbines at the end of the feeders. Nevertheless, in the case that a fault occurs at the cable between the first turbine of a feeder and the collector hub, the full output power of the wind turbines in the faulted feeder must be diverted through the other, meaning that the cable at the hub end of the latter needs to be dimensioned for the power output of double the number of wind turbines. This does not mean that the entire feeder needs to have double power capacity; one can taper the cable capacity as the distance from the hub increases. This will be an economical issue, where the extra installation costs must be weighed against the expected value of lost load over the lifetime of the wind farm. Again, after conferring with professor Terje Gjengedal at NTNU (Gjengedal, 2009), this option is not considered here as the extra costs during the cable installation are considered too high for this to be feasible.

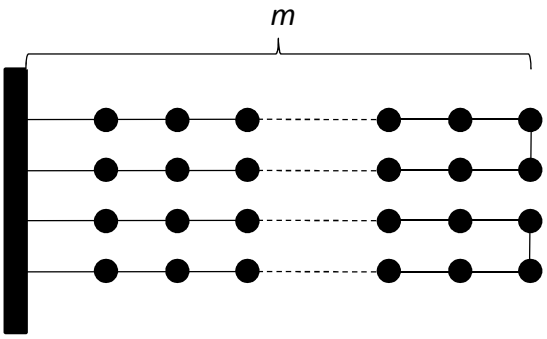

Figure 19 - Double sided ring offshore grid

3.5.4 Star design

Figure 20shows the star design concept. The design allows reduced cable ratings and improved security, since a cable outage will only affect one wind turbine (except in the case where the fault occurs in the connection to the collector hub). The voltage regulation is also likely to be better in this configuration. The drawback is the increased expenses due to the longer diagonal cable runs and the short section of the higher rated connection to the feeder. However, these costs are not likely to be significant, especially in the presented star shape where nine turbines are coupled together. The major cost of this arrangement is the more complex switchgear requirement at the central turbine. To provide redundancy in the connection to the collector hub, two stars could be connected in parallel and the cable rating of the connections to the collector hub increased. Nevertheless, the cost of this redundancy is considered too high to be a competitive alternative compared with the current design, as the probability of a cable failure in the short connection to the collector hub is very low.

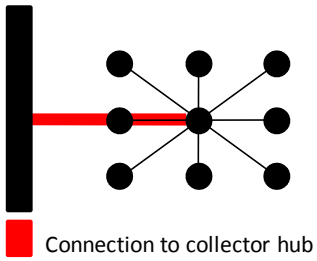

Figure 20 - Star offshore grid

3.5.5 Shared ring design

Figure 21 shows the configuration which is given the name " shared ring design" in this thesis. This design was developed by the DOWNVInD project group and consists of four feeders connected in parallel to a redundant cable. The redundant circuit is designed to potentially deliver the full power output of a failing feeder within the four-feeder arrangement. The probability of two or more feeders failing at the same time is considered sufficiently small to avoid having higher rated cable capacity for the redundant cable.

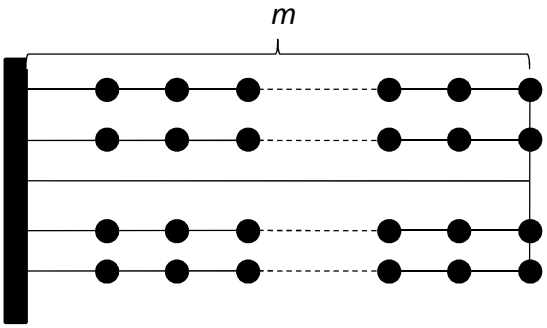

Figure 21 - Shared ring offshore grid

3.5.6 *N*-sided ring design

As an alternative to the double sided ring, the *n*-sided ring design (Figure 22) is suggested in this thesis. The difference from the double sided ring is that instead of simply connecting two feeders in parallel, a higher number, *n* feeders, are connected in parallel. The idea is to reduce the high power rating of cables and equipment which is necessary in the double sided feeder design.

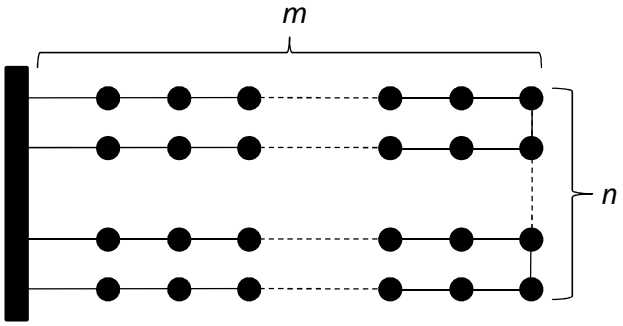

Figure 22 - *n*-sided ring offshore grid

Defining the numbers of wind turbines in each feeder as *m*, this means that during steady state, each feeder *j* must be able to carry the power S_j defined as

$$S_j = \sum_{i=1}^{m} S_i \qquad \textbf{3-5}$$

When connecting *n* feeders in parallel, each feeder *j* will be dimensioned to carry its own power production plus the amount of power delivered to the feeder when a fault occurs closest to the collector hub at one of the other feeders. This power will be divided between the *n*-1 feeders still in operation, meaning that each feeder must be dimensioned to handle the worst case fault situation power flow $S_{j,fault}$. This power can be found by using the basic current division formula as:

$$S_{j,fault} = S_j\left(1 + \frac{Z_{th}}{Z_{radial} + Z_{th}}\right) \quad \textbf{3-6}$$

Z_{radial} is the impedance of the radial closest to the fault, while Z_{th} is the thevenin impedance of the rest of the cables in the *n* feeders and *n*-1 cables that connect the feeders in parallel.

When choosing the amount of feeders to be connected in parallel, one must consider the extra costs of the parallel connection of one more turbine versus the saved cost of reduced power ratings of the equipment due to this extra connection. The correct amount of parallel connections is the one where these costs cross each other.

4 Transmission technologies

This chapter will present the transmission technologies that are available for the transmission from the offshore wind farm to the PCC. Also, overhead AC transmission is presented since, from a mathematical point of view, an underground or subsea cable can be modeled in exactly the same way as an overhead line. The only difference will be the parameter values. The contents of the chapter are based on the project work performed the fall of 2008 (Haugsten Hansen, 2008), where a more detailed description of the technologies is presented.

4.1 HVAC transmission

HVAC transmission is used to connect synchronized AC networks that oscillate at the same frequency and in phase. Three phase systems are used since they minimize the material needed to transfer the same amount of power compared to one or two phase systems. In addition, a three phase system applies the rotating magnetic field needed in the stator of electrical AC-machines, without having to use extra equipment. Both synchronous machines and induction machines have a simpler configuration than DC-machines, and thus are cheaper to buy and easier to maintain than DC-machines.
The power losses in an AC-connection are proportional to the square of the current, while the power transferred is proportional with the square of the voltage. Therefore, it is desirable to have as high voltage as possible when transferring power.

4.1.1 Overhead lines

When transferring power, an overhead line's impedance consists of the resistance in the line, the capacitance to the ground, and the line inductance. A single phase equivalent circuit of a transmission line with distributed parameters is shown in Figure 23:

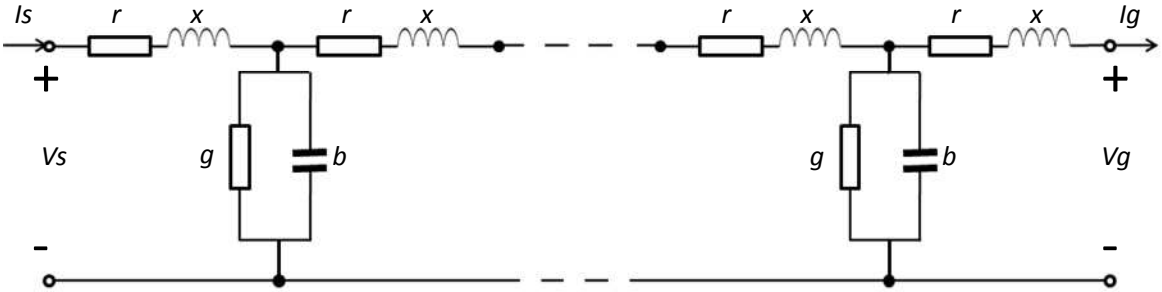

Figure 23 - Single phase equivalent circuit of AC transmission line

The parameters describing the circuit are:

r	=	Series resistance per km per phase	[Ω/km]
L	=	series inductance per phase	[H/km]
$x = \omega L$	=	Series reactance per km per phase	[Ω/km].
g	=	Shunt conductance per km per phase	[S/km]
C	=	Shunt capacitance per phase	[F/km]
$B = \omega C$	=	Shunt susceptance per unit length per phase	[S/km]
l	=	Line length	[km]

The series impedance per km per phase and the shunt admittance per km per phase can be expressed according to the following equations:

$$\bar{z} = r + jx \quad \textbf{4-1}$$

$$\bar{y} = g + jb \quad \textbf{4-2}$$

By multiplying the above values with the line length, one can find the line total series impedance per phase, and the line total shunt admittance per phase.

$$\bar{Z} = \bar{z}l \quad \textbf{4-3}$$

$$\bar{Y} = \bar{y}l \quad \textbf{4-4}$$

One can also define the transmission line's characteristic impedance and propagation constant

$$\overline{Z_c} = \sqrt{\frac{\bar{z}}{\bar{y}}} \quad \textbf{4-5}$$

$$\bar{\gamma} = \sqrt{\bar{z}\bar{y}} \quad \textbf{4-6}$$

As power systems consist of many lines, a simpler model of a power line is to describe each line by its π-equivalent, as shown in Figure 24:

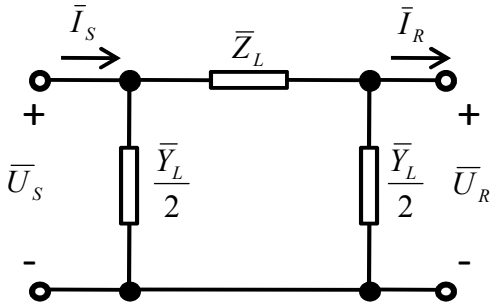

Figure 24 - Equivalent π-circuit of a transmission line

An analysis of this circuit shows that the π-equivalent elements can be expressed as:

$$\bar{Z}_L = \bar{Z}\frac{\sinh(\bar{\gamma}l)}{\bar{\gamma}l} \quad \textbf{4-7}$$

$$\bar{Y}_L = \bar{Y}\frac{\tanh(\bar{\gamma}l/2)}{\bar{\gamma}l/2} \quad \textbf{4-8}$$

For a typical high voltage transmission line *g* can be neglected whilst $r << x$. By considering the lossless line, i.e. neglecting *r*, the characteristic impedance is purely resistive, and the propagation constant is purely imaginary:

$$\bar{Z}_C = \sqrt{\frac{L}{C}} \quad \textbf{4-9}$$

$$\bar{\gamma} = j\omega\sqrt{LC} \quad \textbf{4-10}$$

With the previously mentioned assumptions, the reactive power loss in a transmission line can be expressed according to equation 4-11:

$$\Delta Q = \frac{V_S^2 \cos(\beta l) - 2V_S V_R \cos(\delta_{SR}) + V_R^2 \cos(\beta l)}{Z_C \sin(\beta l)} \quad \textbf{4-11}$$

, where:

V_S	=	Sending end voltage	[V]
β	=	The phase constant (= the value of the imaginary part of the propagation constant)	
V_R	=	Receiving end voltage	[V].
δ_{SR}	=	Transmission angle, by which V_S leads V_R	[°]

Assuming $V_S \approx V_R \approx V_N$, this equation can be rewritten as:

$$\Delta Q(P_R) \approx \frac{2P_{SIL}}{\sin \beta l}(\cos \beta l - \sqrt{1 - (\frac{P_R \sin \beta l}{P_{SIL}})^2}) \quad \textbf{4-12}$$

, where P_{SIL} is the surge impedance load, defined as the power delivered at nominal voltage(V_n) to a load impedance equal to the characteristic impedance (Z_C). It is given by:

$$P_{SIL} = \frac{V_n^2}{Z_C} \quad \textbf{4-13}$$

P_R is the receiving end active power. For a more detailed derivation of these equations, see (Machowski, Bialek, & Bumby, pp. 47-50). In Figure 25, ΔQ is plotted as a function of P_R/P_{SIL}:

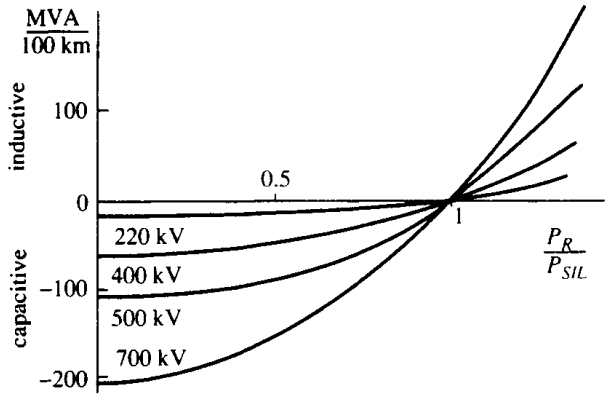

Figure 25 - Examples of reactive power absorbed by a lossless line as a function of its real load for various voltage ratings

When $P_R > P_{SIL}$, $V_S > V_R$, from Figure 25, it is clear that the overhead line is consuming reactive power. This is the case when power is transmitted from node S to node R. The larger P_R is, the larger the reactive power is, which is in accordance with equation 4-12. The longer the line, the higher the value of the line impedance, and thus the reactive power consumption is. To cope with these losses, one must feed reactive power into the grid. This can be done for instance by connecting series or shunt capacitors to the line, ideally so that the inductive part of the line impedance is equal to the capacitive part of the impedance. A DC-transmission does not meet these problems. The reactance and susceptance of a line are proportionally connected to the frequency of the system, and disappear for a DC-transmission. Even though the conversion equipment is quite expensive, the economical benefit due to the non-existence of reactive losses makes HVDC the preferred choice for overhead line distances longer than 600-800 km. It can also be mentioned that HVDC does not suffer from skin effects as AC does. Also, for a given power

ratio, the peak value of the AC voltage is higher than the constant DC voltage. This means that for the same conductor, more power can be transmitted through the same conductor area if it is DC instead of AC.

4.1.2 Cables

A cable has a large capacitance per length unit. When the cable reaches a certain length, the value of the capacitance is so large that the cable's impedance can be considered purely capacitive. In such a case, the cable only provides reactive power, due to the phase shift between the voltage and the current. The possible length of the cable can be made longer with phase compensations in both ends of the line. Figure 26 shows the transmission capacity as a function of the transmission length for three different voltage levels.

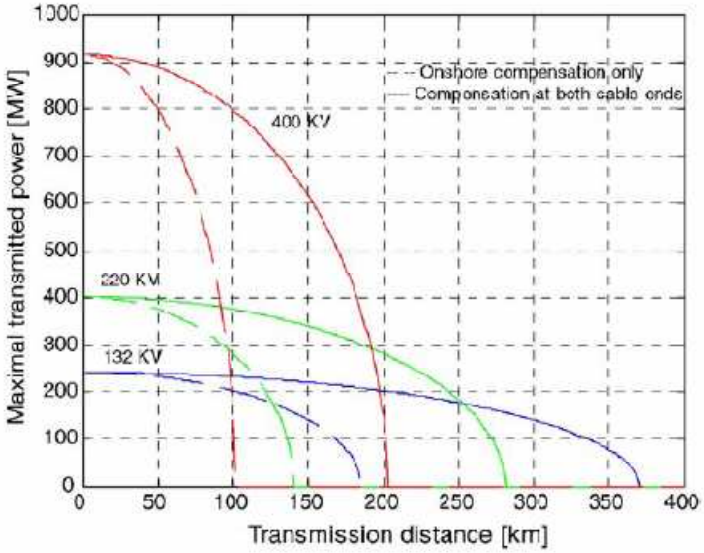

Figure 26 - Transmission capacity as a function of the transmission length for AC cables (Barberis, Todorovic, & Ackermann, 2005)

By using HVDC for this purpose, no reactive power is produced or consumed in the cables. This means that all of the cable's transfer capacity can be used to transfer active power. For subsea cables, the length where HVDC is more feasible than AC is approximately 50 km (ABB, 2008).

4.2 HVDC transmission

In an HVDC system, the electric power is converted from AC to DC in a converter station, transmitted to the receiving end of the transmission, converted back to AC in a second converter station and injected into the receiving AC system. It is used to connect areas which are not synchronous, like for instance the Scandinavian system NORDEL and the western European system UCTE1. An HVDC transmission line costs less than an AC line for the same transmission capacity. However, the terminal stations are more expensive in the HVDC case due to the fact that they must perform the conversion from AC to DC and vice versa. At a certain length of the transmission, called the break even distance, the HVDC solution becomes more feasible than the AC solution. In addition to this, other factors like controllability and reliability must also be considered when choosing the transmission technology.
The principle of an HVDC-transmission is shown in Figure 27. The three phase AC power is converted to DC power in a rectifying circuit before it is transferred as DC current to the receiving end of the transmission. At the end station, the DC power is inverted back to three phase AC power.

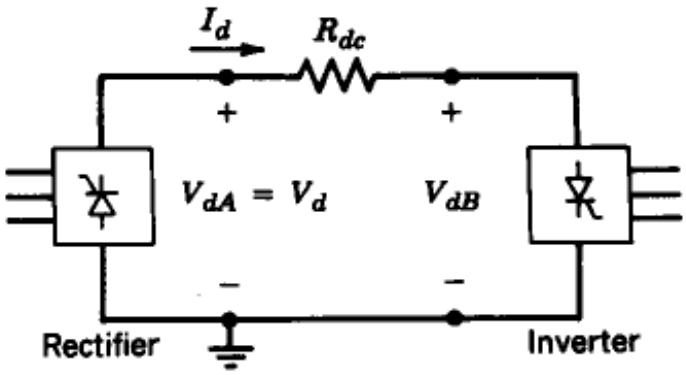

Figure 27 - Principle of HVDC connection

4.3 Traditional HVDC

A typical traditonal HVDC converter station is shown in Figure 28. The converter station itself consists of two poles, i.e. the link is bipolar. Each of the poles have the configuration as shown in Figure 28. In addition to the smoothing inductance L_d, DC filters help to minimize the ripple in the DC transmission. After passing the DC filter, the power is sent to the receiving end, shown in the figure as terminal B. The terminal has the same configuration as terminal A, and the power is converted to AC. This AC power is sent into power system B.

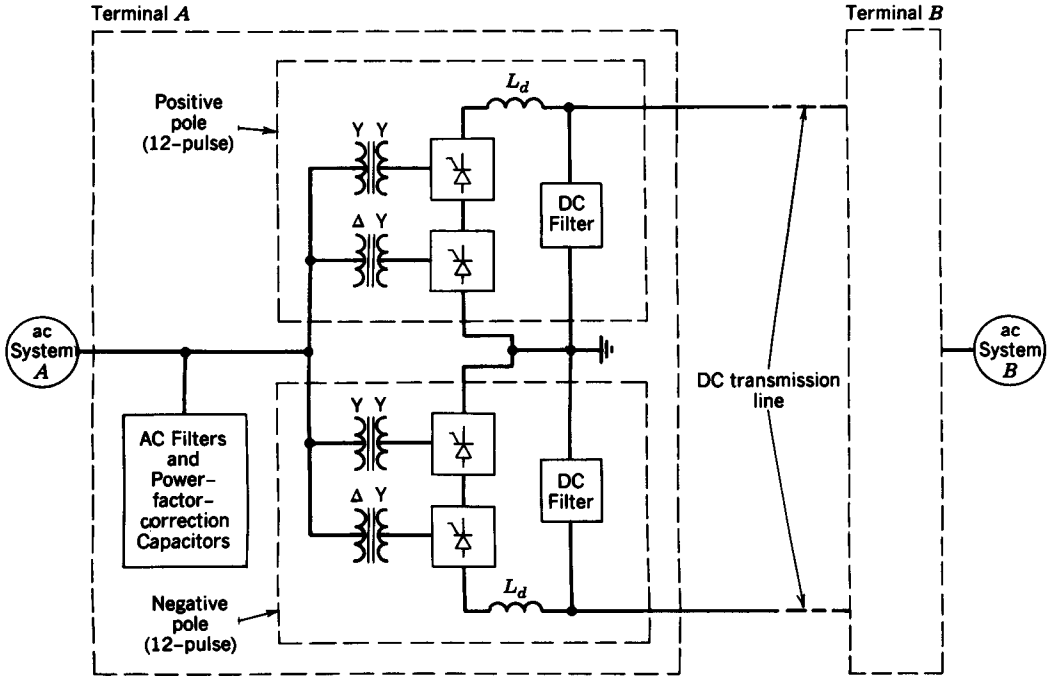

Figure 28 - The configuration of a typical bipolar twelve pulse HVDC connection(Mohan & Undeland, 2006)

4.4 HVDC Light

HVDC Light, developed by ABB, is based on the use of Voltage Source Converters (VSC). The technology uses semiconductors in the form of insulated gate bipolar transistors (IGBTs), and operate with

high frequency pulse width modulation in order to achieve high speed and, as a consequence, small filters and independent control of both active and reactive power. It was introduced in 1997 and ranges from a few tens of megawatts to the upper range of 1200 MW at 320 kV (ABB, 2008). ABB lists many advantages with the technology; the electromagnetic fields are neutral, the cables are oil free and the converter stations are more compact than for traditional HVDC. What is most relevant to this study is that the technology increases the reliability of power grids.

Unlike conventional HVDC converters which usually require a 5% minimum current, the HVDC Light converter can operate at zero power. The active and reactive powers are controlled independently, and at zero active power the full range of reactive power can be utilized. Actually, at zero power, the HVDC Light will have the properties of a Static Synchronous Compensator, or STATCOM (Machowski, Bialek, & Bumby, 1998, p. 34). The active power transfer can be reversed very quickly with HVDC Light. The reversion does not require converter blocking, filter switching or change of control mode, like traditional HVDC. The power is reversed by changing the direction of the DC *current* instead of changing the polarity of the DC *voltage* as in traditional HVDC technology.

The topology of an HVDC Light connection is the same as for traditional HVDC. Figure 27 shows this principle. The areas in which HVDC Light disengages from traditional HVDC are the cable and the converter stations. The HVDC Light cables use extruded polymer insulation while traditional HVDC cables have used paper-oil insulated cables. This eliminates the risk of oil spillage. The cables are laid in pairs with DC currents in opposite directions. This configuration eliminates the magnetic fields outside the cables.

The complete topology of a converter station for HVDC Light is shown in Figure 29. The AC power is transformed to the right voltage level and passes through an LC filter and a converter reactor before it is converted to DC current in the converter valves. These are based on transistor technology, assuring very good controllability of the active and reactive power. The DC current produced in the valves is filtered in the DC capacitors before it is transmitted to the receiving end converter station. The DC current is then inverted to AC, filtered in the converter reactor and LC filter, transformed to the voltage level of the grid and sent into the receiving AC grid.

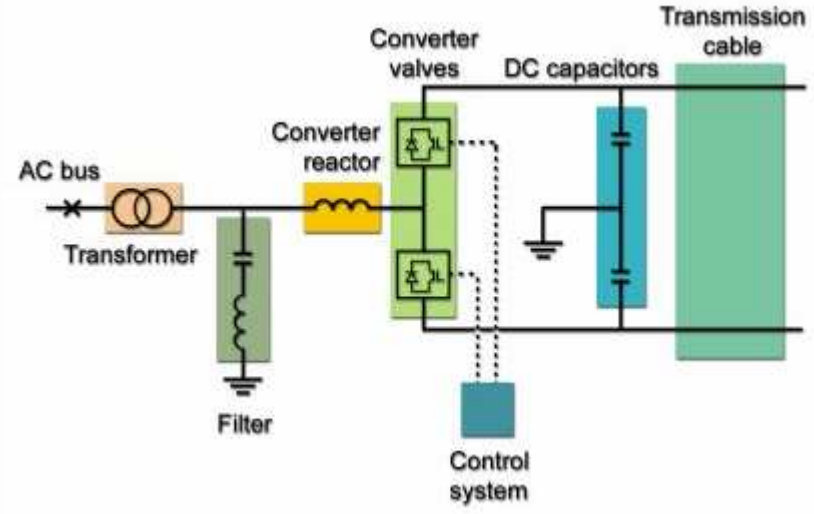

Figure 29 - HVDC Light configuration (ABB, 2008)

4.4.1 Converters

In the converter station, the AC power is rectified to DC power and vice versa. The IGBTs provide pulse width modulation (PWM), which means that AC voltage can be produced by fast switching between positive and negative DC voltage. Figure 31 shows this. Since the IGBTs are self commutating, the amplitude and power angle of the AC voltage signal can be chosen freely. This means that the converter can control the active and reactive power independent of each other. The six pulse transistor bridge is the main part of the converter, as shown in Figure 30. On the DC side, capacitors are used to filter the harmonics.

One of the disadvantages when it comes to this converter type is the high switching losses. For a converter, the losses are proportional to the switching frequency according to the formula

$$P_{conv;loss} = k \cdot f_{sw} \qquad \text{4-14}$$

In an HVDC Light converter, the switching frequency is 2 kHz, i.e. in one period in the 50 Hz system, the voltage direction is reversed 40 times. This is shown in Figure 31. Traditional HVDC technology has line commutated converters, which means that the switching frequency is the same as the line frequency. At the pilot HVDC Light installation in 1997, the converter losses were approximately 4% of the total capacity. Today, the losses have been reduced with 60%, and are now down to approximately 1.6% of the total capacity for each converter. For traditional HVDC, these losses are 0.6-0.7% per converter.

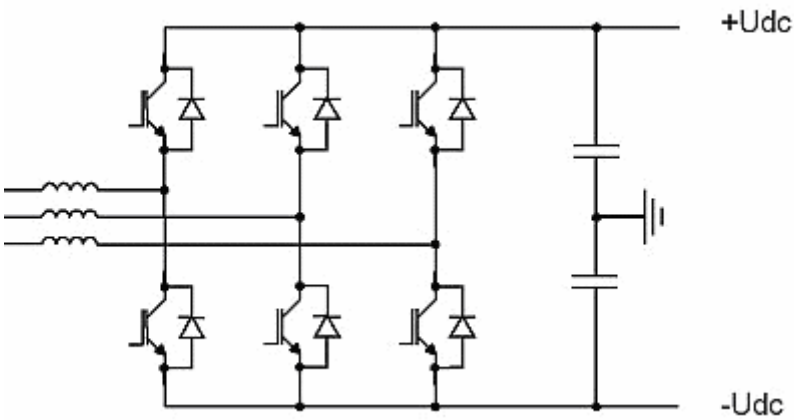

Figure 30 - Six pulse transistor based converter configuration (Mohan & Undeland, 2006)

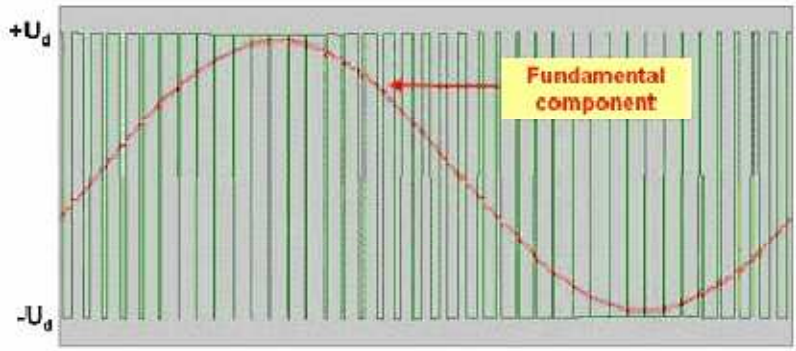

Figure 31 – HVDC Light AC side voltage signal and the fundamental component of the harmonics (ABB, 2008)

4.4.2 Filters

An HVDC Light converter has a high switching frequency, as described in the previous chapter, and shown in Figure 31. Because of the high switching frequency, there will only arise high frequency harmonics. The shunt filters in Figure 29 are therefore relatively small. There is only need for a high pass filter, unlike for the traditional HVDC solution, where tuned filters are also needed.

4.5 HVDC PLUS

HVDC PLUS (Power Link Universal System) is Siemens' version of VSC HVDC technology. Just like HVDC Light, HVDC PLUS is based on VSCs in the form of IGBTs. A consequence of the switching technology used in the HVDC Light converters is that harmonics arise, resulting in high converter losses. Siemens' solution to this problem is to have a modular multilevel converter (MCC) consisting of several modules. For each module, there is a capacitor. The topology is shown in Figure 32. This topology ensures that each module get a small voltage level, without ripple. By controlling all the modules separately, the output voltage is very close to a pure sine wave. The technology has less harmonics than HVDC Light, and also a low level of high frequency noise. As a consequence of this, HVDC PLUS needs only small or even no filters. This is a big advantage due to lower costs and lower maintenance requirement. In HVDC PLUS converters, the switching frequency is only three times as high as the line frequency of the AC grid, which gives smaller losses than for the HVDC Light switching.

As shown in Figure 32, the converter consists of three legs. Each leg is divided in series connected sub modules. Each sub module consists of two IGBTs, a DC storage capacitor and an electronic control system (illustrated by the gray arrows in the sub module shown in Figure 32). The topology provides the possibility of using individual, selective control of the individual sub modules in a phase, and thus obtains a voltage level selectable in small steps at the AC terminal, and, at the same time, a nearly constant DC voltage at the DC terminals.

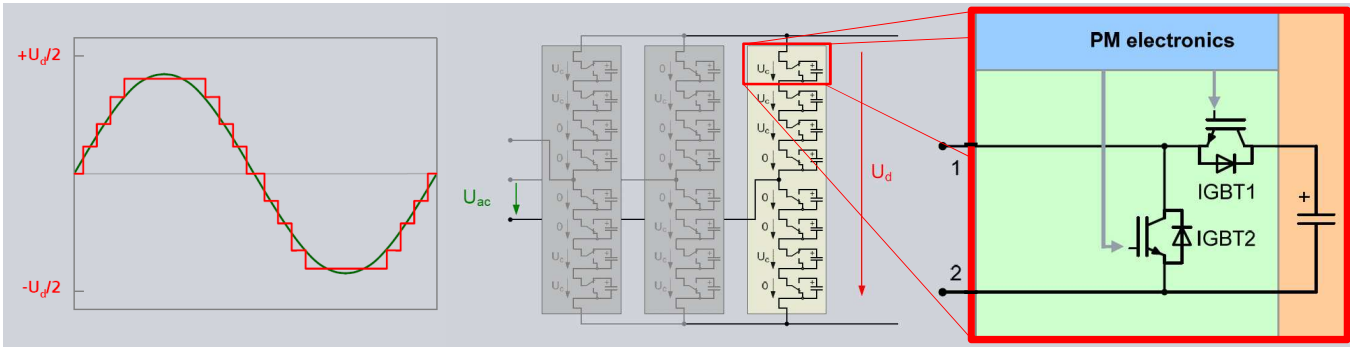

Figure 32 - HVDC PLUS output signal (left) and converter configuration (middle and right) (Siemens PTD, 2008)

5 Power system performance

In this master thesis, the term power system performance is used as a generic term for power system stability, power system security and power system reliability. Even though these are related, they are not the same. This chapter will give a presentation of each of the three terms and relate these to the operation of an offshore wind farm. Details regarding the mathematical description of these phenomena are not presented in this report. Instead, readers are referred to (Machowski, Bialek, & Bumby, 1998) and (Kundur P. , 1994) for detailed descriptions of power system performance phenomena.

5.1 Power system stability

Power system stability is similar to the stability of any other dynamic system, and is based on the same fundamental mathematics. It is simply stated an issue of remaining equilibrium between opposing forces.

The term denotes the ability of a power system to regain a state of operation equilibrium after being subject to a physical disturbance, so that the system integrity is preserved. This means that practically the entire power system shall remain intact, with no tripping of loads or generators, except for those disconnected by isolation of the faulted elements or intentionally tripped to preserve the continuity of operation of the rest of the system.

The disturbances might be of different nature, and they can be small or large. Small disturbances, such as change in generation and load occur continuously. Large disturbances can for instance be the short circuit of a line, or the loss of a large generating unit. A stable system will reach a new equilibrium after a transient disturbance, while an unstable system will result in a run-away or run-down situation, for instance a progressive decrease in system voltages or a progressive increase in rotor angle differences.

5.1.1 Classification of power system stability issues

The classification of power system stability issues facilitates the analysis of stability issues. By dividing the issues into separate areas of interest, it is easier both to identify the factors that lead to instability and to find effective methods to improve stable operation of power systems. Figure 33 shows how the IEEE Power system dynamics committee classifies power system stability issues:

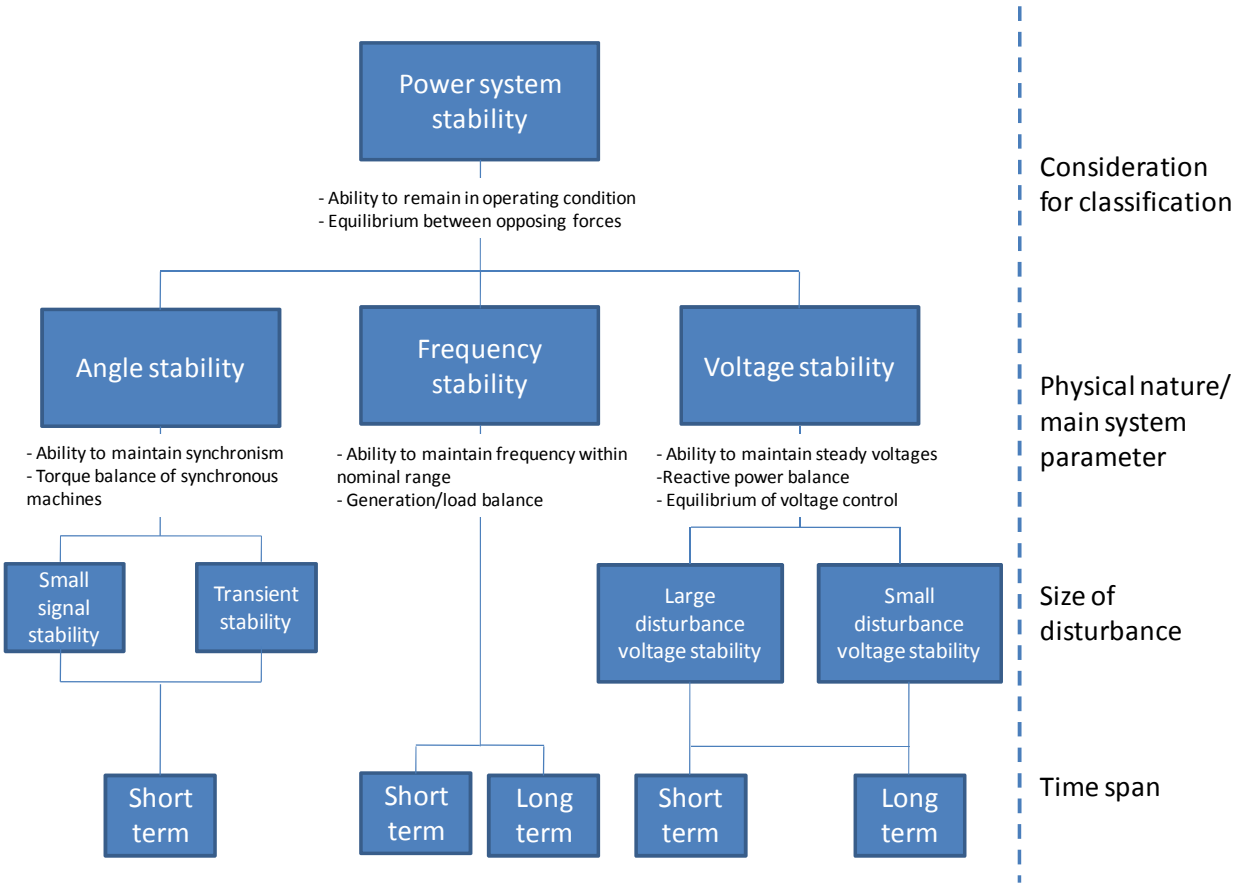

Figure 33 - Classification of power system stability. Based on(Kundur, et al., 2003)

As the figure shows, power system stability can be divided into three main topics; angle stability (or rotor angle stability), frequency stability and voltage stability.

5.1.2 Rotor angle stability

Rotor angle stability denotes the ability of interconnected generators to operate in synchronism during all operating conditions of the system. It depends on the ability of the machines in the system to maintain equilibrium between the electromagnetic torque and mechanical torque of each generator in the system, so if this kind of instability occurs, it is due to torque imbalance. This kind of instability occurs in the form of increasing swings in the rotor angle of certain generators, finally leading to loss of synchronism with the other generators in the system.

Small signal rotor angle stability issues are usually associated with the oscillations of one generator against the rest of the system, called *local plant mode oscillations*. The stability of these issues depends on the strength of the transmission system as seen from the generator, the generator excitation systems and the plant output. Global problems might be caused by interactions among a large amount of generators in the same area. These might oscillate as a group against another group of generators at another part of the area. These oscillations are called *interarea mode oscillations*. The characteristics of such oscillations are quite different from the local plant mode oscillations, and are very much affected by load characteristics. The time frame for small signal rotor angle stability is in the order of 10 to 20 seconds following a disturbance.

Transient stability issues are associated with the ability of the power system to withstand a large disturbance, such as line tripping or the short circuit of a line. When such a fault occurs, large currents and torques are produced, and often action must be taken quickly to remain system stability. The instability is usually related to insufficient synchronizing torque, resulting in *first swing instability*. However, in large power systems, transient instability may also be the result of nonlinear effects affecting a single mode causing instability in a preceding swing. It could also be a result of superposition of a slow interarea swing mode and a faster local area swing mode, resulting in rotor angle instability.
The time frame for transient stability studies is usually up to five seconds following the disturbance, but for very large systems, the time span of interest may extend to as much as 20 seconds.

5.1.3 Frequency stability

Frequency stability denotes the ability of the system to maintain nominal frequency following a disturbance of the system leading to an imbalance between load and generation. Frequency instability occurs in the form of sustained frequency swings that lead to the tripping of generators and/or loads. In a small system, frequency instability could be of concern for any large disturbance causing a significant loss of generation or load, while in a large system, this kind of problem is only of concern if a severe disturbance occurs, dividing the system into separate islands operating independently of each other. In islanded operation, frequency instability may occur for any disturbance causing a relatively large loss of load compared to the total island load.
Frequency stability problems are associated with inadequacies in equipment responses and poor coordination of control and protection systems. During frequency mismatches, the characteristic time of the process may vary from hundreds of milliseconds, corresponding to generator excitation systems, protection or load shedding, up to minutes, corresponding to the response of devices like for instance load voltage regulators or prime movers. Thus, frequency stability issues can be divided into short term or long term issues.

Short term frequency stability issues can be the formation of an undergenerated island with insufficient underfrequency load shedding, causing a blackout of the system within seconds. The time of interest is from hundreds of milliseconds up to seconds.
Long term frequency stability issues may be a more complex situation, where for instance the control system of a power plant is incorrectly tuned so that there is inadequate overspeed controls. The time of interest is from tens of seconds up to minutes.

5.1.4 Voltage stability

Voltage stability denotes the ability of the system to maintain steady voltages at all buses following a disturbance from a given initial condition. Voltage instability is the progressive and uncontrollable rise or fall in voltage of one or more buses due to a disturbance from the initial operating conditions. The main factor causing voltage instability is the inability of power systems to maintain a proper balance of reactive power and voltage control actions. The driving force for voltage instability is usually the loads. Following a condition of reduced transmission system voltages, the power consumed by the loads tends to be restored by the action of thermostats, tap changing transformers or voltage regulators. Voltage instability may lead to loss of load or loss of system integrity.

Short term voltage stability involves the dynamics of fast acting power system components, such as induction generators, power electronic devices and electrically controlled loads. The time interval for short term voltage stability issues is in the seconds range. This type of analysis is based on sets of differential equations, and the dynamic modeling of loads is therefore often essential to get good results.

Long term voltage stability involves slower working elements, such as tap-changers, thermostatically controlled loads and generator current limiters. The time interval of interest may extend to several minutes. The long term voltage stability of a system is often determined by the outage of equipment, rather than the severity of the initial disturbance. Instabilities occur due to long term imbalance, for instance when loads try to restore their power beyond the capability of the transmission network feeding the load, the post-disturbance steady state operating point being small-signal unstable, or a failure to reach the post-disturbance steady state operating point. Also, long term load buildups can cause this kind of instability.

5.2 Power system security

Power system security denotes the ability of a power system to survive disturbances without the interruption of customer service. To be secure, the system must, in addition to being stable, be secure against contingencies that are not classified as stability problems, for instance sabotage, fall of transmission towers due to ice loading or an explosive failure of a cable. Also, security includes the issue of the consequences of instability. Two systems might both be stable and have the same stability margins, but unequally secure due to the fact that the consequences of instability are more severe in one system than the other.

The security analysis of a power system is made to determine the robustness of the system when subject to one or more of the already mentioned disturbances. There are two important components of security analysis; *Static security analysis* and *dynamic security analysis*. Static security analysis involves steady state analysis of post disturbance system conditions to determine whether the equipment ratings or voltage constraints are violated. Dynamic security analysis involves examining different categories of stability issues as described in chapter 5.1. Hence, stability analysis is an integrated part of security analysis.

A common way to perform a security assessment is to use *the N-1-criterion.* For an N-component power system to fulfill the N-1-criterion, the system must withstand the loss of any of its components and still be in a stable steady state operation mode. In practice, this means that the disconnection of the largest power plant should not cause the disconnection of any consumer. The criterion can be checked by defining a certain amount of contingencies that have a significant likelihood of occurring, and study how these will affect the system by simulating it in a power system simulation tool.

5.3 Power system reliability

Power system reliability deals with the probability of satisfactory operation over the long run. It denotes the ability to supply adequate electrical service on a nearly continuous basis, with few interruptions over an extended time period. To be reliable, the system must be secure most of the time. While security and stability are time-varying issues that can be judged by studying the performance of the power system under a particular set of conditions, for instance by using simulation tools, there is a need for probability distributions and consequence analysis when performing a reliability analysis.

Reliability can be addressed by studying two basic functions of the power system; *Adequacy* and *Security*. Adequacy is the ability of the power system to supply the electric power demanded by the customer at all times, accounting for possible outages of system components. Security is already described.

In order to estimate reliability indices, one must be able to predict the system behavior. The components in the system, such as cables, transformers, generators and gearboxes, can either be functioning (100% operability) or out of function (0% operability). The mean time to failure (MTTF) is the mean time spent

in the on-state, i.e. the time the component is working between two faults. The mean time to repair (MTTR) is the mean time it takes to repair a fault on the component in question or replace the faulted part, i.e. the mean downtime when a fault occurs. The mean time between failures (MTBF) is the sum of the mean time to failure and the mean time to repair. This is illustrated in Figure 34:

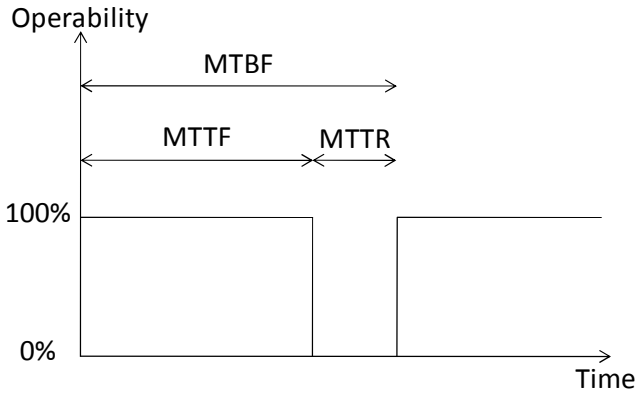

Figure 34 - The failure and reparation process of a component

When it comes to offshore wind power plants, reliability is even more important than for onshore wind power plants. The consequences of a fault offshore may be severe, with reparation times up to several months and planned power ratings up to 1000 MW. Up until today, providing redundancy has not been considered for existing wind farms since the likelihood for a fault and the associated costs has been assumed to be lower than the costs of the extra equipment needed to provide redundancy. As wind farm sizes increase, the amount of energy (and income) lost might be high enough for redundancy to become profitable. Cost/benefit calculations regarding redundancy should be performed for all projects.

In a Garrad Hassan study (Gardner, Craig, & Smith), based on statistical data from 1950 to 1980, a cable failure rate of 0.32 failures/100km of cable/year was found. Since these data are old, the study suggests a cable failure rate of 0.1 failures/100km of cable/year instead. In the literature study conducted as a part of this thesis, it was found that estimates for cable failure rates vary from 0.08 to 0.32 failures/100km/year.

Another important reliability issue is related to the capacity margin of the power system. There must be enough capacity available in the power system to cover the peak load. Adding wind power to the power system the installed power increases, meaning that the capacity of the producers in the grid also increases. The *capacity factor* of a wind farm (CF) depends on the wind resources and the type of wind turbine. It denotes the average power as a percentage of the nominal capacity, and can be expressed as:

$$CF = \frac{W}{8760 \cdot P_m} \cdot 100\% \qquad \textbf{5-1}$$

, where W is the annual energy production, and P_m is the mean power production of the wind farm, which can be expressed as:

$$P_m = \int_0^{C_{IC}} x \cdot f_p(x) dx \qquad \textbf{5-2}$$

C_{IC}	=	total installed capacity	[MW]
x	=	Production level of the wind farm	[MW]
$f_p(x)$	=	probability density function of the total wind power from the wind farm over one year	

The CF of most wind power plants on land lies between 20% and 40%, which can be expressed as 1800 – 3500 h/a.. Offshore wind power plants can reach up to 4000-5000 full load hours, corresponding to a CF of 45% - 60%. In comparison, combined heat and power has full load hours in the range 4000-5000 h/a, coal power plants has 5000-6000 h/a. and nuclear power plants have 7000-8000 h/a (Ackermann, 2005, p. 149). This shows that moving wind power plants offshore might improve the reliability of the wind power production.

5.4 Grid codes

There are no specific grid codes regulating the operation of the internal grid of an offshore wind farm directly. Nevertheless, all countries have specified grid codes, regulating the operation of the national electricity grid, and the offshore wind farm will have to fulfill the operational criterions described in these codes. The grid codes are decided by the TSO, and might vary from country to country The Norwegian TSO, Statnett, has defined a set of grid codes (Statnett SF, 2008) that must be fulfilled by all power plants in the Norwegian power system, and in this thesis the Norwegian grid codes are used as reference. In the following it is described how these codes apply for the offshore wind farm, relating them to the power system performance issues described in the previous chapters.

For an offshore wind farm, rotor angle stability is a matter of maintaining synchronism for all wind turbines. The fault ride through demands for a power plant coupled to a point in the Norwegian power system with voltage above 200kV state that the power plant needs to withstand a voltage drop to 0 pu lasting up to 150 ms (Figure 35). For a fault occurring in the offshore grid, there is no such demand. The main idea of improving transient stability of a generating unit is to decrease the available energy for acceleration of the generating unit during a grid disturbance.

As equations 2-7 to 2-14, show, the rotor angle is highly dependent on the power output of the wind turbine. Hence, rotor angle control can be done by rapidly changing the output power of the generators in the system. Equation 2-11 shows that to control the electrical output power P_e one can lower the output voltage by applying voltage control, or one can control the stator currents. The predefined generic wind model in PSS/E® contains control systems for the DFIG. These are described in Appendix 4.

When it comes to frequency stability, this is a matter of keeping the frequency in the PCC within the descriptions given in the grid code. The permitted stationary frequency deviation in the Nordic system is ±0.2% = 0.1 Hz. The permitted frequency drop during a dimensioning fault is 1%, or 0.5 Hz, i.e. the frequency is not allowed to drop below 49.5 Hz. In the Nordic system this control is above all situated in the hydro generators. Grid frequency oscillations can be counteracted with controlled power injection into the grid. For the wind farm to be able to provide this, the need for active power regulation of the wind farm arises, either in the turbines or by controlling the active power transmission in the transmission system. It must be possible to adjust the production to any value in the area 20-100% of nominal power, and it must also be possible to regulate the production from nominal output power to stop in maximum 30 seconds (Statnett SF, 2008). As a general comment, it should be noted that in the Norwegian power system, the use of wind power plants as frequency regulators would not be a good solution as long as there is hydro power available. Since there is no storage opportunity for wind power, the alternative value for the wind is zero. The wind power production should therefore be kept at maximum at all times. The

frequency regulation should therefore be performed by hydro power plants as long as that is an opportunity. Nevertheless, in islanded operation, active power control of the wind farm can be necessary. Also, as the amount of wind power in the grid increases, the offshore wind farms must also contribute to frequency stabilization, not just be able to stay connected to the grid.

Table 3 shows the boundaries for the operational area of power plants, regarding frequency, voltage level and time duration. Within these boundaries, the power production plant must be able to operate continuously for the time requirements stated in the table.

Frequency [Hz]	Voltage [pu]	Time
45.0 – 47.5	0.90 – 1.05	>20 s
47.5 – 49.0	0.90 – 1.05	>30 min
49.0 – 52.0	0.90 – 1.05	Continuously
52.0 – 53.0	0.90 – 1.05	> 30 min
53.0 – 55.0	0.90 – 1.05	>20 s
55.0 – 57.0	0.90 – 1.05	>10 s

Table 3- Functional area of power production plants (Statnett SF, 2008).

Operating an induction machine at a significantly different frequency than what it is designed for can cause a significant change in the magnetizing reactance of the machine and, because of this, an out-of-proportion increase in magnetizing current. The net result might be overheating of the machine windings. To prevent this, the ratio of volts per hertz in the machine should be kept constant, or expressed mathematically:

$$V_{f2} = \frac{f_2}{f_{nom}} V_{fnom} \quad \textbf{5-3}$$

$$P_{f2} = \frac{f_2}{f_{nom}} P_{fnom} \quad \textbf{5-4}$$

, where f_{nom} denotes the nominal frequency (50 Hz) and f_2 denotes the frequency when there is a frequency deviation in the system.

The main voltage stability issue for an offshore wind farm is the fault ride through demand. For connection points where the voltage is higher than 200 kV, the Norwegian TSO, Statnett, has the following fault ride through demands to power plants connected to the grid: The power plant has to stay connected and deliver power at a voltage at the connection point above the voltage profile described as follows:

- Voltage reduction to 0 pu for up to 150 ms, followed by instant voltage increase to 0.25 pu.
- Linear voltage increase from 0.25 pu to 0.90 pu for 750 ms
- Constant voltage at a minimum value of 0.90 pu

The offshore wind farm will have to supply a voltage that meets these demands, which are shown graphically in Figure 35 :

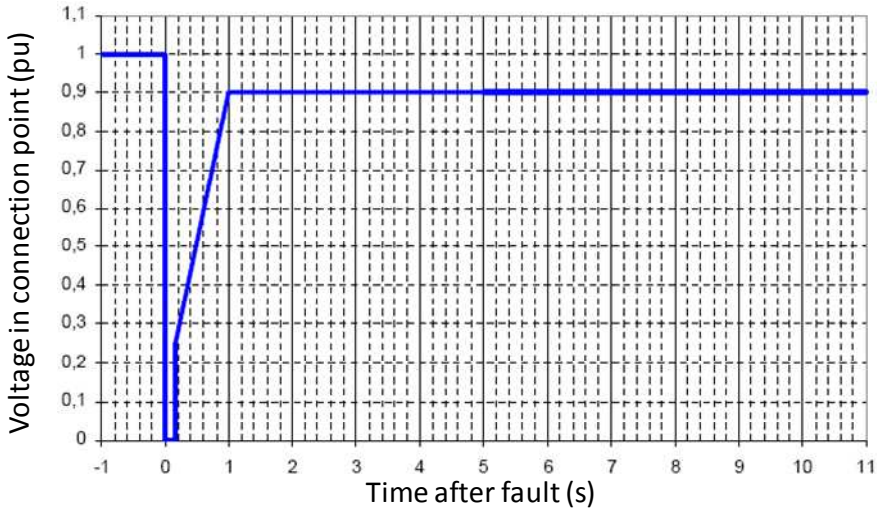

Figure 35 - Fault ride through requirements for power plants connected to a grid point with voltage >200kV in the Norwegian grid (Statnett SF, 2008)

In addition to meeting the fault ride through demands, the wind farm is required to keep the voltage level in the range of 0.9 pu to 1.1 pu at the connection point at all other times.

Another issue when it comes to voltage stability is the control of reactive power. According to the grid codes, the wind farm at nominal production shall have a reactive power rating at a level where the power factor is kept between 0.95 leading and 0.95 lagging. At production below rated power, there shall be no limitations when it comes to using the reactive capacity of the plant. Figure 36 shows the reactive power regulation area for wind power plants:

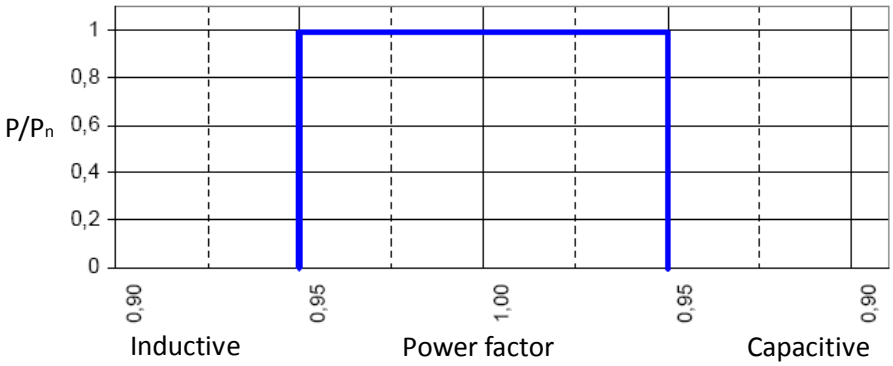

Figure 36 - Reactive power capacity for wind power plants in the Norwegian grid (Statnett SF, 2008)

With an HVDC transmission to shore, this demand is taken care of by the onshore converter station control. With an AC transmission system, this must be taken care of by adjusting the power factor of the wind turbines, or by applying some kind of reactive power compensation device in the PCC.

6 Simulation models

This chapter describes the setup of the simulations that are executed in this thesis. A short presentation of the simulation tool that is used to perform the simulations is given, and the choice of parameters and models are presented and justified.

All simulations have been executed in the program PSS/E (*Power System Simulator for Engineering*).The program, which is developed by Siemens PTI (*Power Technologies International*), is widely used in electrical transmission planning for static and dynamic analysis of power systems. In this thesis it is used to perform load flow calculations and to study the dynamic behavior of the wind farm layouts that are being compared.

6.1 Physical parameters for the wind farm site

The wind farm is placed in the North Sea and connected to the Norwegian grid. It is assumed that the wind turbines must be placed at water depths shallow enough for existing installation technologies to be used, i.e. floating offshore wind turbines are not considered. For the existing technologies to be utilized, the wind farm should be placed outside the Norwegian trench. The trench is from 50 to 95 kilometers wide, and therefore a transmission distance of 100 km is chosen in this thesis. This distance is from the onshore PCC to the offshore substation.

The wind farm consists of 108 wind turbines rated at 5MW. Most sources suggest that the distance between the turbines should be three to four rotor diameters in the direction perpendicular to the dominating wind direction, and five to nine rotor diameters in the dominating wind direction, to minimize wake losses. Using data from an existing 5 MW wind turbine, the RE power 5M wind turbine (RePower Systems AG), a rotor diameter of 126 m is used for the turbines. Based on this diameter, the distances between the wind turbines are chosen to be 500 m in the direction perpendicular to the dominating wind direction and 900 m in the dominating wind direction. The electrical connection of the wind turbines is done by dividing the wind farm into twelve feeders consisting of nine turbines each, where all turbines in one feeder are connected to each other either in a radial, looped or star design, as described in chapter 3.5. It is assumed that the distance from the first wind turbine in the feeder to the offshore substation is 5 km.

6.2 Static models

The cables, transformers, generators, shunt elements and loads are modeled using the predefined models in PSS/E . For all simulation cases, there is only one load. This is placed at the onshore swing bus, which is representing the onshore power system. For the systems using AC transmission to shore, the SVC and fixed reactors are designed so that zero reactive power is delivered to the PCC.

6.2.1 Wind turbines

Version 31 of PSS/E includes a wind turbine model, which is used for all wind turbines studied in this thesis. The data for the wind turbines are the same for all simulations. All wind turbines are rated at 5 MW, with a maximum power factor of 0.95. This gives an apparent power-rating of 5.26 MVA for the turbines. PSS/E version 31 includes three options for reactive power control of the turbines:

1) The wind machine participates in voltage control, with user defined reactive power limits. The values of QT and QB on the data record in PSS/E specify the machine's reactive power limits.

2) The wind machine participates in voltage control, with a specified power factor and the machine's active power setting (PG on the data record in PSS/E) used to set the machine's reactive power limits.

3) The wind machine operates at fixed active and reactive power. The machine's reactive power output and reactive power upper and lower limits all equal, and set based on the specified power factor and the machine's active power setting (PG on the data record in PSS/E).

Option 2) is chosen for all simulations in this thesis.

6.2.2 Transformers

All transformers in the system models have impedance values based on the transformer's MVA rating. (Hubert, 2002, p. 72) determines that the efficiency of large transformers may be higher than 99%, and based on this, all transformers are designed to have active power losses in the range of 0.5-1.0%. The parameter values for the transformer resistance and inductance for all transformers[1] are:

R = 0.007 pu
X = 0.1 pu

6.2.3 Cables

To decide the cable parameters of all cables in the system models, two parameters are considered; the cable length and the power rating of the cable.

For all models, the cable length is given by the physical parameters of the wind farm. The distances between the wind turbines are 500 m in the direction perpendicular to the dominating wind direction and 900 m in the dominating wind direction. The distance from the first wind turbine in the feeder to the offshore substation is 5 km. The cable to shore is 100 km.

When it comes to the power rating of the cable, this is decided by looking at the maximum power it must be able to handle in a worst case scenario. It is assumed that no tapering of cable capacity is done, and thus all cables in one feeder must be able to carry the worst case scenario power. The offshore cable ratings differ from layout to layout. Table 4 shows the cable parameter values for the AC cables used in this thesis:

Cable type	Manufacturer	U_{nom}	I_{nom}	r [Ω(km]	x [Ω(km]	c [µF/km]
1x3x95 XLPE-M-AL-LRT	Ericsson	11	265	0,32	0,11	0,34
TSLE 3x1x800 Al/-	Nexans	33	780	0,037	0,16	0,36
TSLE 3x1x2000 Al/-	Nexans	33	1050	0,015	0,14	0,53
TSLE 3x1x150AQ	Nexans	48	1025	0,0186	0,09	0,13
XLPE 3x1x 1000 CU-LRT	Ericsson	400	1220	0,0151	0,12	0,17

Table 4 - Cable parameters of the AC cables used in the different wind farm layouts

[1] The transformers that are included in the ABB HVDC Light-model have parameter values as stated in the classified information from ABB. These values are not recited in this thesis.

6.2.4 HVDC Light

The user model of HVDC Light is developed and provided by ABB. The standard elements from PSS/E are used in order to establish the load flow. Table 5 shows the available modules for HVDC Light technology: All parameters are taken from the ABB document "It's time to connect" (ABB, 2008).

HVDC Light® modules		Currents		
		580A (2 sub)	1140A (4 sub)	1740A (6 sub)
Voltages	± 80 kV	**M1**	**M2**	**M3**
	± 150 kV	**M4**	**M5**	**M6**
	± 320 kV	**M7**	**M8**	**M9**

Table 5 - HVDC Light modules(ABB, 2008)

For all load flows, the module M6 is used to represent the HVDC Light transmission. This has a rated power, S_{base} , of 570 MVA.

The rectifier is modeled as a PU bus connected to a generator and shunt. Because the power is going from the AC to the DC side, the specified power to the generator has to be negative. The generator impedance Z_{source} in PSS/E specifies the converter reactance in Figure 29. The shunt AC filter in the same figure is represented by the reactive power generation of the fixed shunt capacitor at the rectifier bus in PSS/E . Additionally, a converter transformer has to be added. One side is connected to the rectifier bus, and the other side is connected to the offshore substation bus. The AC voltage at the converter bus is 195 kV for the HVDC Light converter in module M6. The inverter is modeled using the same units as the rectifier, but the power from the generator has to be positive, because the power is going from the DC side to the AC side.

The reactive power limits to be specified in the power flow for the generator equivalents depend on the active power. The HVDC Light converter has a capability curve according to Figure 37:.

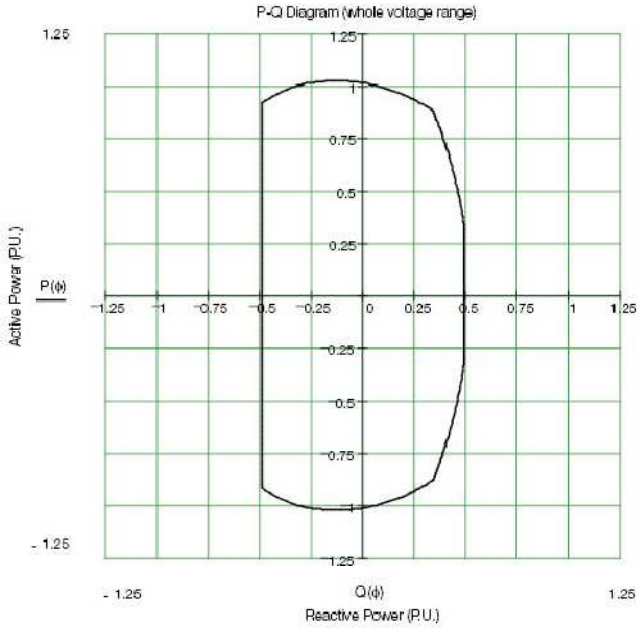

Figure 37 – Capability curve for HVDC converter

It is up to the user to select the right reactive power limits for the converter, based on this curve.

The DC cable is not modeled in the load flow. The power loss in the HVDC Light system must be calculated, and the received power at the onshore converter bus generator must be specified based on this calculation in order to represent the HVDC losses correctly in the load flow simulation. Equation 6-1 describes the power loss in the HVDC Light system.

$$P_{loss,DC} = P_{rectifier} - P_{inverter} \quad \text{6-1}$$

The power loss in the DC system can be split into converter losses and line losses. Table 6 shows the full power ratings of HVDC Light modules M4 to M6:

Converter	DC voltage	DC current	DC cable	Sending power	Receiving power (MW)					
types	kV	A	Cu in mm²	MW	Back-to-back	50 km	100 km	200 km	400 km	800 km
M4	150	627	800	191.3	185.0	182.0	179.0	174.0		
M5	150	1233	1200	376.0	363.7	361.0	358.0	353.0	342.0	
M6	150	1881	2800	573.9	555.1	552.0	549.5	544.0	533.0	

Table 6 – Sending and receiving power in the 150kV HVDC Light modules

From Table 6, the converter losses at full power can be calculated by comparing the sending power with the receiving power when the system is has a back-to-back configuration.

The dynamic converter losses are calculated as a constant part, no load losses, and a load loss which is estimated to be linear with the load

- The no load losses are estimated as 0.3 pu of the nominal losses
- The load losses are estimated as 0.7 pu at nominal load (Sbase)
- The nominal losses are estimated to 0.0165 pu of Sbase, according to (ABB, 2008)

This can be expressed mathematically by equations 6-2 to 6-4:

$$P_{nom} = 0.0165 \cdot S_{base} \quad \text{6-2}$$

$$P_{noload} = 0.30 \cdot P_{nom} \quad \text{6-3}$$

$$P_{load} = 0.7 \cdot P_{nom} \cdot \frac{P_{sent}}{P_{sent,\max}} \quad \text{6-4}$$

Total converter losses for one converter can be expressed as:

$$P_{loss,conv} = P_{load} + P_{noload} \quad \text{6-5}$$

For a bipolar transmission, the DC cable loss for can be calculated by finding the DC current, given a certain cable dimension and length. The DC current in each cable can be expressed as:

$$I_{DC} = 1000 \cdot \frac{P_{sent} - P_{loss,conv}}{2 \cdot U_{base}} \quad \text{6-6}$$

In (ABB, 2008), an overview of the resistance for different cables for different conductor areas is presented. From Table 6, it can be found that the copper conductor area of the DC cable needs to be 2800

mm^2. Looking at the resistance overview, the resistance is found to be 0.0079 Ω/km. With a 100 km distance to shore, the total resistance of the cable is 0.79Ω This can be used to calculate the cable losses as:

$$P_{loss,cables} = 2RI_{DC}^2 \quad \textbf{6-7}$$

Finally, the received power at the inverter bus can be expressed as:

$$P_{received} = \cdot P_{sent} - 2P_{loss,conv} - P_{loss,cables} \quad \textbf{6-8}$$

6.2.5 Onshore generator and SVC

The onshore power system is modeled as one bus with one generator and one load. The generator representing the power system is modeled by the predefined generator model in PSS/E . In addition to the generator at the PCC, a load of 540 MW is connected at the same bus. This way, the active power production at the generator in the PCC equals the total active power losses of the wind farm.

For the AC/AC-models, an SVC is placed at the onshore transmission bus. The SVC is modeled using the standard generator model, defining the active power output as zero.

6.2.6 Fixed shunts

For the AC/AC-models, two fixed shunt reactors are placed at the onshore transmission bus to provide reactive power compensation to the AC cables. The shunts are modeled using the predefined "fixed shunt"-model in PSS/E .

6.3 Dynamic models

All generators and power electronic devices in a power system consist not only of the device itself. To make sure that the system fulfills the system requirements, all devices are equipped with control systems such as automatic voltage regulators (AVRs), power factor correctors (PFCs) and power system stabilizers (PSSes). Thus, for PSS/E to run dynamic simulation, the program demands that dynamic models are defined for all generators, SVCs and VSC HVDC lines. In the following, the models used in this thesis are presented.

6.3.1 Wind turbine model

In this thesis, the DFIG is chosen to represent the wind turbine generators. PSS/E contains a predefined model of this turbine type, the WT3 generic wind model, which comprises the following modules:

- WT3G: generator/converter module
- WT3E: electrical control module
- WT3T: mechanical control (wind turbine) module
- WT3P: pitch control module.

The model was developed to simulate performance of a wind turbine employing a doubly fed induction generator (DFIG) with the active control by a power converter connected to the rotor terminals. The model is described in detail in the application guide of PSS/E (Siemens PTI, 2007), and the model is described and all block diagrams reproduced in Appendix 4. The chosen parameter values for the wind turbine model are also given in the appendix. When conducting the DC simulations, the control parameter

VLTFLG (see the block diagram of the WT3E1 module in appendix 4) had to be changed as compared to the AC simulations. VLTFLG had to be equal to 1 for the AC/DC simulations, and 0 for the AC/AC simulations, in order to get the initial conditions check to be OK.

6.3.2 Onshore generator model

The onshore generator model is modeled as a salient pole hydro generator, since the Norwegian power system is based on almost only hydro power generation. To represent the dynamic behavior of the generator, the model GENSAL is used. The exciter and governor systems are represented by the models SCRX and HYGOV, respectively. All parameters can be found in appendix 4.

6.3.3 SVC model

The SVC used in the simulations is modeled as a generator, producing zero active power during the load flow simulations. In the dynamic simulations, the PSS/E model CSVGN5 is used. All parameters can be found in appendix 4.

6.3.4 HVDC Light model

In order to represent the dynamic behavior of the HVDC Light system, ABB has developed two user models called CABBL2 and CEMPTY. Each module presented in Table 5 has its own dynamic file, which is given in the user manual provided by ABB(ABB Power technologies AB, 2009). The dynamic file corresponding to the module M6 is applied for the dynamic simulations in this thesis.

Figure 38 shows the structure of the load flow and dynamic model of HVDC Light.

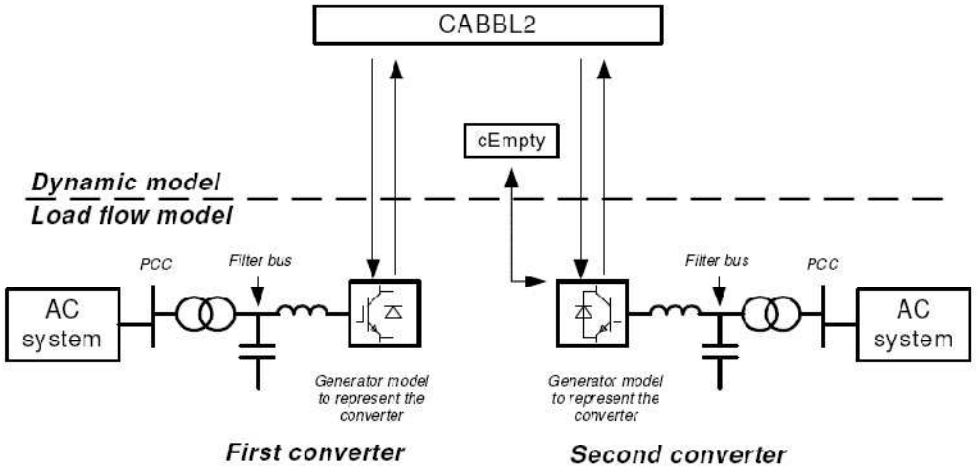

Figure 38 - The HVDC Light model used in PSS/E

In the load flow, the PSS/E generic generator model represents the converters. The user model CABBL2 is used to calculate the current injection to be applied by this generic generator. This user model includes a representation of the cable, including the cable resistance. The user model CABBL2 is applied as the "primary" dynamic model for the generator used as the first converter in PSS/E. Still CABBL2 controls both the first and the second converter. An additional dummy user model CEMPTY is applied as the "primary" dynamic model for the generator used as the second converter. Without this dummy user model, PSS/E will disconnect the second converter in the dynamic simulation.

.

7 Load flow simulations

This chapter describes the load flow simulations executed as a part of the work with this thesis. For each wind farm layout, two cases are studied:

In the first case, the simulation is setup so that the active power delivered to the PCC is maximized. This is done by varying the voltage level at the offshore transmission bus and choosing the voltage level that gives the highest amount of active power delivered to the PCC, given that all elements of the system is rated below 100%, and that the voltage level at all buses does not exceed its upper and lower limit. For each simulation, PU-curves, showing the optimum voltage/power-level have been created. The PU-curves are given in appendix 2. This load flow situation is from now on referred to as "normal operating conditions".

In the second case, it is assumed that a fault has occurred at the most critical cable in one of the feeders. This fault has led to the cable being disconnected. The voltage at the offshore transmission bus is the same as before the fault occurred. This load flow condition is from now on referred to as "worst case operating conditions".

In chapter 3.5, six options for the design of the offshore grid were presented, and these are all studied by running load flow simulations on them. In addition, the impact of the choice of transmission system to shore is studied. Two options are studied. The first option is to use AC transmission, using two AC cables to provide redundancy. The second option is to use HVDC Light transmission, using two HVCD links to provide redundancy. Having six offshore grid designs, two transmission system options and two load flow cases, this means that a total of 24 load flow simulations are executed in this thesis.

7.1 Large AC wind farm layouts

The large AC wind farm layout was presented in chapter 3.2.2 . It consists of an offshore AC network with an AC transmission to shore. Figure 39 shows the transmission system to shore. A 33/400 kV transformer provides the right voltage level. The cables are 400 kV XLPE cables, rated at 845.2 MVA. The cable data are gathered from an Ericsson datasheet, available at their web page (Ericsson nkt).

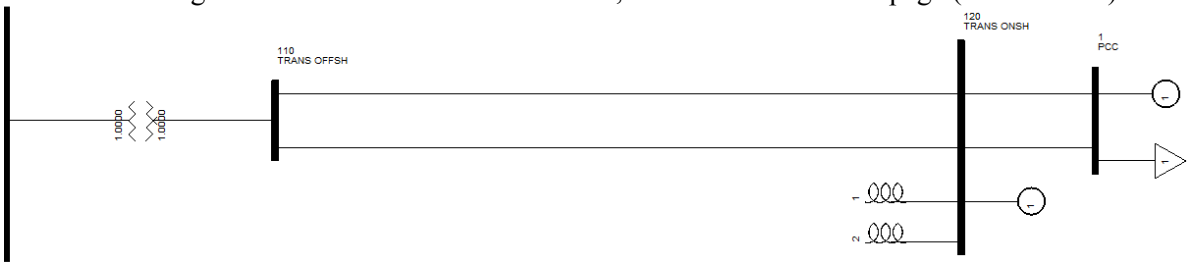

Figure 39 - Single line diagram showing the connection to shore, using two AC cables to provide redundancy

At the onshore side, there is a considerable need of reactive compensation. This is taken care of by having a constellation consisting of two fixed shunt reactors and one SVC at the onshore transmission bus. The constellation is designed so that the SVC provides zero reactive power at unity power factor at the PCC. The SVC assures that the reactive capacity requirement of being able to provide cos φ = 0.95 at nominal power output is fulfilled. At normal operating conditions, the offshore wind farm delivers 515 – 530 MW to the PCC, depending on the wind farm layout. With a power factor limit of 0.95, the SVC must be rated at a minimum of 170 – 175 MVAr. The total reactive power delivered to the onshore transmission bus

from the two AC cables is in the range of 1611 to 1613 MVAr for the simulation cases. The reason why this is so high is the high capacitive rating of the cable (0.20 µF/km, giving 17 µF in total per cable), combined with the fact that there is no reactive compensation offshore.

The fixed shunts are rated at the same reactive power level as what is delivered to the onshore transmission bus by the AC cables. If one of the transmission lines is lost, one of the fixed shunts are disconnected, so that the SVC still does not have to provide reactive power compensation at unity power factor. This running condition is indicated in Figure 40 :

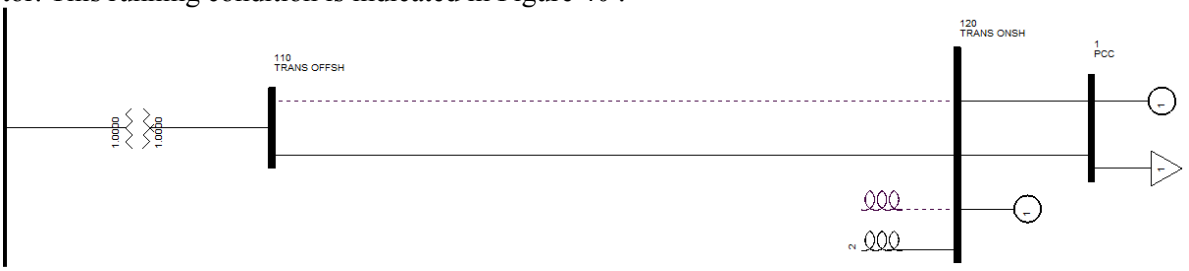

Figure 40 - Single line diagram showing the connection to shore with one AC cable disconnected

For all simulations, the disconnected shunt varies between 845MVAr and 846 MVAr, while the shunt still in connection varies between 765 and 766 MVAr. This situation is not studied as a load flow case, only during the dynamic simulations.

7.2 AC/DC wind farm layouts

The AC/DC wind farm layout was presented in chapter 3.3. In the simulations, the AC/DC configuration consists of an offshore AC network with a double HVDC Light transmission to shore. Traditional HVDC-technology is not studied. Figure 41 shows the transmission system to shore.

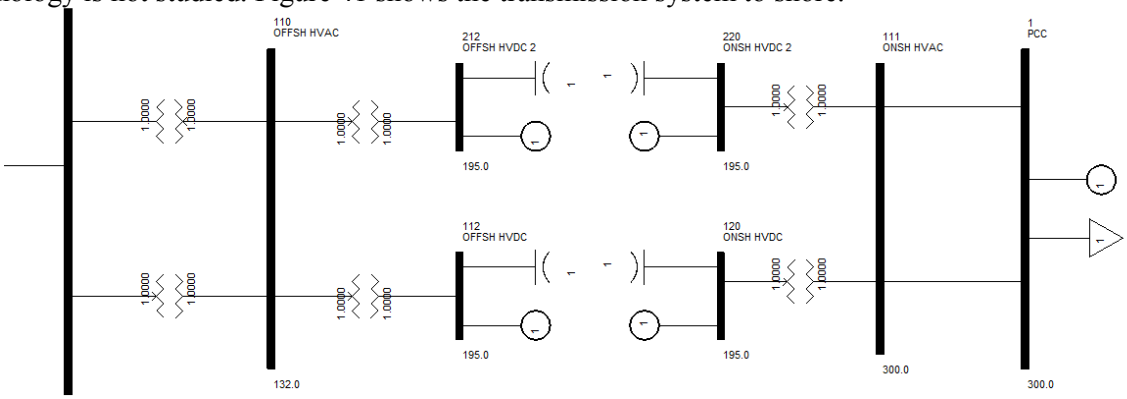

Figure 41 - Single line diagram showing the connection to shore, using two HVDC Light connections

A 33/132 kV transformer offshore boosts the voltage before the power is converted from AC to DC in the HVDC Light converter station. Onshore, the power is transformed from 195 kV DC voltage to 300 kV AC voltage before it is transmitted to the PCC. The DC cables are 195 kV XLPE cables, rated at 570 MVA.

7.3 Radial design

In the radial design, nine wind turbines are connected in a radial, as described previously. The wind turbines are rated at 5MW, with a power factor limit of 0.95. The wind turbines are operating at 0.69kV. Each wind turbine is equipped with a 0.69/33kV transformer, rated at 5.26 MVA. The cable ratings are 48.6 MVA throughout the loop, operating at 33 kV. The maximum rated voltage of the cable is 36 kV, or

1.091 pu. Thus, all voltage levels lower than 1.091 pu are considered acceptable in the offshore grid. A value of 0.9 pu is used as the minimum acceptable voltage level.

7.3.1 AC/AC

Figure 42 shows the load flow result during *normal operating conditions* for one feeder of the radial design while using AC transmission to shore. All elements of the feeder operate at below their maximum rating. The most heavily loaded cable is the one connecting the first wind turbine to the offshore substation. This is loaded at 92%. The most heavily loaded devices in the feeder are the wind turbines, which operate at 95% of their maximum rating. All voltage levels are within their boundaries.

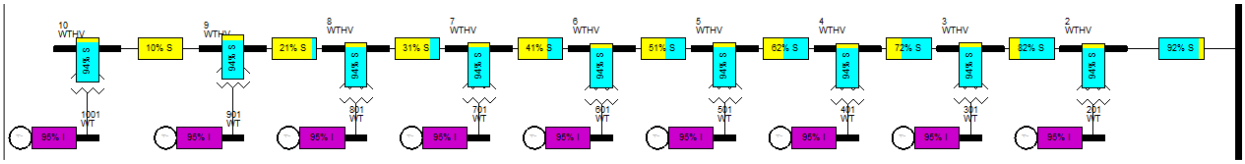

Figure 42 - Radial design with AC transmission – normal operating conditions

The active power delivered to the grid is 524.6 MW, giving total losses of 2.85%. The most heavily loaded elements of the system are the transmission cables, rated at 100%.

Figure 43 shows the load flow result during *worst case operating conditions* for one feeder of the radial design while using AC transmission to shore. All elements of the feeder operate at ratings below their maximum rating. The most heavily loaded devices in the feeder are the wind turbines and wind turbine transformers, which operate at 95% of their maximum rating.

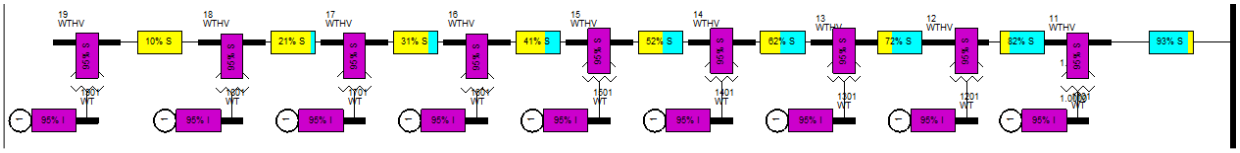

Figure 43 - Radial design with AC transmission - worst case operating conditions

During worst case operating conditions, that is, during operating conditions where one radial is out of service, the active power delivered to the grid is 480.9 MW. This means that the total losses are 10.94% when compared to the total installed power of the wind farm, 540 MW. The SVC must consume 6.2 MVAr in order to provide unity power factor in the PCC.

7.3.2 AC/DC

Figure 44 shows the load flow result during *normal operating conditions* for one feeder of the radial design while using AC transmission to shore. All elements of the feeder operate at below their maximum rating, but slightly higher than in the AC/AC-system. The most heavily loaded cable is the one connecting the first wind turbine to the offshore substation. This is loaded at 94%. The most heavily loaded devices in the feeder are the wind turbines, which operate at 98% of their maximum rating. All voltage levels are within their boundaries.

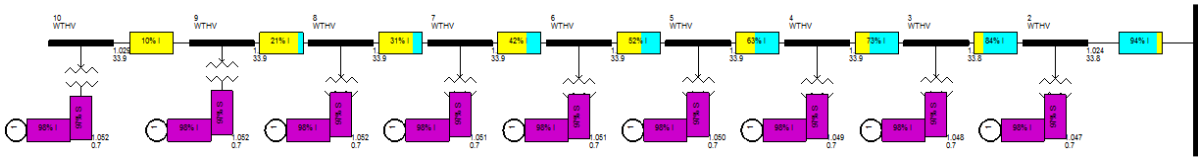

Figure 44 - Radial design with DC transmission – normal operating conditions

The active power delivered to the grid is 502.7 MW, giving total losses of 6.91%. The most heavily loaded elements of the system are the wind turbines, at 98%. The generators representing the HVDC Light connection are running at 48% and 46% at the offshore and onshore stations respectively (shown in appendix 2).

Figure 45 shows the load flow result during *worst case operating conditions* for one feeder of the radial design while using AC transmission to shore. All elements of the feeder operate at ratings below their maximum rating. The cable ratings are as in the normal operating conditions. The most heavily loaded devices in the feeder are the wind turbines and the wind turbine transformers, which operate at 97% of their maximum rating. All voltage levels are within their boundaries.

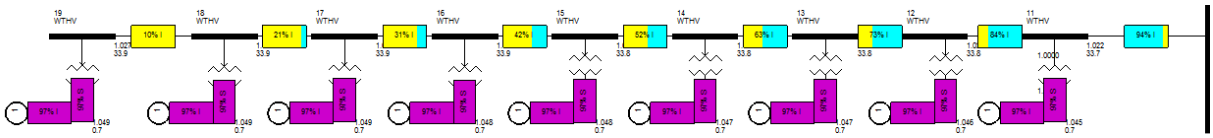

Figure 45 - Radial design with DC transmission - worst case operating conditions

During worst case operating conditions, which is during operating conditions where one feeder is out of service, the active power delivered to the grid is 460.2 MW, corresponding to 14.78% losses when comparing to the nominal power output. The most heavily loaded elements of the system are the wind turbines and the wind turbine transformers. The generators representing the HVDC Light connection are running at 45% and 43% at the offshore and onshore stations respectively (shown in appendix 2).

7.4 Single sided ring

In the single sided design, nine wind turbines are connected in series, with a safety cable from the last wind turbine to the offshore substation. The wind turbines are rated at 5MW, with a power factor limit of 0.95. The wind turbines are operating at 0.69kV. Each wind turbine is equipped with a 0.69/33kV transformer, rated at 5.26 MVA. The cable ratings are 48.6 MVA throughout the loop, operating at 33 kV. The maximum rated voltage of the cable is 36 kV, or 1.091 pu. Thus, all voltage levels lower than 1.091 pu are considered acceptable in the offshore grid. A value of 0.9 pu is used as the minimum acceptable voltage level.

7.4.1 AC/AC

Figure 46 shows the single sided ring design during *normal operating conditions*. Due to the extra cable connection from the last wind turbine in the feeder to the offshore substation, none of the cables are rated higher than 55%. The most heavily loaded devices are the wind turbine transformers, which are rated at 96%. All voltage levels are within their boundaries.

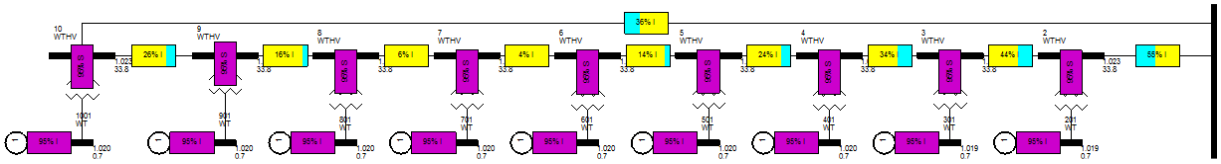

Figure 46 - Single sided ring, normal operating conditions

The active power delivered to the grid is 526.6 MW, giving total losses of 2.48%. The most heavily loaded elements of the system are the transmission cables, rated at 100%.

Figure 47 shows the *worst case* load flow situation for the single sided ring design. The line between the first wind turbine and the offshore substation is lost, meaning that the direction of the power flow is reversed through the feeder. The most heavily loaded cable is now running at 91% of its current rating. The most heavily loaded devices of the feeders are still the wind turbine transformers, at 96%. All voltage levels are within their boundaries.

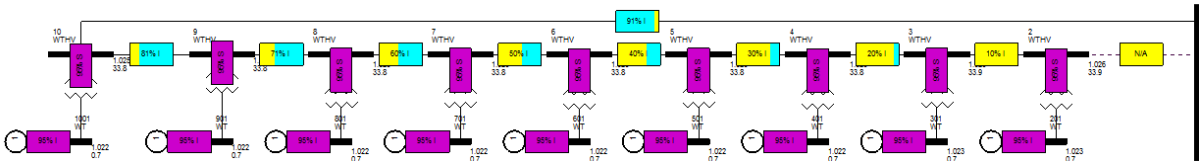

Figure 47 - Single sided ring, worst case operating conditions

The active power delivered to the grid is 526.2 MW, corresponding to 2.56% losses when comparing to the nominal power output. The most heavily loaded elements of the system are the transmission cables, rated at 100%. The SVC must consume 0.1 MVAr in order to provide unity power factor in the PCC.

7.4.2 AC/DC

Figure 48 shows the single sided ring design during *normal operating conditions*. Due to the extra cable connection from the last wind turbine in the feeder to the offshore substation, none of the cables are rated higher than 55%. The most heavily loaded devices are the wind turbine transformers, which are rated at 96%. All voltage levels are within their boundaries.

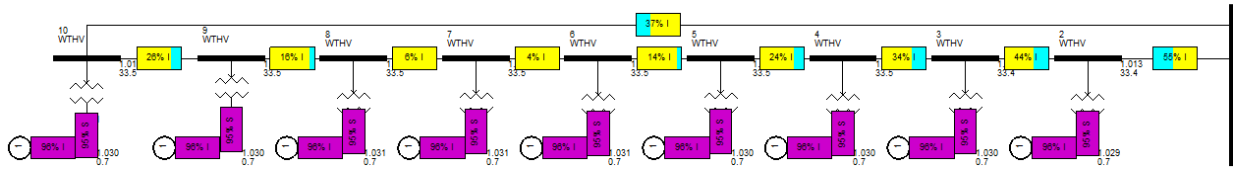

Figure 48 - Single sided ring, normal operating conditions

The active power delivered to the grid is 504.6 MW, giving total losses of 6.56%. The most heavily loaded elements of the system are the wind turbines. The generators representing the HVDC Light connection are running at 48% and 47% at the offshore and onshore stations respectively (shown in appendix 2).

Figure 49 shows the *worst case* load flow situation for the single sided ring design. The line between the first wind turbine and the offshore substation is lost, meaning that the direction of the power flow is reversed through the feeder. The most heavily loaded devices of the feeders are the wind turbines and the wind turbine transformers, at 96%. All voltage levels are within their boundaries.

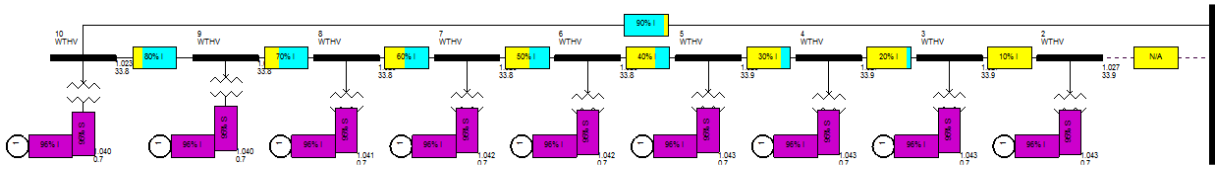

Figure 49 - Single sided ring, worst case operating conditions

The active power delivered to the grid is 504.2 MW, corresponding to 6.63% losses when comparing to the nominal power output. The most heavily loaded elements of the system are the wind turbines and the

wind turbine transformers. The generators representing the HVDC Light connection are running at 48% and 46% at the offshore and onshore stations respectively (shown in appendix 2).

7.5 Double sided ring

In each feeder of the double sided design, nine wind turbines are connected in series, and two feeders are connected in parallel to provide redundancy. The wind turbines are rated at 5MW, with a power factor limit of 0.95. The wind turbines are operating at 0.69kV. Each wind turbine is equipped with a 0.69/48kV transformer, rated at 5.26 MVA. The cable ratings are 92.3 MVA throughout the loop, operating at 48 kV due to the high power rating of the cable. The maximum rated voltage of the cable is 52 kV, or 1.083 pu. Thus, all voltage levels lower than 1.083 pu are considered acceptable in the offshore grid. A value of 0.9 pu is used as the minimum acceptable voltage level.

7.5.1 AC/AC

Figure 50 shows the load flow situation of the double sided ring during *normal operating conditions*. The most heavily loaded cables are running at 48%, since they are rated to provide redundancy. The most heavily loaded elements of the feeders are the wind turbine transformers, which are rated at 96%. All voltage levels are within their boundaries.

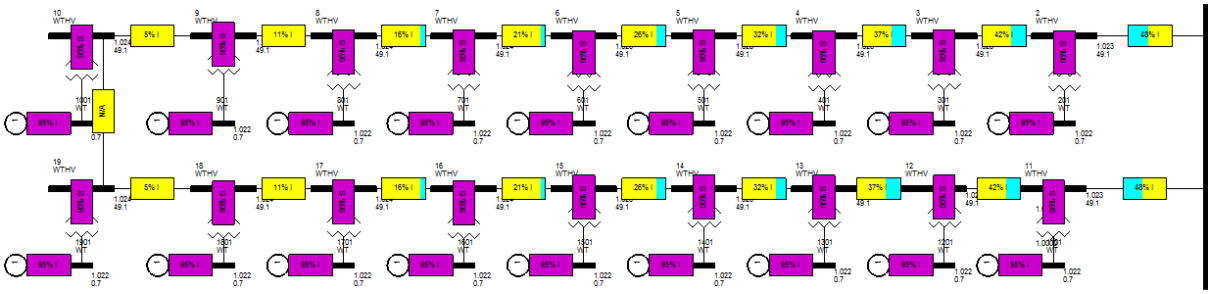

Figure 50 - Double sided ring, normal operating conditions

The active power delivered to the grid is 526.9 MW, giving total losses of 2.43%. The most heavily loaded elements of the system are the transmission cables, rated at 100%.

Figure 51 shows the *worst case* load flow situation of the double sided ring-system. In this situation, one of the lines connecting the first turbine of a feeder to the offshore substation is lost. The direction of the power flow in this feeder is reversed, and all the turbines can continue to operate at full production. The most heavily loaded cable now operates at 95%, and is the most heavily loaded device of the feeders, together with the wind turbines which are also loaded at 95%. All voltage levels are within their boundaries.

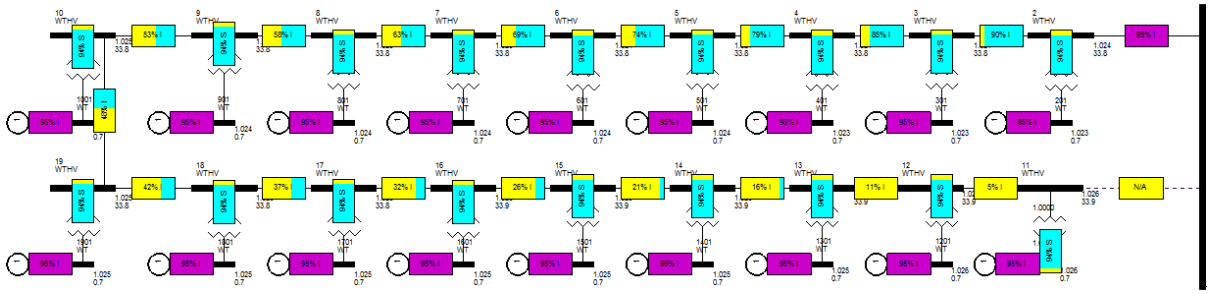

Figure 51 - Double sided ring, worst case operating conditions

The active power delivered to the grid is 526.3 MW, giving total losses of 2.54%. The most heavily loaded elements of the system are the transmission cables, rated at 100%. The SVC must consume 0.1 MVAr in order to provide unity power factor in the PCC.

7.5.2 AC/DC

Figure 50 shows the load flow situation of the double sided ring during *normal operating conditions*. None of the cables are rated above 48%, since they are rated to provide redundancy. The most heavily loaded elements of the feeders are the wind turbine transformers, which are rated at 97%. All voltage levels are within their boundaries.

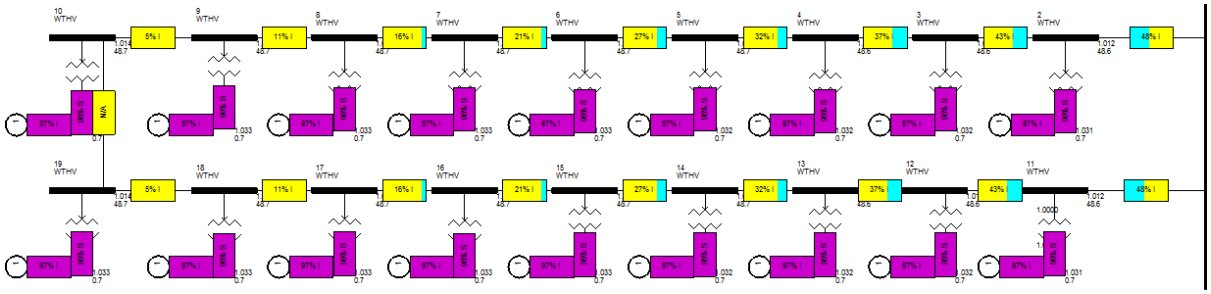

Figure 52 - Double sided ring, normal operating conditions

The active power delivered to the grid is 505.0 MW, corresponding to 6.48% losses when comparing to the nominal power output. The most heavily loaded elements of the system are the wind turbines and the wind turbine transformers. The generators representing the HVDC Light connection are running at 48% and 46% at the offshore and onshore stations respectively (shown in appendix 2).

Figure 53 shows the *worst case* load flow situation of the double sided ring-system. In this situation, one of the lines connecting the first turbine of a feeder to the offshore substation is lost. The direction of the power flow in this feeder is reversed, and no turbines need to be out of production. The most heavily loaded cable is now running at 95% capacity. The most heavily loaded devices of the feeders are still the wind turbines, at 97%. All voltage levels are within their boundaries.

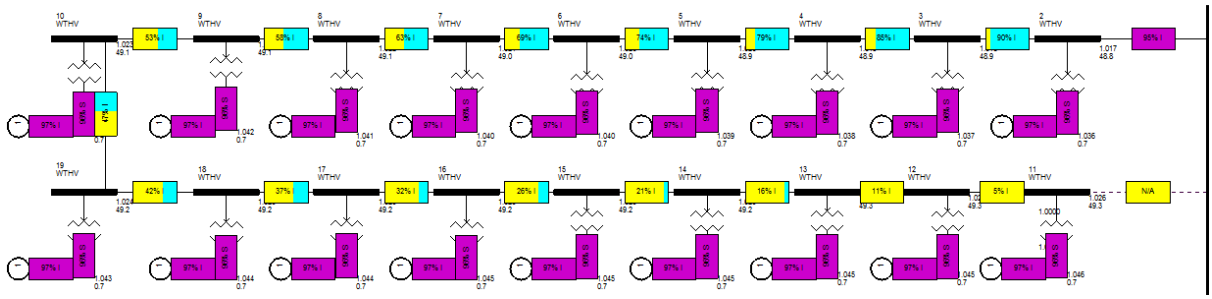

Figure 53 - Double sided ring, worst case operating conditions

The active power delivered to the grid is 504.4 MW, corresponding to 6.59% losses when comparing to the nominal power output. The most heavily loaded elements of the system are the wind turbines. The generators representing the HVDC Light connection are running at 48% and 46% at the offshore and onshore stations respectively (shown in appendix 2).

7.6 Shared ring

In each feeder in the shared ring design, nine wind turbines are connected in series, and four feeders share a safety cable that provides redundancy. The wind turbines are rated at 5MW, with a power factor limit of 0.95. The wind turbines are operating at 0.69kV. Each wind turbine is equipped with a 0.69/33kV transformer, rated at 5.26 MVA. The cable ratings are 48.6 MVA throughout the loop, operating at 33 kV. The maximum rated voltage of the cable is 36 kV, or 1.091 pu. Thus, all voltage levels lower than 1.091 pu are considered acceptable in the offshore grid. The cables from the last wind turbine to the extra buses at the feeder ends (see Figure 54) are modeled as lossless lines, representing the breaker system that is used to rearrange the power flow if a cable is disconnected. A value of 0.9 pu is used as the minimum acceptable voltage level.

7.6.1 AC/AC

Figure 54 shows the load flow situation for the shared ring design during *normal operating conditions*. Due to the redundancy provided by the extra cable, no cables are rated higher than 76%. In the feeders, the highest rated elements are the wind turbines, rated at 95%. All voltage levels are within their boundaries.

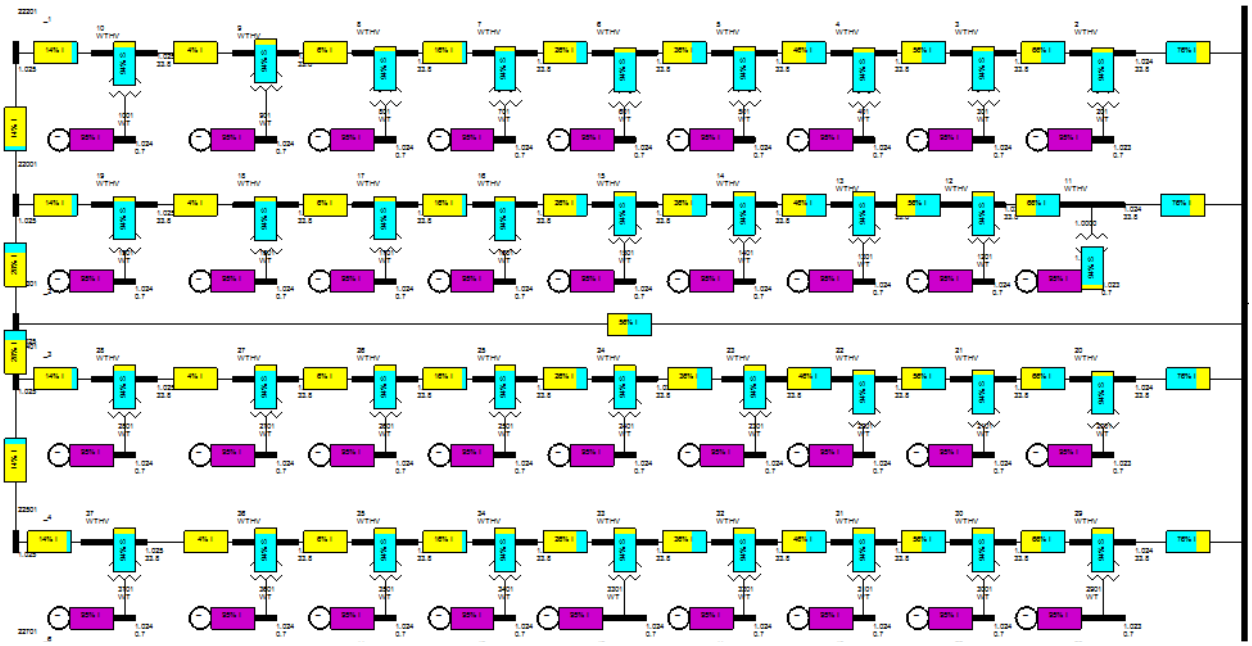

Figure 54 - Shared ring, normal operating conditions

The active power delivered to the grid is 525.5 MW, giving total losses of 2.69%. The most heavily loaded elements of the system are the transmission cables, rated at 100%.

Figure 55 shows the *worst case* load flow situation for the shared ring design. The line between the first wind turbine and the offshore substation of the feeder the furthest away from the redundant cable is lost, meaning that the direction of the power flow is reversed through that feeder. To avoid overloading of the cables at the other feeders, the connections from these to the redundant cable are disconnected, as indicated by the dashed lines in Figure 55. The most heavily loaded cables are the ones connecting the first wind turbine of each feeder to the offshore substation, and the redundant cable, all loaded at 92%. The most heavily loaded devices of the power system are the wind turbines, which are running at 95%. All voltage levels are within their boundaries.

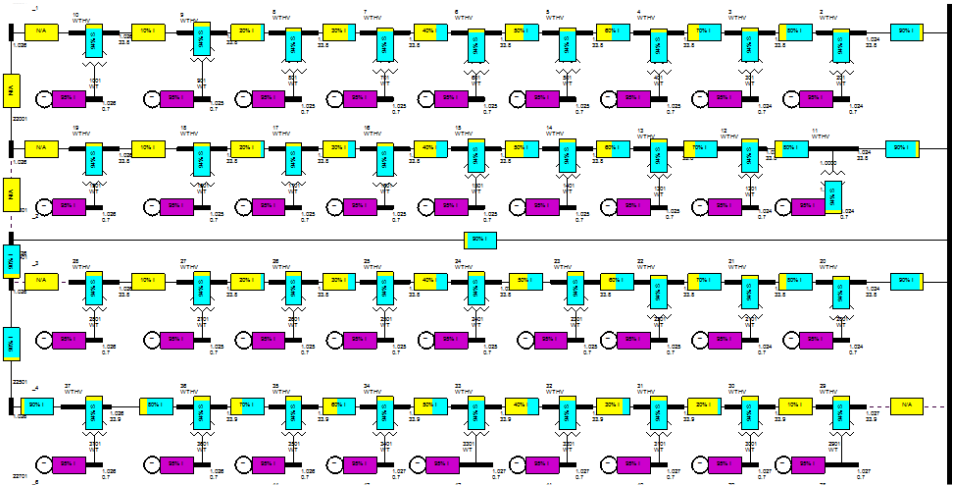

Figure 55 - Shared ring, worst case operating conditions

The active power delivered to the grid is 524.9 MW, giving total losses of 2.80%. The most heavily loaded elements of the system are the transmission cables, rated at 100%. The SVC must consume 0.1 MVAr in order to provide unity power factor in the PCC.

7.6.2 AC/DC

Figure 56 shows the load flow situation for the shared ring design during *normal operating conditions*. Due to the redundancy provided by the extra cable, no cables are rated higher than 77%. In the feeders, the highest rated elements are the wind turbines, rated at 97%. All voltage levels are within their boundaries.

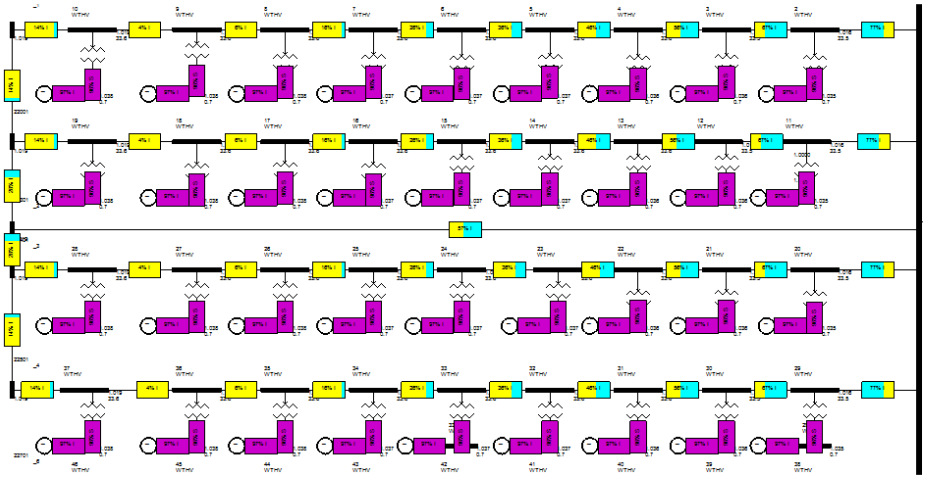

Figure 56 - Shared ring, normal operating conditions

The active power delivered to the grid is 502.4 MW, corresponding to 6.78% losses when comparing to the nominal power output. The most heavily loaded elements of the system are the wind turbines and the wind turbine transformers. The generators representing the HVDC Light connection are running at 48% and 46% at the offshore and onshore stations respectively (shown in appendix 2).

Figure 57 shows the *worst case* load flow situation for the shared ring design. The line between the first wind turbine and the offshore substation of the feeder the furthest away from the redundant cable is lost,

meaning that the direction of the power flow is reversed through that feeder. To avoid overloading of the cables at the other feeders, the connections from these to the redundant cable are disconnected, as indicated by the dashed lines in Figure 57. The most heavily loaded devices of the power system are the wind turbines and the wind turbine transformers, running at 97% capacity. All voltage levels are within their boundaries.

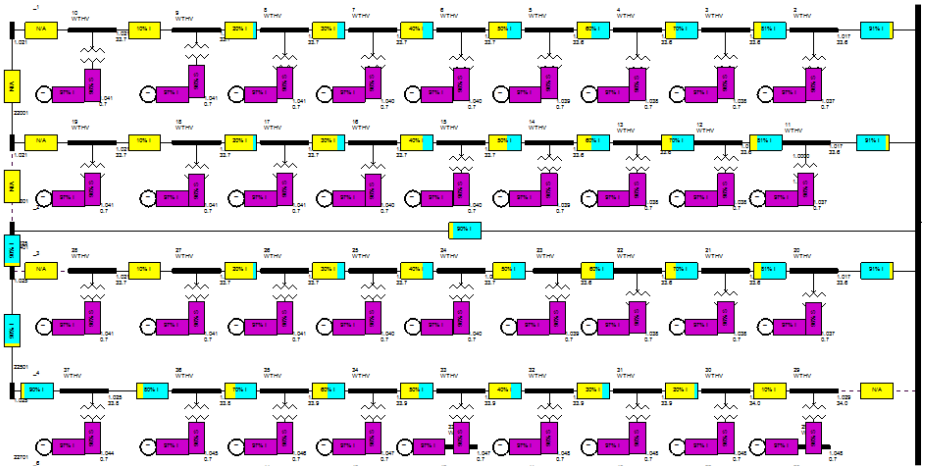

Figure 57 - Shared ring, worst case operating conditions

The active power delivered to the grid is 502.8 MW, corresponding to 6.89% losses when comparing to the nominal power output. The most heavily loaded elements of the system are the wind turbines and the wind turbine transformers. The generators representing the HVDC Light connection are running at 48% and 46% at the offshore and onshore stations respectively (shown in appendix 2).

7.7 *N*-sided ring (n=4)

In each feeder the *n*-sided ring design, where *n*=4 in the simulations in this thesis, nine wind turbines are connected in series, and four feeders are connected in parallel to provide redundancy. The wind turbines are rated at 5MW, with a power factor limit of 0.95. The wind turbines are operating at 0.69kV. Each wind turbine is equipped with a 0.69/33kV transformer, rated at 5.26 MVA. The cable ratings are 65.5 MVA throughout the loop, operating at 33 kV. The maximum rated voltage of the cable is 36 kV, or 1.091 pu. Thus, all voltage levels lower than 1.091 pu are considered acceptable in the offshore grid. A value of 0.9 pu is used as the minimum acceptable voltage level.

7.7.1 AC/AC

Figure 58 shows the n-sided ring design during *normal operating conditions*. Due to the redundancy provided by the high cable rating (see equation 3-6), no cables are rated higher than 67%.The most heavily loaded devices are the wind turbines and the wind turbine transformers, which are rated at 96%. All voltage levels are within their boundaries.

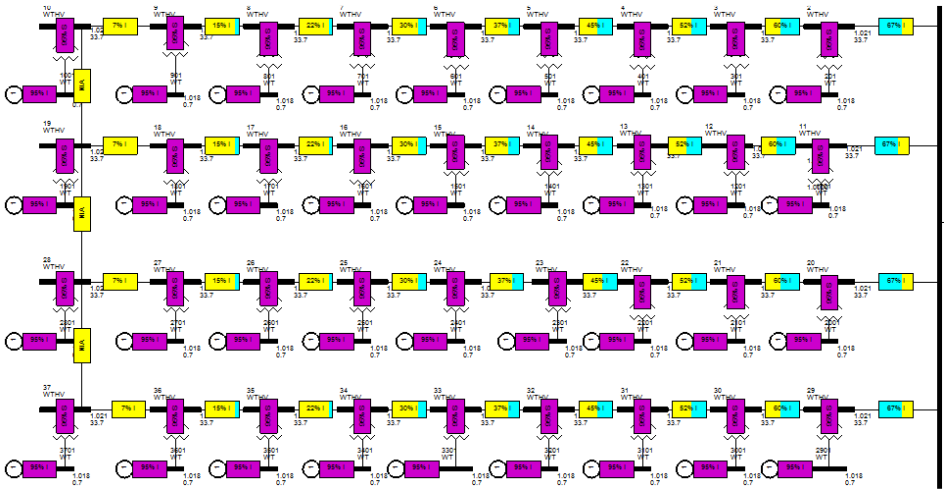

Figure 58 - N-sided ring, normal operating conditions

The active power delivered to the grid is 527.4 MW, giving total losses of 2.33%. The most heavily loaded elements of the system are the transmission cables, rated at 100%.

Figure 59 shows the *n*-sided ring during *worst case operating conditions*. In this situation, a fault occurs at one of the outermost feeders. This means that the direction of the power flow is reversed through the feeder. The most heavily loaded cable is the one closest to the outermost feeder. The most heavily loaded devices of the feeders are still the wind turbines and the wind turbine transformers, at 95%. All voltage levels are within their boundaries.

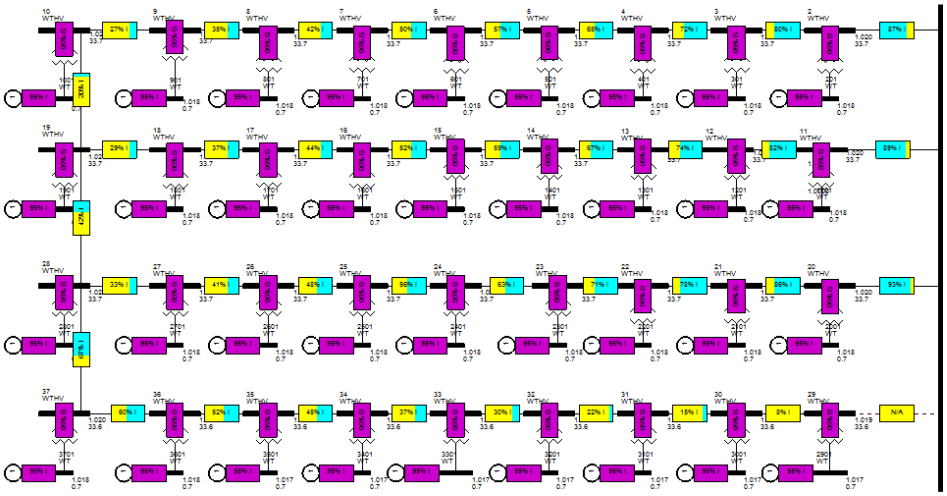

Figure 59 - N-sided ring, worst case operating conditions

The active power delivered to the grid is 527.1 MW, giving total losses of 2.39%. The most heavily loaded elements of the system are the transmission cables, rated at 100%. The SVC must consume 0.1 MVAr in order to provide unity power factor in the PCC.

7.7.2 AC/DC

Figure 60 shows the *n*-sided ring design during *normal operating conditions*. Due to the redundancy provided by the high cable rating (see equation 3-6), no cables are rated higher than 68%.The most heavily

loaded devices are the wind turbines and the wind turbine transformers, which are rated at 96%. All voltage levels are within their boundaries.

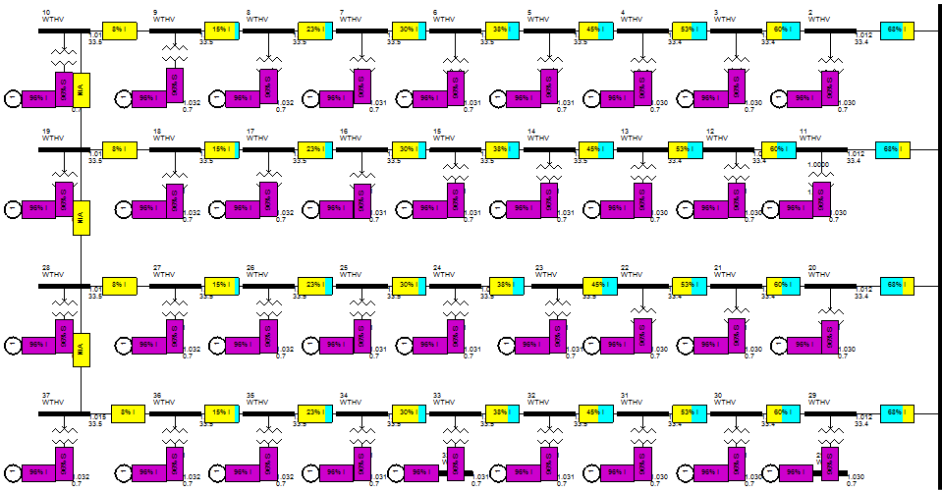

Figure 60 - N-sided ring, normal operating conditions

The active power delivered to the grid is 505.4 MW, corresponding to 6.41% losses when comparing to the nominal power output. The most heavily loaded elements of the system are the wind turbines and the wind turbine transformers. The generators representing the HVDC Light connection are running at 48% and 46% at the offshore and onshore stations respectively (shown in appendix 2).

Figure 61 shows the n-sided ring during *worst case operating conditions*. In this situation, a fault occurs at one of the outer feeders of the *n* feeders that are connected in parallel. This means that the direction of the power flow is reversed through the feeder. The most heavily loaded cable is the one connecting the first wind turbine of the feeder closest to the fault to the offshore substation. This is running at 93% of its full capacity.The most heavily loaded devices of the feeders are still the wind turbines and the wind turbine transformers, at 96%. All voltage levels are within their boundaries.

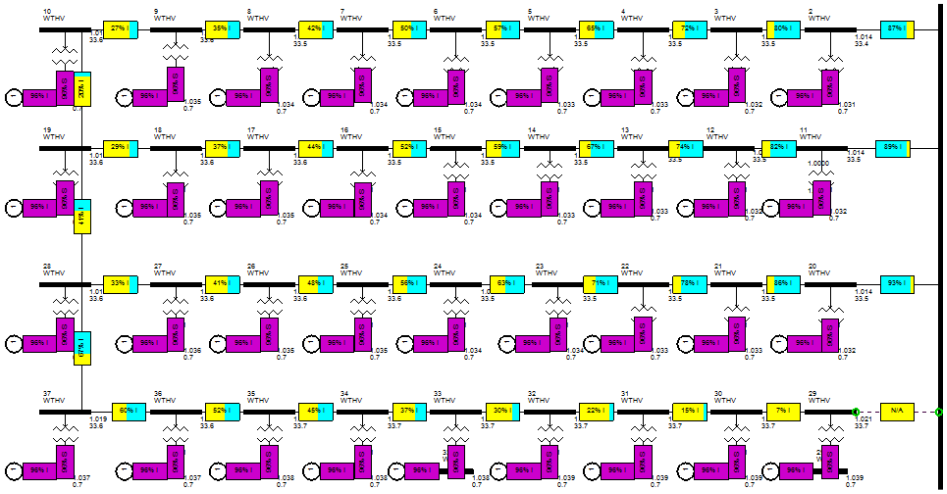

Figure 61 - N-sided ring, worst case operating conditions

The active power delivered to the grid is 504.7 MW, corresponding to 6.54% losses when comparing to the nominal power output. The most heavily loaded elements of the system are the wind turbines and the wind turbine transformers. The generators representing the HVDC Light connection are running at 48% and 46% at the offshore and onshore stations respectively (shown in appendix 2).

7.8 Star design

In the star design, nine wind turbines are connected in a star to the same connection point. From this point, the power is transmitted in a common cable to the offshore substation. The wind turbines are rated at 5MW, with a power factor limit of 0.95. The wind turbines are operating at 0.69kV. Each wind turbine is equipped with a 0.69/11kV transformer, rated at 5.26 MVA. The cable ratings are 5.5 MVA, operating at 11 kV. The maximum rated voltage of the cable is 12 kV, or 1.091 pu. Thus, all voltage levels lower than 1.091 pu are considered acceptable in the star. From the centre bus, the voltage is transformed from 11kV to 33kV. The cable rating of the cable between the centre bus of the star and the offshore substation is 48.6 MVA, rated at 33 kV. The maximum rated voltage of the cable is 36 kV, or 1.091 pu. Thus, for the transmission from the star to the offshore substation, a voltage level lower than 1.091 pu are considered acceptable in the offshore grid. A value of 0.9 pu is used as the minimum acceptable voltage level.

7.8.1 AC/AC

Figure 62 shows the star design during *normal operating conditions*. The 11 kV cables are loaded at 90% and the 33 kV cable is loaded at 95%. The most heavily loaded devices in the system are the wind turbines and the33 kV cable connecting the star and the substation, being loaded at 95%. All voltage levels are within their boundaries.

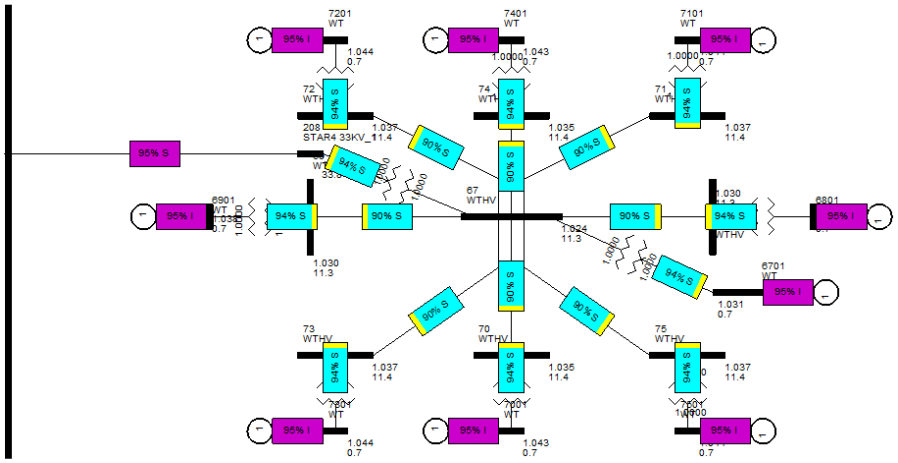

Figure 62 - Star design, normal operating conditions

The active power delivered to the grid is 517.5 MW, giving total losses of 4.17%. The most heavily loaded elements of the system are the transmission cables, rated at 100%.

Figure 63 shows the load flow result during *worst case operating conditions*, that is, when one star is out of service. The only difference in the running conditions is that the star draws slightly more reactive power. Except from that, the devices are running at the same load levels as earlier. All voltage levels are within their boundaries.

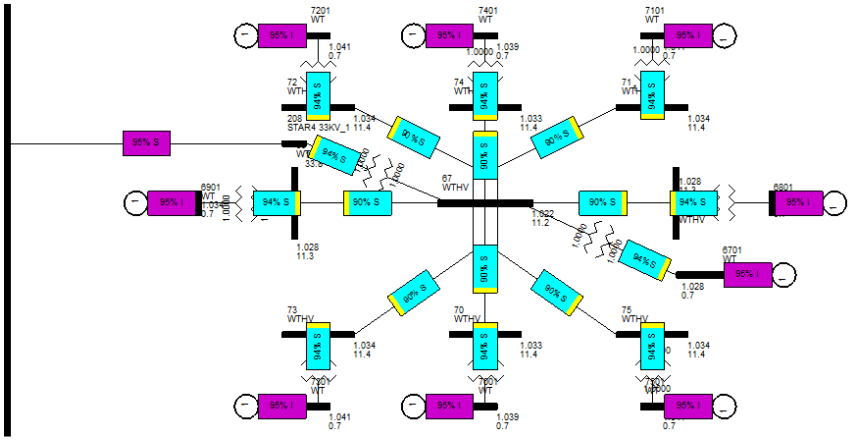

Figure 63 - Star design, worst case operating conditions

The active power delivered to the grid is 474.4 MW, giving total losses of 12.15% when comparing to the nominal power output. The most heavily loaded elements of the system are the transmission cables, rated at 100%. The SVC must consume 6.1 MVAr in order to provide unity power factor in the PCC.

7.8.2 AC/DC

Figure 64 shows the star design during *normal operating conditions*. The 11 kV cables are loaded at 93% and the 33kV connection to the offshore substation is running at 95%. The most heavily loaded devices in the system are the wind turbines and the wind turbine transformers, running at 99%. All voltage levels are within their boundaries.

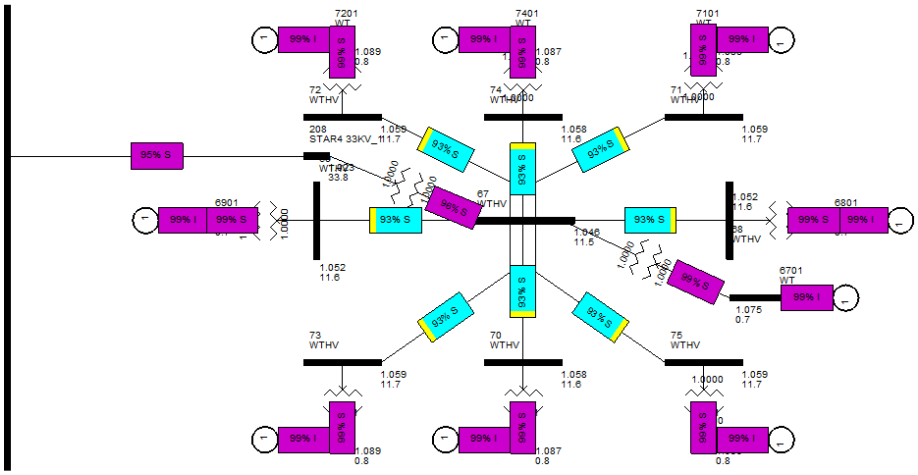

Figure 64 - Star design, normal operating conditions

The active power delivered to the grid is 495.8 MW, corresponding to 8.79% losses when comparing to the nominal power output. The most heavily loaded elements of the system are the wind turbines and the wind turbine transformers. The generators representing the HVDC Light connection are running at 48% and 46% at the offshore and onshore stations respectively (shown in appendix 2).

Figure 65 shows the load flow result during *worst case operating conditions*, that is, when one star is out of service. The 11kV cables now run at 92%, and the wind turbine transformers are running at 98%. The

most heavily loaded elements of the star are still the wind turbines, running at 99%. All voltage levels are within their boundaries.

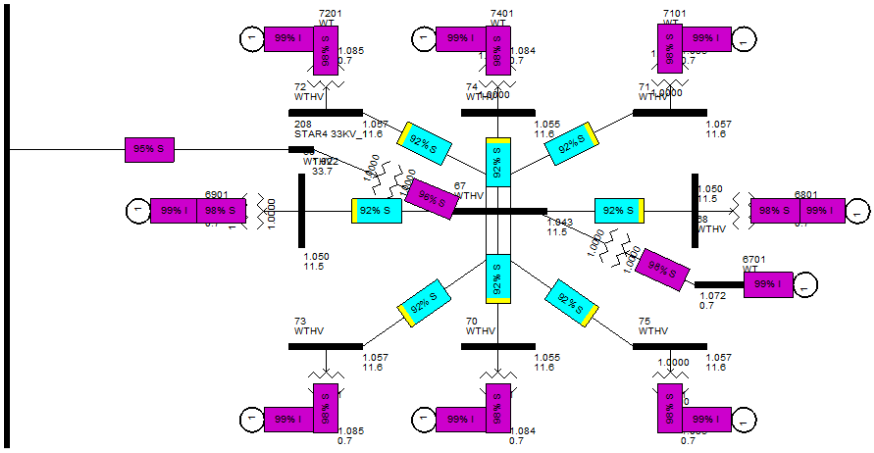

Figure 65 - Star design, DC transmission, worst case operating conditions

The active power delivered to the grid is 453.8 MW, corresponding to 15.96% losses when comparing to the nominal power output. The most heavily loaded elements of the system are the wind turbines. The generators representing the HVDC Light connection are running at 44% and 42% at the offshore and onshore stations respectively (shown in appendix 2).

8 Dynamic simulations

This chapter describes the dynamic simulations that have been executed as a part of the work with this thesis. In chapter 3.5, six options for the design of the offshore grid were presented. In this chapter, their dynamic behavior is studied and compared. In addition, the impact of the choice of transmission technology from the wind farm to the PCC is studied. Three fault scenarios are presented. This means that a total of 36 dynamic simulations are executed. For all wind farm layouts, the active power P, the reactive power Q, the generator speed ω and the voltage U are plotted at selected generator buses. It has been chosen to study the rotor speed instead of the rotor angle, since the DFIG can control the rotor angle in the partial scale frequency controller. (see Figure 5) Only the most relevant plots are reproduced in this chapter, but all plots can be found in appendix 5.

All dynamic simulations are based on the "normal operating conditions"-load flow situation, as described in chapter 7. For all three fault scenarios, the fault applied to the system is a three phase short circuit to ground, lasting 150 ms before the circuit breakers on the faulted cable open, and the cable is disconnected.

When comparing the wind farm layouts, two main factors are studied; how the grid design influences the dynamic behavior, and how the transmission choice influences the dynamic behavior. This is done by studying the rotor speed stability and voltage stability in the system. The maximum oscillation and time it takes for the rotor speed to stabilize is studied, as is the voltage response in terms of maximum voltage dip and the maximum overvoltage preceding a fault. As the initial rotor speed of all the wind turbines of all the systems are similar, at 0.2 pu, the oscillations are studied by looking at the per unit values of the deviation from the initial value.

The voltage level is case specific and also varies from turbine to turbine. In order to compare the voltage dips, the value has been calculated as percentage of the original voltage level at the bus in question. The original voltage level values are gathered from the" normal operating conditions"-load flow cases.

8.1 Fault scenario one

In fault scenario one, a fault is applied to one of the two transmission lines between the offshore wind farm and the PCC, as illustrated in Figure 66:

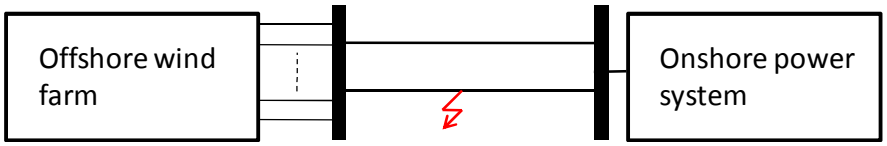

Figure 66 - Fault scenario one

This scenario is studied to investigate two issues:

1) How does the offshore wind farm layout influence the dynamic behavior following a transmission fault?
2) How does the transmission choice influence the dynamic behavior of the wind turbines following a transmission fault?

A fault in the transmission system will have the largest impact on the generators closest to the fault, i.e. the wind turbine generators situated at the buses that lie the closest to the offshore substation. Therefore, only the dynamic behavior of the generator at one of these buses is studied. Figure 67 shows this plot for the radial design. For the five other designs, the dynamic behavior is similar. Thus, their dynamic response is not shown here, but can be seen in appendix 5.

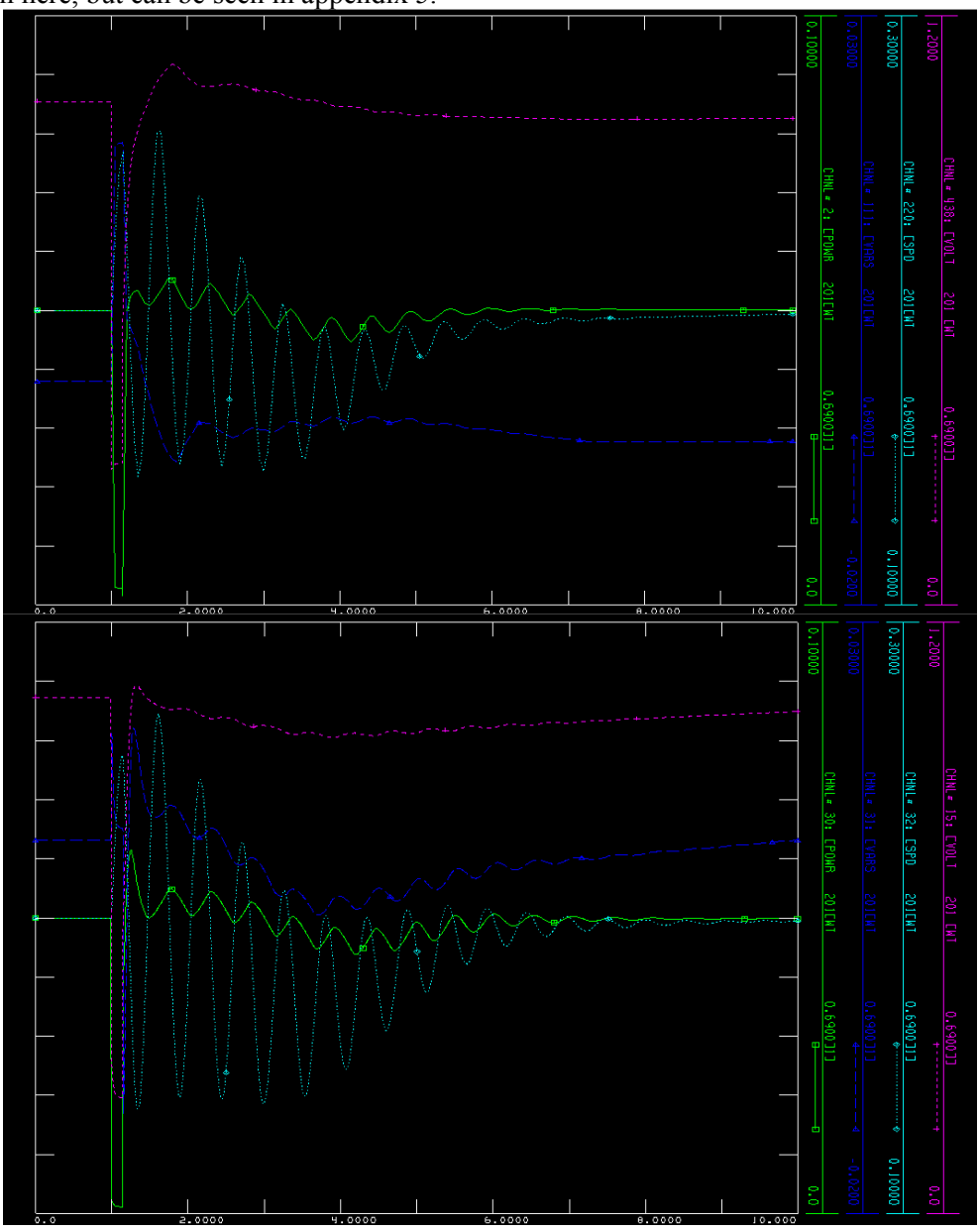

Figure 67 – Fault scenario one. Radial design. P (green), Q (blue), ω (light blue) and U (purple) of the wind turbine generator closest to the substation. Top: AC/AC Bottom: AC/DC.

The dynamic response is clearly stable, with the oscillations being fully damped at approximately seven seconds for the AC/AC system and eight seconds for the AC/DC system. The minimum and maximum deviations of the twelve designs are compared below:

For fault scenario one, Figure 68 shows the maximum and minimum deviation of the generator speed ω and voltage level U at the bus closest to the offshore substation for all 12 designs.

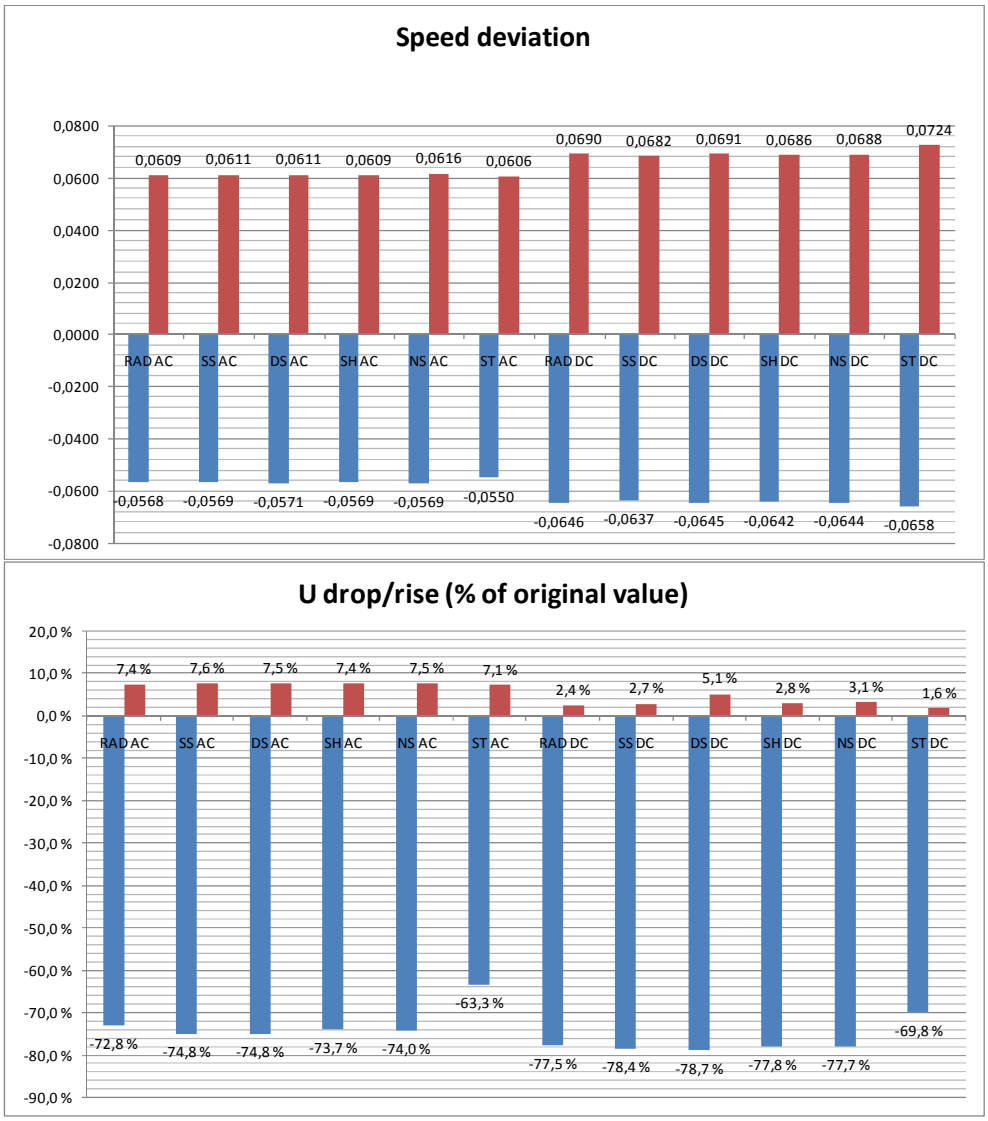

Figure 68 - Fault scenario one. Maximum speed deviation [pu on system base] and voltage deviation [% of initial value]) of the wind turbine generator closest to the substation.

ω:
The choice of offshore grid does not have a large impact on the maximum and minimum speed deviation. Only small differences are observable.
The impact of the choice of transmission system is clearly of importance. For all designs, the speed deviation is clearly and consequently higher for the AC/DC systems than for the AC/AC systems.

U:
The star design separates clearly from the other designs. The voltage drop is lower than for the rest of the designs, and the maximum voltage is also smaller. The other designs show small variations in the voltage deviation.
The impact of the choice of transmission system is clearly of importance. For all designs, the voltage drop is larger for DC transmission than for AC transmission. Nevertheless, the maximum values of the voltages are clearly and consequently smaller for the AC/DC systems than the AC/AC systems.

8.2 Fault scenario two

In fault scenario two, a fault is applied to the cable connecting the innermost turbine of one of the feeders to the offshore substation. For the radial and star design, this means that the entire feeder is lost as a consequence of this fault, since no redundancy is provided. This is illustrated in Figure 69:

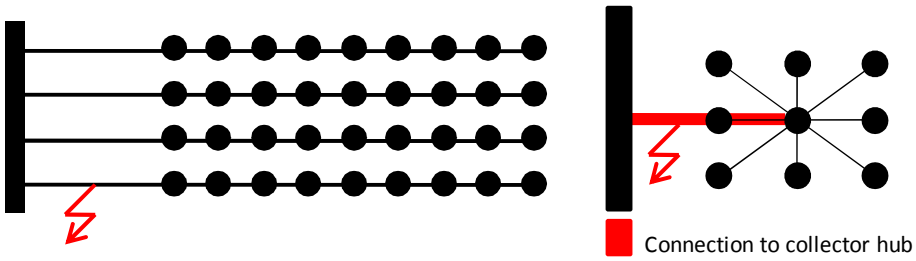

Figure 69 - Fault scenario two

For fault scenario two, the dynamic response at two buses is plotted. The scope is to investigate how a fault of type two affects:

1) The buses in the same feeder as the one subject to the fault
2) The buses in the rest of the offshore wind farm.

The first bus to be studied is the bus the closest to the fault, i.e. the innermost bus of the feeder, when seen from the offshore substation. For the radial and star design, when the feeder is disconnected it is isolated from the rest of the network, and the dynamic behavior in the isolated feeder is unstable. For the redundant designs, this problem is avoided. This is illustrated in Figure 70 and Figure 71:

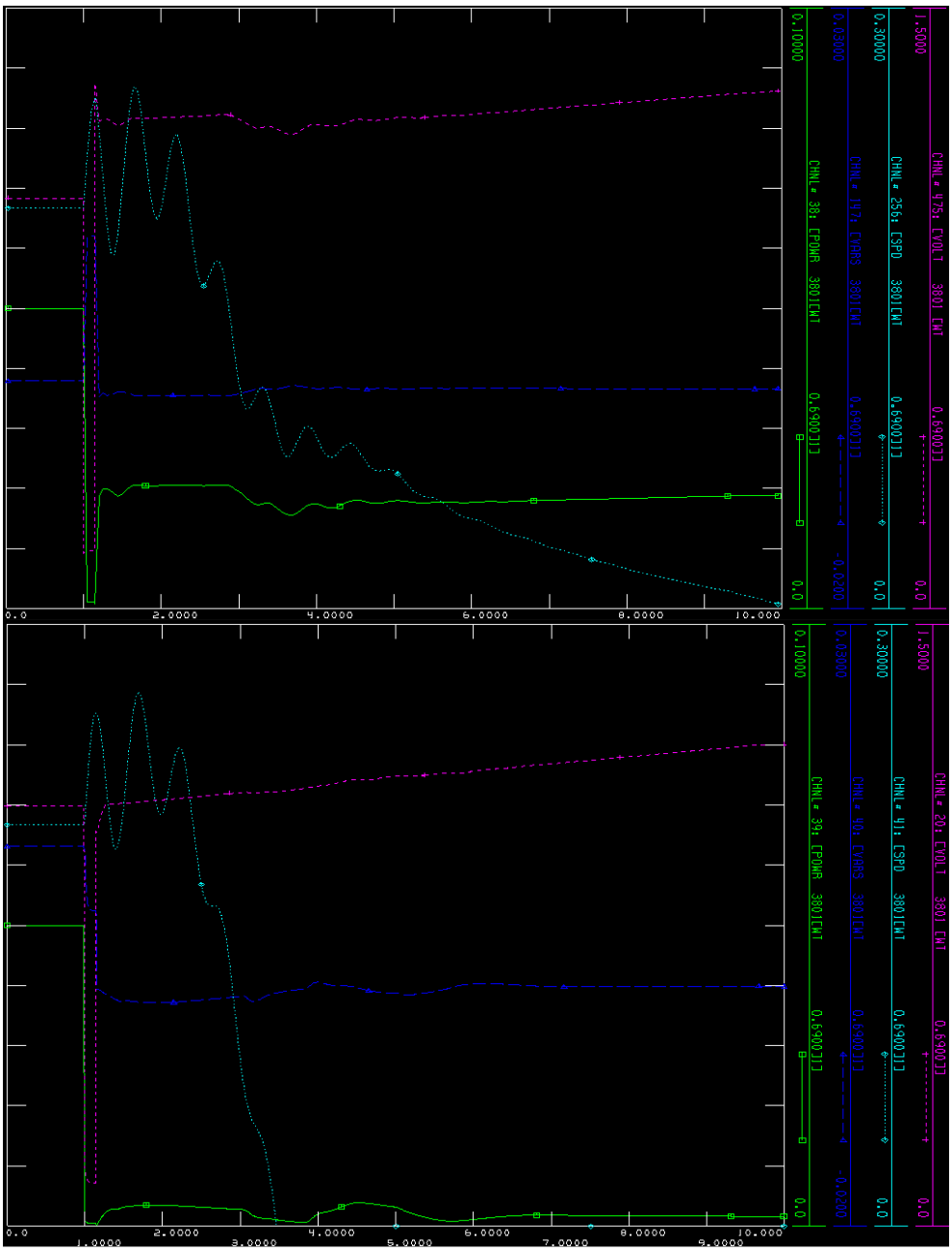

Figure 70 – Fault scenario two. Radial design. P (green), Q (blue), ω (light blue) and U (purple) of the wind turbine generator closest to the substation in the same feeder as the fault occurs. Top: AC/AC Bottom: AC/DC.

The rotor speed does not return to its original value and there is a drop in the active and reactive power. The instability occurs faster for the AC/DC system than for the AC/AC system. The voltage increases throughout the first ten seconds after the fault. For the redundant designs, these post-fault problems are avoided. Figure 71 shows the dynamic behavior of the wind turbine generator closest to the substation in the feeder that is isolated when the shared ring concept is applied to the offshore grid:

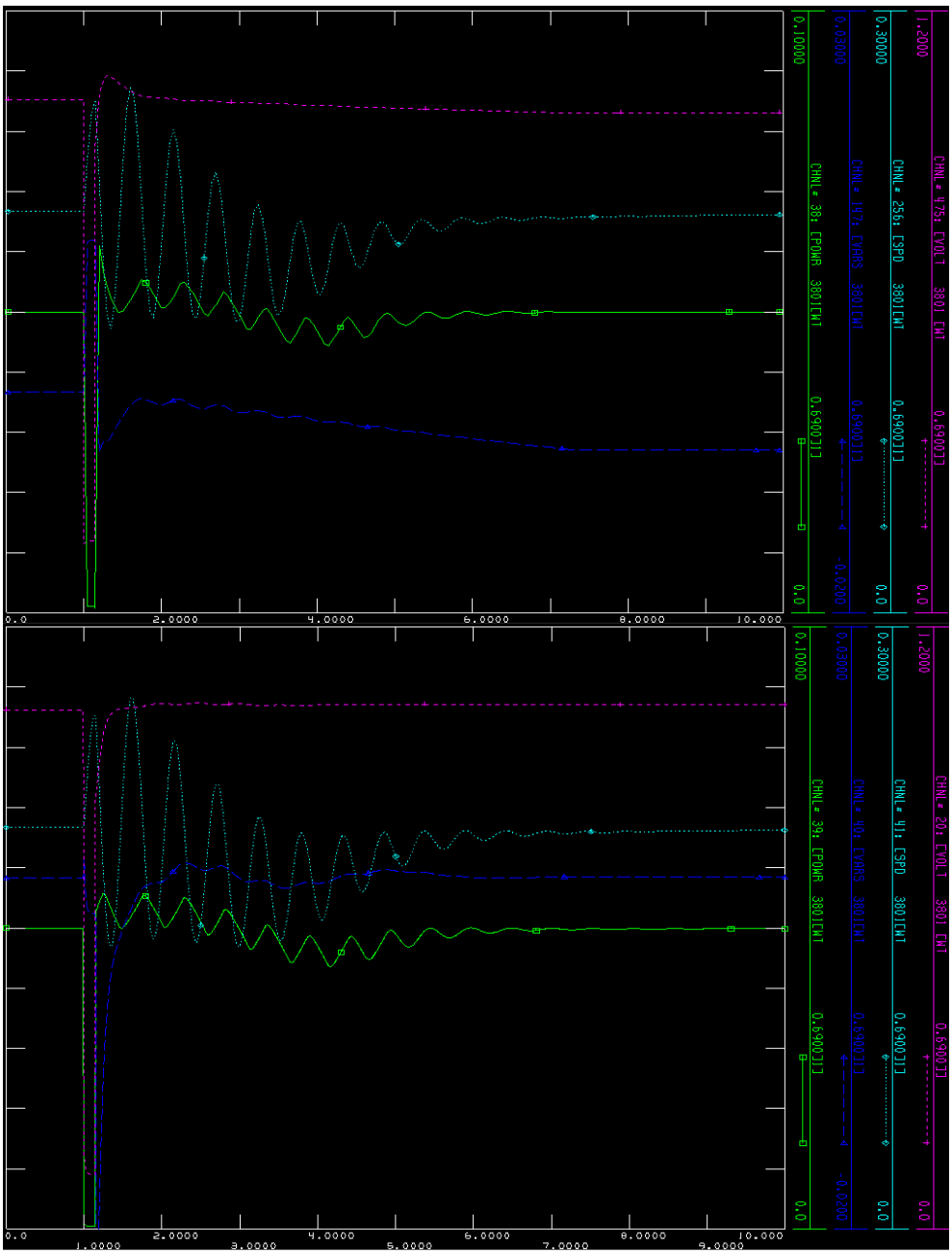

Figure 71 – Fault scenario two. Shared ring design. P (green), Q (blue), ω (light blue) and U (purple) of the wind turbine generator closest to the substation when the fault occurs in the same feeder. Top: AC/AC Bottom: AC/DC.

The figure shows that all values return to their original values after approximately seven seconds. The dynamic behavior of the different wind farm layout options are compared in Figure 72:

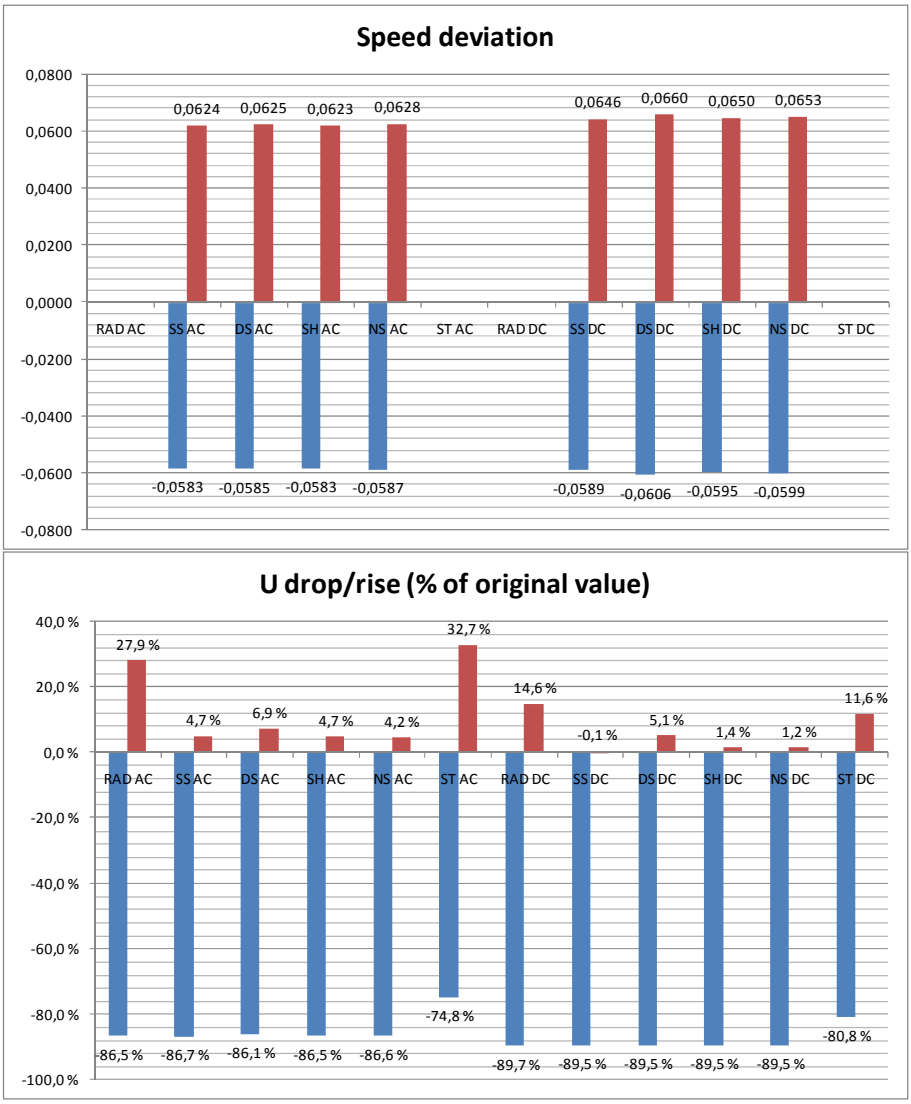

Figure 72 –Fault scenario two. Maximum speed deviation [pu on system base] and voltage deviation [% of initial value]) of the wind turbine generator closest to the substation when the fault occurs in the same feeder as the generator is placed.

ω:
The choice of offshore electrical collector does not affect the maximum and minimum speed deviation considerably. The speed deviation at the radial and star design is not considered, as the speed is clearly unstable at these buses.
The impact of the choice of transmission system is of importance even though the differences are quite small, the AC/DC system consequently gives higher speed deviations than the AC/AC system.

U:
There is no big difference in the voltage drop at the layouts that does not lead to unstable post-fault operation. The maximum voltage is clearly highest at the two buses where unstable operation is obtained after the fault. The star design gives the lowest voltage drop, but clearly the highest voltage rise for the AC/AC system. For the AC/DC system, the radial design gives the highest voltage rise, while the star

design still gives the smallest drop. For all cases, the AC/DC system gives larger drops and smaller maximum values than for the AC/AC systems.

The second bus to be studied is the first bus of one of the feeders in the wind farm that was not subject to the fault. The response of the bus that is directly connected to the offshore substation is shown in Figure 73:

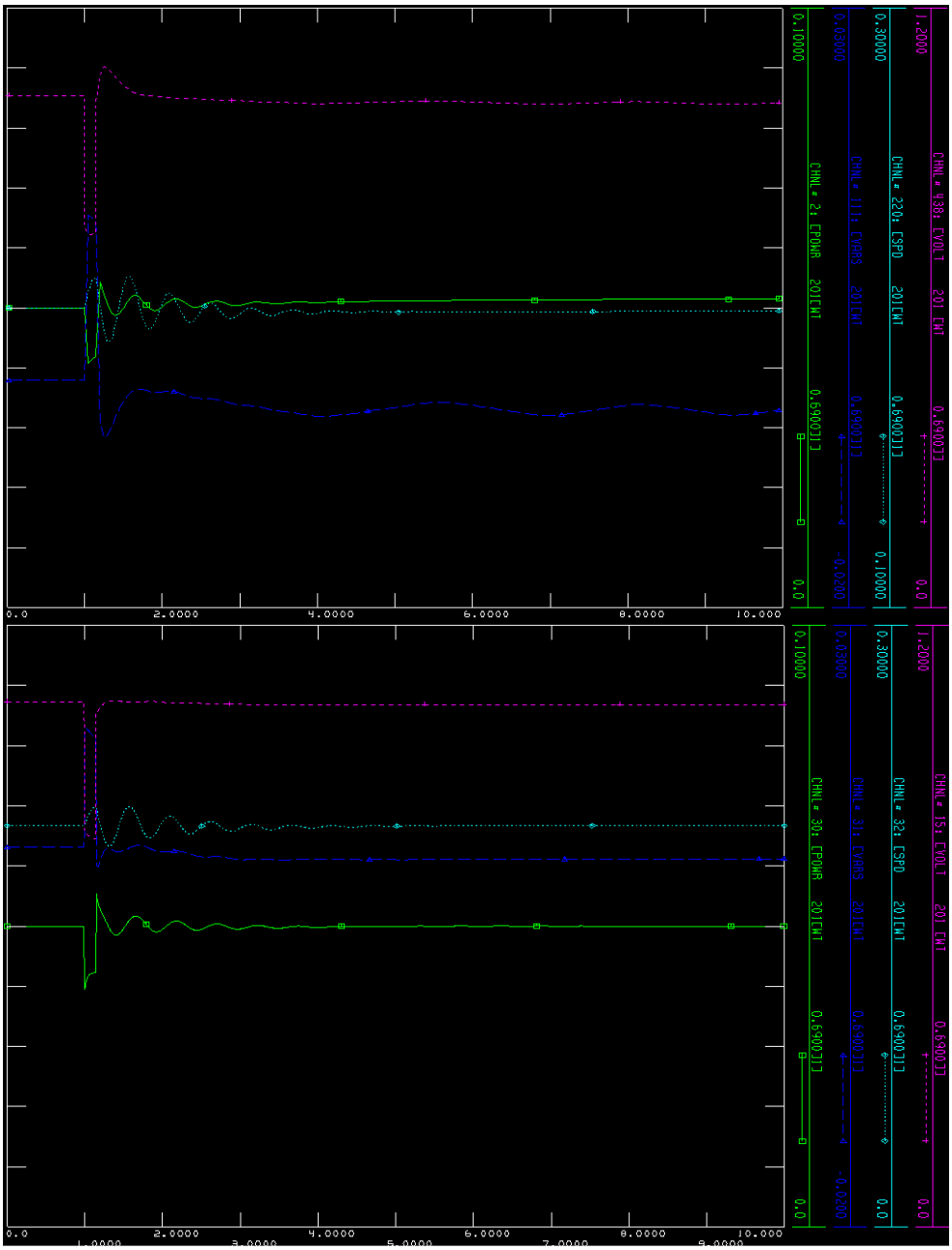

Figure 73 – Fault scenario two. Radial design. P (green), Q (blue), ω (light blue) and U (purple) of the wind turbine generator closest to the substation when the fault occurs in one of the other feeders. Top: AC/AC Bottom: AC/DC.

All dynamic responses are clearly stable. It takes approximately five seconds for the oscillations to be fully damped. The voltage drop and reactive power rise are relatively small.

The minimum and maximum deviations of the twelve designs at the relevant buses are compared below:

For fault scenario two, Figure 74 shows the maximum and minimum deviation of the generator speed ω and voltage level U at the bus closest to the offshore substation in one of the other feeders for all 12 designs:

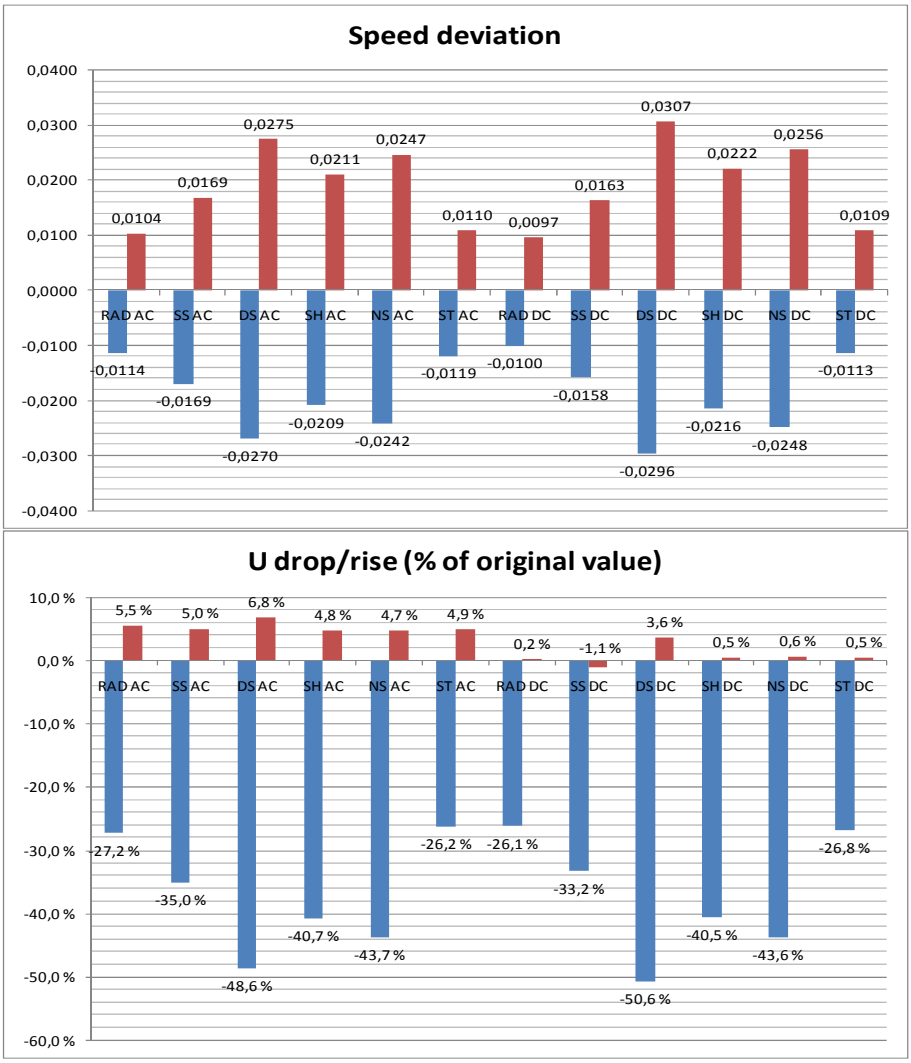

Figure 74 –Maximum speed deviation [pu on system base] and voltage deviation [% of initial value]) of the wind turbine generator closest to the substation following fault 2 when the fault occurs in a different feeder than where the generator is placed.

ω:
The choice of offshore electrical collector clearly influences the maximum and minimum speed deviation. The radial design gives the smallest deviations, with the star design as number two, giving slightly higher oscillations. The rest of the order is as follows: Single sided, shared, *n*-sided, double sided.

The impact of the choice of transmission system is also clearly of importance. For the star and radial design, the oscillations are smaller for the AC/DC system than for the AC/AC system. For the rest of the systems, the AC/DC system gives larger oscillations than for the AC/AC system

U:
The star and radial designs clearly stand out as the ones giving the smallest voltage drops. Using AC transmission, the star design gives the smallest voltage deviations, while the radial design gives the smallest deviations when using DC transmission. The double sided design clearly gives the largest drop in the voltage.
The impact of the choice of transmission system varies when it comes to the voltage drops, but all AC/DC layouts consequently give smaller maximum values of the voltage.

8.3 Fault scenario three

In fault scenario three, a fault is applied in the outermost cable of the feeder. For the radial and looped designs, this means that the fault occurs between the eighth and ninth turbine. For the star design, the fault occurs between the centre bus and one of buses at the end of one of the "arms" of the star. This is illustrated in Figure 75:

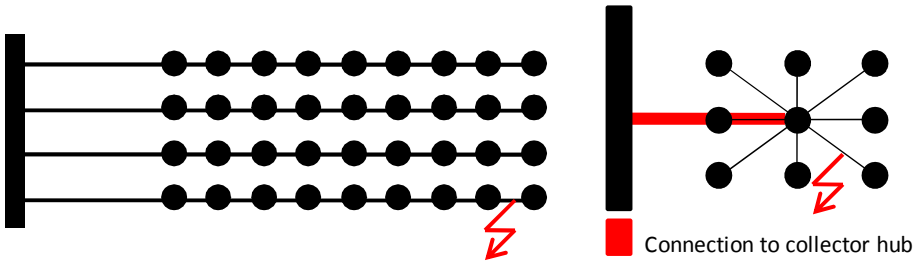

Figure 75 - Fault scenario three

For fault scenario three, the dynamic response at three buses is plotted. The scope is to investigate how a fault of type two affects the following buses:

1) The bus next to the fault that is further away from the offshore substation than the fault (the bus right of the fault in the left drawing, and the lower right bus of the right drawing, of Figure 75).
2) The bus next to the fault that is closer to the substation than the fault (the bus left of the fault in the left drawing, and the central bus of the right drawing, of Figure 75)
3) The bus the closest to the offshore substation in the same feeder as the fault occurs.

As the right drawing of Figure 75 illustrates, for the star design, the buses described in point 2) and 3) is the same, i.e. the central bus of the star.

The dynamic response for the bus described in point 1) is shown for the radial design in Figure 76:

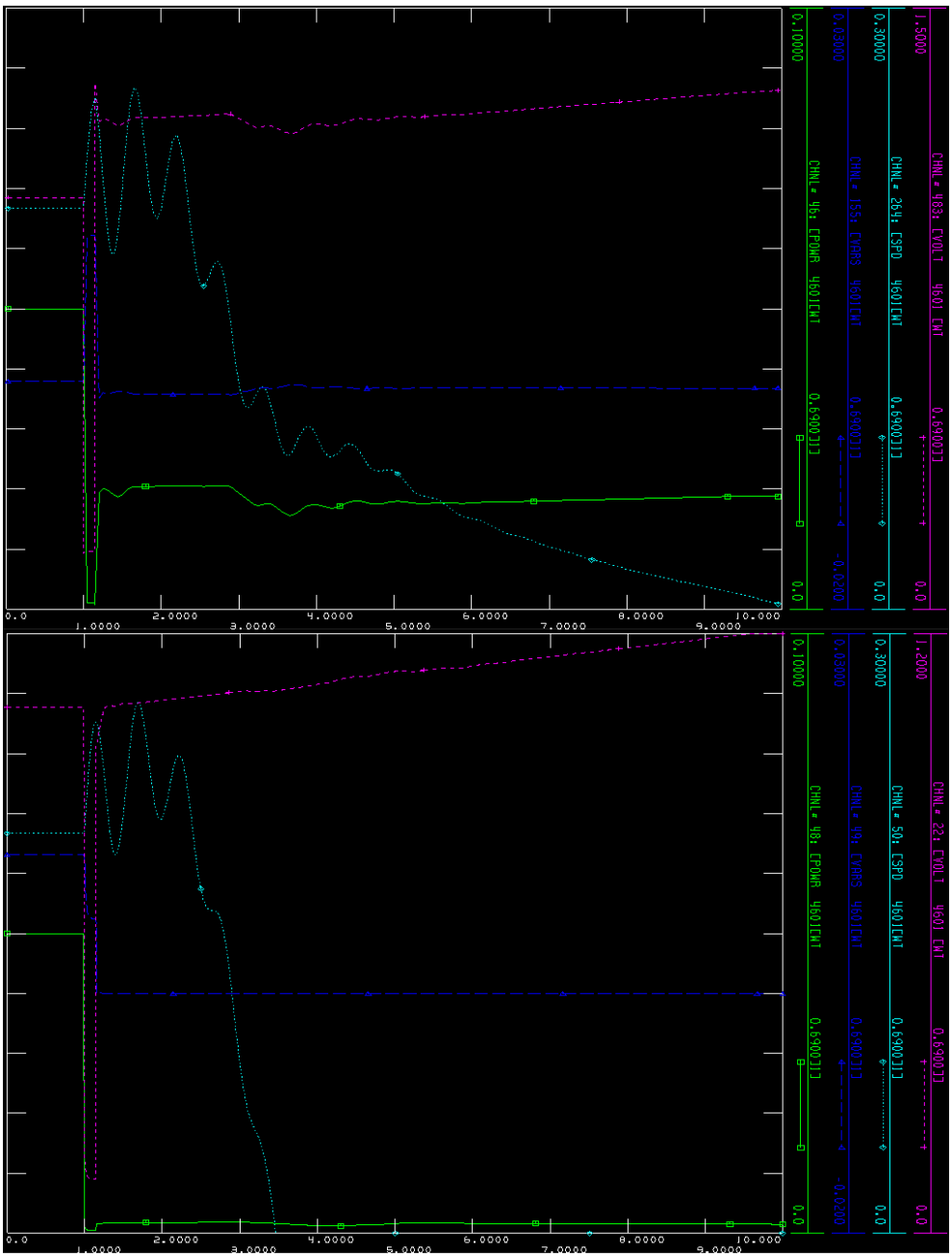

Figure 76 - Fault scenario three. Radial design. P (green), Q (blue), ω (light blue) and U (purple) of the wind turbine generator further away from the offshore substation than the fault point. Top: AC/AC Bottom: AC/DC.

The figures show that the response is clearly unstable. The instability occurs faster for the AC/DC system than for the AC/AC system. This instability is the case for the radial and star design. For the redundant designs, this problem is avoided. The dynamic response of the same bus is shown for the shared design below:

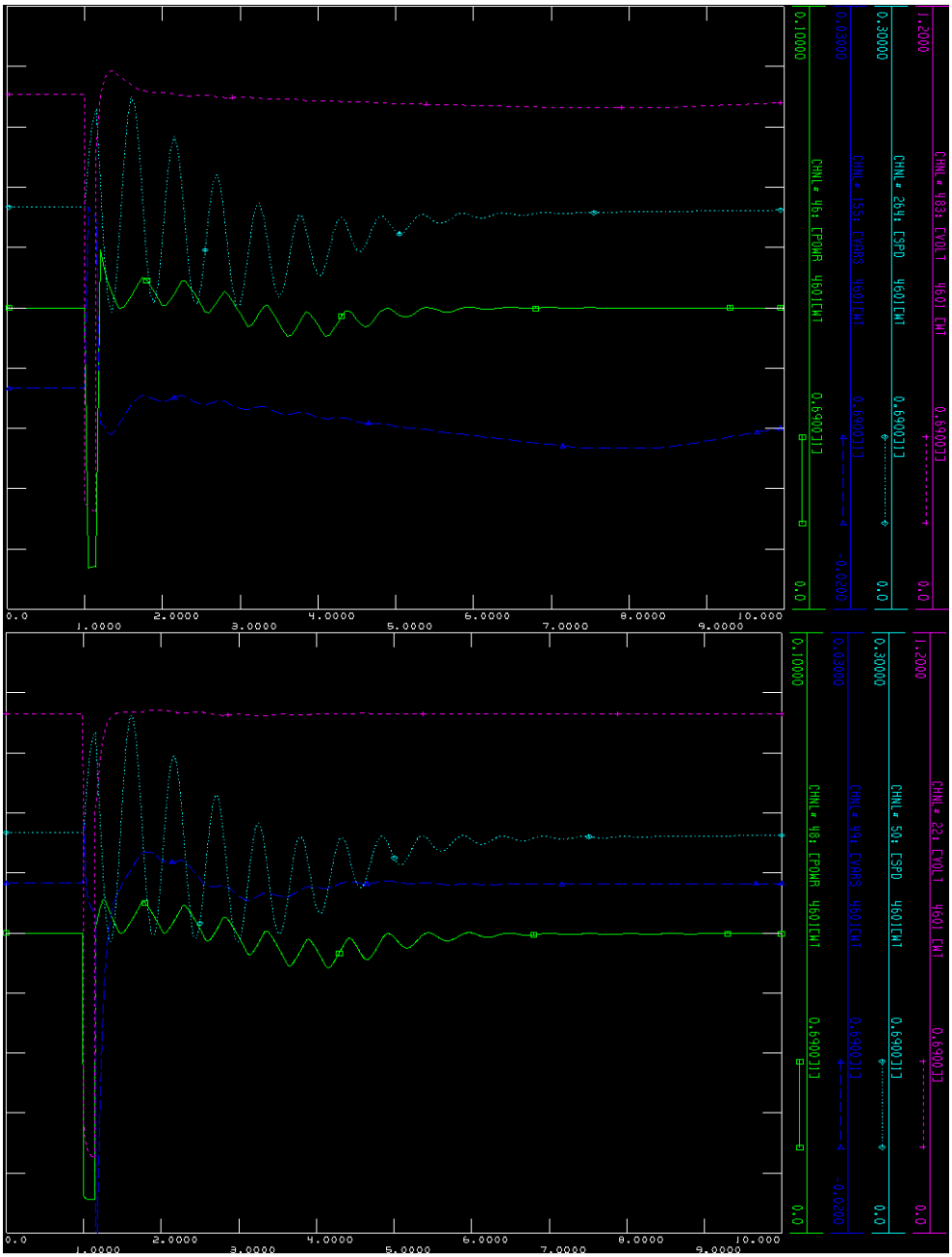

Figure 77 - Fault scenario three. Shared ring design. P (green), Q (blue), ω (light blue) and U (purple) of the wind turbine generator further away from the offshore substation than the fault point. Top: AC/AC Bottom: AC/DC.

The looped design of the shared ring provides stability after the fault. The oscillations are fully damped after approximately seven seconds. The impact of the wind farm layout on the dynamic response is shown in Figure 78:

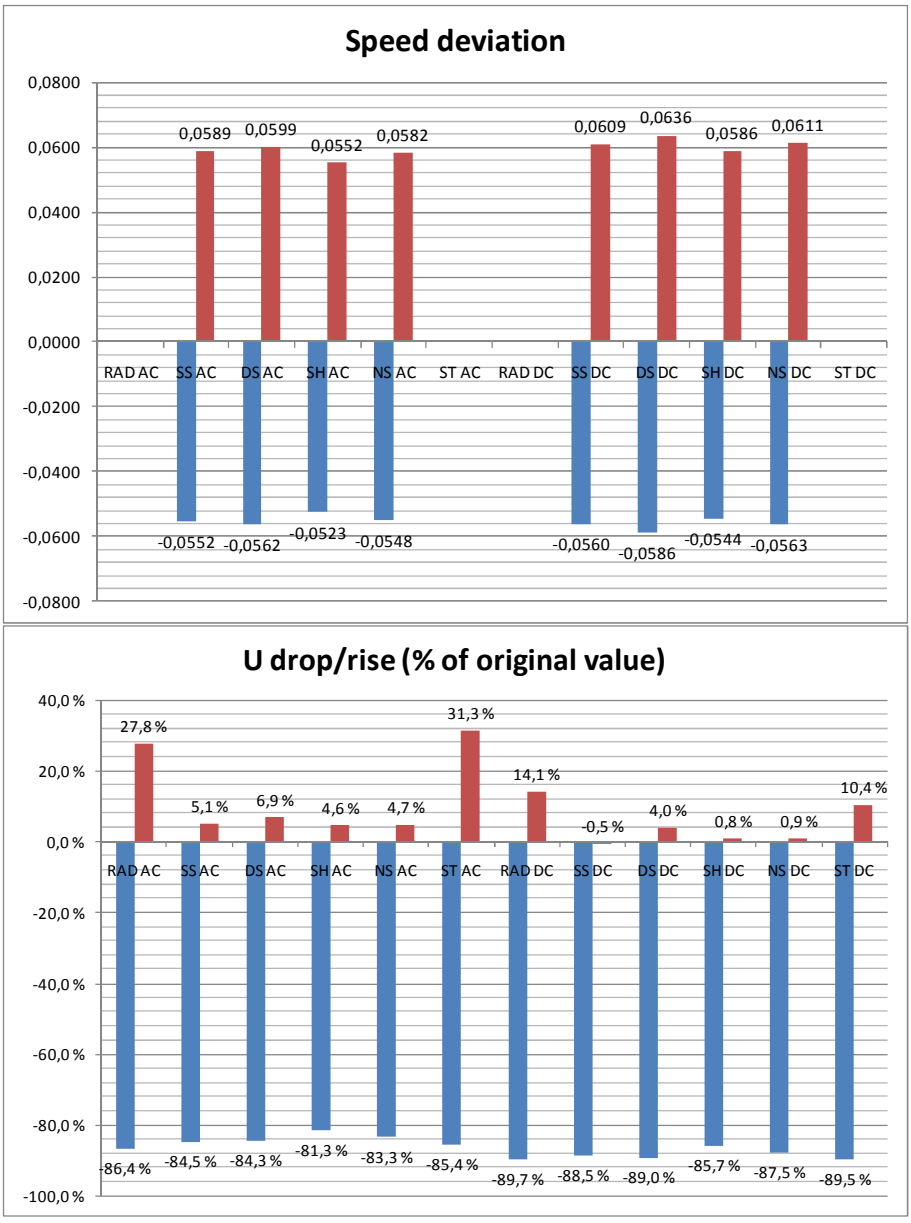

Figure 78 - Fault scenario three. Maximum speed deviation [pu on system base] and voltage deviation [% of initial value]) of the wind turbine generator furthest away from the substation when the fault occurs in the same feeder as the generator is placed.

ω:
The choice of offshore electrical collector affects the maximum and minimum speed deviation considerably. The smallest deviation is for the shared design, and the largest for the doubly sided design, both for the AC/AC systems and the AC/DC systems. The speed deviation at the radial and star design is not considered, as the speed is clearly unstable at these buses.
The impact of the choice of transmission system is of importance. The AC/DC systems consequently give higher speed deviations than the AC/AC system.

U:
There is a noticeable difference in the voltage drop at the layouts that does not lead to unstable post-fault operation. The smallest deviation is for the shared design, and the largest for the doubly sided design, both for the AC/AC systems and the AC/DC systems. The maximum voltage is clearly highest at the two buses where unstable operation is obtained after the fault. The star design gives the lowest voltage drop, but clearly the highest voltage rise for the AC/AC system. For the AC/DC system, the radial design gives the highest voltage rise, while the star design still gives the smallest drop. For all cases, the AC/DC system gives larger drops and smaller maximum values than for the AC/AC systems.

The dynamic response for the bus next to the fault, that is closer to the substation than the fault, is shown for the radial design in Figure 79:

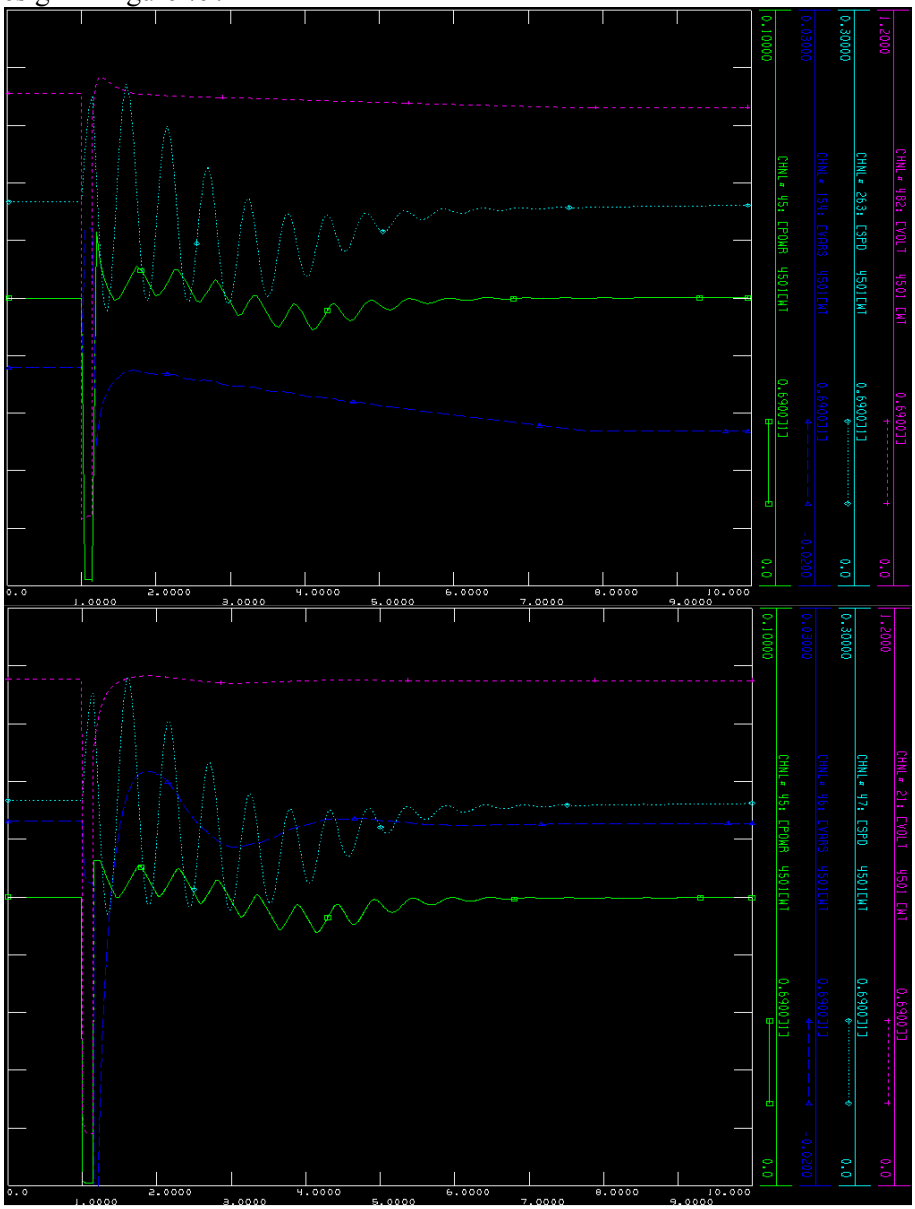

Figure 79 – Fault scenario three. Radial design. P (green), Q (blue), ω (light blue) and U (purple) of the wind turbine generator closer to the offshore substation than the fault point. Top: AC/AC Bottom: AC/DC.

The oscillations in Figure 79 are fully damped after approximately seven seconds, and the post fault response is clearly stable. For the AC/AC system, the reactive power is negatively increasing until it stabilizes at eight seconds. For the AC/DC design, it oscillates and stabilizes at the pre-fault value.

The dynamic response for the bus closest to the offshore substation, in the same feeder as the fault occurs, is shown for the radial design in Figure 80:

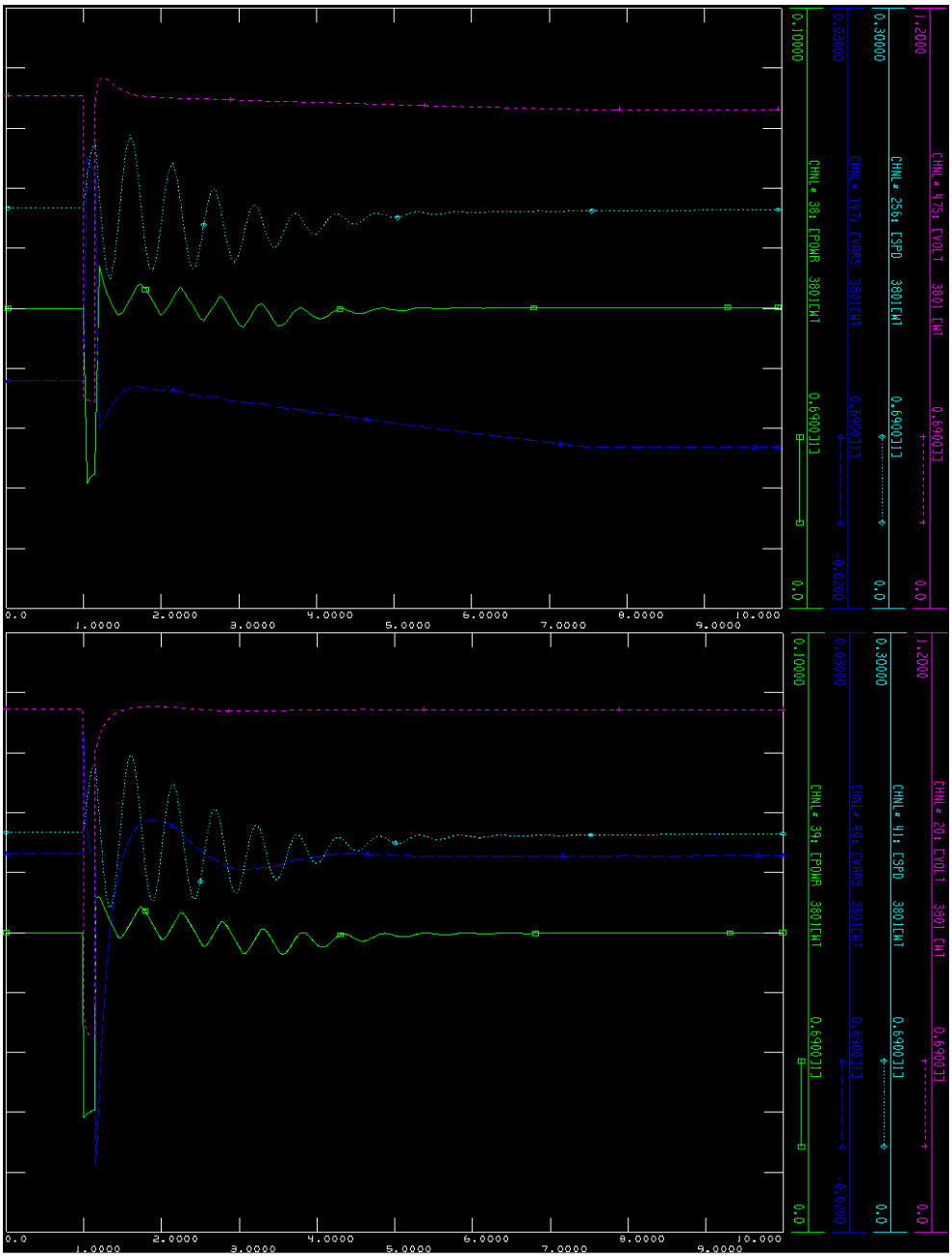

Figure 80 - Fault scenario three. Radial design. P (green), Q (blue), ω (light blue) and U (purple) of the wind turbine generator closest to the offshore substation. Top: AC/AC Bottom: AC/DC.

As expected, the oscillations are smaller, and the time it takes for the oscillations to be fully damped is smaller, approximately six seconds. The reactive power also reaches a stable operating point faster than for the wind turbine further out in the radial.

Finally, the dynamic response of the centre bus of the star design is shown in Figure 81:

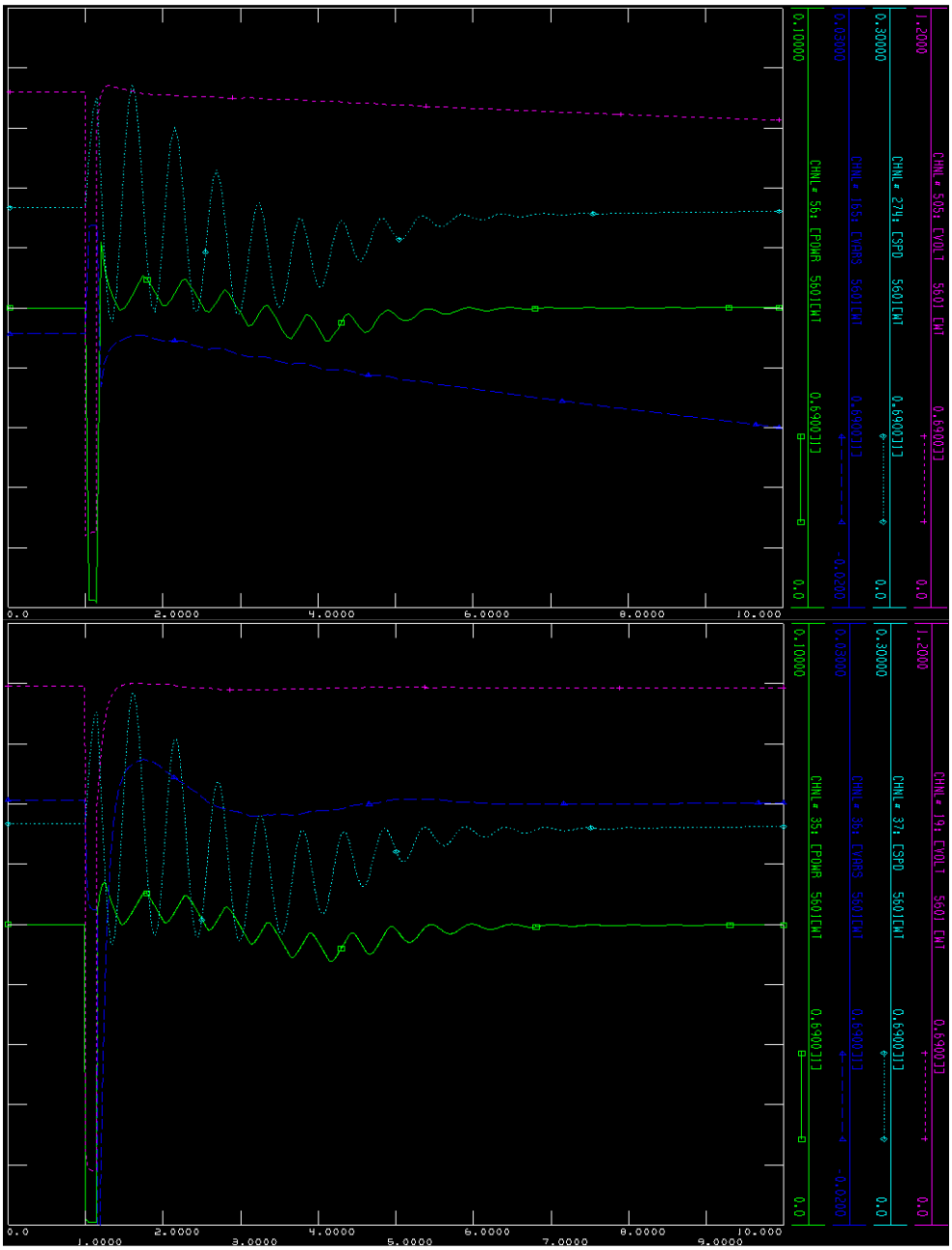

Figure 81 - Fault scenario three. Star design. P (green), Q (blue), ω (light blue) and U (purple) of the wind turbine generator at the central bus of the star. Top: AC/AC Bottom: AC/DC.

The oscillations are fully damped after approximately seven seconds, and the post fault response is clearly stable. For the AC/AC system, the reactive power is negatively increasing all the way up to ten seconds. For the AC/DC design, it oscillates and stabilizes at the pre-fault value.

The minimum and maximum deviations of the twelve designs at the relevant buses are compared below:
For fault scenario three, Figure 82 shows the maximum and minimum deviation of the generator speed ω and voltage level U at the bus next to the fault that is closer to the substation than the fault (the bus left of the fault in the left drawing, and the central bus of the right drawing, of Figure 75)

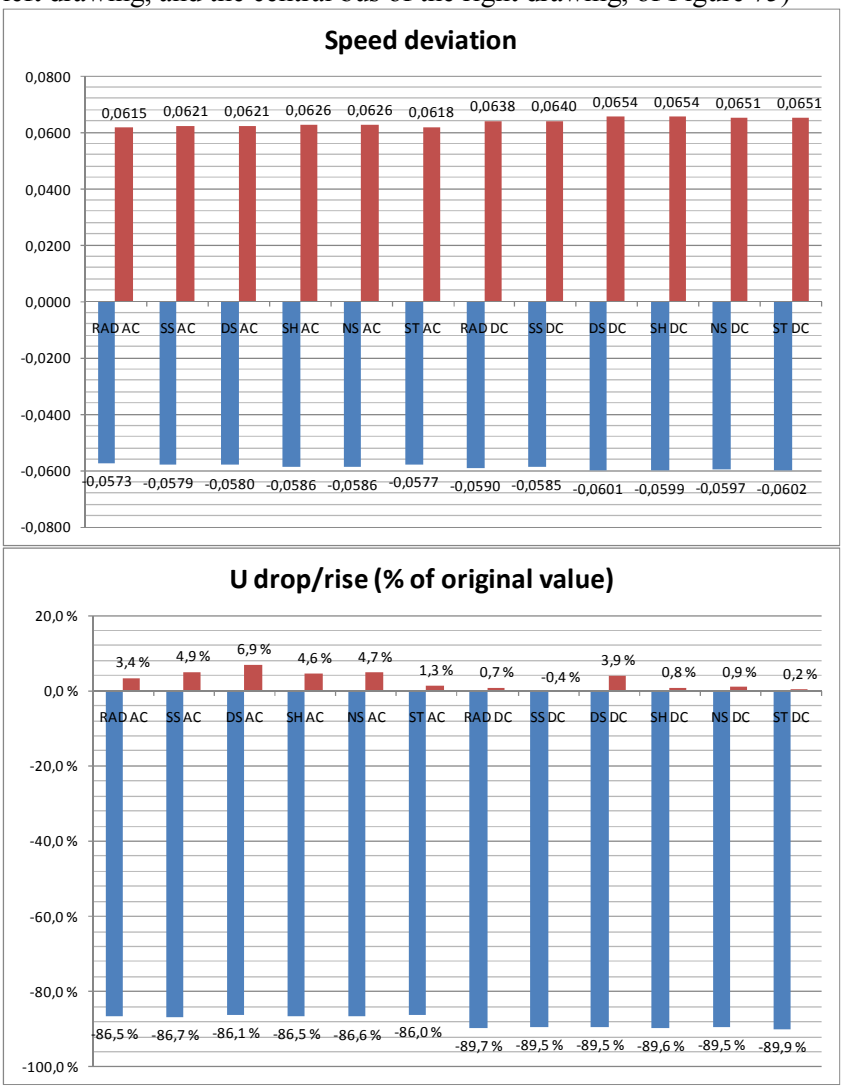

Figure 82 - Fault scenario three. Maximum speed deviation [pu on system base] and voltage deviation [% of initial value]) of the wind turbine generator bus next to the fault, that is closer to the substation than the fault.

ω:
The choice of offshore grid has a small impact on the speed deviations.
The impact of the choice of transmission system is of larger importance. For all designs, the speed deviation is higher for the AC/DC systems than for the AC/AC systems.

U:
The choice of offshore grid has a small impact on the voltage drops, but impacts the voltage rise. The double sided design has the highest rise in the voltage following the fault.
The impact of the choice of transmission system is of larger importance. For all designs, the voltage drop is larger for the AC/DC systems than for the AC/AC systems, while the maximum values of the voltage are clearly smaller.

For fault scenario three, Figure 83 shows the maximum and minimum deviation of the generator speed ω and voltage level U at the bus closest to the offshore substation in the same feeder as the one where the fault occurs for all 12 designs:

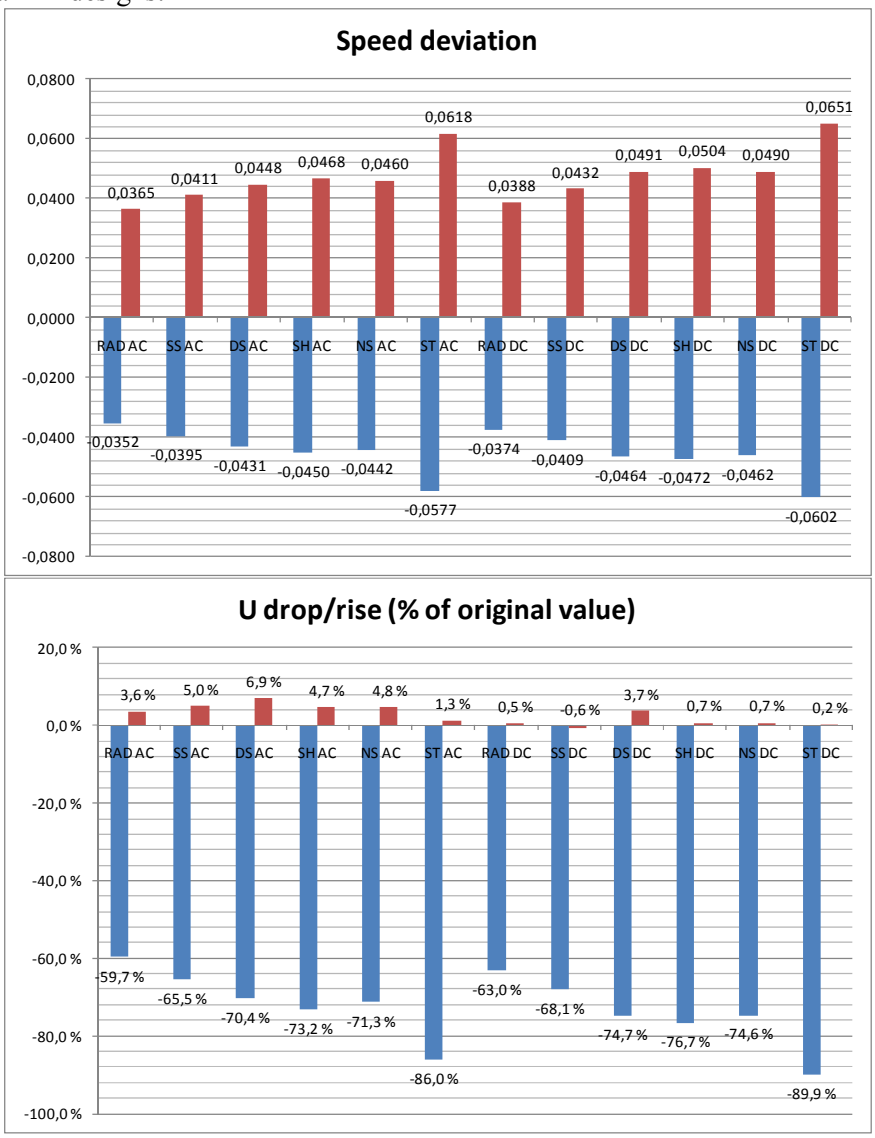

Figure 83 - Fault scenario three. Maximum speed deviation [pu on system base] and voltage deviation [% of initial value]) of the wind turbine generator bus closest to the offshore substation in the same feeder as the fault occurs.

ω:
The choice of offshore electrical collector clearly influences the maximum and minimum speed deviation. The radial design gives the smallest deviations, while the star gives the largest deviations.
The impact of the choice of transmission system is also of importance. The AC/DC systems consequently give larger deviations than the AC/DC systems.

U:
The choice of offshore electrical collector clearly influences the maximum and minimum voltage deviation as well. The radial design gives the smallest deviations, while the star gives the largest deviations, just as for the speed.
The impact of the choice of transmission system is also of importance. The AC/DC systems consequently give larger voltage drops than the AC/DC systems, while the maximum values of the voltage are clearly smaller.

9 Discussion

In this chapter, the most important results from the load flow simulations and dynamic simulations are presented and discussed. For the load flow situation, this is done mainly by comparing the system losses at the two operating situations. For the dynamic simulations, this is done by comparing the behavior of the

9.1 Load flow simulations

Figure 84 shows that the losses are considerably lower in the AC/AC layouts than in the AC/DC layouts. For the AC/AC systems, the losses vary from 2,33% to 4,17% of the total power production, while for the AC/DC layouts, this percentage is higher, varying between 6,41% and 8,19%.

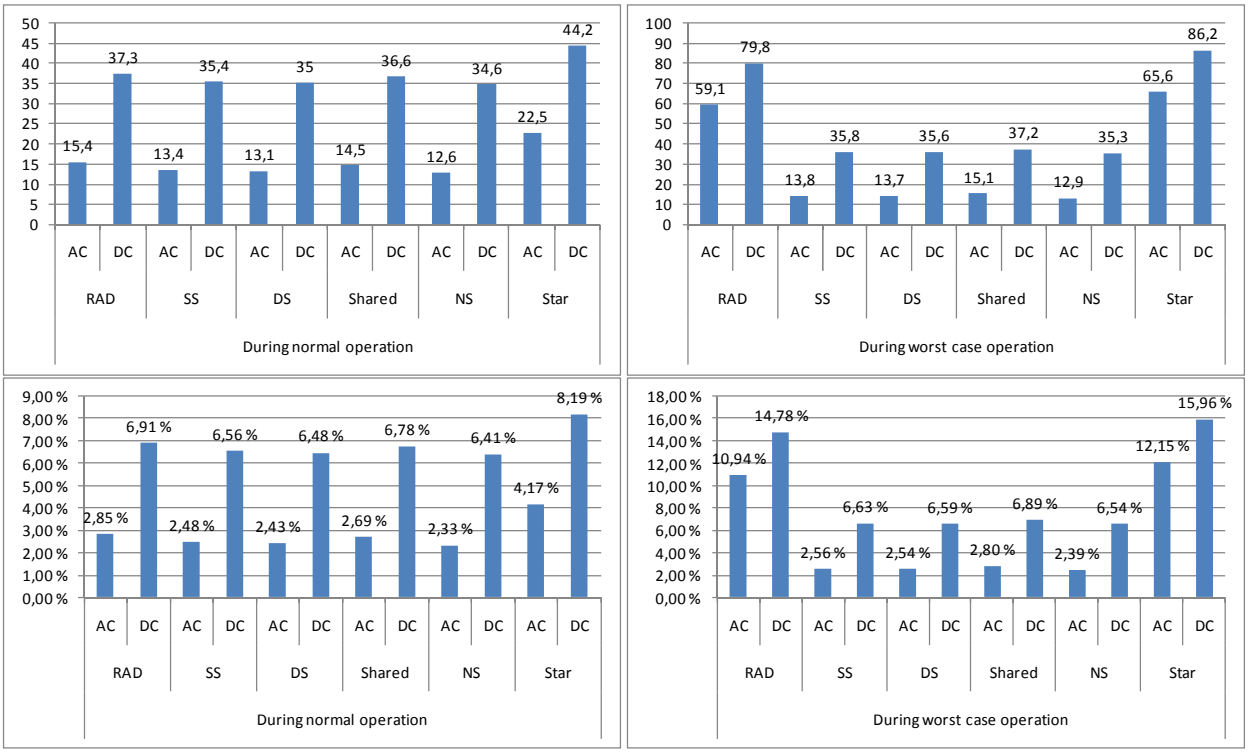

Figure 84 - Active power losses for the different wind farm layouts. The top two diagrams show MW losses, the bottom two show losses as percentage of the total produced power in the wind farm.

During normal operating conditions, the difference between the AC/DC system losses and the AC/AC system losses varies from 22.1 MW for the shared ring design to 21.7 MW for the star design.

The layout giving the smallest losses, both for AC and DC transmission to shore, is the *n*-sided ring design, giving total losses of 12.6MW (2.33%) for the AC/AC system, and 34.6MW (6.41%) for the AC/DC system. The layout giving the highest losses is the star system, giving 46-79% higher losses than the other designs for the AC/AC layout, and 19-28% higher losses than the other designs for the AC/DC layout.

By comparing the top right and top left diagram of Figure 84, it is clear that the radial and star designs are the ones giving the highest increase in the active power losses when the operating conditions change from

normal to worst case. This is because the worst case running conditions for these two systems imply the loss of production from nine wind turbines, since no redundancy is provided. The difference for the radial design is 43.7MW for the AC/AC system and 42.5MW for the AC/DC system. For the star design, the difference is 43.1MW for the AC/AC system and 42.0MW for the AC/DC system.

For the rest of the wind farm layouts, the differences in power losses are small when comparing the normal operating conditions to the worst case operating conditions, ranging from 0.3MW to 0.7MW.

It should be noted that the AC transmission cables are running at 100% of their power ratings. This is due to the high capacitive charging currents produced in the cables. Also, in the AC/AC layouts, there was a need for fixed reactors at a total size of approximately 1600 MVAr (!) for all cases, larger than any produced shunt reactor in the world today. In addition, an SVC of minimum 175 MVArs had to be installed in order to fulfill the grid codes regarding power factor control of the wind farm output power. This confirms what was written in the introduction, where it was stated that long AC cable connections to shore can lead to the need of very large and expensive reactive power compensators.

If the distance were to increase further, the cable rating would be violated, and yet another AC cable would have to be added to the transmission to be able to transport the power to shore. This would lead to the need for yet another shunt reactor in the several hundreds of megawatts range. The SVC would not have to be increased, as it is based on the active power transmitted, and a maximum power factor of 0.95. No economical calculations have been conducted in this thesis, but based on the amount of extra equipment needed for an AC connection with three cables it is likely that the HVDC Light link would give considerably better profitability. With no calculations to back this assertion, this is only speculations. The issue should be further looked into by conducting a feasibility study prior to the construction of the wind farm.

The load flow results describe the *consequences* of a fault, but says nothing about the *probability* of a fault occurring. This comparison does not take into consideration that the probability for faults may decrease as the cable ratings increase. Instead, the best case and worst case cable failure rate numbers from chapter 5.3 are used as a basis for the calculations. Based on those failure rates, the number of failures for each design is calculated as,:

$$N_{faults} = CFR \cdot \frac{l_{cable}}{100} \cdot LT_{wf} \qquad \textbf{9-1}$$

, where N_{fault} denotes the number of faults per year and:

LT_{wf}	=	Life time of the wind farm	[years]
l_{cable}	=	length of cable	[km]
CFR	=	cable failure rate	[failures/100km/year]

Based on a wind farm lifetime of 30 years, the expected numbers of faults for each design are shown in Table 7 and Table 8:

Cable \design:	*Radial*	*Single sided*	*Double sided*	*Shared*	*N-sided*	*Star*
WT1-Offshore substation	1,4	1,4	1,4	1,4	1,4	1,4
WT1-WT2	0,1	0,1	0,1	0,1	0,1	0,1
WT2-WT3	0,1	0,1	0,1	0,1	0,1	0,1
WT3-WT4	0,1	0,1	0,1	0,1	0,1	0,3
WT4-WT5	0,1	0,1	0,1	0,1	0,1	0,3
WT5-WT6	0,1	0,1	0,1	0,1	0,1	0,3
WT6-WT7	0,1	0,1	0,1	0,1	0,1	0,3
WT7-WT8	0,1	0,1	0,1	0,1	0,1	0,3
WT8-WT9	0,1	0,1	0,1	0,1	0,1	0,3
WT9-Offshore substation	0	2,6	0	2,6	0	0
Feeder to feeder	0	0	0,1	0,1	0,1	0
In total	**2,6**	**5,2**	**2,7**	**5,3**	**2,7**	**3,4**

Table 7 - Expected number of failures during the lifetime of the wind farm (LT = 30 years, CFR = 0.08)

Cable \design:	*Radial*	*Single sided*	*Double sided*	*Shared*	*N-sided*	*Star*
WT1-Offshore substation	3,6	3,6	3,6	3,6	3,6	3,6
WT1-WT2	0,4	0,4	0,4	0,4	0,4	0,4
WT2-WT3	0,4	0,4	0,4	0,4	0,4	0,4
WT3-WT4	0,4	0,4	0,4	0,4	0,4	0,6
WT4-WT5	0,4	0,4	0,4	0,4	0,4	0,6
WT5-WT6	0,4	0,4	0,4	0,4	0,4	0,7
WT6-WT7	0,4	0,4	0,4	0,4	0,4	0,7
WT7-WT8	0,4	0,4	0,4	0,4	0,4	0,7
WT8-WT9	0,4	0,4	0,4	0,4	0,4	0,7
WT9-Offshore substation	0	6,5	0	6,5	0	0
Feeder to feeder	0	0	0,2	0,4	0,3	0
In total	**6,5**	**13**	**6,7**	**13,3**	**6,8**	**8,6**

Table 8 - Expected number of failures during the lifetime of the wind farm (LT= 30 years, CFR = 0.20)

The lowest number of expected faults can be found at the radial design, while the shared design gives the highest amount of expected faults. Nevertheless, the consequences of losing the lines vary. Table 9 shows the extra power losses in the system as a consequence of a failure in one of the cables:

	$P_{loss,extra}$ *[MW]*					
Cable \design:	*Radial*	*Single sided*	*Double sided*	*Shared*	*N-sided*	*Star*
WT1-Offshore substation	43,7	0,4	0,6	0,6	0,3	43,1
WT1-WT2	38,8	0,2	0,5	0,4	0,2	4,7
WT2-WT3	33,9	0,1	0,4	0,3	0,2	4,7
WT3-WT4	29	0	0,3	0,2	0,1	4,7
WT4-WT5	24,1	0	0,2	0,2	0,1	4,7

WT5-WT6	19,3	-0,1	0,1	0,1	0	4,7
WT6-WT7	14,4	-0,1	0,1	0,1	0	4,7
WT7-WT8	9,6	0	0	0	0	4,7
WT8-WT9	4,8	0	0	0	0	4,7
WT9-Offshore substation		0,1		0,1		
Feeder to feeder				0,3	0	

Table 9 – Extra power losses compared to normal operating conditions, when a cable is lost.

The table shows that the consequences of losing a line in terms of power losses is a lot bigger for the radial design than for the others. The star design is a clear number two, while the looped designs are clearly superior when it comes to providing redundancy. When knowing the mean time to repair of a cable offshore, and having a good forecast for the electricity price, the expected loss of income for the wind farm due to non-provided redundancy can be calculated. Since this will only be speculations, and are beyond the scope of this thesis, this will not be done here.

9.2 Dynamic simulations

For the dynamic simulations, Table 11 shows how the maximum speed deviations are dependent on transmission technology and offshore grid design:

SPEED DEVIATIONS		FAULT 1	FAULT 2	FAULT 3
First bus of neighboring feeder	*Transmission*	DC > AC	DC>AC except for star and radial.	Not studied
	Design	Small differences	DS>NS>Shared>SS> Star>Rad for both AC and DC	Not studied
First bus of same feeder	*Transmission*	Not studied	DC > AC.	DC > AC
	Design	Not studied	Rad and star unstable. Small differences	AC: Star>Shared>NS>DS>SS>Rad DC: Star>Shared>DS>NS>SS>Rad
Bus closest to the fault and closer to the substation	*Transmission*	Not studied	Not studied	DC > AC
	Design	Not studied	Not studied	Small differences
Bus closest to the fault, further away from the substation	*Transmission*	Not studied	Not studied	DC > AC
	Design	Not studied	Not studied	Rad and star unstable AC:DS>SS>NS>SH DC: DS>NS>SS>SH

Table 10 - Comparison of the speed deviation for dynamic simulations. A>B means that the maximum deviation from the steady state value is larger for A than for B, i.e. the response is worse.

For all cases except two, the AC/DC layouts give larger maximum speed deviation from the steady state value during a fault. The two exceptions are found at the first bus of the generator at the neighboring feeder to the fault, when using the star and radial design during fault scenario two.

The speed deviations are also consequently larger when using HVDC Light transmission compared to using AC cable transmission, with two exceptions, as described in the beginning of this chapter. The reason why the speed deviations are bigger for the DC systems than for the AC systems can be explained by looking at equation 2-8. The offshore electric power is plotted in the dynamic simulations chapter. Diagrams showing the maximum and minimum values of the electric power can be found in appendix 5. The diagrams show that for all cases, the electric power during the fault is larger for AC transmission than for HVDC Light transmission, $P_{E,AC}>P_{E,DC}$. during the fault. From equation 2-8, it can be seen that when the electrical power P_E increases, the rotor speed change decreases. This explains to some degree why the maximum speed deviation is larger for the DC systems than for the AC systems. The above reasoning only considers the rotor speed change during the three phase fault, and thus only describes the rotor speed change during the fault. It does not take into consideration the damping capability of the system. When conducting the DC simulations, the control parameter VLTFLG is equal to 1 for the AC/DC simulations, and 0 for the AC/AC simulations, in order to get the initial conditions check to be OK. This change in the wind turbine controller settings will affect the dynamic behavior, and might be the explanation to why the rotor speed deviation is smaller for the AC/AC system than the AC/DC system.

When looking at how the design affects the speed response, it is difficult to range the designs from best to worse, since different faults give different results. What can be noted is that for fault scenario three, the star design gives the highest deviation for the first bus of the same feeder, since this bus is directly coupled to the fault. The different systems have different cables, with different cable parameters. The dynamic response depends on the total impedance between the generator and fault, and with different impedances comes different dynamic responses. The star and radial designs are the only ones giving unstable operation, since the fault isolates certain generators. All other generators in all systems have a very stable operation.

Table 11 shows how the voltage drop and rise is dependent on transmission technology and offshore grid design:

VOLTAGE DEVIATIONS		FAULT 1	FAULT 2	FAULT 3
First bus of neighboring feeder	*Transmission*	Drop: DC > AC Rise: AC > DC	Drop: DC > AC Rise: AC > DC	Not studied
	Design	Star clearly lowest. AC: DS=SS>NS>Shared>Rad>Star DC: DS>SS >Shared>NS>Rad>Star	AC: DS>NS>Shared>SS> Rad>Star DC: DS>NS>Shared>SS> Star>Rad	Not studied
First bus of same feeder	*Transmission*	Not studied	Drop: DC > AC Rise: AC > DC	Drop: DC > AC Rise: AC > DC
	Design	Not studied	Designs: Small differences for stable cases. Rad and star unstable.	AC: Star>Shared>NS>DS>SS>Rad DC: Star>Shared>DS>NS>SS>Rad
Bus closest to the fault and closer to the substation	*Transmission*	Not studied	Not studied	Drop: DC > AC Rise: AC > DC
	Design	Not studied	Not studied	Small differences
Bus closest to the fault, further away from the substation	*Transmission*	Not studied	Not studied	Drop: DC > AC Rise: AC > DC
	Design	Not studied	Not studied	AC: SS>DS>NS>Shared DC: DS>SS>Shared>NS Rad and star unstable

Table 11 - Comparison of the voltage deviation for dynamic simulations. A>B means that the maximum deviation from the steady state value is larger for A than for B, i.e. the response is worse.

The table shows that there is a clear difference between using HVDC Light transmission and AC cable transmission to shore. The AC/DC layouts consequently give larger voltage drops and lower voltage tops than the AC/AC layouts.

The voltage response can be explained by looking at the short circuit power at the offshore substation. Short circuit power, SC MVA, is a normal parameter for measuring the strength at a bus in an AC network. The definition of short circuit power is given in equation 9-2:

$$SCMVA = I_{fault} V_{nom,ac} = \frac{V_{nom,ac}^2}{Z_{th}} \quad \textbf{9-2}$$

The HVDC Light connection provides a limited short circuit current, upwards limited to 1pu , based on the converter rating. The short circuit power contribution to the offshore substation is therefore limited to the nominal pu value of the AC voltage, which is 1 pu. This gives that the maximum short circuit power delivered by the HVDC Light converter is 1 pu, referred to the converter MVA base. This is 570 MVA for each converter, giving that the maximum short circuit current from the HVDC Light converter at the offshore substation is 1140 MVA. Referring this to the base power for the offshore substation, which is the system base (100 MVA), the maximum short circuit power from the two HVDC Light converters is 11.4 pu based on the system base.

For an AC transmission, there is no such upper limit. By performing an automatic sequence short circuit fault calculation at the offshore substation bus in PSS/E. it was found that for the different designs, the short circuit current contribution from the transmission system was 25.64 to 25.91 pu, or 2564MVA to 2591MVA. From Ohm's law, one can conclude that, for constant short circuit impedance, the higher the short circuit current is, the higher the short circuit voltage is. Therefore, all systems using AC transmission to shore give smaller voltage drops than the systems using HVDC Light transmission.

10 Conclusion

Presently, there is a debate among the offshore wind community regarding the value of redundancy required in the offshore grid to maximize the energy yield, and the impact it may impose on the capital costs of the wind farm. The major concern is related to the cost of supplementary subsea cabling, either in terms of extra length or higher ratings, versus the value of the decreased losses during normal operation and contingency operation.

In this thesis, six different designs of the electrical grid of a 540 MW offshore wind farm, placed 100km off the Norwegian coast, have been studied. The six different designs are the radial design, the single sided ring, the double sided ring, the shared ring, the *n*-sided ring (with *n* equal to four in this thesis*)* and the star design. In addition, two transmission options to shore have been studied. For both of the transmission options, two parallel connections to shore were installed in order to provide redundancy. The first option was to have two parallel AC cable connections to shore, with a rated voltage level of 400 kV. The second option was to have two parallel HVDC Light connections to shore, rated at ±150kV DC. The main scope has been to study the performance of the different wind farm layouts. The power losses during normal and contingency running conditions have been found and compared. In addition to this, the reliability of the systems has been compared by looking at the expected amount of cable failures and the consequence of any cable fault in the offshore grid. Finally, the dynamic response following a fault has been studied in order to evaluate which layout is the most robust when it comes to withstanding a fault in the offshore system.

All simulations have been executed in version 31 of the program PSS/E .The wind farm was modeled full scale, consisting of 108 wind turbines rated at 5MW. The wind turbines were modeled as doubly fed induction generators, using the generic wind model that comes with version 31 of PSS/E.

The load flow simulations showed that the differences in power losses were quite large, both when comparing the six grid designs and when looking at the transmission to shore. The choice of transmission system had a larger impact on the system losses than the choice of offshore grid design. Nevertheless, the design also influenced the losses considerably. A connection using two AC cable connections to shore gave lower total system losses than using two HVDC light connections.

The lowest losses when using AC cables were found at the *n*-sided ring design. The losses in this design were found to be 12.6MW, which is 2.33% of the total produced power in the wind farm. The highest losses were found in the star design. The losses in this design were 22.5MW, which is 4.17% of the total produced power in the wind farm. When using HVDC Light, the losses were considerably higher: The lowest losses when using HVDC Light were found at the *n*-sided bus. The losses in this design were 34.6MW, which is 6.41% of the total produced power in the wind farm. The highest losses were found in the star design. The losses in this design were 44.2MW, which is 8.19% of the total produced power in the wind farm.

An additional load flow simulation was run, studying the offshore wind farm under worst case running conditions. Under these conditions, it is assumed that a fault has led to the disconnection of one of the cables connecting the innermost wind turbine of one of the feeders to the offshore substation. The radial design and the star design provide no redundancy, so for these systems the entire feeder where the cable is disconnected is unable to deliver any power to the offshore substation. The lowest losses were still found for the *n*-sided design, using AC cable transmission to shore. These losses are now 12.9MW, which is

2.39% of the total produced power in the wind farm. The highest losses are again found at the star design, using HVCD Light transmission to shore. For this system design, the losses are 86.2MW, which is 15.96% of the total produced power in the wind farm with all cables in function.

It must be noted that in the AC/AC layouts, there was a need for fixed reactors at a total size of approximately 1600 MVAr for all cases. In addition, an SVC of minimum 175 MVArs had to be installed in order to fulfill the grid codes regarding power factor control of the wind farm output power. This confirms what was written in the introduction, where it was stated that long AC cable connections to shore can lead to the need of very large and expensive reactive power compensators.

In terms of reliability, the looped designs had the superiorly smallest consequences of losing a cable. Also, for the *n*-sided and double sided designs, the expected number of faults was only slightly higher than for the radial design, since the amount of extra cabling is small.

To decide what effect the offshore grid design and transmission system design had on the dynamic response of the offshore wind turbines following a fault, the voltage response and rotor speed response of selected generators in the wind farm was studied when subject to a three phase short circuit fault, lasting 150ms. Three fault points were studied. The first fault point was in the connection to shore, the second was in the cable connecting the innermost wind turbine in a feeder to the offshore substation, and the third was in the cable connecting the two outermost wind turbines of a feeder. The faults gave varying results when comparing the different grid designs. It is difficult to draw any conclusions as regarding which offshore grid design gives the best offshore dynamic response, as this seems to be more dependent on where the fault occurs than what grid design was chosen. When comparing the transmission systems though, it was clear that for nearly all offshore grid designs and all fault types, the speed deviations were larger when using HVDC Light transmission compared to using AC cables. Also, for all simulations, the HVDC Light transmission to shore gave increased voltage drops offshore. This is due to the low short circuit power capability of the HVDC connection compared to the AC cable connection. Thus, the results indicate that HVDC Light has a negative influence on the offshore stability when compared to AC cables.

11 Further work

This thesis is the end of the work that started in the project work executed during the fall of 2008. After working with the subject of offshore wind power and the connection of offshore wind power to the grid, it has become increasingly clear that the work that has been executed in this thesis only covers a small part of the challenges attached to the offshore wind power field.

This thesis does not focus on the control systems of the wind turbines. To compare the dynamic behavior of different layouts without optimizing the control system for each design might lead to different results than what could be achieved with better tuned and better designed control systems. A natural way to pick up and continue the work with this thesis is to develop the control systems of the wind turbines and the SVC. Also, several studies indicate that an offshore DC grid, as presented in chapter 3.4, might be competitive to an offshore AC grid in terms of profitability. This has not been studied in this thesis, and should be further looked into.

When using an offshore DC grid, there are several fields that should be investigated. The design of the power electronics in this system, covering the DC generator, an offshore DC transformer and a medium or high frequency transformer for the wind turbine are suggestions to what the

The wind farm economy should be investigated in order to better compare the different layouts. When given the power production and power losses of the wind farm, it would be very interesting to dig into the issues of reliability and to conduct a feasibility study, where the profitability of the different layouts is compared.

Furthermore, in the offshore wind power community the idea of having an offshore multi terminal DC (MTDC) grid in the North Sea, connecting the countries surrounding it to a cluster of offshore wind farms and also to each other has been discussed. The first offshore MTDC grid is planned at Kriegers Flak, connecting Sweden, Denmark and Germany together and to the offshore wind farm. The effects of a similar offshore grid on the Norwegian power system should be studied. Also, the effect on the power market should be investigated.

Also, the idea of connecting the MTDC-grid to one or more oil platforms, or to connect smaller wind farms to the platforms in isolated power systems, should be investigated as this would provide environmentally friendly energy to the oil platforms, the idea of connecting the MTDC-grid to one or more oil platforms, or to connect smaller wind farms to the platforms in isolated power systems should be investigated as this would provide environmentally friendly energy to an industry which is not exactly known for its environmentally friendly image

Bibliography

ABB. (2008). Retrieved september 23, 2008, from ABB HVDC - Power T&D solutions: http://www.abb.com/hvdc
ABB. (2008). *It's time to connect - Technical description of HVDC Light® technology.* ABB.
ABB Power technologies AB. (2009). *User guide for the PSS/E implementation of the HVDC Light detailed model Version 1.1.7.* Ludvika: ABB.
Ackermann, T. (2005). *Wind power in power systems.* John Wiley & Sons, Ltd.
Barberis, N., Todorovic, J., & Ackermann, T. (2005). *Loss evaluation of HVAC and HVDC transmission solutions for large offshore wind farms.* Science Direct.
Elkington, K. (2009). *Modelling and control of doubly fed induction generators in power systems (Licentiate thesis).* Stockholm, Sweden: KTH, electrical engineering.
Ericsson nkt. (n.d.). *http://www.encv.co.uk/Products/Datasheets.aspx.* Retrieved May 30, 2009, from Ericsson nkt cables Venture Ltd: http://www.encv.co.uk/Products/Datasheets.aspx
Gardner, P., Craig, L. M., & Smith, G. J. *Electrical Systems for Offshore Wind Farms.* Glasgow, UK: Garrad Hassan & Partners.
Gjengedal, T. (2009, May 13). Telephone conversation.
Haugsten Hansen, T. (2008). *Offshore wind power - power system studies.* Project work at Department of Electrical Engineering, NTNU.
Hubert, C. I. (2002). *Electric Machines - Theory, Operations, Applications, Adjustment, and Control.* Prentice Hall.
Kundur, P. (1994). *Power System Stability and Control.* McGraw-Hill.
Kundur, P., Paserba, J., Ajjarapu, V., Andersson, G., Bose, A., Canizares, C., et al. (2003). *Definition and classification of power system stability.* IEEE.
Lundberg, S. (2006). *Wind Farm Configuration and Energy Efficiency Studies - Series DC versus AC Layouts.* Department of Energy and Environment, Chalmers University of Technology.
Machowski, J., Bialek, J. W., & Bumby, J. R. (1998). *Power system dynamics and stability.* John Wiley & Sons Ltd.
Martander, O. (2002). *DC grids for wind farms.* Department of electric power engineering, Chalmers university of technology.
Mohan, & Undeland. (2006). *Power Electronics.* John Wiley & Sons.
NordPool. (2009). *All Spot - NordPool*. Retrieved May 18, 2009, from ASA NordPool web site: http://www.nordpool.com/system/flags/elspot/area/all/
Quinonez-Varela, G., Ault, G., Anaya-Lara, O., & McDonald, J. (2007, June). Electrical collector system options for large offshore wind farms. *IET Renewable Power Generation, Vol.1, No.2* .
RePower Systems AG. (n.d.). *RePower Systems AG: Wind Turbines*. Retrieved May 13, 2009, from http://www.repower.de/index.php?id=12&L=1
Schütte, T., Gustavsson, B., & Ström, M. (2001). *The use of low frequency AC for Offshore Wind Power.* Proceedings of the second international workshop on transmission networks for offshore wind farms. Edited by Thomas Ackermann, Royal institute of technology.
Siemens PTD. (2008, april 14). Power point presentation: HVDC plus; technology benefits & applications.
Siemens PTI. (2007). *PSSE users manual - Program application guide - Volume II.* Siemens Power Transmission & Distribution, Inc., Power Technologies International.

Statnett SF. (n.d.). *Dokumenter - Statnett - Samfunnsøkonomi.pdf.* Retrieved May 15, 2009, from Statnett SF (Norwegian): http://www.statnett.no/Prosjekter/Kabel-til-Nederland-NorNed/Dokumenter/
Statnett SF. (2008). *Funksjonskrav i kraftsystemet (Norwegian).* Statnett SF.
Tavner, P. (2009, april 23). Reliability & availability of wind turbine electrical & electronic components (power point presentation). Wind power to the grid - EPE Wind Energy Chapter - 2nd seminar, Stockholm, Sweden.
Vestas Wind systems AS. (n.d.). *Vestas V90 - 3.0 MW - information brochure.* Retrieved april 26, 2009, from Vestas web page: http://www.vestas.com/en/wind-power-solutions/wind-turbines/3.0-mw
www.hornsrev.dk. (n.d.). *Horns rev offshore wind farm*. Retrieved May 8, 2009, from http://www.hornsrev.dk/index.en.html

Appendix 1: Load flow reports

Radial design

ACAC, normal running conditions:

```
************************  SUMMARY FOR COMPLETE SYSTEM ************************
                                SYSTEM SWING BUS SUMMARY

 X------ SWING BUS ------X          X---- AREA -----X X---- ZONE -----X
BUS#  X-- NAME --X BASKV      #           X-- NAME --X      MW       MVAR   MVABASE
  1   PCC          400.00      1           1                 15.4     0.0    1000.0

220 BUSES     110 PLANTS      110 MACHINES           2 FIXED SHUNTS     0 SWITCHED SHUNTS
1 LOADS     221 BRANCHES    109 TRANSFORMERS       0 DC LINES         0 FACTS DEVICES

                        X------ ACTUAL ------X X----- NOMINAL ------X
                        MW          MVAR         MW          MVAR
FROM GENERATION         555.4       -11.4        555.4       -11.4
TO CONSTANT POWER LOAD  540.0         0.0        540.0         0.0
TO CONSTANT CURRENT     0.0           0.0        0.0           0.0
TO CONSTANT ADMITTANCE  0.0           0.0        0.0           0.0
TO BUS SHUNT            0.0           1611.8     0.0           1611.8
TO FACTS DEVICE SHUNT   0.0           0.0        0.0           0.0
TO LINE SHUNT           0.0           0.0        0.0           0.0
FROM LINE CHARGING      0.0           1769.6     0.0           1715.5

VOLTAGE                 X----- LOSSES -----X    X-- LINE SHUNTS --X     CHARGING
LEVEL       BRANCHES      MW        MVAR          MW      MVAR          MVAR
400.0       5             7.06      75.41         0.0     0.0           1762.8
33.0        216           8.30      70.96         0.0     0.0           6.7
TOTAL       221           15.35     146.38        0.0     0.0           1769.6
```

ACAC, worst case:

```
************************  SUMMARY FOR COMPLETE SYSTEM  ************************
                                SYSTEM SWING BUS SUMMARY

 X------ SWING BUS ------X          X---- AREA -----X       X---- ZONE -----X
BUS#  X-- NAME -X  BASKV            #     X-- NAME -X MW    MVAR  MVABASE
  1   PCC          400.00           1     1           59.1  0.0   1000.0

202 BUSES     101 PLANTS      101 MACHINES           2 FIXED SHUNTS     0 SWITCHED SHUNTS
1 LOADS     203 BRANCHES    100 TRANSFORMERS       0 DC LINES         0 FACTS DEVICES

                        X------ ACTUAL ------X  X----- NOMINAL ------X
                        MW    MVAR              MW    MVAR
 FROM GENERATION        554.1 -24.4             554.1 -24.4
 TO CONSTANT POWER LOAD 540.0  0.0              540.0 0.0
 TO CONSTANT CURRENT     0.0   0.0              0.0   0.0
 TO CONSTANT ADMITTANCE  0.0   0.0              0.0   0.0
 TO BUS SHUNT            0.0   1611.8           0.0   1611.8
 TO FACTS DEVICE SHUNT   0.0   0.0              0.0   0.0
 TO LINE SHUNT           0.0   0.0              0.0   0.0
 FROM LINE CHARGING      0.0   1769.0           0.0   1714.9
```

VOLTAGE	X----- LOSSES -----X			X-- LINE SHUNTS -X	CHARGING
LEVEL	BRANCHES	MW	MVAR	MW	MVAR	MVAR
400.0	5	6.42	67.35	0.0	0.0	1762.8
33.0	198	7.65	65.42	0.0	0.0	6.2
TOTAL	203	14.07	132.76	0.0	0.0	1769.0

ACDC, normal running conditions:

```
************************  SUMMARY FOR COMPLETE SYSTEM  ************************
                                SYSTEM SWING BUS SUMMARY

X------ SWING BUS ------X     X---- AREA -----X X---- ZONE -----X
BUS#  X-- NAME -X BASKV    #   X-- NAME -XMW       MVAR     MVABASE
1         PCC     300.00   1   1          37.4     -32.3    1000.0
112 OFFSH HVDC  195.00     1   1        -264.2     -78.6     570.0
212 OFFSH HVDC 2195.00     1   1        -264.2     -78.6     570.0

    224 BUSES     113 PLANTS      113 MACHINES           4 FIXED SHUNTS     0 SWITCHED
SHUNTS
      1 LOADS     222 BRANCHES    113 TRANSFORMERS       0 DC LINES         0 FACTS
DEVICES

                          X------ ACTUAL ------X X----- NOMINAL ------X
                                  MW        MVAR        MW        MVAR
FROM GENERATION                551.6     -223.1       551.6     -223.1
TO CONSTANT POWER LOAD         540.0      -44.9       540.0      -44.9
TO CONSTANT CURRENT              0.0        0.0         0.0        0.0
TO CONSTANT ADMITTANCE           0.0        0.0         0.0        0.0
TO BUS SHUNT                     0.0     -342.0         0.0     -342.0
TO FACTS DEVICE SHUNT            0.0        0.0         0.0        0.0
TO LINE SHUNT                    0.0        0.0         0.0        0.0
FROM LINE CHARGING               0.0        6.7         0.0        6.4

VOLTAGE                   X----- LOSSES -----X    X-- LINE SHUNTS   X   CHARGING
LEVEL       BRANCHES            MW  MVAR         MW        MVAR    MVAR
300.  0     3                 0.00      25.11   0.0         0.0   0.0
195.0       2                 0.00      27.76   0.0         0.0   0.0
132.0       1                 3.24      46.26   0.0         0.0   0.0
33.0        216               8.35      71.37   0.0         0.0   6.7
TOTAL       222              11.59     170.50   0.0         0.0   6.7
```

ACDC, worst case:

```
************************ SUMMARY FOR COMPLETE SYSTEM ************************
                         SYSTEM SWING BUS SUMMARY

X------ SWING BUS ------X X---- AREA -----X X---- ZONE -----X
BUS# X-- NAME --X BASKV    # X-- NAME --X    # X-- NAME --X       MW       MVAR   MVABASE
   1 PCC          300.00    1                 1                   79.8      10.5    1000.0
 112 OFFSH HVDC  195.00     1                 1                 -242.3     -79.7     570.0
 212 OFFSH HVDC 2195.00     1                 1                 -242.3     -79.7     570.0

  206 BUSES     104 PLANTS      104 MACHINES          4 FIXED SHUNTS     0 SWITCHED SHUNTS
    1 LOADS     204 BRANCHES    104 TRANSFORMERS      0 DC LINES         0 FACTS DEVICES

                          X------ ACTUAL ------X X----- NOMINAL ------X

                                  MW        MVAR        MW        MVAR
  FROM GENERATION              550.4     -199.3       550.4     -199.3
  TO CONSTANT POWER LOAD       540.0        0.0       540.0        0.0
  TO CONSTANT CURRENT            0.0        0.0         0.0        0.0
  TO CONSTANT ADMITTANCE         0.0        0.0         0.0        0.0
  TO BUS SHUNT                   0.0     -342.0         0.0     -342.0
  TO FACTS DEVICE SHUNT          0.0        0.0         0.0        0.0
  TO LINE SHUNT                  0.0        0.0         0.0        0.0
```

FROM LINE CHARGING		0.0	6.1	0.0	5.9	
VOLTAGE LEVEL	BRANCHES	LOSSES MW	LOSSES MVAR	LINE SHUNTS MW	LINE SHUNTS MVAR	CHARGING MVAR
300.0	3	0.00	21.05	0.0	0.0	0.0
195.0	2	0.00	23.34	0.0	0.0	0.0
132.0	1	2.72	38.91	0.0	0.0	0.0
33.0	198	7.66	65.50	0.0	0.0	6.1
TOTAL	204	10.38	148.80	0.0	0.0	6.1

Single sided loop design

ACAC, normal running conditions:

```
************************  SUMMARY FOR COMPLETE SYSTEM  ************************

                                  SYSTEM SWING BUS SUMMARY
 X------ SWING BUS ------X X---- AREA -----X X---- ZONE -----X
BUS# X-- NAME --X BASKV    # X-- NAME --X    # X-- NAME --X       MW       MVAR   MVABASE
    1    PCC    400.00    1                 1                  13.3       0.0    1000.0

220 BUSES     110 PLANTS      110 MACHINES          2 FIXED SHUNTS     0 SWITCHED SHUNTS
1 LOADS     233 BRANCHES    109 TRANSFORMERS       0 DC LINES         0 FACTS DEVICES

                         X------ ACTUAL ------X X----- NOMINAL ------X
                                  MW        MVAR         MW        MVAR
 FROM GENERATION                553.3      -34.4       553.3      -34.4
 TO CONSTANT POWER LOAD         540.0        0.0       540.0        0.0
 TO CONSTANT CURRENT              0.0        0.0         0.0        0.0
 TO CONSTANT ADMITTANCE           0.0        0.0         0.0        0.0
 TO BUS SHUNT                     0.0     1611.5         0.0     1611.5
 TO FACTS DEVICE SHUNT            0.0        0.0         0.0        0.0
 TO LINE SHUNT                    0.0        0.0         0.0        0.0
 FROM LINE CHARGING               0.0     1783.5         0.0     1728.8

  VOLTAGE       X----- LOSSES -----X   X-- LINE SHUNTS --X   CHARGING
  LEVEL BRANCHES      MW        MVAR        MW        MVAR       MVAR
  400.0      5       7.09      75.80        0.0        0.0     1762.8
   33.0    228       6.25      61.76        0.0        0.0       20.6
  TOTAL    233      13.34     137.56        0.0        0.0     1783.5
```

ACAC, worst case:

```
************************  SUMMARY FOR COMPLETE SYSTEM  ************************

                                  SYSTEM SWING BUS SUMMARY

 X------ SWING BUS ------X X---- AREA -----X X---- ZONE -----X
BUS# X-- NAME --X BASKV    # X-- NAME --X    # X-- NAME --X       MW       MVAR   MVABASE
    1     PCC     400.00    1                  1                  13.8       0.0    1000.0

220 BUSES     110 PLANTS      110 MACHINES          2 FIXED SHUNTS     0 SWITCHED SHUNTS
1 LOADS     232 BRANCHES    109 TRANSFORMERS       0 DC LINES         0 FACTS DEVICES

                         X------ ACTUAL ------X X----- NOMINAL ------X
                                  MW        MVAR         MW        MVAR
 FROM GENERATION                553.8      -32.2       553.8      -32.2
 TO CONSTANT POWER LOAD         540.0        0.0       540.0        0.0
 TO CONSTANT CURRENT              0.0        0.0         0.0        0.0
 TO CONSTANT ADMITTANCE           0.0        0.0         0.0        0.0
 TO BUS SHUNT                     0.0     1611.5         0.0     1611.5
 TO FACTS DEVICE SHUNT            0.0        0.0         0.0        0.0
 TO LINE SHUNT                    0.0        0.0         0.0        0.0
 FROM LINE CHARGING               0.0     1782.9         0.0     1728.3

  VOLTAGE       X----- LOSSES -----X   X-- LINE SHUNTS --X   CHARGING
  LEVEL BRANCHES      MW        MVAR        MW        MVAR       MVAR
  400.0      5       7.08      75.72        0.0        0.0     1762.8
   33.0    227       6.68      63.55        0.0        0.0       20.1
  TOTAL    232      13.76     139.27        0.0        0.0     1782.9
```

ACDC, normal running conditions:

```
************************  SUMMARY FOR COMPLETE SYSTEM  ************************

                                  SYSTEM SWING BUS SUMMARY
 X------ SWING BUS ------X X---- AREA -----X X---- ZONE -----X

BUS# X-- NAME --X BASKV    # X-- NAME --X    # X-- NAME --X       MW       MVAR   MVABASE
   1 PCC         300.00    1                 1                   35.4      12.7    1000.0
   112 OFFSH HVDC  195.00    1                 1                 -265.2     -68.4     570.0
   212 OFFSH HVDC 2195.00    1                 1                 -265.2     -68.4     570.0

224 BUSES     113 PLANTS      113 MACHINES          4 FIXED SHUNTS     0 SWITCHED SHUNTS
1 LOADS     234 BRANCHES    113 TRANSFORMERS       0 DC LINES         0 FACTS DEVICES

                          X------ ACTUAL ------X X----- NOMINAL ------X
                                  MW        MVAR         MW        MVAR
 FROM GENERATION               549.5     -200.2       549.5     -200.2
 TO CONSTANT POWER LOAD        540.0        0.0       540.0        0.0
 TO CONSTANT CURRENT             0.0        0.0         0.0        0.0
 TO CONSTANT ADMITTANCE          0.0        0.0         0.0        0.0
 TO BUS SHUNT                    0.0     -342.0         0.0     -342.0
 TO FACTS DEVICE SHUNT           0.0        0.0         0.0        0.0
 TO LINE SHUNT                   0.0        0.0         0.0        0.0
 FROM LINE CHARGING              0.0       20.1         0.0       19.7

  VOLTAGE       X----- LOSSES -----X   X-- LINE SHUNTS --X   CHARGING
  LEVEL BRANCHES      MW        MVAR        MW        MVAR       MVAR
  300.0      2       0.00      12.65        0.0        0.0        0.0
  195.0      3       0.00      40.72        0.0        0.0        0.0
   33.0    229       9.54     108.56        0.0        0.0       20.1
  TOTAL    234       9.54     161.93        0.0        0.0       20.1
```

ACDC, worst case:

```
************************  SUMMARY FOR COMPLETE SYSTEM  ************************

                                  SYSTEM SWING BUS SUMMARY
 X------ SWING BUS ------X X---- AREA -----X X---- ZONE -----X
 BUS# X-- NAME --X BASKV    # X-- NAME --X    # X-- NAME --X       MW       MVAR   MVABASE
  1       PCC     300.00    1                 1                   35.8      12.6    1000.0
  112 OFFSH HVDC  195.00    1                 1                 -265.0     -68.4     570.0
  212 OFFSH HVDC 2195.00    1                 1                 -265.0     -68.4     570.0

224 BUSES     113 PLANTS      113 MACHINES          4 FIXED SHUNTS     0 SWITCHED SHUNTS
1 LOADS     233 BRANCHES    113 TRANSFORMERS       0 DC LINES         0 FACTS DEVICES

                          X------ ACTUAL ------X X----- NOMINAL ------X
                                  MW        MVAR         MW        MVAR
 FROM GENERATION               550.0     -198.1       550.0     -198.1
 TO CONSTANT POWER LOAD        540.0        0.0       540.0        0.0
 TO CONSTANT CURRENT             0.0        0.0         0.0        0.0
 TO CONSTANT ADMITTANCE          0.0        0.0         0.0        0.0
 TO BUS SHUNT                    0.0     -342.0         0.0     -342.0
 TO FACTS DEVICE SHUNT           0.0        0.0         0.0        0.0
 TO LINE SHUNT                   0.0        0.0         0.0        0.0
 FROM LINE CHARGING              0.0       19.7         0.0       19.2

  VOLTAGE       X----- LOSSES -----X   X-- LINE SHUNTS --X   CHARGING
  LEVEL BRANCHES      MW        MVAR        MW        MVAR       MVAR
```

300.0	2	0.00	12.63	0.0	0.0	0.0
195.0	3	0.00	40.66	0.0	0.0	0.0
33.0	228	9.96	110.27	0.0	0.0	19.7
TOTAL	233	9.96	163.56	0.0	0.0	19.7

Double sided loop design

ACAC, normal running conditions:

```
************************  SUMMARY FOR COMPLETE SYSTEM  ************************

                                  SYSTEM SWING BUS SUMMARY
 X------ SWING BUS ------X X---- AREA -----X X---- ZONE -----X
 BUS# X-- NAME --X BASKV    # X-- NAME --X    # X-- NAME --X       MW       MVAR   MVABASE
  1       GRID   400.00       1                 1                13.0       0.0    1000.0

220 BUSES     110 PLANTS      110 MACHINES          2 FIXED SHUNTS     0 SWITCHED SHUNTS
1 LOADS     227 BRANCHES    109 TRANSFORMERS       0 DC LINES         0 FACTS DEVICES

                         X------ ACTUAL ------X X----- NOMINAL ------X
                                   MW        MVAR         MW        MVAR
 FROM GENERATION                 553.0      -19.9       553.0      -19.9
 TO CONSTANT POWER LOAD          540.0        0.0       540.0        0.0
 TO CONSTANT CURRENT               0.0        0.0         0.0        0.0
 TO CONSTANT ADMITTANCE            0.0        0.0         0.0        0.0
 TO BUS SHUNT                      0.0     1611.5         0.0     1611.5
 TO FACTS DEVICE SHUNT             0.0        0.0         0.0        0.0
 TO LINE SHUNT                     0.0        0.0         0.0        0.0
 FROM LINE CHARGING                0.0     1768.1         0.0     1714.1

  VOLTAGE       X----- LOSSES -----X   X-- LINE SHUNTS --X   CHARGING
  LEVEL BRANCHES      MW        MVAR        MW        MVAR       MVAR
  400.0      5       7.09       75.87        0.0        0.0     1762.8
   33.0    222       5.90       60.84        0.0        0.0        5.3
  TOTAL    227      12.99      136.71        0.0        0.0     1768.1
```

ACAC, worst case:

```
************************  SUMMARY FOR COMPLETE SYSTEM  ************************

                                  SYSTEM SWING BUS SUMMARY
 X------ SWING BUS ------X X---- AREA -----X X---- ZONE -----X
   BUS# X-- NAME --X BASKV    # X-- NAME --X    # X-- NAME --X       MW    MVAR  MVABASE
      1 GRID        400.00    1                 1                 13.6     0.0  1000.0

220 BUSES     110 PLANTS      110 MACHINES          2 FIXED SHUNTS     0 SWITCHED SHUNTS
1 LOADS     226 BRANCHES    109 TRANSFORMERS       0 DC LINES         0 FACTS DEVICES

                         X------ ACTUAL ------X X----- NOMINAL ------X
                                   MW        MVAR         MW        MVAR
 FROM GENERATION                 553.6      -16.9       553.6      -16.9
 TO CONSTANT POWER LOAD          540.0        0.0       540.0        0.0
 TO CONSTANT CURRENT               0.0        0.0         0.0        0.0
 TO CONSTANT ADMITTANCE            0.0        0.0         0.0        0.0
 TO BUS SHUNT                      0.0     1611.5         0.0     1611.5
 TO FACTS DEVICE SHUNT             0.0        0.0         0.0        0.0
 TO LINE SHUNT                     0.0        0.0         0.0        0.0
 FROM LINE CHARGING                0.0     1767.9         0.0     1713.9

  VOLTAGE       X----- LOSSES -----X   X-- LINE SHUNTS --X   CHARGING
  LEVEL BRANCHES      MW        MVAR        MW        MVAR       MVAR
  400.0      5       7.08       75.75        0.0        0.0     1762.8
   33.0    221       6.51       63.71        0.0        0.0        5.0
  TOTAL    226      13.59      139.47        0.0        0.0     1767.9
```

ACDC, normal running conditions:

```
************************  SUMMARY FOR COMPLETE SYSTEM  ************************

                                  SYSTEM SWING BUS SUMMARY
 X------ SWING BUS ------X X---- AREA -----X X---- ZONE -----X
 BUS# X-- NAME --X BASKV    # X-- NAME --X    # X-- NAME --X       MW       MVAR   MVABASE
  1       GRID    300.00    1                 1                  35.0      12.7   1000.0
  112 OFFSH HVDC  195.00    1                 1                -265.4     -68.4     570.0
  212 OFFSH HVDC 2195.00    1                 1                -265.4     -68.4     570.0

224 BUSES     113 PLANTS      113 MACHINES          4 FIXED SHUNTS     0 SWITCHED SHUNTS
1 LOADS     228 BRANCHES    113 TRANSFORMERS       0 DC LINES         0 FACTS DEVICES

                         X------ ACTUAL ------X X----- NOMINAL ------X
                                MW        MVAR         MW        MVAR
 FROM GENERATION              549.3     -185.4       549.3     -185.4
 TO CONSTANT POWER LOAD       540.0        0.0       540.0        0.0
 TO CONSTANT CURRENT            0.0        0.0         0.0        0.0
 TO CONSTANT ADMITTANCE         0.0        0.0         0.0        0.0
 TO BUS SHUNT                   0.0     -342.0         0.0     -342.0
 TO FACTS DEVICE SHUNT          0.0        0.0         0.0        0.0
 TO LINE SHUNT                  0.0        0.0         0.0        0.0
 FROM LINE CHARGING             0.0        5.2         0.0        5.0

  VOLTAGE       X----- LOSSES -----X   X-- LINE SHUNTS --X   CHARGING
  LEVEL BRANCHES      MW        MVAR        MW        MVAR       MVAR
  300.0      1       0.00       0.00        0.0        0.0        0.0
  195.0      3       0.00      39.40        0.0        0.0        0.0
  132.0      2       3.28      60.88        0.0        0.0        0.0
   33.0    222       5.97      61.52        0.0        0.0        5.2
  TOTAL    228       9.25     161.80        0.0        0.0        5.2
```

ACDC, worst case:

```
************************  SUMMARY FOR COMPLETE SYSTEM  ************************

                                  SYSTEM SWING BUS SUMMARY
 X------ SWING BUS ------X X---- AREA -----X X---- ZONE -----X
BUS# X-- NAME --X BASKV    # X-- NAME --X    # X-- NAME --X       MW       MVAR   MVABASE
 1       GRID    300.00    1                 1                  35.6      12.6   1000.0
 112 OFFSH HVDC  195.00    1                 1                -265.1     -68.4     570.0
 212 OFFSH HVDC 2195.00    1                 1                -265.1     -68.4     570.0

224 BUSES     113 PLANTS      113 MACHINES          4 FIXED SHUNTS     0 SWITCHED SHUNTS
1 LOADS     227 BRANCHES    113 TRANSFORMERS       0 DC LINES         0 FACTS DEVICES

                         X------ ACTUAL ------X X----- NOMINAL ------X
                                MW        MVAR         MW        MVAR
 FROM GENERATION              549.9     -182.5       549.9     -182.5
 TO CONSTANT POWER LOAD       540.0        0.0       540.0        0.0
 TO CONSTANT CURRENT            0.0        0.0         0.0        0.0
 TO CONSTANT ADMITTANCE         0.0        0.0         0.0        0.0
 TO BUS SHUNT                   0.0     -342.0         0.0     -342.0
 TO FACTS DEVICE SHUNT          0.0        0.0         0.0        0.0
 TO LINE SHUNT                  0.0        0.0         0.0        0.0
 FROM LINE CHARGING             0.0        4.9         0.0        4.8

  VOLTAGE       X----- LOSSES -----X   X-- LINE SHUNTS --X   CHARGING
  LEVEL BRANCHES      MW        MVAR        MW        MVAR       MVAR
```

300.0	1	0.00	0.00	0.0	0.0	0.0
195.0	3	0.00	39.31	0.0	0.0	0.0
132.0	2	3.27	60.74	0.0	0.0	0.0
33.0	221	6.58	64.40	0.0	0.0	4.9
TOTAL	227	9.85	164.45	0.0	0.0	4.9

Shared loop design

ACAC, normal running conditions:

```
************************  SUMMARY FOR COMPLETE SYSTEM  ************************

                                  SYSTEM SWING BUS SUMMARY
 X------ SWING BUS ------X X---- AREA -----X X---- ZONE -----X
 BUS# X-- NAME --X BASKV    # X-- NAME --X    # X-- NAME --X       MW       MVAR   MVABASE
    1 PCC          400.00    1                 1                  14.5       0.0    1000.0

235 BUSES     110 PLANTS      110 MACHINES          2 FIXED SHUNTS     0 SWITCHED SHUNTS
1 LOADS     248 BRANCHES    109 TRANSFORMERS       0 DC LINES         0 FACTS DEVICES

                         X------ ACTUAL ------X X----- NOMINAL ------X
                                  MW        MVAR         MW        MVAR
 FROM GENERATION                554.5      -17.8       554.5      -17.8
 TO CONSTANT POWER LOAD         540.0        0.0       540.0        0.0
 TO CONSTANT CURRENT              0.0        0.0         0.0        0.0
 TO CONSTANT ADMITTANCE           0.0        0.0         0.0        0.0
 TO BUS SHUNT                     0.0     1611.7         0.0     1611.7
 TO FACTS DEVICE SHUNT            0.0        0.0         0.0        0.0
 TO LINE SHUNT                    0.0        0.0         0.0        0.0
 FROM LINE CHARGING               0.0     1772.4         0.0     1718.1

  VOLTAGE       X----- LOSSES -----X   X-- LINE SHUNTS --X   CHARGING
  LEVEL BRANCHES      MW        MVAR        MW        MVAR       MVAR
  400.0      5       7.07      75.57        0.0        0.0     1762.8
   33.0    231       7.47      67.33        0.0        0.0        9.5
    0.0     12       0.00       0.00        0.0        0.0        0.0
  TOTAL    248      14.54     142.90        0.0        0.0     1772.4
```

ACAC, worst case:

```
************************  SUMMARY FOR COMPLETE SYSTEM  ************************

                                  SYSTEM SWING BUS SUMMARY
 X------ SWING BUS ------X X---- AREA -----X X---- ZONE -----X
 BUS# X-- NAME --X BASKV    # X-- NAME --X    # X-- NAME --X       MW       MVAR   MVABASE
    1 PCC          400.00    1                 1                  15.0       0.0    1000.0

235 BUSES     110 PLANTS      110 MACHINES          2 FIXED SHUNTS     0 SWITCHED SHUNTS
1 LOADS     247 BRANCHES    109 TRANSFORMERS       0 DC LINES         0 FACTS DEVICES

                         X------ ACTUAL ------X X----- NOMINAL ------X
                                  MW        MVAR         MW        MVAR
 FROM GENERATION                555.0      -15.1       555.0      -15.1
 TO CONSTANT POWER LOAD         540.0        0.0       540.0        0.0
 TO CONSTANT CURRENT              0.0        0.0         0.0        0.0
 TO CONSTANT ADMITTANCE           0.0        0.0         0.0        0.0
 TO BUS SHUNT                     0.0     1611.7         0.0     1611.7
 TO FACTS DEVICE SHUNT            0.0        0.0         0.0        0.0
 TO LINE SHUNT                    0.0        0.0         0.0        0.0
 FROM LINE CHARGING               0.0     1771.8         0.0     1717.6

  VOLTAGE       X----- LOSSES -----X   X-- LINE SHUNTS --X   CHARGING
  LEVEL BRANCHES      MW        MVAR        MW        MVAR       MVAR
  400.0      5       7.06      75.47        0.0        0.0     1762.8
   33.0    230       7.98      69.60        0.0        0.0        9.0
    0.0     12       0.00       0.00        0.0        0.0        0.0
```

TOTAL	247	15.04	145.07	0.0	0.0	1771.8

ACDC, normal running conditions:

```
************************  SUMMARY FOR COMPLETE SYSTEM  ************************

                                  SYSTEM SWING BUS SUMMARY
 X------ SWING BUS ------X X---- AREA -----X X---- ZONE -----X
 BUS# X-- NAME --X BASKV    # X-- NAME --X    # X-- NAME --X       MW       MVAR   MVABASE
    1 GRID        300.00    1                 1                  36.6      12.6    1000.0
    112 OFFSH HVDC  195.00    1                   1               -264.6     -68.5   570.0
    212 OFFSH HVDC 2195.00    1                   1               -264.6     -68.5   570.0

239 BUSES     113 PLANTS      113 MACHINES          4 FIXED SHUNTS     0 SWITCHED SHUNTS
1 LOADS     249 BRANCHES    113 TRANSFORMERS       0 DC LINES         0 FACTS DEVICES

                         X------ ACTUAL ------X X----- NOMINAL ------X
                                 MW        MVAR         MW        MVAR
 FROM GENERATION              550.8     -183.8       550.8     -183.8
 TO CONSTANT POWER LOAD       540.0        0.0       540.0        0.0
 TO CONSTANT CURRENT            0.0        0.0         0.0        0.0
 TO CONSTANT ADMITTANCE         0.0        0.0         0.0        0.0
 TO BUS SHUNT                   0.0     -342.0         0.0     -342.0
 TO FACTS DEVICE SHUNT          0.0        0.0         0.0        0.0
 TO LINE SHUNT                  0.0        0.0         0.0        0.0
 FROM LINE CHARGING             0.0        9.3         0.0        9.1

  VOLTAGE       X----- LOSSES -----X   X-- LINE SHUNTS --X   CHARGING
  LEVEL BRANCHES      MW        MVAR        MW        MVAR       MVAR
  300.0      3       0.00      25.19        0.0        0.0        0.0
  195.0      2       0.00      27.94        0.0        0.0        0.0
  132.0      1       3.26      46.56        0.0        0.0        0.0
   33.0    231       7.54      67.87        0.0        0.0        9.3
    0.0     12       0.00       0.00        0.0        0.0        0.0
  TOTAL    249      10.80     167.56        0.0        0.0        9.3
```

ACDC, worst case:

```
************************  SUMMARY FOR COMPLETE SYSTEM  ************************

                                  SYSTEM SWING BUS SUMMARY
 X------ SWING BUS ------X X---- AREA -----X X---- ZONE -----X
 BUS# X-- NAME --X BASKV    # X-- NAME --X    # X-- NAME --X       MW       MVAR   MVABASE
      1 GRID        300.00    1                 1                  37.2      12.6 1000.0
    112 OFFSH HVDC  195.00    1                   1               -264.3     -68.5  570.0
    212 OFFSH HVDC 2195.00    1                   1               -264.3     -68.5  570.0

239 BUSES     113 PLANTS      113 MACHINES          4 FIXED SHUNTS     0 SWITCHED SHUNTS
1 LOADS     246 BRANCHES    113 TRANSFORMERS       0 DC LINES         0 FACTS DEVICES

                         X------ ACTUAL ------X X----- NOMINAL ------X
                                 MW        MVAR         MW        MVAR
 FROM GENERATION              551.3     -181.1       551.3     -181.1
 TO CONSTANT POWER LOAD       540.0        0.0       540.0        0.0
 TO CONSTANT CURRENT            0.0        0.0         0.0        0.0
 TO CONSTANT ADMITTANCE         0.0        0.0         0.0        0.0
 TO BUS SHUNT                   0.0     -342.0         0.0     -342.0
 TO FACTS DEVICE SHUNT          0.0        0.0         0.0        0.0
 TO LINE SHUNT                  0.0        0.0         0.0        0.0
 FROM LINE CHARGING             0.0        8.8         0.0        8.6

  VOLTAGE       X----- LOSSES -----X   X-- LINE SHUNTS --X   CHARGING
```

LEVEL	BRANCHES	MW	MVAR	MW	MVAR	MVAR
300.0	3	0.00	25.13	0.0	0.0	0.0
195.0	2	0.00	27.88	0.0	0.0	0.0
132.0	1	3.25	46.47	0.0	0.0	0.0
33.0	229	8.07	70.26	0.0	0.0	8.8
0.0	11	0.00	0.00	0.0	0.0	0.0
TOTAL	246	11.33	169.74	0.0	0.0	8.8

N-sided loop design (N=4)

ACAC, normal running conditions:

```
************************  SUMMARY FOR COMPLETE SYSTEM  ************************

                                  SYSTEM SWING BUS SUMMARY
 X------ SWING BUS ------X X---- AREA -----X X---- ZONE -----X
 BUS# X-- NAME --X BASKV    # X-- NAME --X    # X-- NAME --X       MW       MVAR   MVABASE
      1 PCC         400.00    1                  1                  12.6       0.0 1000.0

220 BUSES     110 PLANTS      110 MACHINES          2 FIXED SHUNTS     0 SWITCHED SHUNTS
1 LOADS     230 BRANCHES    109 TRANSFORMERS       0 DC LINES         0 FACTS DEVICES

                         X------ ACTUAL ------X X----- NOMINAL ------X
                                  MW        MVAR         MW        MVAR
 FROM GENERATION                552.6      -29.3       552.6      -29.3
 TO CONSTANT POWER LOAD         540.0        0.0       540.0        0.0
 TO CONSTANT CURRENT              0.0        0.0         0.0        0.0
 TO CONSTANT ADMITTANCE           0.0        0.0         0.0        0.0
 TO BUS SHUNT                     0.0     1611.4         0.0     1611.4
 TO FACTS DEVICE SHUNT            0.0        0.0         0.0        0.0
 TO LINE SHUNT                    0.0        0.0         0.0        0.0
 FROM LINE CHARGING               0.0     1784.8         0.0     1730.1

  VOLTAGE       X----- LOSSES -----X   X-- LINE SHUNTS --X   CHARGING
  LEVEL BRANCHES      MW        MVAR        MW        MVAR       MVAR
  400.0      5       7.10       75.95       0.0         0.0     1762.8
   33.0    225       5.46       68.09       0.0         0.0       21.9
  TOTAL    230      12.56      144.04       0.0         0.0     1784.8
```

ACAC, worst case:

```
************************  SUMMARY FOR COMPLETE SYSTEM  ************************
                                  SYSTEM SWING BUS SUMMARY
 X------ SWING BUS ------X X---- AREA -----X X---- ZONE -----X
 BUS# X-- NAME --X BASKV    # X-- NAME --X    # X-- NAME --X       MW       MVAR   MVABASE
      1 PCC         400.00    1                  1                  12.9       0.0 1000.0

220 BUSES     110 PLANTS      110 MACHINES          2 FIXED SHUNTS     0 SWITCHED SHUNTS
1 LOADS     229 BRANCHES    109 TRANSFORMERS       0 DC LINES         0 FACTS DEVICES

                         X------ ACTUAL ------X X----- NOMINAL ------X
                                  MW        MVAR         MW        MVAR
 FROM GENERATION                552.9      -25.2       552.9      -25.2
 TO CONSTANT POWER LOAD         540.0        0.0       540.0        0.0
 TO CONSTANT CURRENT              0.0        0.0         0.0        0.0
 TO CONSTANT ADMITTANCE           0.0        0.0         0.0        0.0
 TO BUS SHUNT                     0.0     1611.4         0.0     1611.4
 TO FACTS DEVICE SHUNT            0.0        0.0         0.0        0.0
 TO LINE SHUNT                    0.0        0.0         0.0        0.0
 FROM LINE CHARGING               0.0     1783.8         0.0     1729.2

  VOLTAGE       X----- LOSSES -----X   X-- LINE SHUNTS --X   CHARGING
  LEVEL BRANCHES      MW        MVAR        MW        MVAR       MVAR
  400.0      5       7.09       75.89       0.0         0.0     1762.8
   33.0    224       5.81       71.31       0.0         0.0       21.0
  TOTAL    229      12.91      147.20       0.0         0.0     1783.8
```

ACDC, normal running conditions:

```
************************  SUMMARY FOR COMPLETE SYSTEM  ************************

                                  SYSTEM SWING BUS SUMMARY
 X------ SWING BUS ------X X---- AREA -----X X---- ZONE -----X
 BUS# X-- NAME --X BASKV    # X-- NAME --X    # X-- NAME --X       MW       MVAR   MVABASE
      1 PCC         300.00    1                 1                  34.6      12.7 1000.0
    112 OFFSH HVDC  195.00    1                 1                -265.6     -68.4  570.0
    212 OFFSH HVDC 2195.00    1                 1                -265.6     -68.4  570.0

224 BUSES     113 PLANTS      113 MACHINES          4 FIXED SHUNTS     0 SWITCHED SHUNTS
1 LOADS     231 BRANCHES    113 TRANSFORMERS       0 DC LINES         0 FACTS DEVICES

                         X------ ACTUAL ------X X----- NOMINAL ------X
                                MW        MVAR         MW        MVAR
 FROM GENERATION              548.8     -194.9       548.8     -194.9
 TO CONSTANT POWER LOAD       540.0        0.0       540.0        0.0
 TO CONSTANT CURRENT            0.0        0.0         0.0        0.0
 TO CONSTANT ADMITTANCE         0.0        0.0         0.0        0.0
 TO BUS SHUNT                   0.0     -342.0         0.0     -342.0
 TO FACTS DEVICE SHUNT          0.0        0.0         0.0        0.0
 TO LINE SHUNT                  0.0        0.0         0.0        0.0
 FROM LINE CHARGING             0.0       21.5         0.0       21.1

  VOLTAGE       X----- LOSSES -----X   X-- LINE SHUNTS --X   CHARGING
  LEVEL BRANCHES      MW        MVAR        MW        MVAR       MVAR
  300.0      2       0.00      12.69        0.0        0.0        0.0
  195.0      3       0.00      40.85        0.0        0.0        0.0
  132.0      1       3.28      46.92        0.0        0.0        0.0
   33.0    225       5.48      68.16        0.0        0.0       21.5
  TOTAL    231       8.76     168.61        0.0        0.0       21.5
```

ACDC, worst case:

```
************************  SUMMARY FOR COMPLETE SYSTEM  ************************

                                  SYSTEM SWING BUS SUMMARY
 X------ SWING BUS ------X X---- AREA -----X X---- ZONE -----X
 BUS# X-- NAME --X BASKV    # X-- NAME --X    # X-- NAME --X       MW       MVAR   MVABASE
      1 PCC         300.00    1                 1                  35.3      12.7 1000.0
    112 OFFSH HVDC  195.00    1                 1                -265.4     -68.4  570.0
    212 OFFSH HVDC 2195.00    1                 1                -265.4     -68.4  570.0

224 BUSES     113 PLANTS      113 MACHINES          4 FIXED SHUNTS     0 SWITCHED SHUNTS
1 LOADS     230 BRANCHES    113 TRANSFORMERS       0 DC LINES         0 FACTS DEVICES

                         X------ ACTUAL ------X X----- NOMINAL ------X
                                MW        MVAR         MW        MVAR
 FROM GENERATION              549.1     -190.9       549.1     -190.9
 TO CONSTANT POWER LOAD       540.0        0.0       540.0        0.0
 TO CONSTANT CURRENT            0.0        0.0         0.0        0.0
 TO CONSTANT ADMITTANCE         0.0        0.0         0.0        0.0
 TO BUS SHUNT                   0.0     -342.0         0.0     -342.0
 TO FACTS DEVICE SHUNT          0.0        0.0         0.0        0.0
 TO LINE SHUNT                  0.0        0.0         0.0        0.0
 FROM LINE CHARGING             0.0       20.7         0.0       20.1

  VOLTAGE       X----- LOSSES -----X   X-- LINE SHUNTS --X   CHARGING
  LEVEL BRANCHES      MW        MVAR        MW        MVAR       MVAR
```

300.0	2	0.00	12.67	0.0	0.0	0.0
195.0	3	0.00	40.76	0.0	0.0	0.0
132.0	1	3.28	46.86	0.0	0.0	0.0
33.0	224	5.83	71.42	0.0	0.0	20.7
TOTAL	230	9.11	171.71	0.0	0.0	20.7

Star design

ACAC, normal running conditions:

```
************************  SUMMARY FOR COMPLETE SYSTEM  ************************

                                  SYSTEM SWING BUS SUMMARY
 X------ SWING BUS ------X X---- AREA -----X X---- ZONE -----X
 BUS# X-- NAME --X BASKV    # X-- NAME --X    # X-- NAME --X       MW       MVAR   MVABASE
      1 PCC         400.00    1                 1                   22.5       0.0 1000.0

232 BUSES     110 PLANTS      110 MACHINES          2 FIXED SHUNTS     0 SWITCHED SHUNTS
1 LOADS     233 BRANCHES    121 TRANSFORMERS       0 DC LINES         0 FACTS DEVICES

                         X------ ACTUAL ------X X----- NOMINAL ------X
                                  MW        MVAR         MW        MVAR
 FROM GENERATION               562.5        30.6       562.5        30.6
 TO CONSTANT POWER LOAD        540.0         0.0       540.0         0.0
 TO CONSTANT CURRENT             0.0         0.0         0.0         0.0
 TO CONSTANT ADMITTANCE          0.0         0.0         0.0         0.0
 TO BUS SHUNT                    0.0      1612.8         0.0      1612.8
 TO FACTS DEVICE SHUNT           0.0         0.0         0.0         0.0
 TO LINE SHUNT                   0.0         0.0         0.0         0.0
 FROM LINE CHARGING              0.0      1770.2         0.0      1716.1

  VOLTAGE       X----- LOSSES -----X   X-- LINE SHUNTS --X   CHARGING
  LEVEL BRANCHES      MW        MVAR        MW        MVAR       MVAR
  400.0      5       6.95       74.05       0.0         0.0     1762.8
   33.0     15       4.65       29.42       0.0         0.0        6.2
   11.0    213      10.86       84.56       0.0         0.0        1.1
  TOTAL    233      22.45      188.04       0.0         0.0     1770.2
```

ACAC, worst case:

```
************************  SUMMARY FOR COMPLETE SYSTEM  ************************

                                  SYSTEM SWING BUS SUMMARY
 X------ SWING BUS ------X X---- AREA -----X X---- ZONE -----X
 BUS# X-- NAME --X BASKV    # X-- NAME --X    # X-- NAME --X       MW       MVAR   MVABASE
      1 PCC         400.00    1                 1                   65.6       0.0 1000.0

213 BUSES     101 PLANTS      101 MACHINES          2 FIXED SHUNTS     0 SWITCHED SHUNTS
1 LOADS     214 BRANCHES    111 TRANSFORMERS       0 DC LINES         0 FACTS DEVICES

                         X------ ACTUAL ------X X----- NOMINAL ------X
                                  MW        MVAR         MW        MVAR
 FROM GENERATION               560.6        14.5       560.6        14.5
 TO CONSTANT POWER LOAD        540.0         0.0       540.0         0.0
 TO CONSTANT CURRENT             0.0         0.0         0.0         0.0
 TO CONSTANT ADMITTANCE          0.0         0.0         0.0         0.0
 TO BUS SHUNT                    0.0      1612.8         0.0      1612.8
 TO FACTS DEVICE SHUNT           0.0         0.0         0.0         0.0
 TO LINE SHUNT                   0.0         0.0         0.0         0.0
 FROM LINE CHARGING              0.0      1769.6         0.0      1715.5

  VOLTAGE       X----- LOSSES -----X   X-- LINE SHUNTS --X   CHARGING
  LEVEL BRANCHES      MW        MVAR        MW        MVAR       MVAR
  400.0      5       6.33       66.20       0.0         0.0     1762.8
   33.0     14       4.35       28.11       0.0         0.0        5.7
   11.0    195       9.94       76.95       0.0         0.0        1.0
```

TOTAL	214	20.62	171.27	0.0	0.0	1769.6

ACDC, normal running conditions:

```
************************  SUMMARY FOR COMPLETE SYSTEM  ************************

                                SYSTEM SWING BUS SUMMARY
 X------ SWING BUS ------X X---- AREA -----X X---- ZONE -----X
 BUS# X-- NAME --X BASKV    # X-- NAME --X    # X-- NAME --X       MW       MVAR   MVABASE
      1 PCC         300.00    1                 1                  44.2      12.2 1000.0
    122 OFFSH HVDC  195.00    1                 1                -260.6     -78.7  570.0
    222 OFFSH HVDC 2195.00    1                 1                -260.6     -78.7  570.0

236 BUSES     113 PLANTS      113 MACHINES          4 FIXED SHUNTS     0 SWITCHED SHUNTS
1 LOADS     234 BRANCHES    125 TRANSFORMERS       0 DC LINES         0 FACTS DEVICES

                         X------ ACTUAL ------X X----- NOMINAL ------X
                                MW        MVAR         MW        MVAR
 FROM GENERATION              558.7     -138.4       558.7     -138.4
 TO CONSTANT POWER LOAD       540.0        0.0       540.0        0.0
 TO CONSTANT CURRENT            0.0        0.0         0.0        0.0
 TO CONSTANT ADMITTANCE         0.0        0.0         0.0        0.0
 TO BUS SHUNT                   0.0     -342.0         0.0     -342.0
 TO FACTS DEVICE SHUNT          0.0        0.0         0.0        0.0
 TO LINE SHUNT                  0.0        0.0         0.0        0.0
 FROM LINE CHARGING             0.0        7.4         0.0        7.0

  VOLTAGE       X----- LOSSES -----X   X-- LINE SHUNTS --X   CHARGING
  LEVEL BRANCHES      MW        MVAR        MW        MVAR       MVAR
  300.0      3       0.00      24.43        0.0        0.0        0.0
  195.0      2       0.00      27.01        0.0        0.0        0.0
  132.0      1       3.15      45.02        0.0        0.0        0.0
   33.0     15       4.68      29.61        0.0        0.0        6.2
   11.0    213      10.90      84.90        0.0        0.0        1.2
  TOTAL    234      18.73     210.96        0.0        0.0        7.4
```

ACDC, worst case:

```
************************  SUMMARY FOR COMPLETE SYSTEM  ************************

                                SYSTEM SWING BUS SUMMARY
 X------ SWING BUS ------X X---- AREA -----X X---- ZONE -----X
 BUS# X-- NAME --X BASKV    # X-- NAME --X    # X-- NAME --X       MW       MVAR   MVABASE
      1 PCC         300.00    1                 1                  86.2      10.2 1000.0
    122 OFFSH HVDC  195.00    1                 1                -239.0     -79.8  570.0
    222 OFFSH HVDC 2195.00    1                 1                -239.0     -79.8  570.0

217 BUSES     104 PLANTS      104 MACHINES          4 FIXED SHUNTS     0 SWITCHED SHUNTS
1 LOADS     215 BRANCHES    115 TRANSFORMERS       0 DC LINES         0 FACTS DEVICES

                         X------ ACTUAL ------X X----- NOMINAL ------X
                                MW        MVAR         MW        MVAR
 FROM GENERATION              556.9     -162.6       556.9     -162.6
 TO CONSTANT POWER LOAD       540.0        0.0       540.0        0.0
 TO CONSTANT CURRENT            0.0        0.0         0.0        0.0
 TO CONSTANT ADMITTANCE         0.0        0.0         0.0        0.0
 TO BUS SHUNT                   0.0     -342.0         0.0     -342.0
 TO FACTS DEVICE SHUNT          0.0        0.0         0.0        0.0
 TO LINE SHUNT                  0.0        0.0         0.0        0.0
 FROM LINE CHARGING             0.0        6.7         0.0        6.4
```

VOLTAGE LEVEL	BRANCHES	X----- LOSSES -----X MW	MVAR	X-- LINE SHUNTS --X MW	MVAR	CHARGING MVAR
300.0	3	0.00	20.47	0.0	0.0	0.0
195.0	2	0.00	22.71	0.0	0.0	0.0
132.0	1	2.65	37.86	0.0	0.0	0.0
33.0	14	4.36	28.16	0.0	0.0	5.6
11.0	195	9.93	76.91	0.0	0.0	1.1
TOTAL	215	16.95	186.12	0.0	0.0	6.7

Appendix 2: Load flow figures

PU-curves used to set up the simulations:

AC transmission 2 lines											
RAD		**SS**		**DS**		**Shared**		**NS**		**Star**	
P	**U**	**P**	**U**	**P**	**U**	**P**	**U**	**P**	**U**	**P**	**U**
525,1	1,023	528,2	1,025	528,3	1,024	526,3	1,024	529,1	1,024	511,2	1,02
526,1	1,025	529,4	1,027	529,7	1,027	528,1	1,027	530,3	1,027	515,4	1,023
527,2	1,027	530,1	1,029	530,4	1,029	528,9	1,029	531	1,029	518,3	1,026
528,0	1,029	***530,6***	***1,031***	***530,9***	***1,031***	***529,5***	***1,031***	***531,5***	***1,031***	520,5	1,029
528,7	***1,031***	531	1,033	531,2	1,033	529,9	1,033	531,8	1,033	***521,5***	***1,031***
529,1	1,033	531,2	1,035	531,4	1,035	530,1	1,035	532	1,035	521,9	1,032
529,3	1,035	531,2	1,037	531,4	1,037	530,1	1,037	532	1,037	522,6	1,035
529,2	1,038	531	1,039	531,3	1,039	529,9	1,039	531,9	1,039	522,6	1,037

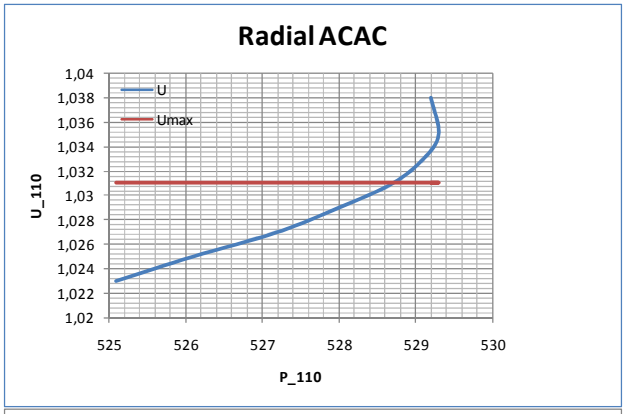
Radial ACAC
U
Umax
U_110
P_110
1,04
1,038
1,036
1,034
1,032
1,03
1,028
1,026
1,024
1,022
1,02
525
526
527
528
529
530

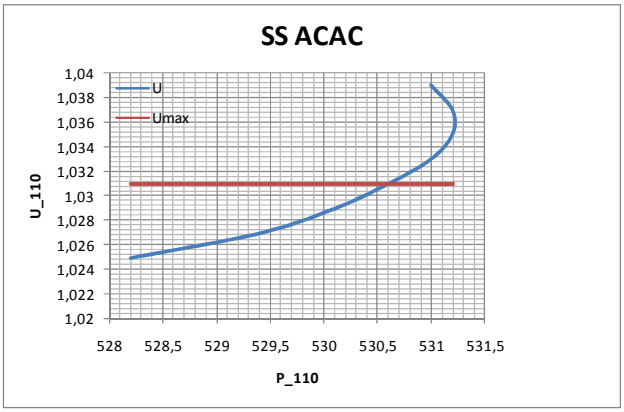
SS ACAC
U
Umax
U_110
P_110
1,04
1,038
1,036
1,034
1,032
1,03
1,028
1,026
1,024
1,022
1,02
528
528,5
529
529,5
530
530,5
531
531,5

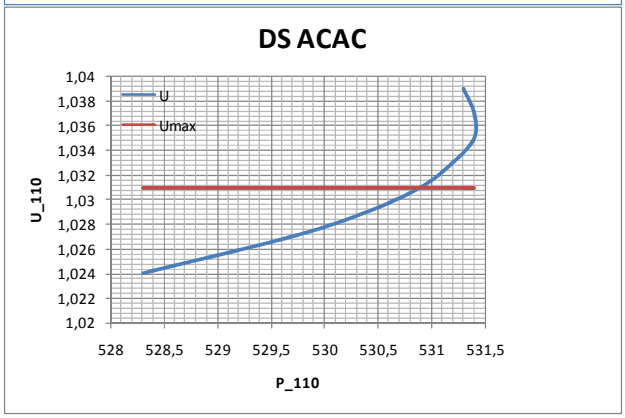
DS ACAC
U
Umax
U_110
P_110
1,04
1,038
1,036
1,034
1,032
1,03
1,028
1,026
1,024
1,022
1,02
528
528,5
529
529,5
530
530,5
531
531,5

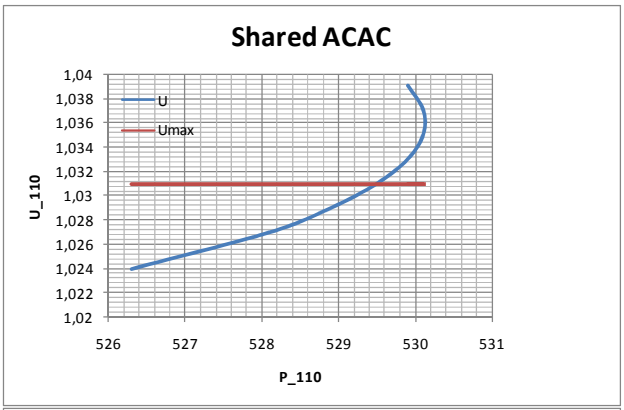
Shared ACAC
U
Umax
U_110
P_110
1,04
1,038
1,036
1,034
1,032
1,03
1,028
1,026
1,024
1,022
1,02
526
527
528
529
530
531

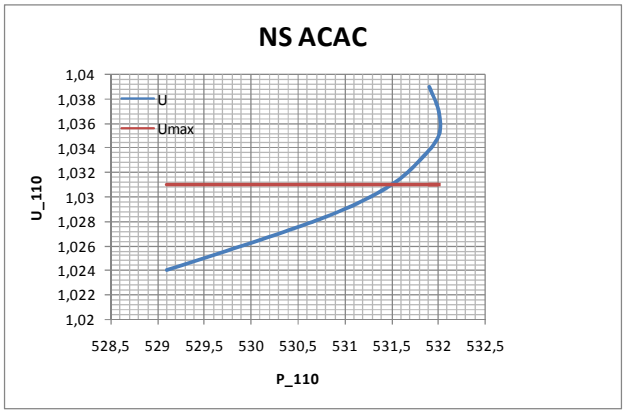
NS ACAC
U
Umax
U_110
P_110
1,04
1,038
1,036
1,034
1,032
1,03
1,028
1,026
1,024
1,022
1,02
528,5
529
529,5
530
530,5
531
531,5
532
532,5

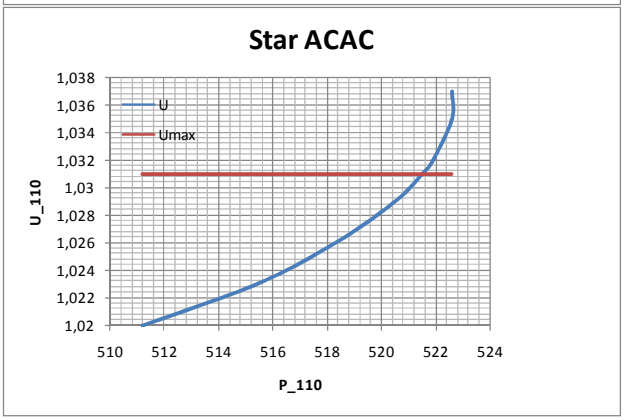
Star ACAC
U
Umax
U_110
P_110
1,038
1,036
1,034
1,032
1,03
1,028
1,026
1,024
1,022
1,02
510
512
514
516
518
520
522
524

DC, 2 Transmission lines											
RAD		SS		DS		Shared		NS		Star	
P	U	P	U	P	U	P	U	P	U	P	U
522	0,962	527,1	0,97	527,6	0,97	525,5	0,97	528,1	0,97	514,7	0,97
524,4	0,97	528,9	0,98	529,3	0,98	527,5	0,98	529,8	0,98	518,2	0,98
526,5	0,98	530	0,99	529,9	0,985	528,2	0,985	530,4	0,985	519,5	0,985
527,9	0,99	530,3	0,995	530,4	0,99	528,7	0,99	530,8	0,99	520,4	0,99
528,2	0,995	*530,5*	*0,998*	530,6	0,994	529	0,994	531,1	0,994	520,7	0,9925
528,4	*1*	530,5	1	*530,7*	*0,998*	*529,2*	*0,998*	531,2	0,997	521	0,995
528,4	1,002	530,5	1,0025	530,7	1	529,2	1	*531,3*	*1*	521,2	0,9975
528,4	1,004	530,5	1,005	530,7	1,003	529,2	1,005	531,3	1,005	*521,3*	*1*
528,4	1,005	530,4	1,0075	530,7	1,006	529,2	1,006	531,2	1,007	521,3	1,001

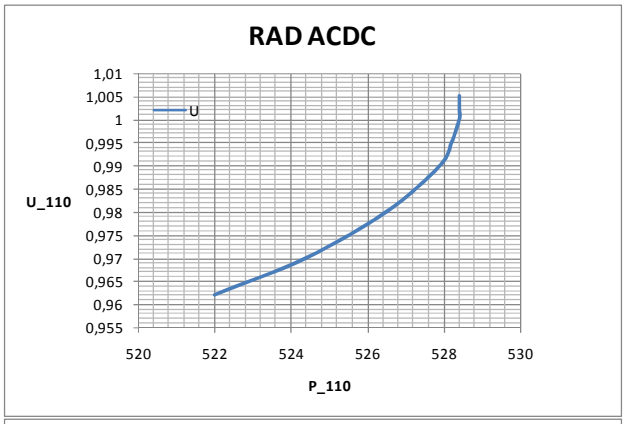
RAD ACDC
U_110
P_110
U
1,01
1,005
1
0,995
0,99
0,985
0,98
0,975
0,97
0,965
0,96
0,955
520
522
524
526
528
530

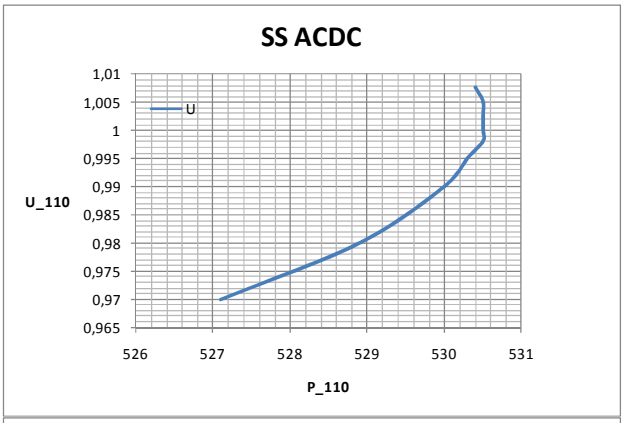
SS ACDC
U_110
P_110
U
1,01
1,005
1
0,995
0,99
0,985
0,98
0,975
0,97
0,965
526
527
528
529
530
531

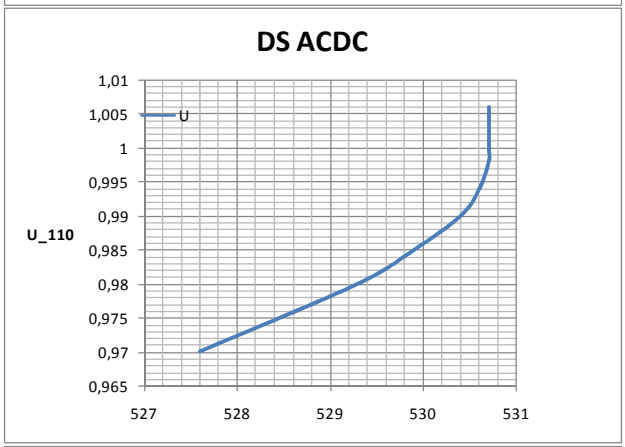
DS ACDC
U_110
U
1,01
1,005
1
0,995
0,99
0,985
0,98
0,975
0,97
0,965
527
528
529
530
531

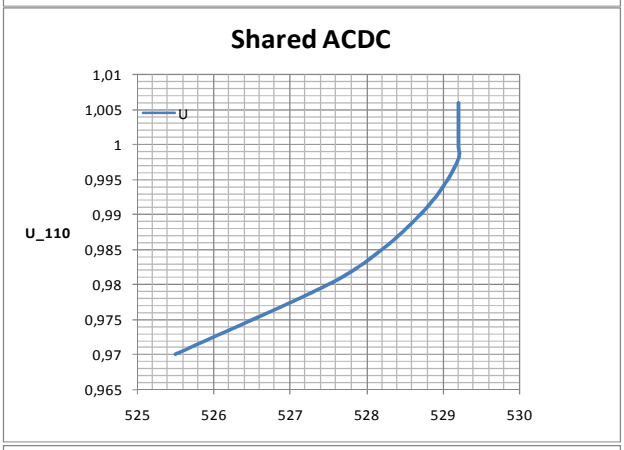
Shared ACDC
U_110
U
1,01
1,005
1
0,995
0,99
0,985
0,98
0,975
0,97
0,965
525
526
527
528
529
530

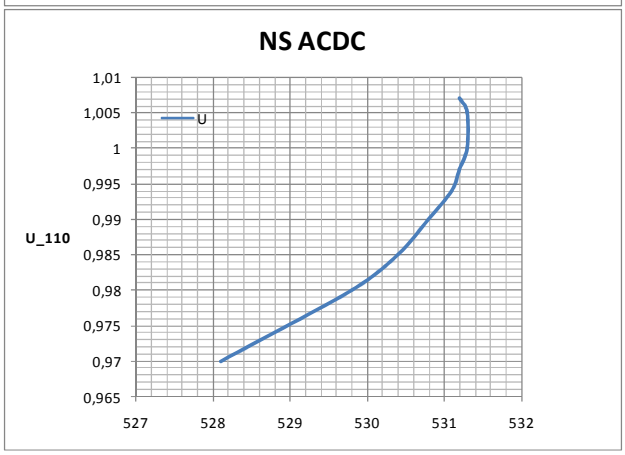
NS ACDC
U_110
U
1,01
1,005
1
0,995
0,99
0,985
0,98
0,975
0,97
0,965
527
528
529
530
531
532

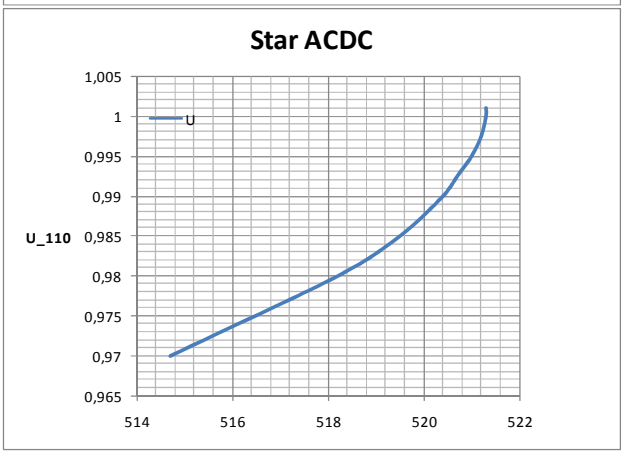
Star ACDC
U_110
U
1,005
1
0,995
0,99
0,985
0,98
0,975
0,97
0,965
514
516
518
520
522

Single line diagrams

In the following, single line diagrams showing the load flow situation for all cases are shown:

AC/AC:

Transmission, both lines operating

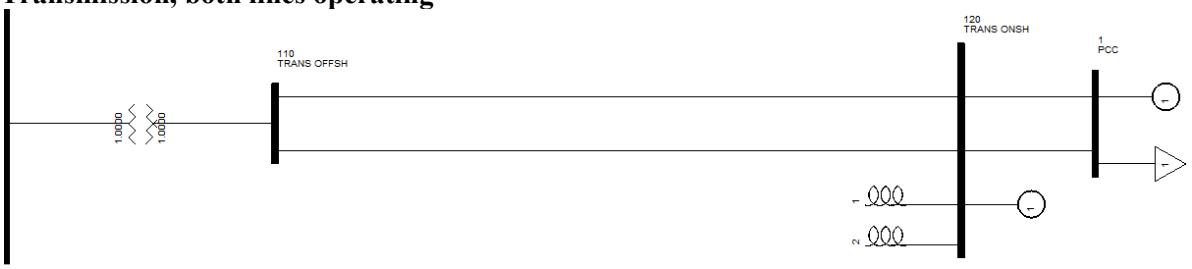

Transmission, one line operating

Radial design, entire system

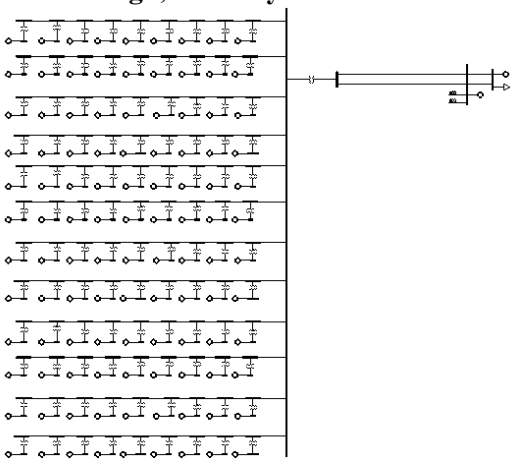

Radial design, transmission, OK

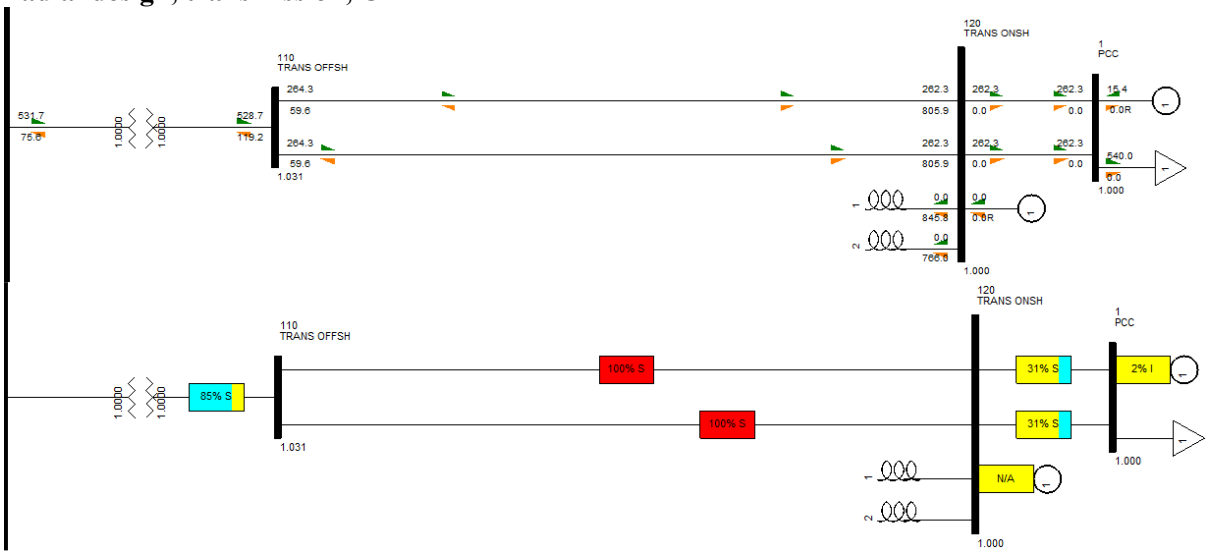

Radial design, feeder OK

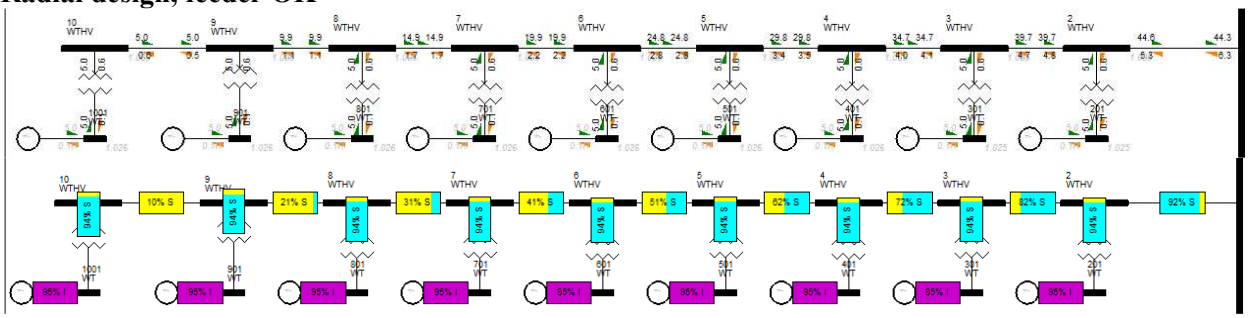

Radial design, transmission, worst case

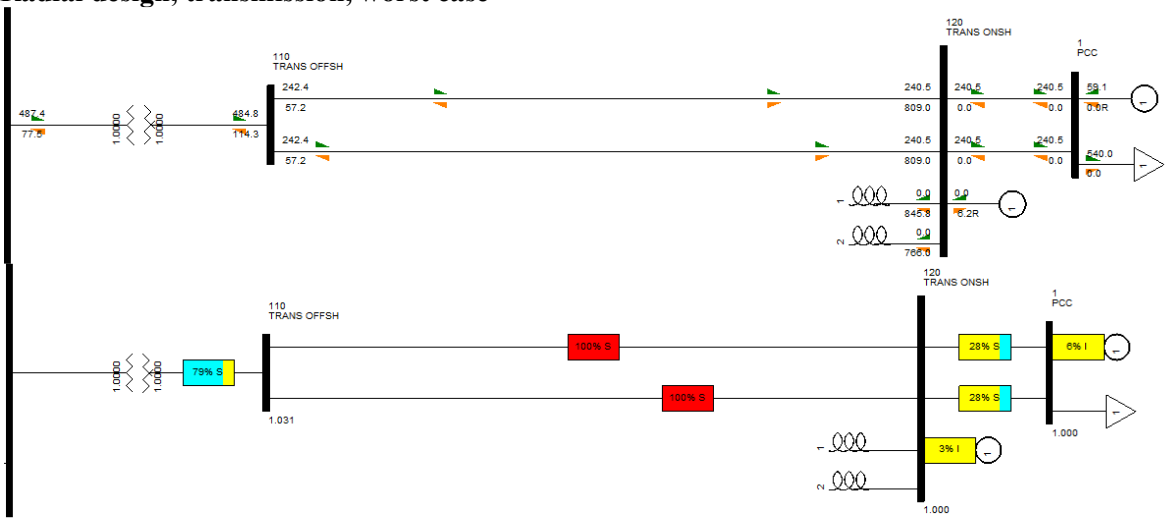

Radial design, feeder, worst case

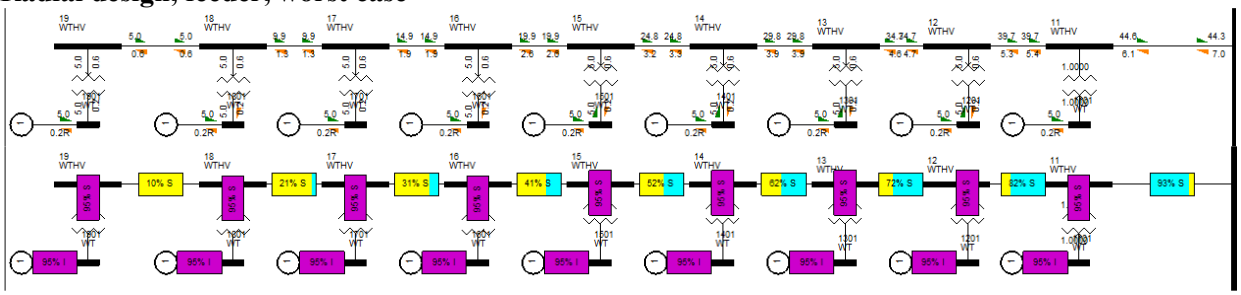

Single sided design, entire system

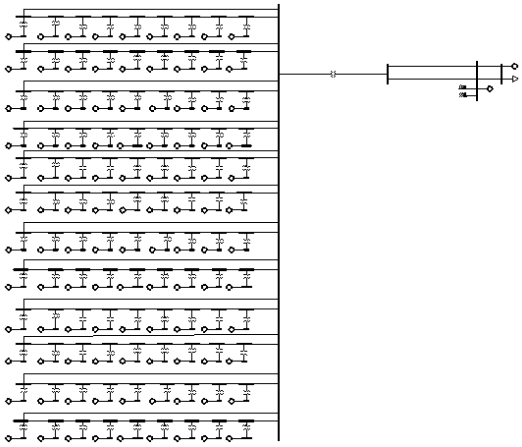

Single sided design, transmission, OK

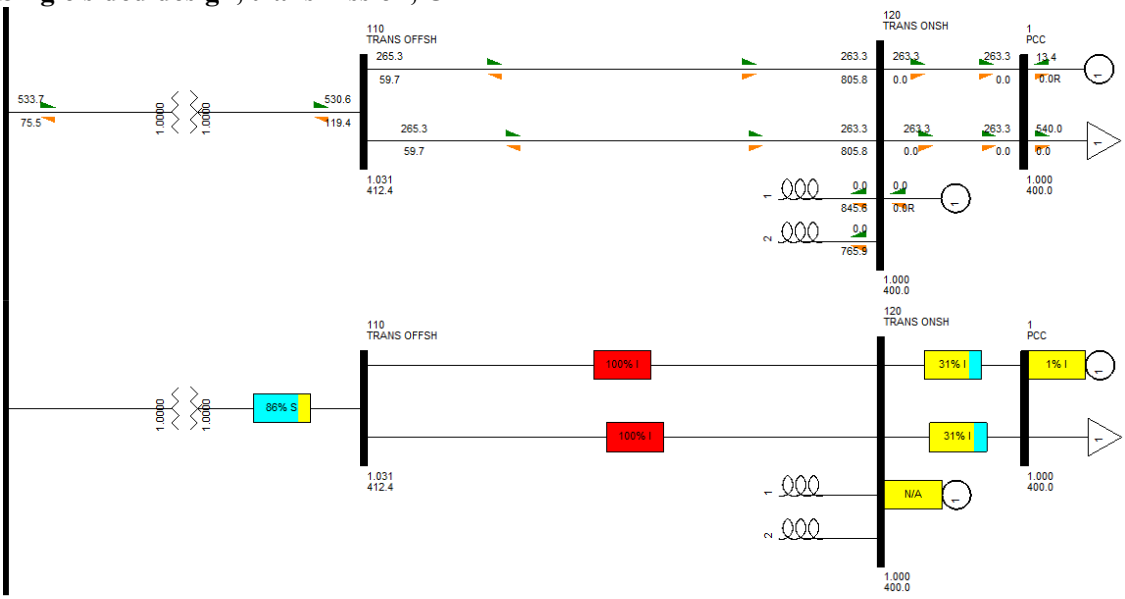

Single sided design, feeder OK

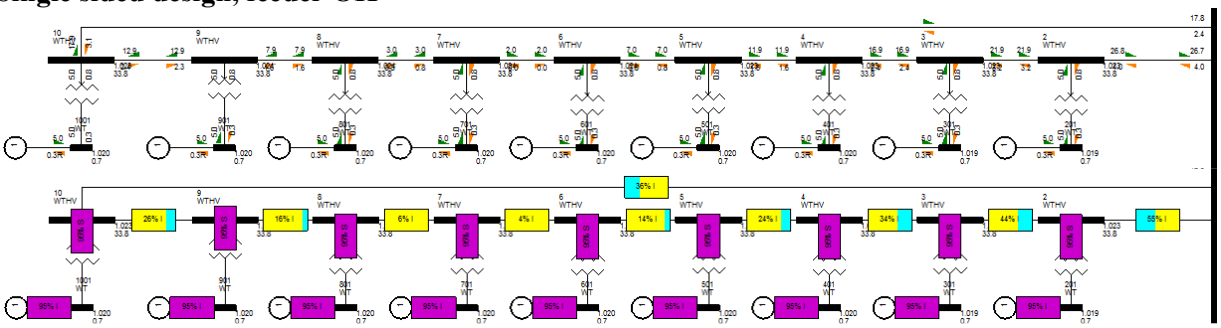

Single sided design, transmission, worst case

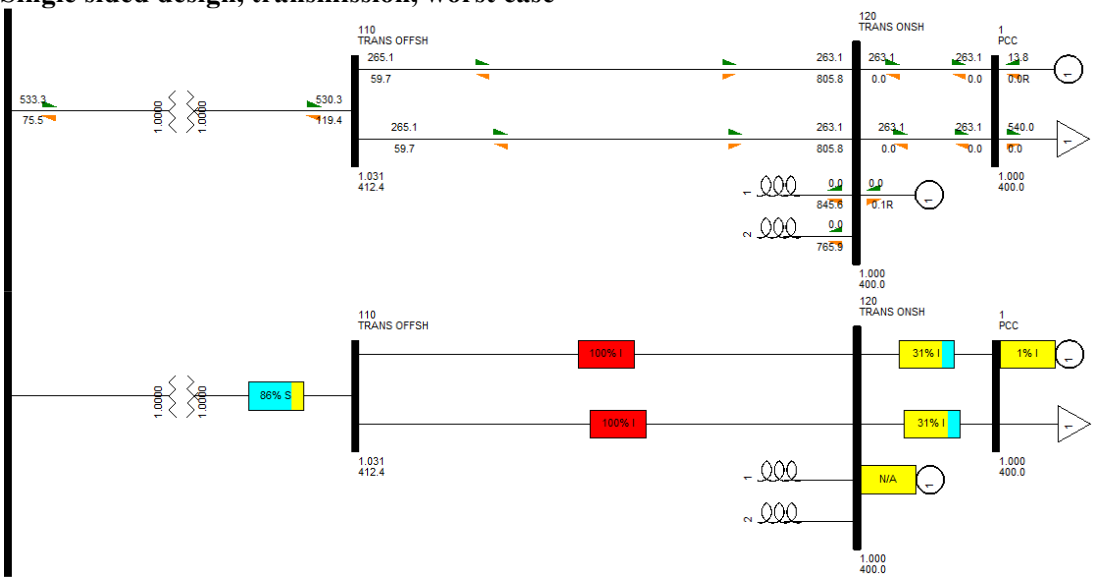

Single sided design, feeder worst case

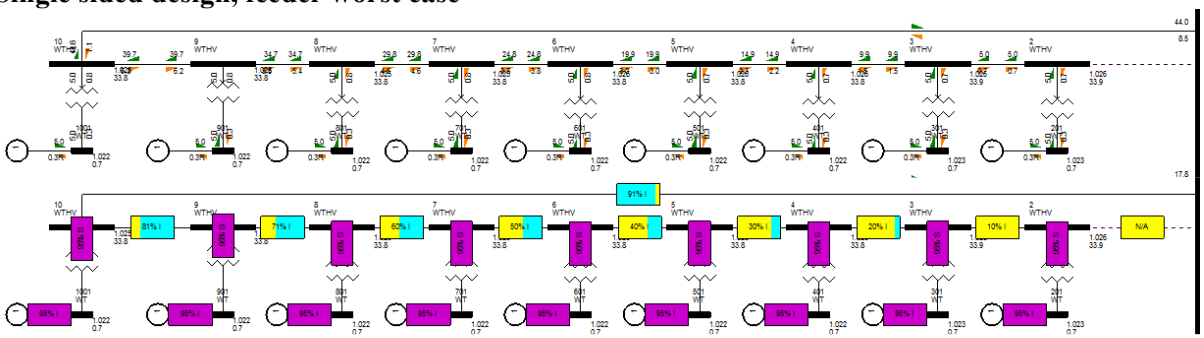

Double sided design, entire system

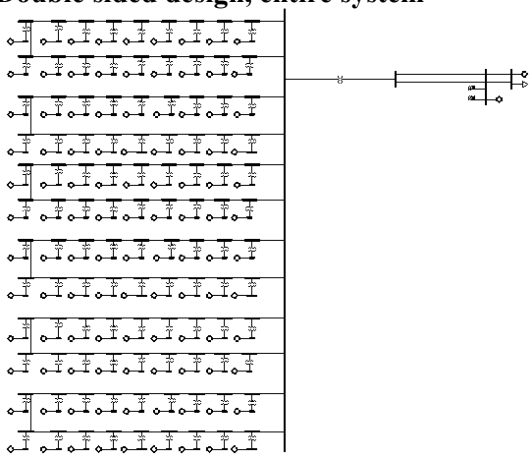

Double sided design, transmission, OK

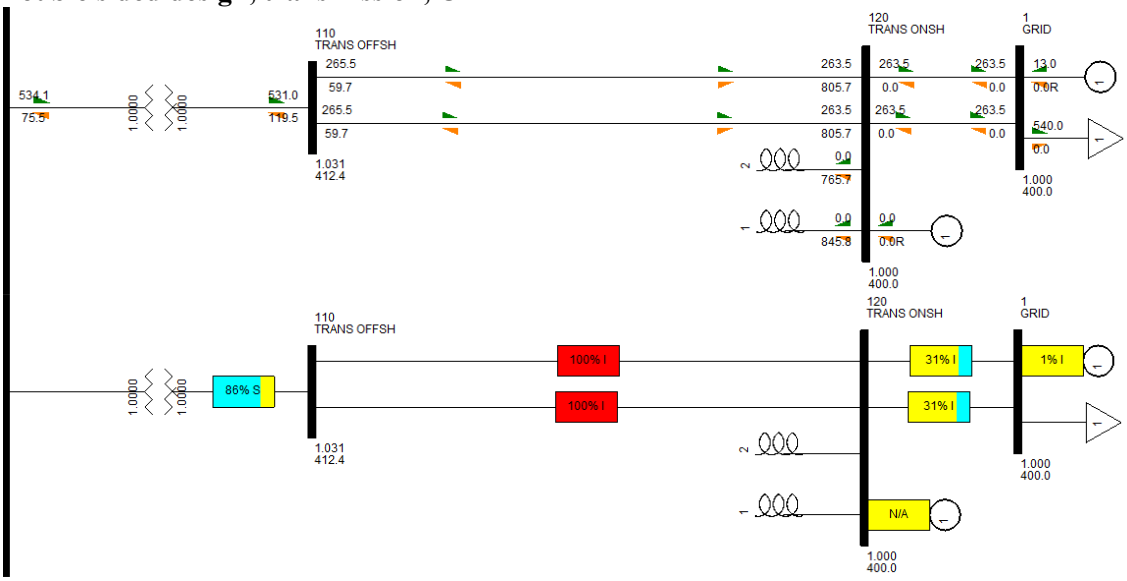

Double sided design, feeder OK

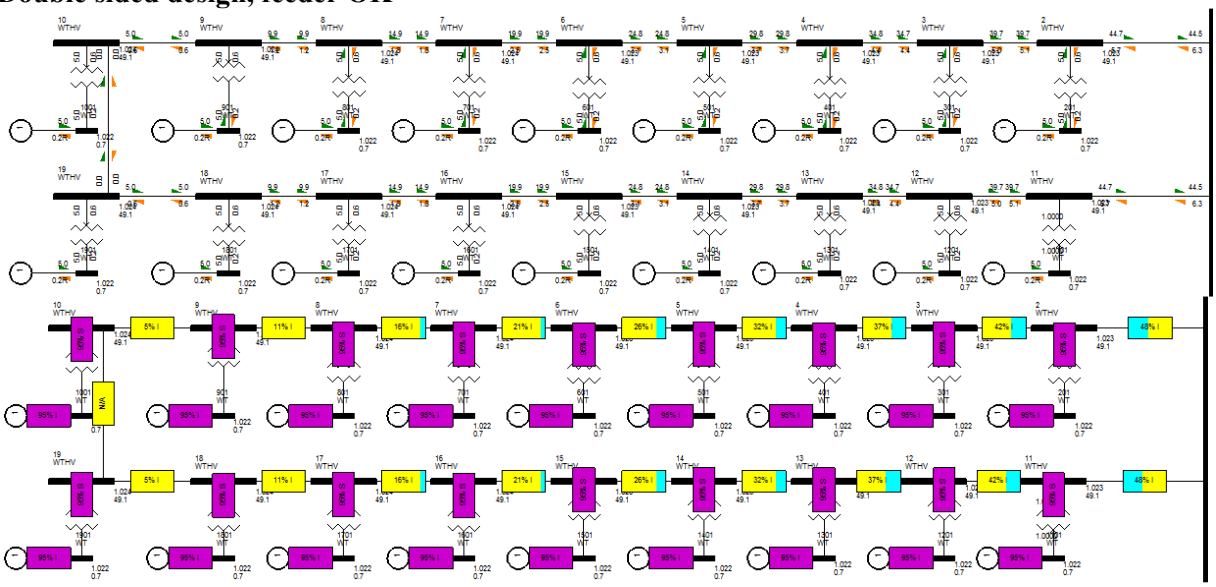

Double sided design, transmission, worst case

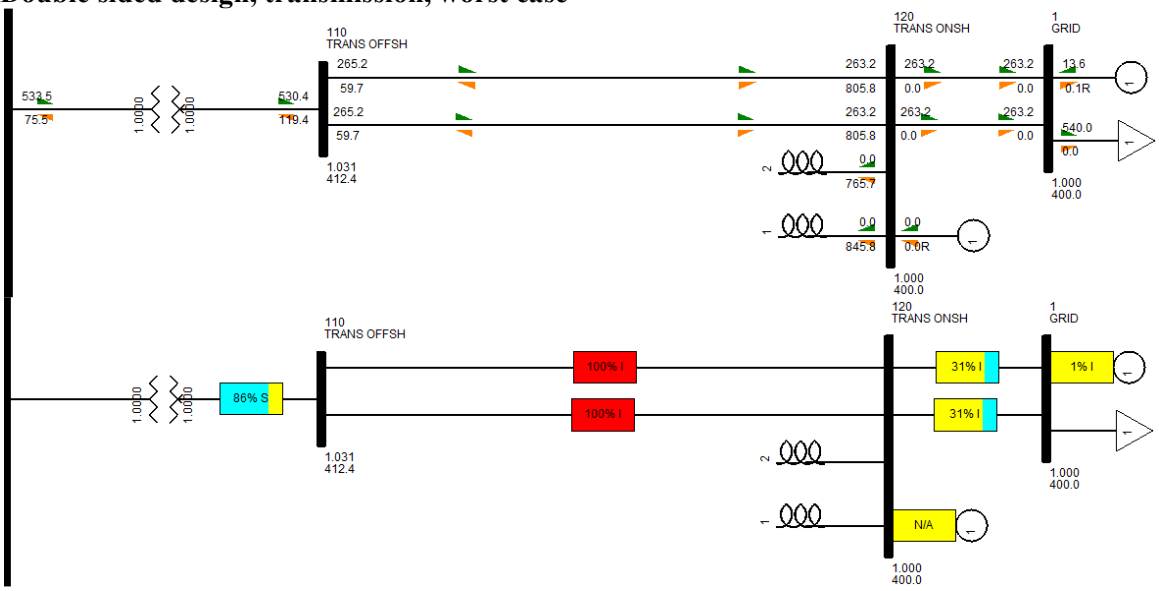

Double sided design, feeder worst case

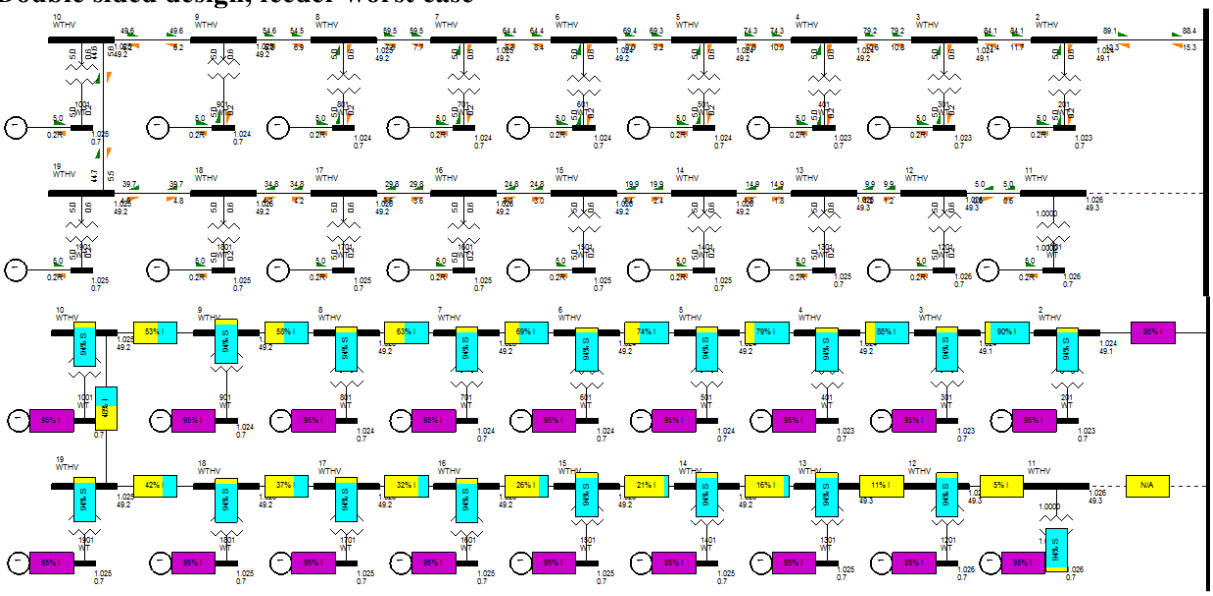

Shared ring design, entire system

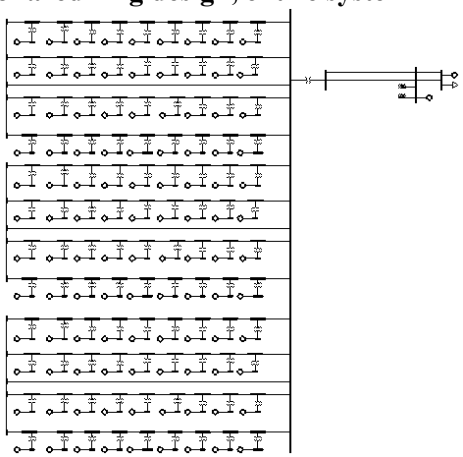

Shared ring design, transmission, OK

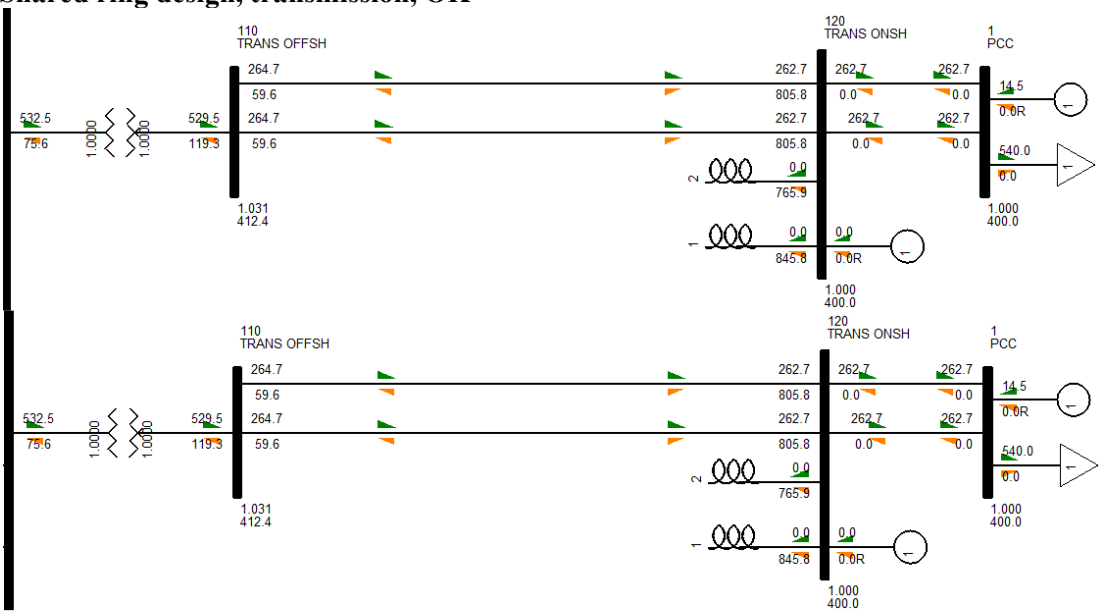

Shared ring design, feeder OK

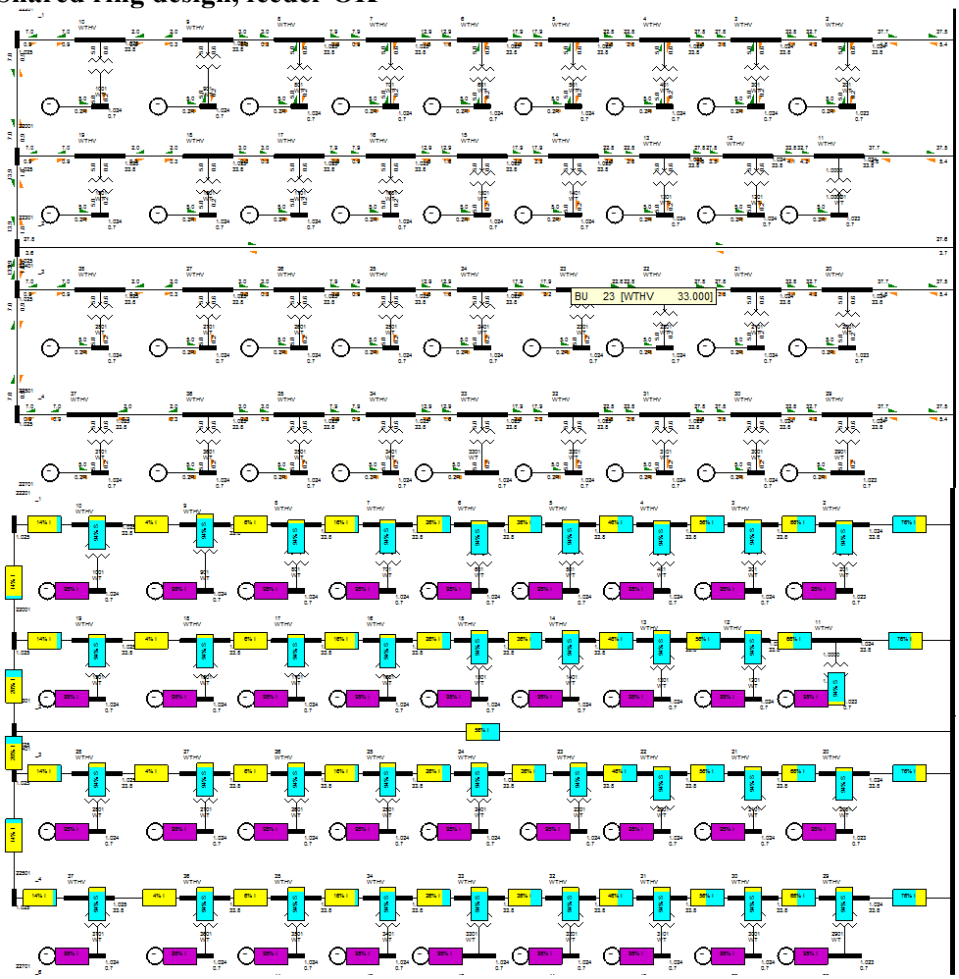

Shared ring design, transmission, worst case

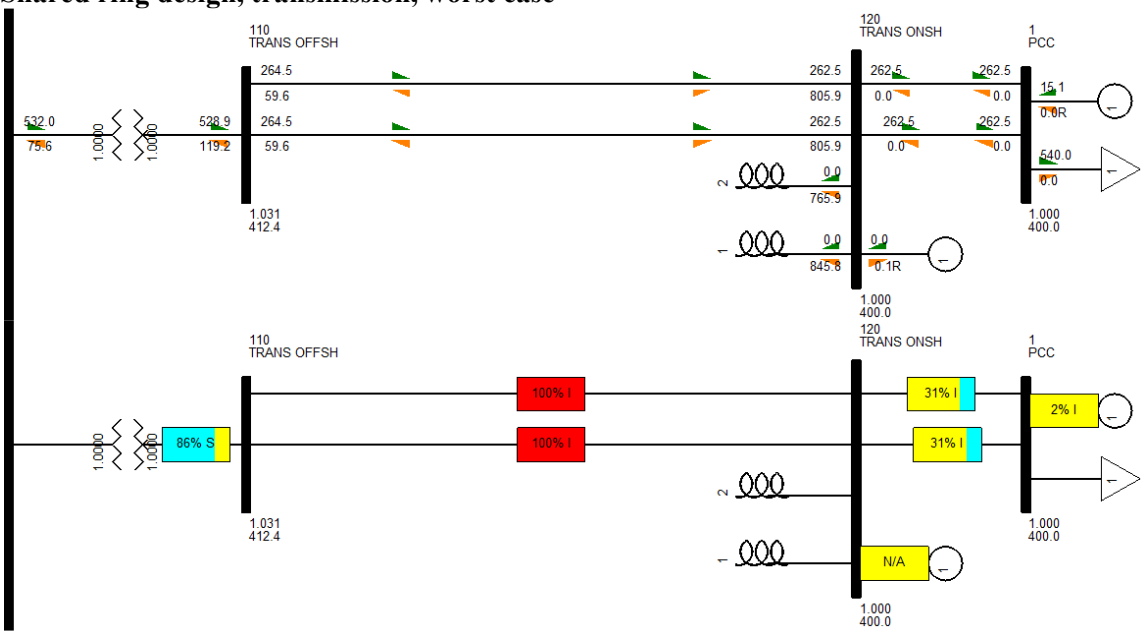

Shared ring design, feeder, worst case

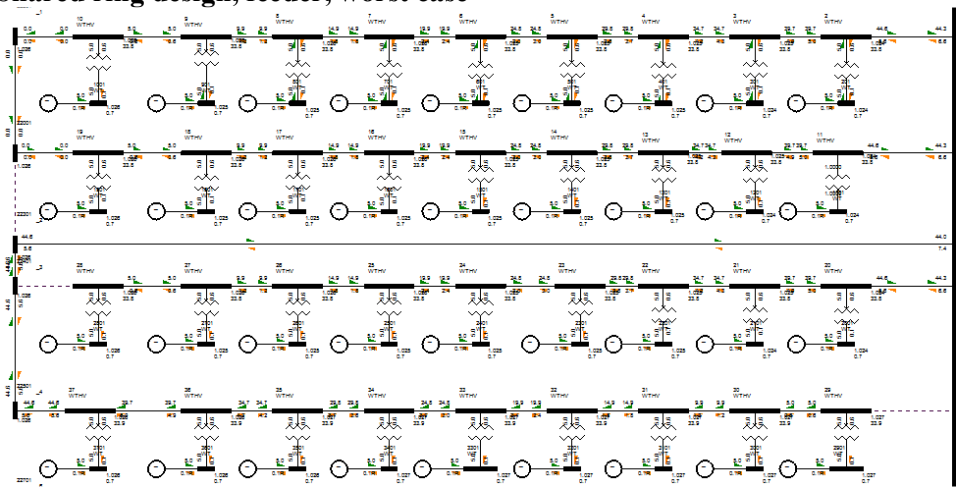

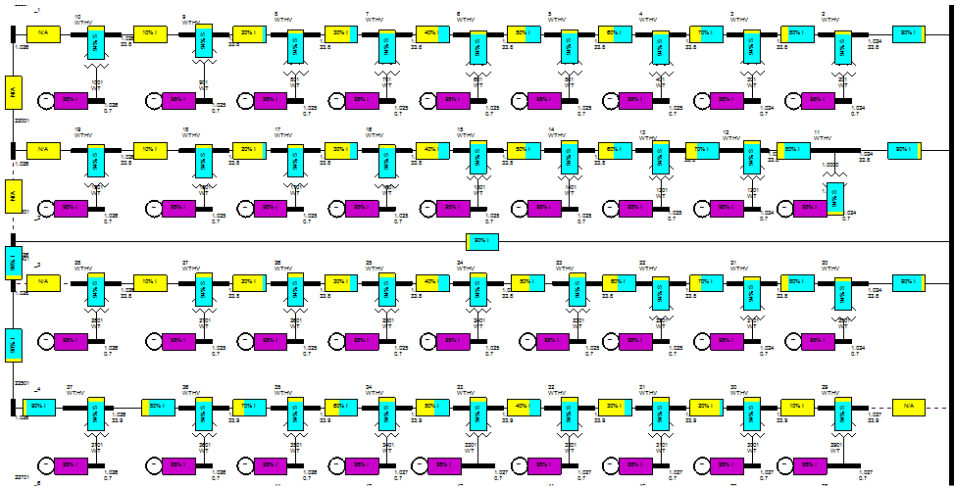

N-sided ring, entire system

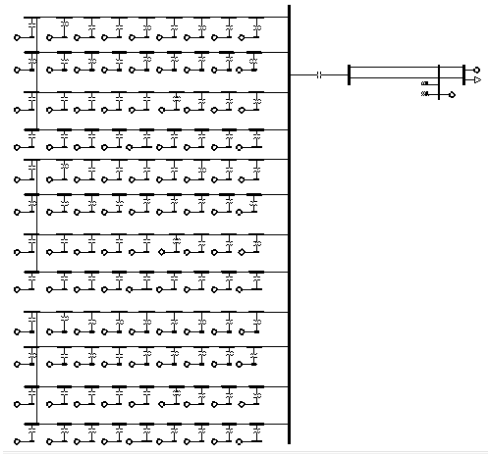

N-sided ring, transmission, OK

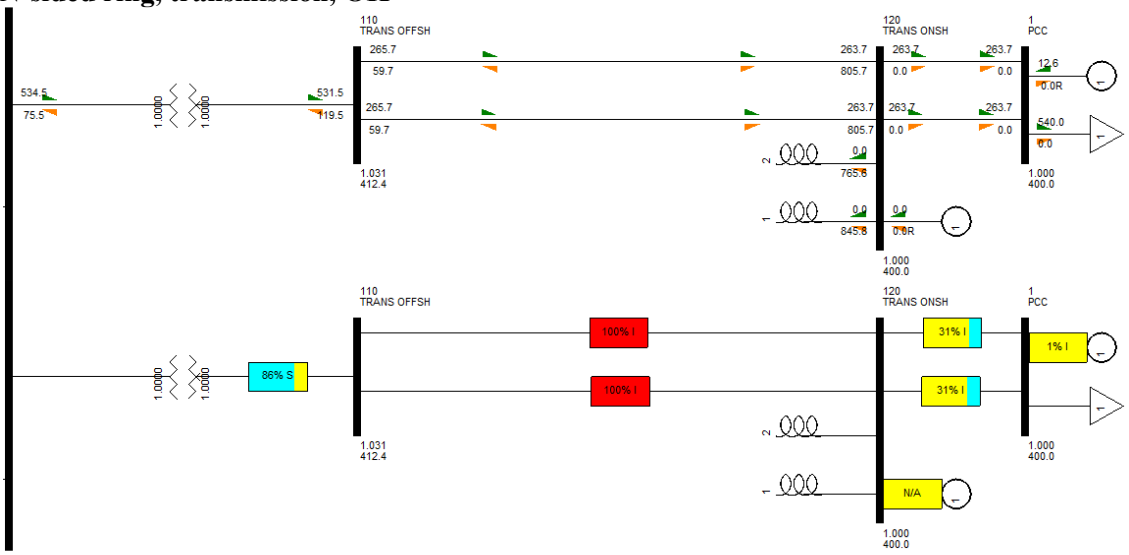

N-sided ring, feeder OK

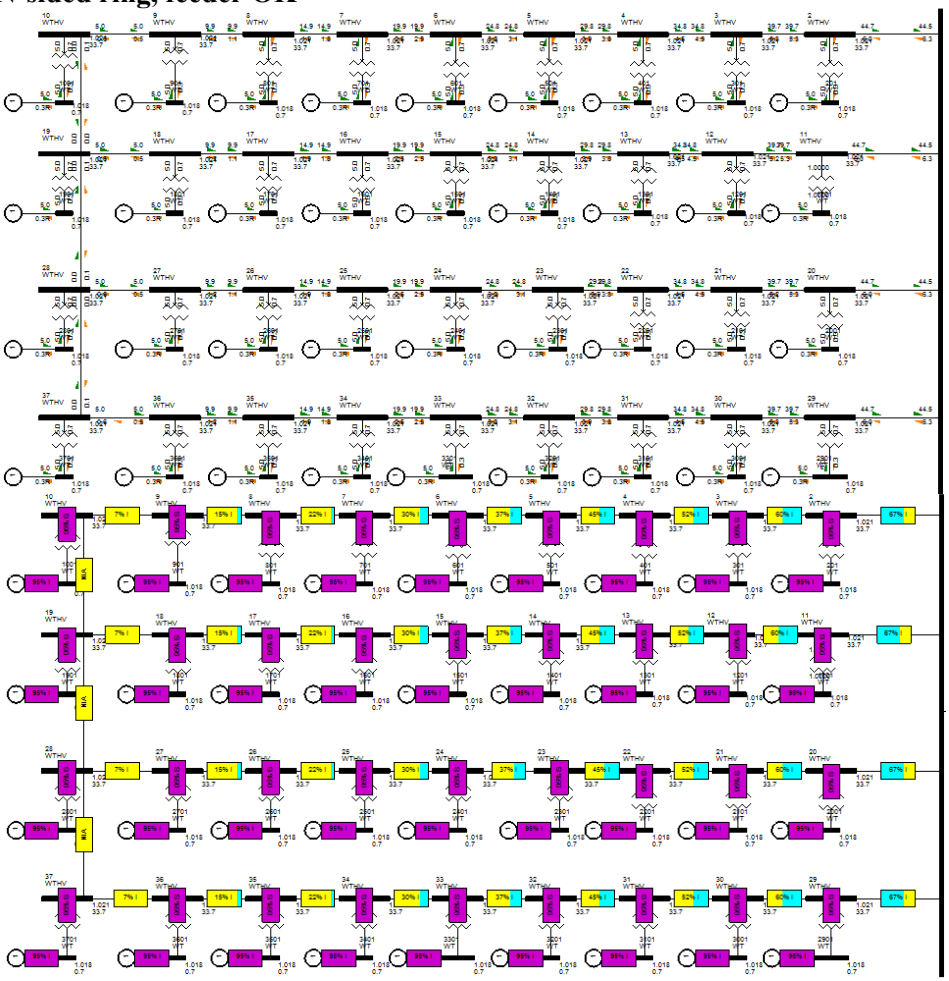

N-sided ring, transmission, worst case

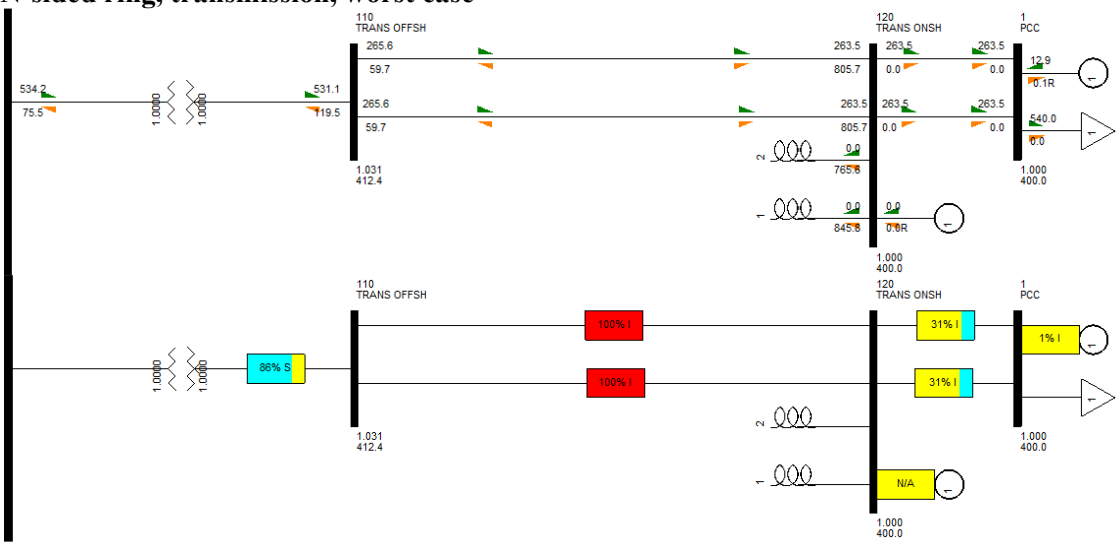

N-sided ring, feeder, worst case

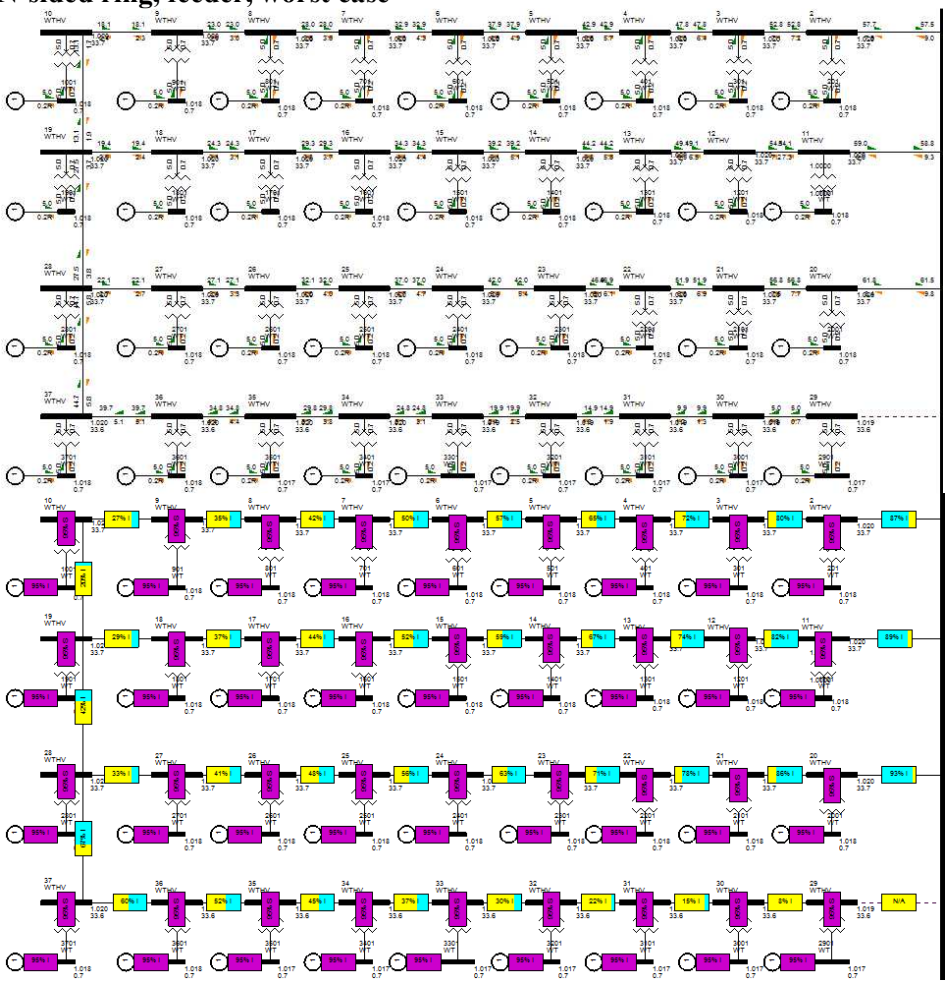

Star design, entire system

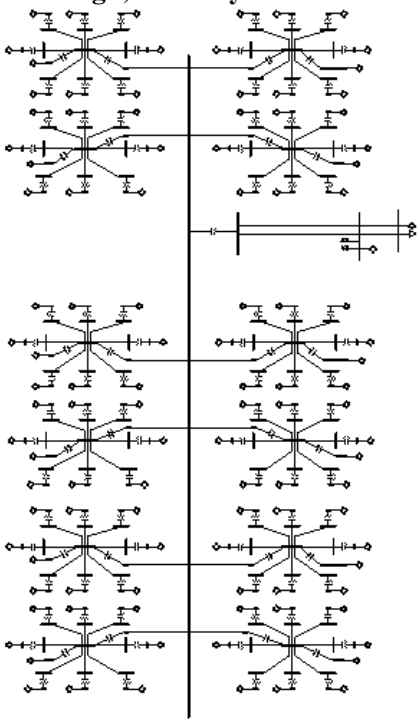

Star design, transmission, OK

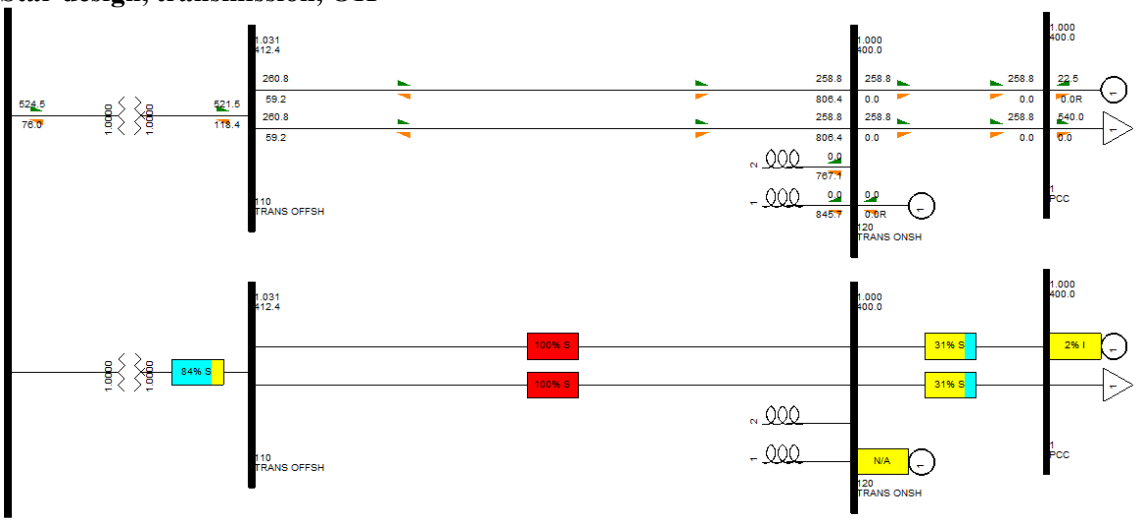

Star design, feeder OK

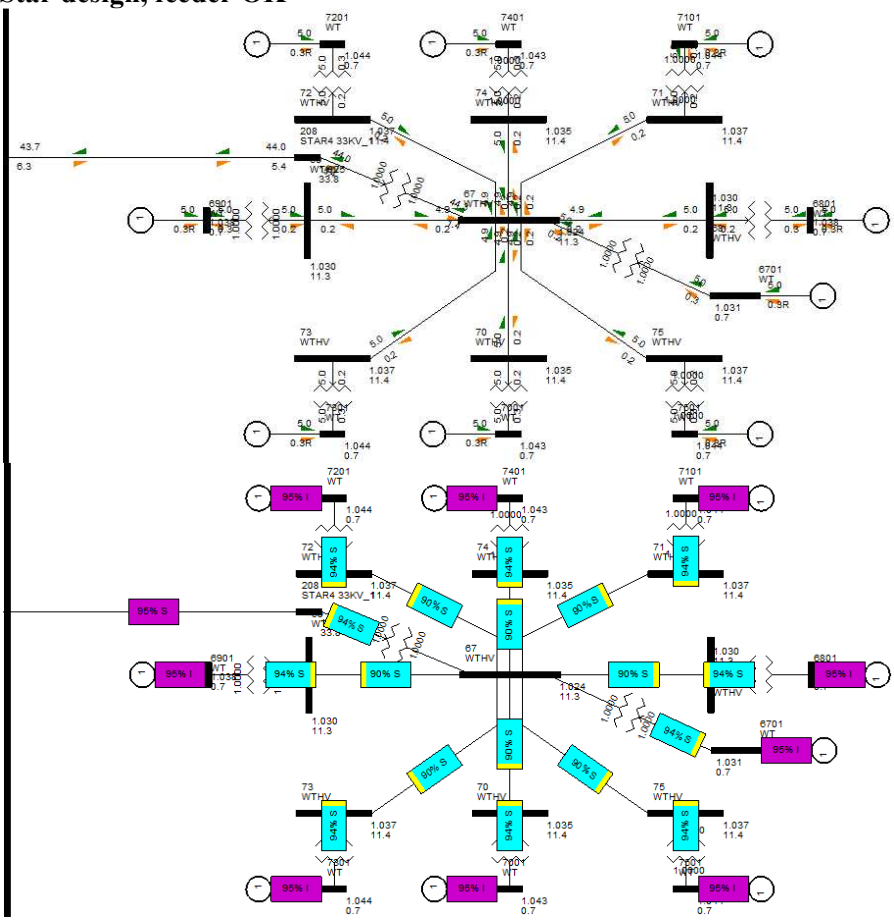

Star design, transmission, worst case

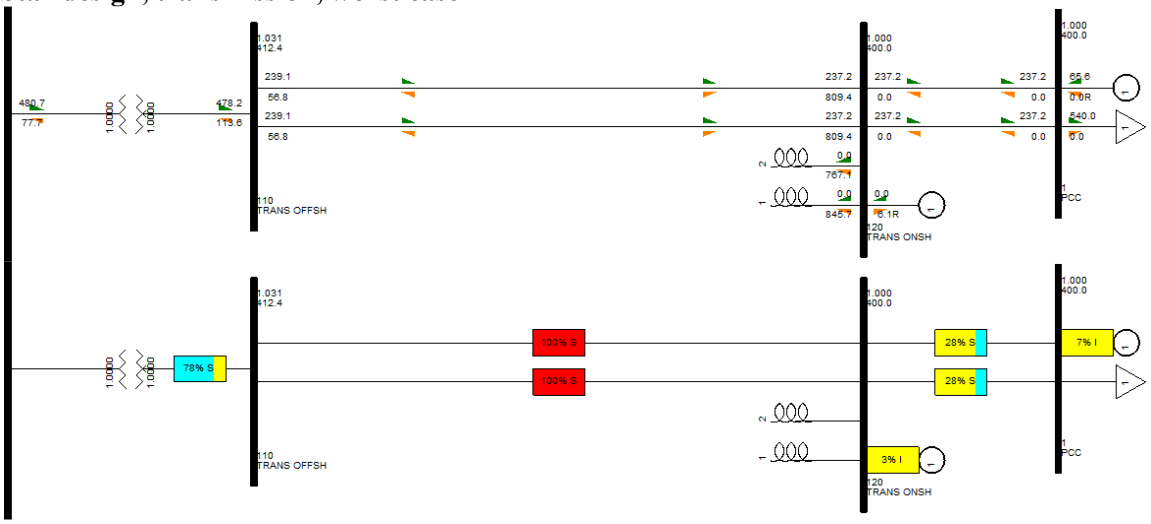

Star design, feeder, worst case

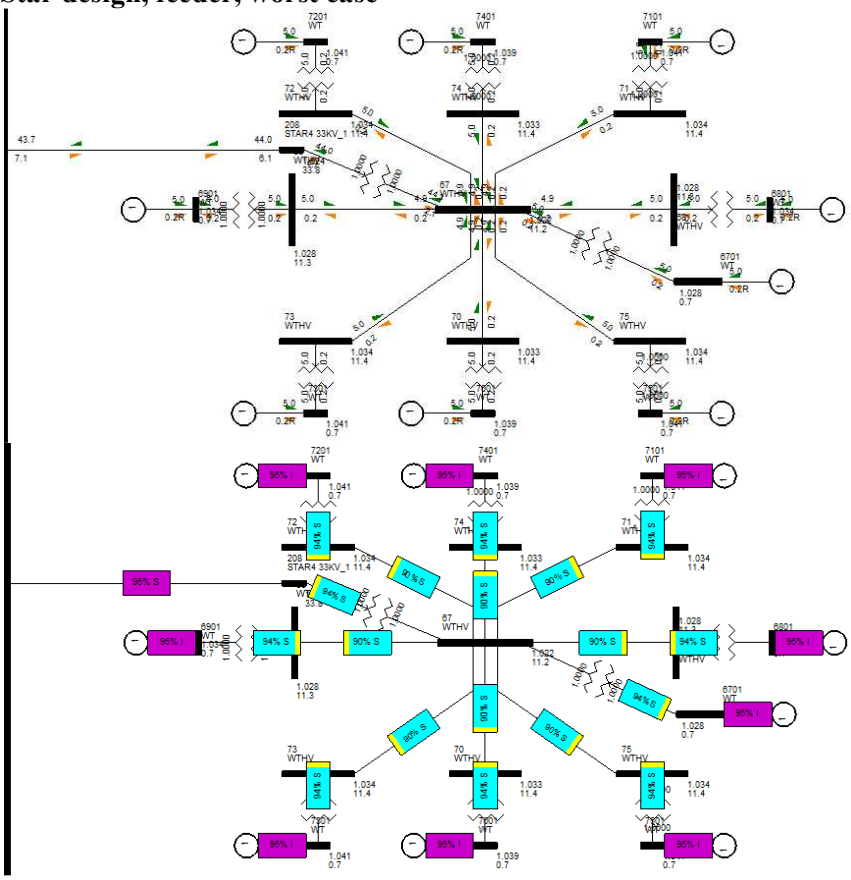

AC/DC

Transmission, both HVDC connections in function

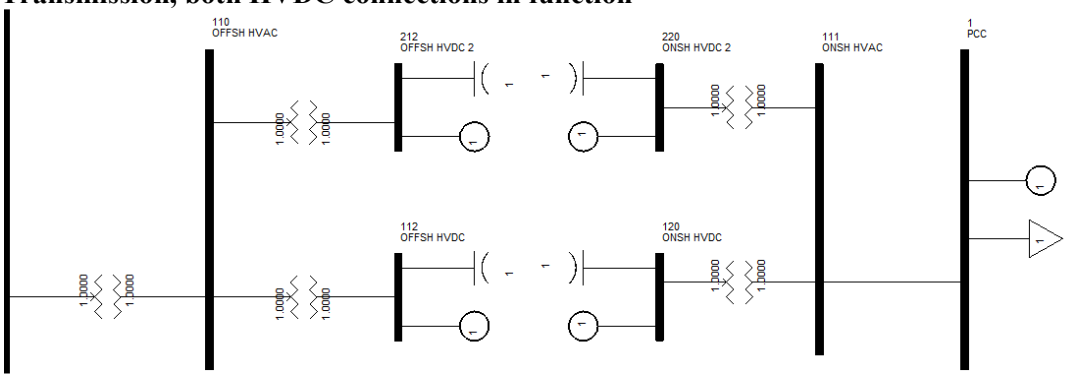

Transmission, one HVDC connection in function

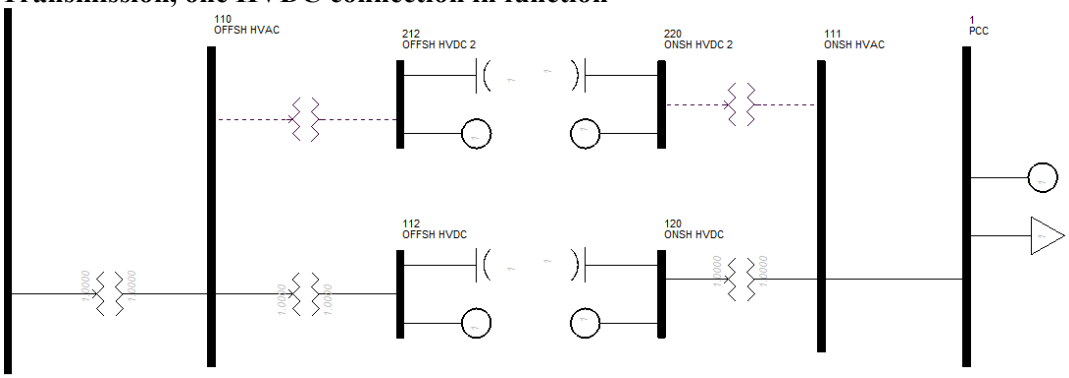

Radial design, entire system

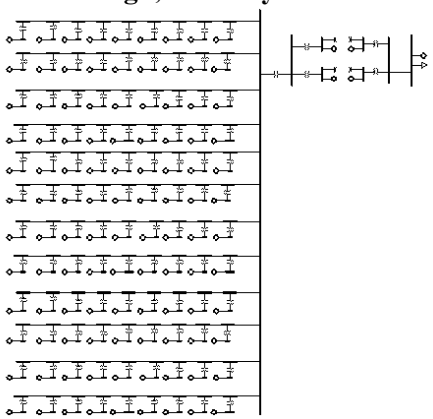

Radial design, transmission, OK

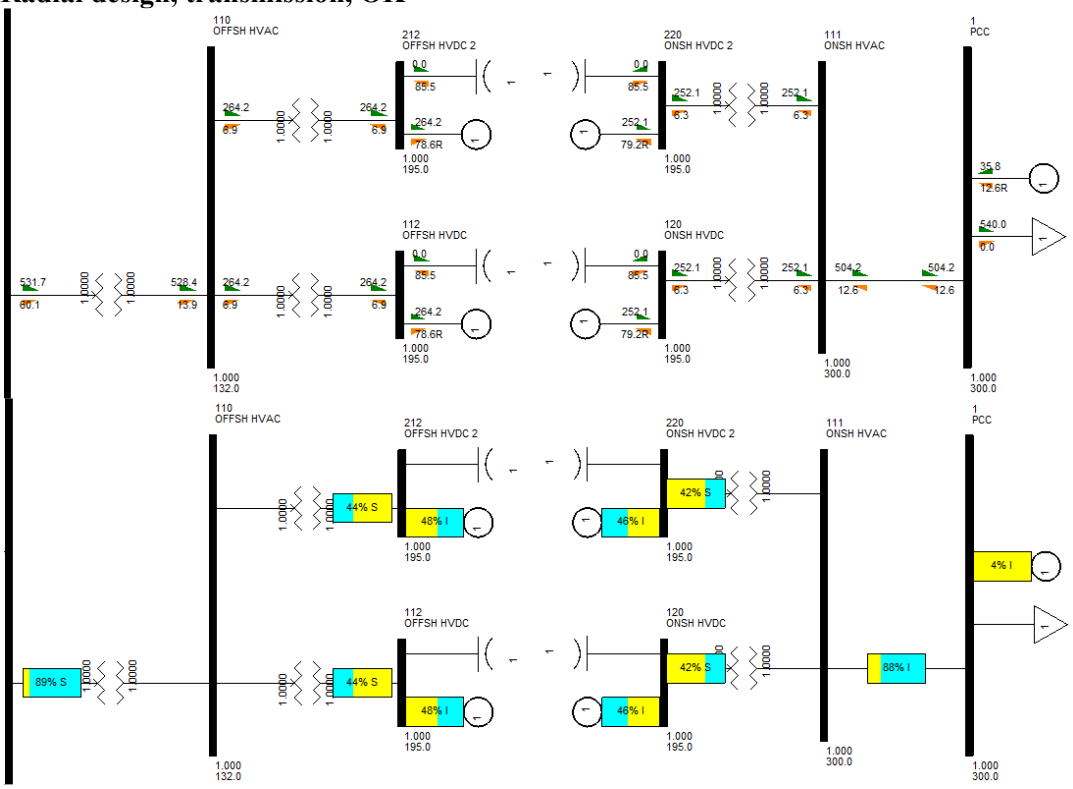

Radial design, feeder OK

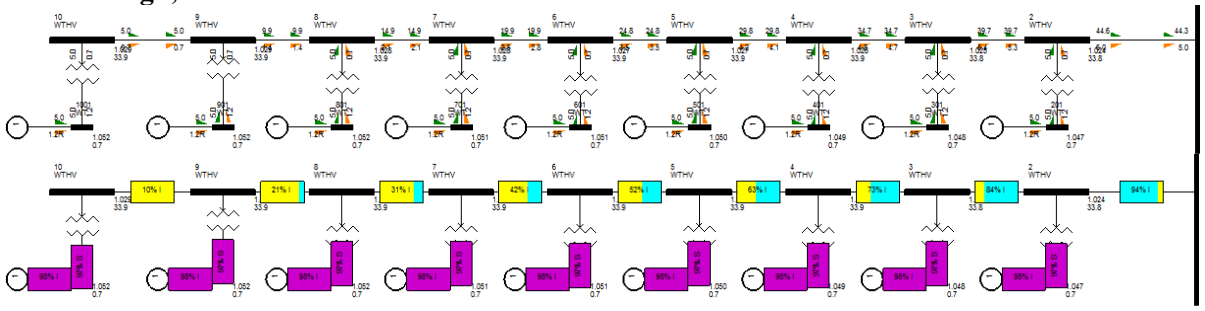

Radial design, transmission, worst case

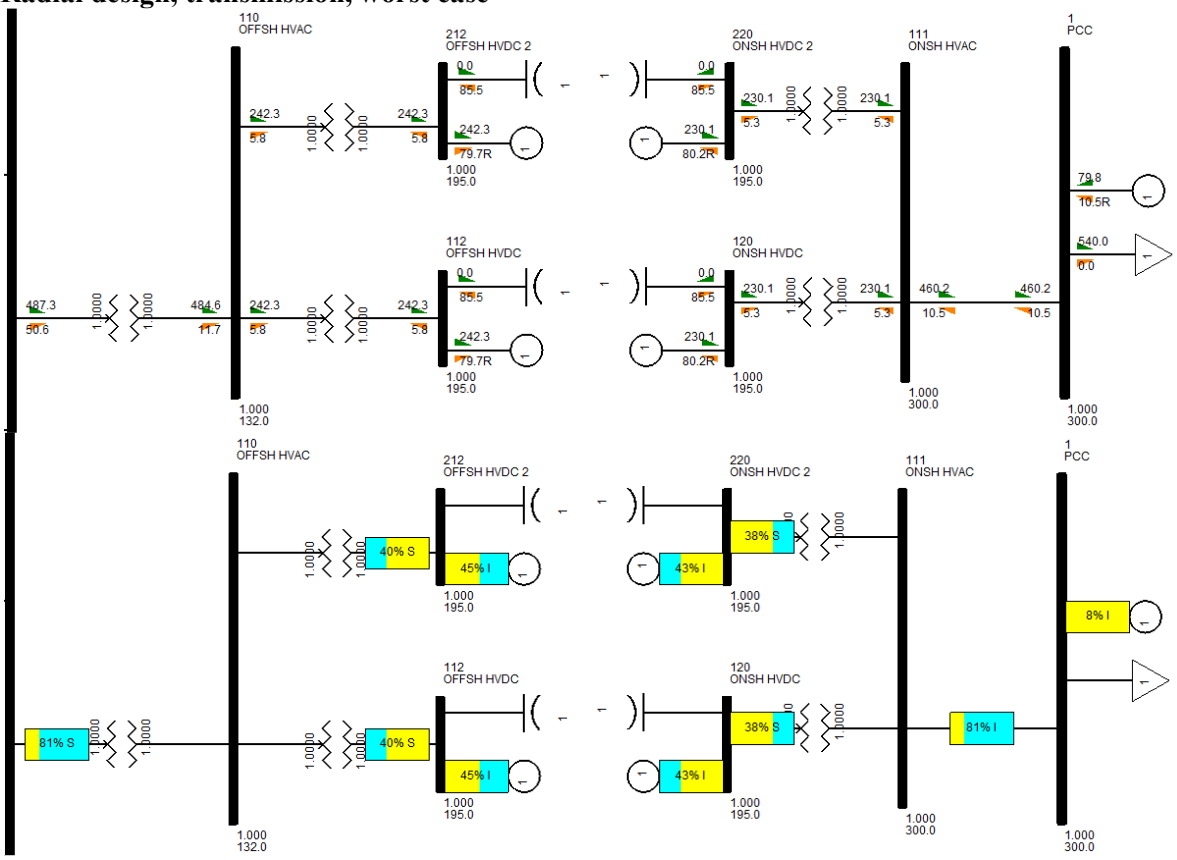

Radial design, feeder, worst case

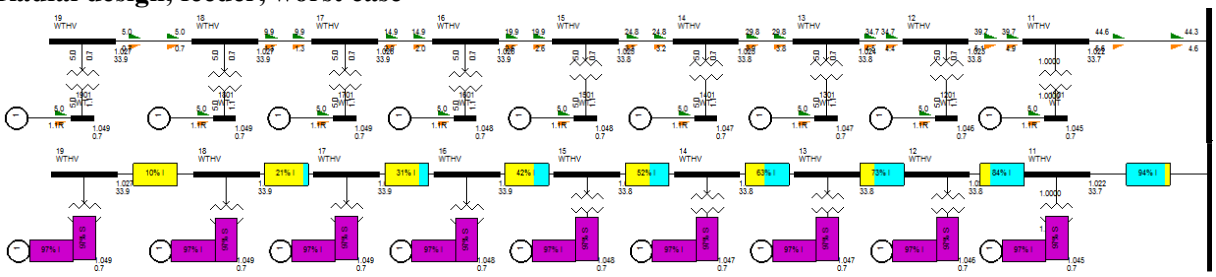

Single sided design, entire system

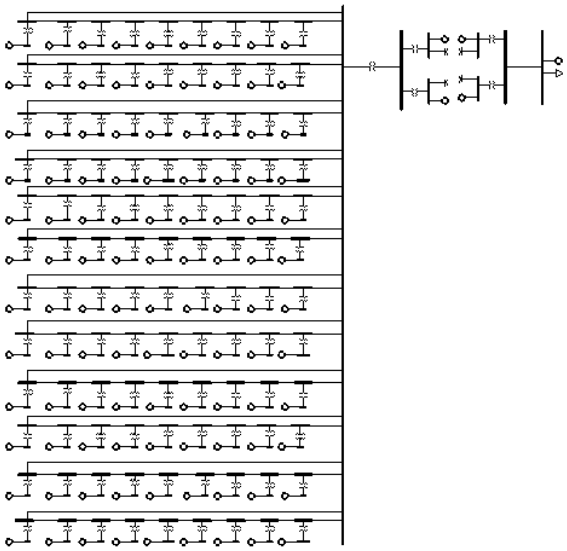

Single sided design, transmission, OK

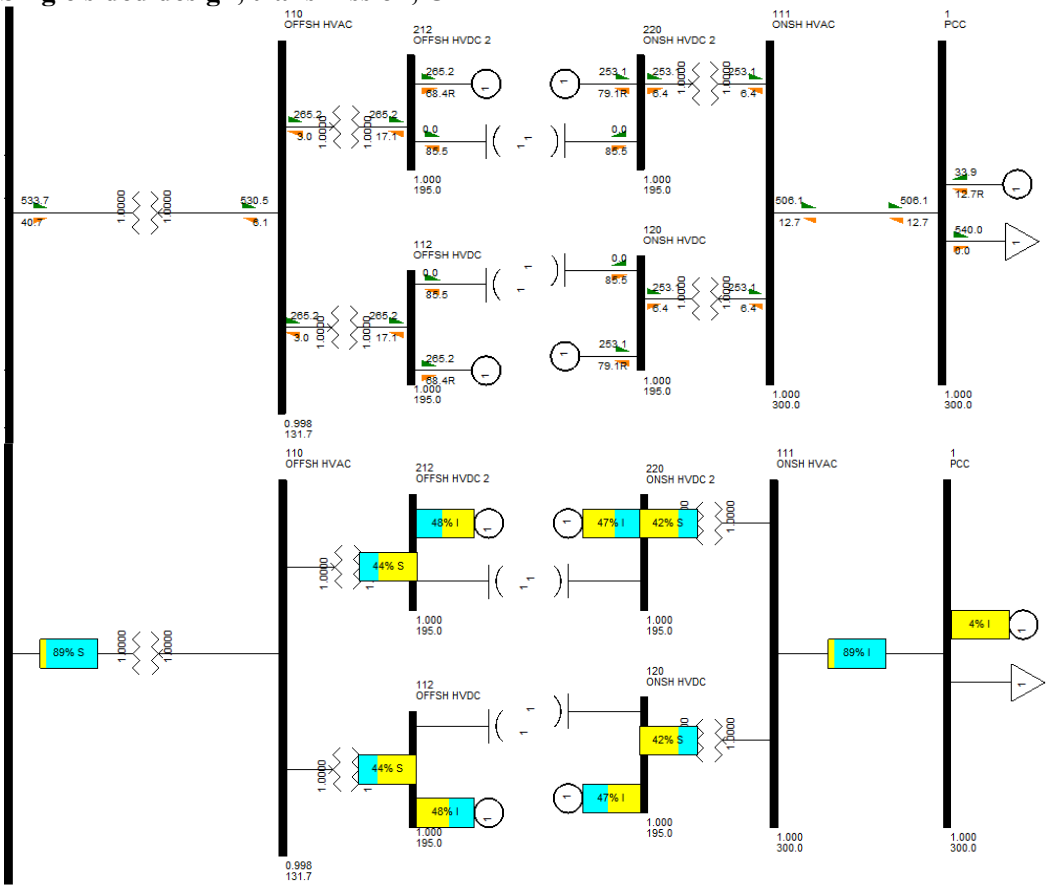

Single sided design, feeder OK

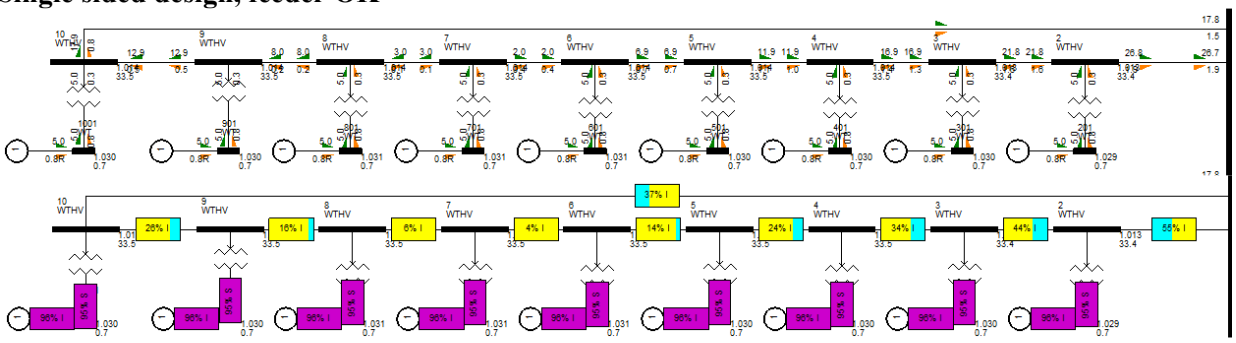

Single sided design, transmission, worst case

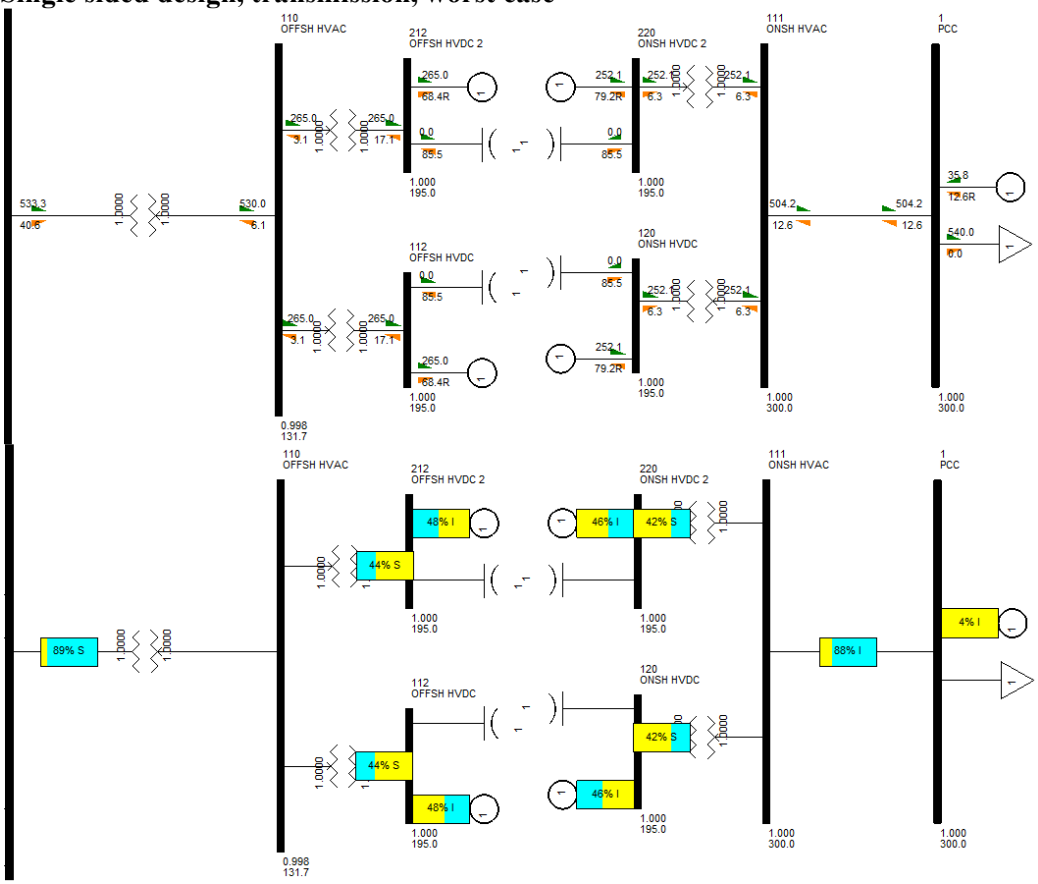

Single sided design, feeder, worst case

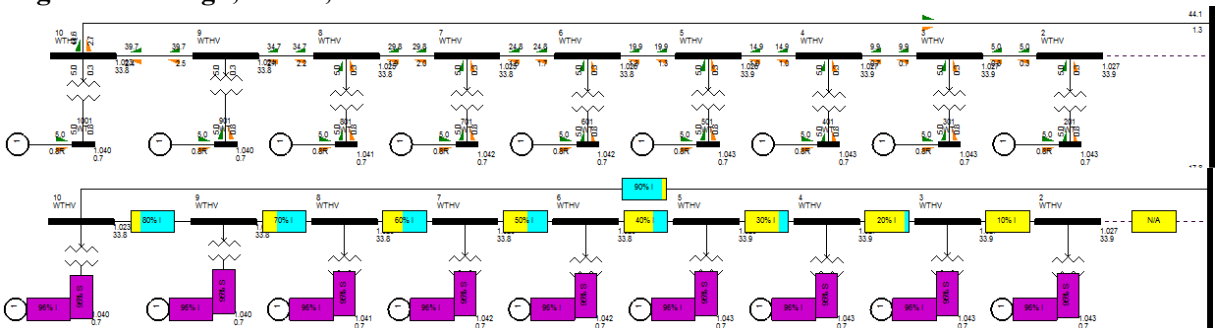

Double sided design, entire system

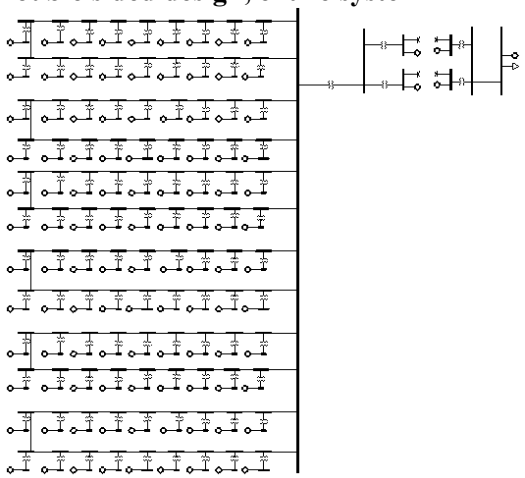

Double sided design, transmission, OK

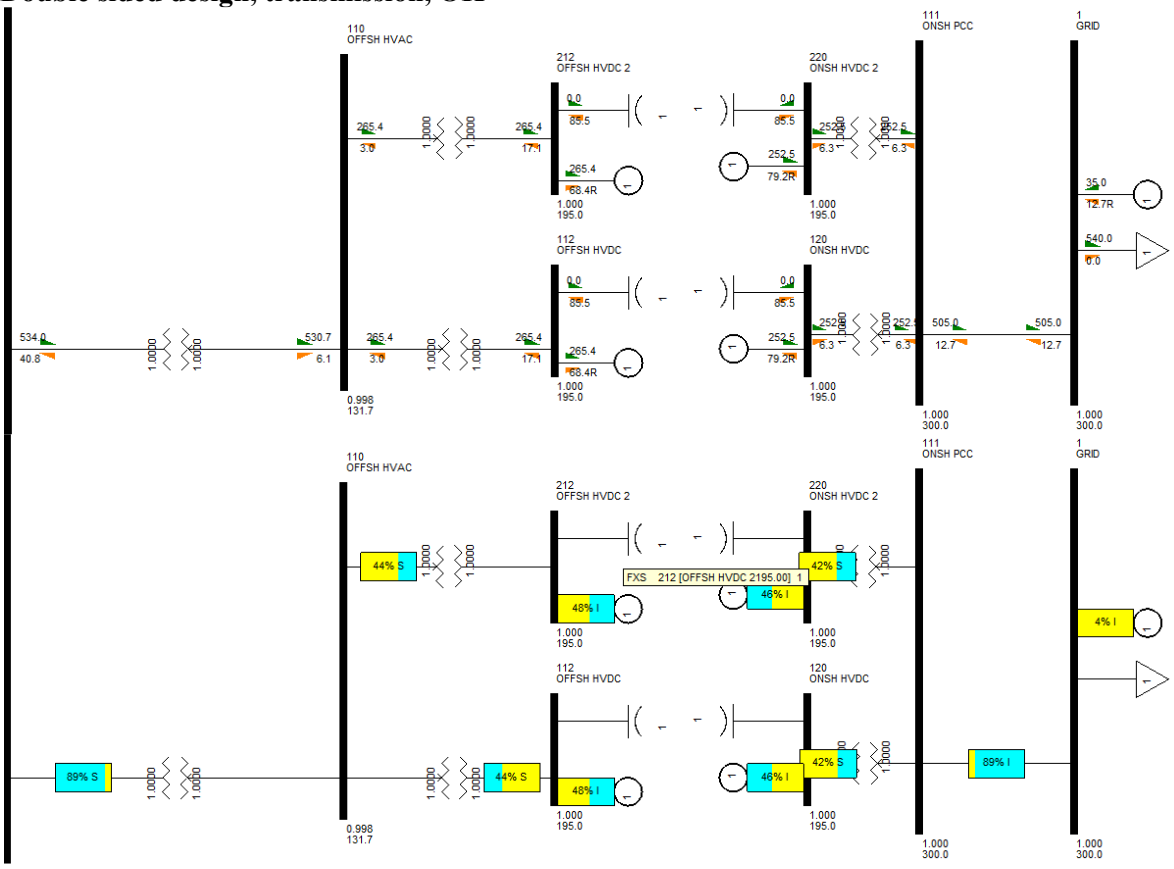

Double sided design, feeder OK

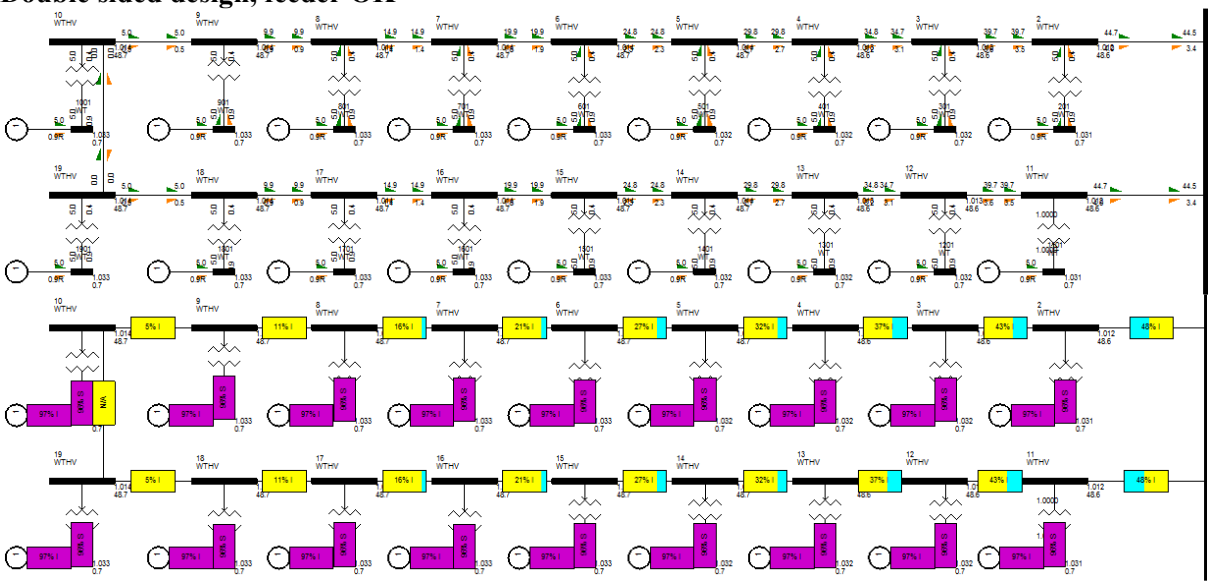

Double sided design, transmission, worst case

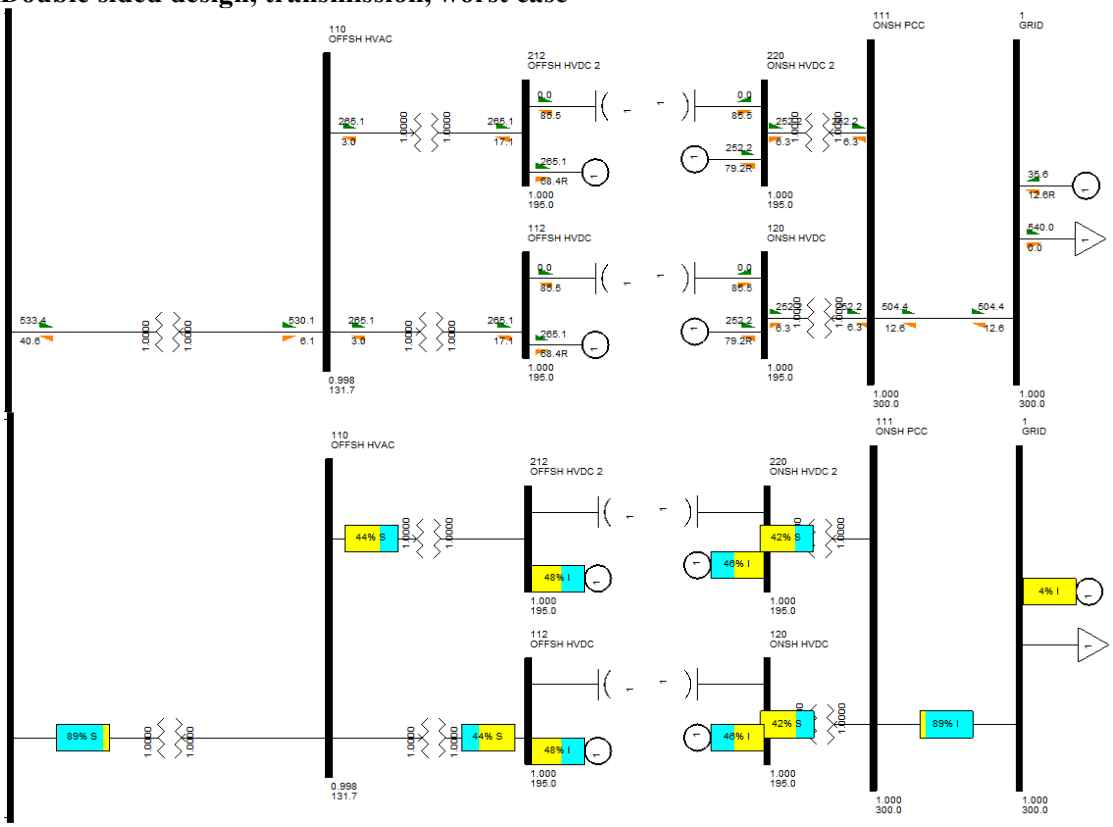

Double sided design, feeder, worst case

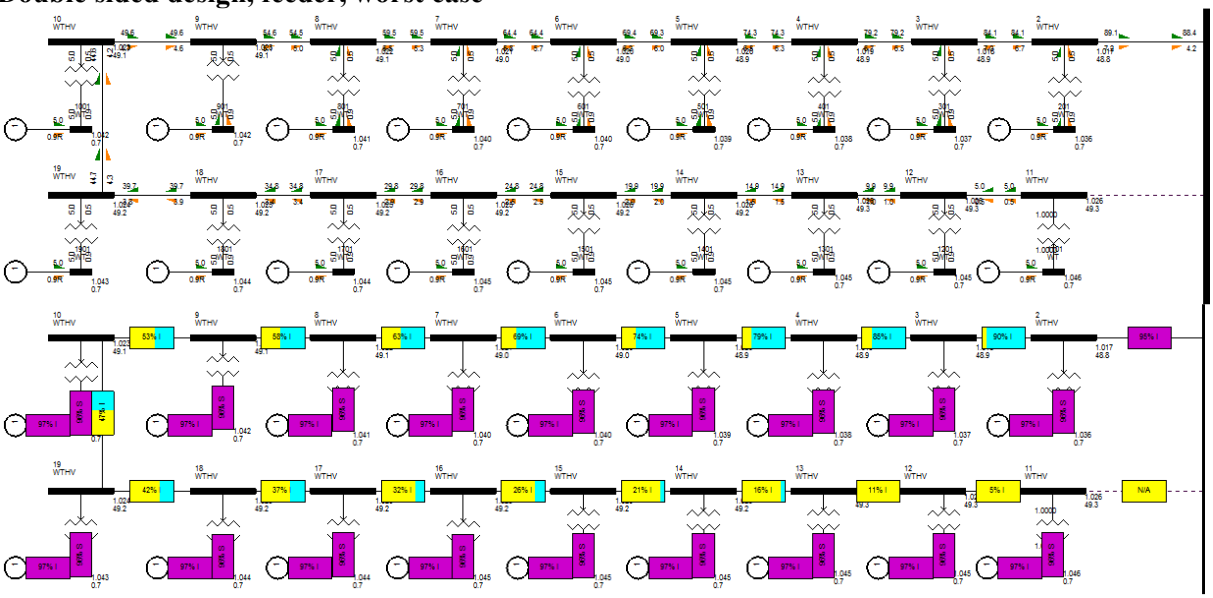

Shared ring design, entire system

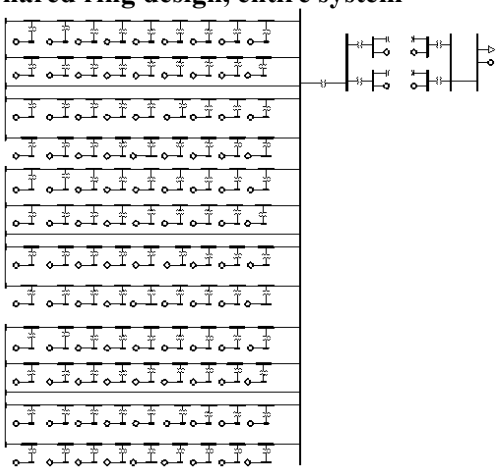

Shared ring design, transmission, OK

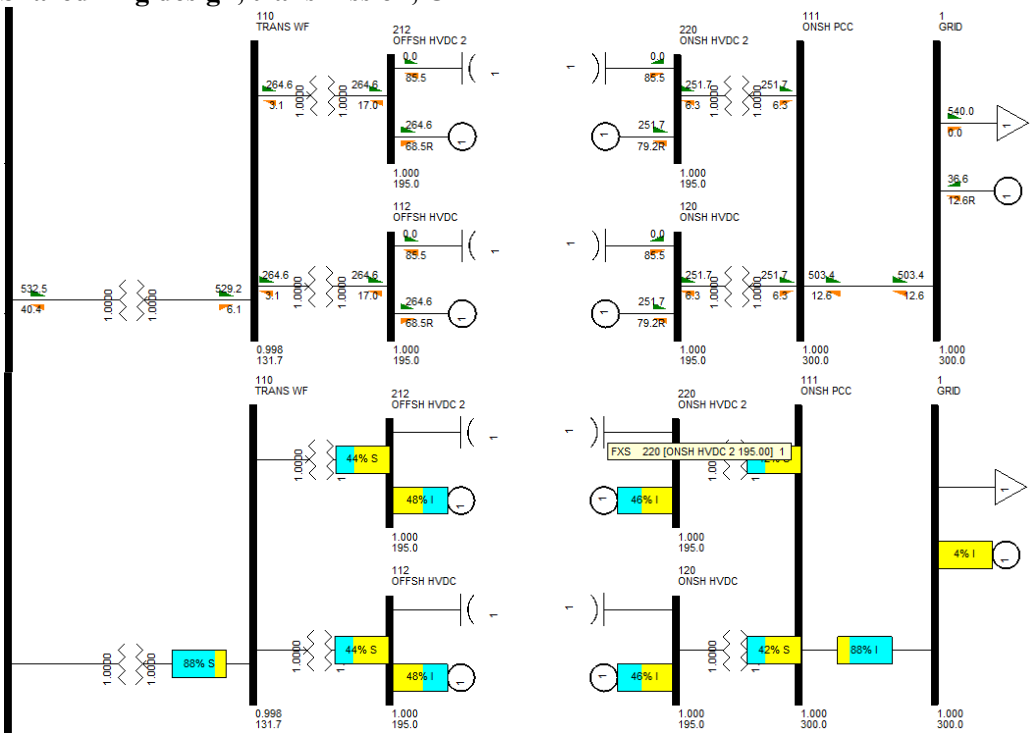

Shared ring design, feeder OK

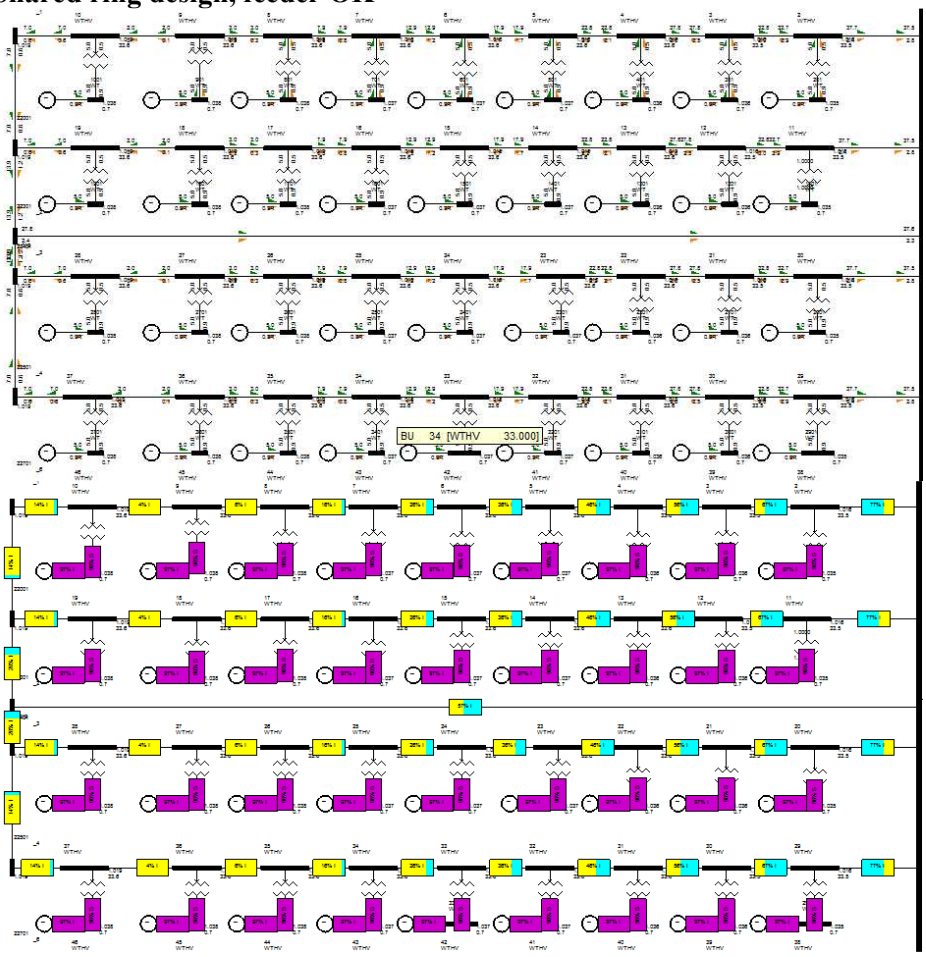

Shared ring design, transmission, worst case

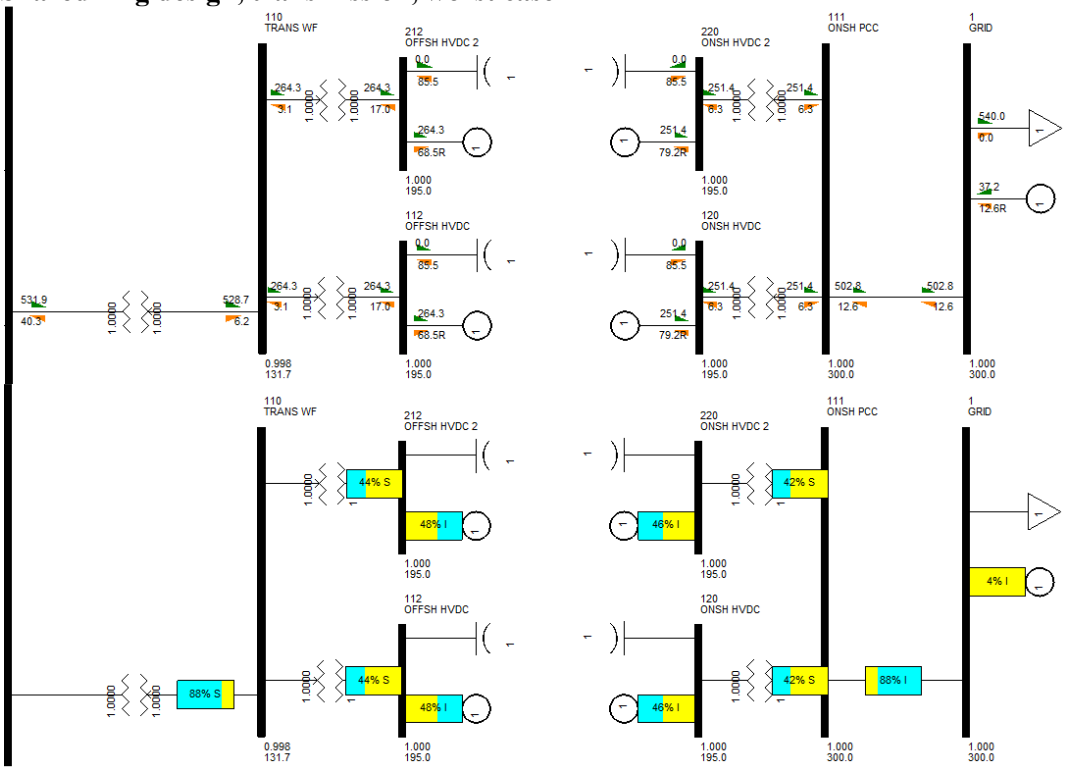

Shared ring design, feeder, worst case

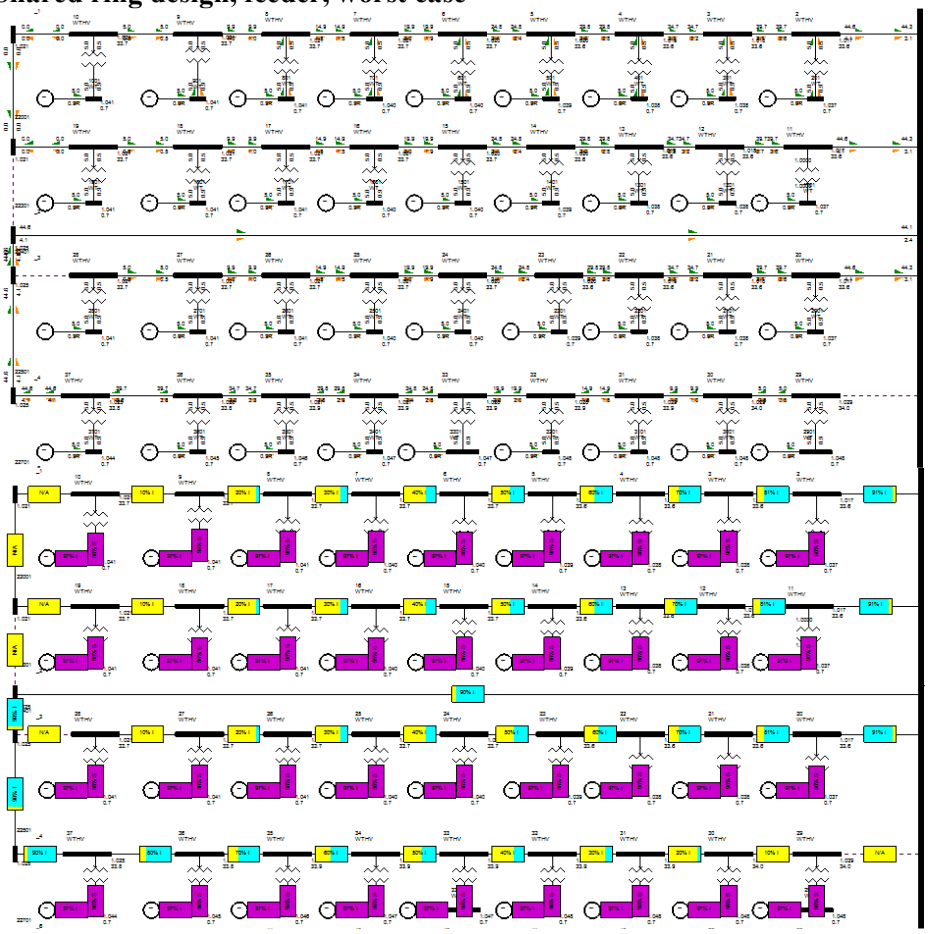

N-sided design, entire system

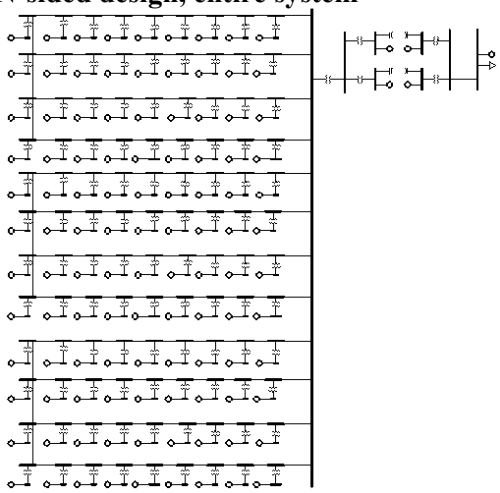

N-sided design, transmission, OK

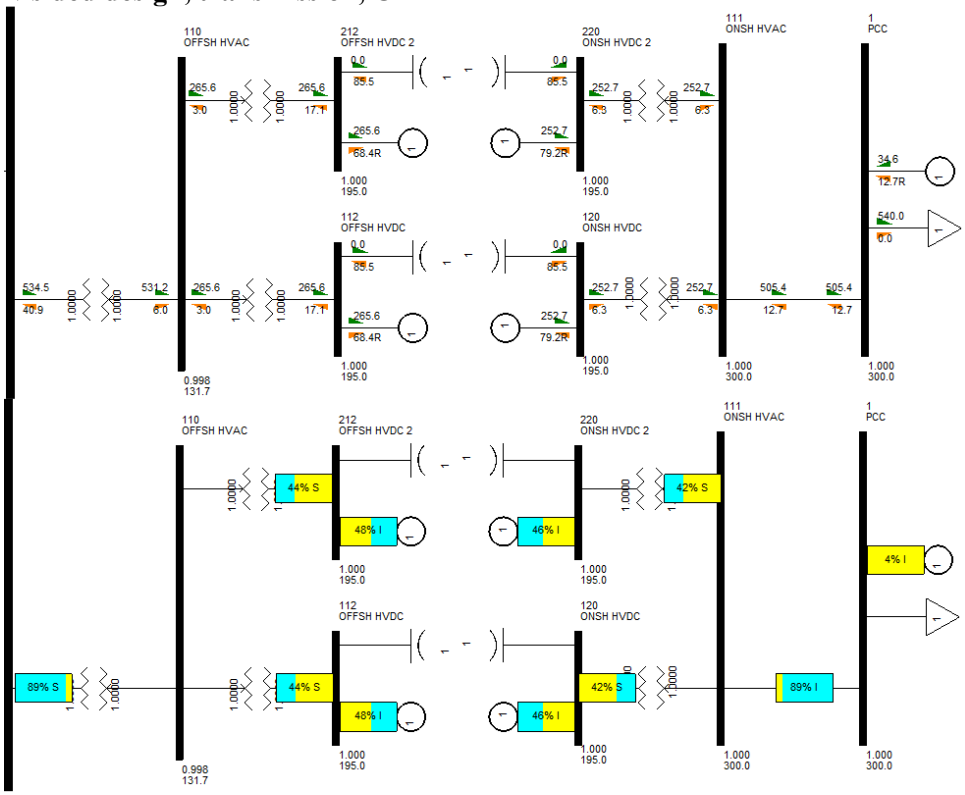

N-sided design, feeder OK

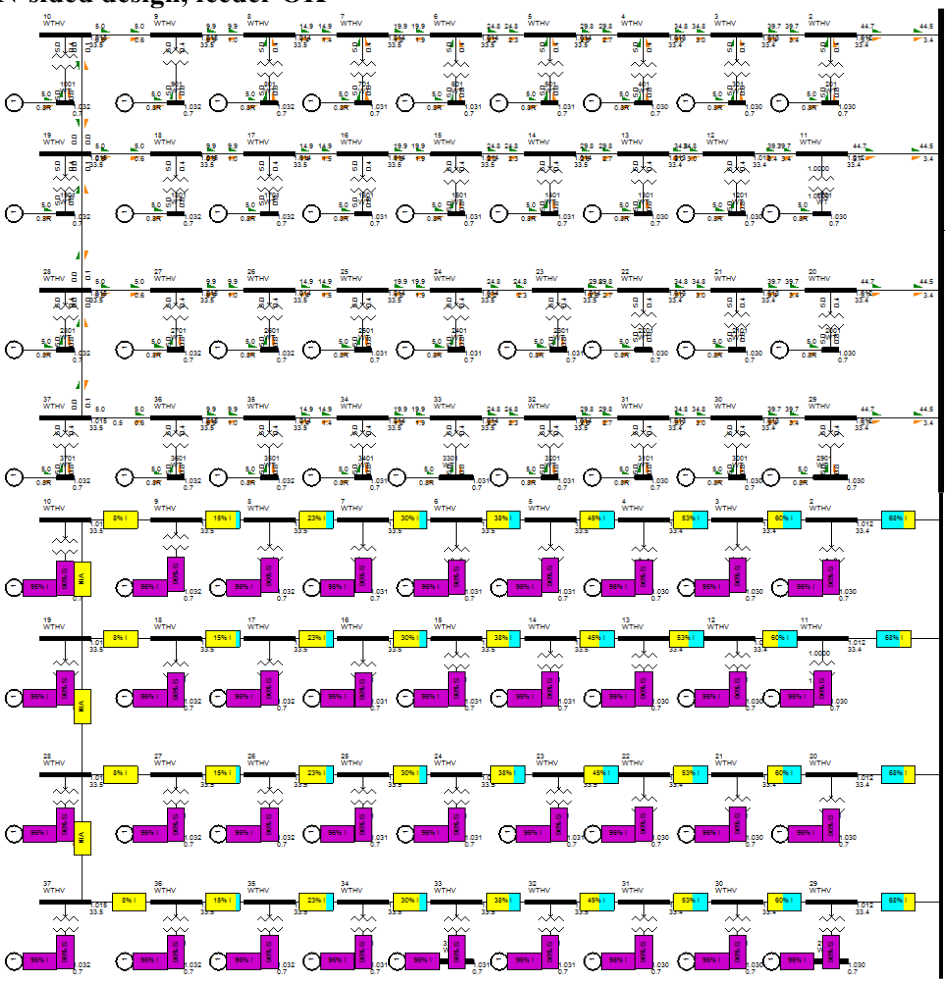

N-sided design, transmission, worst case

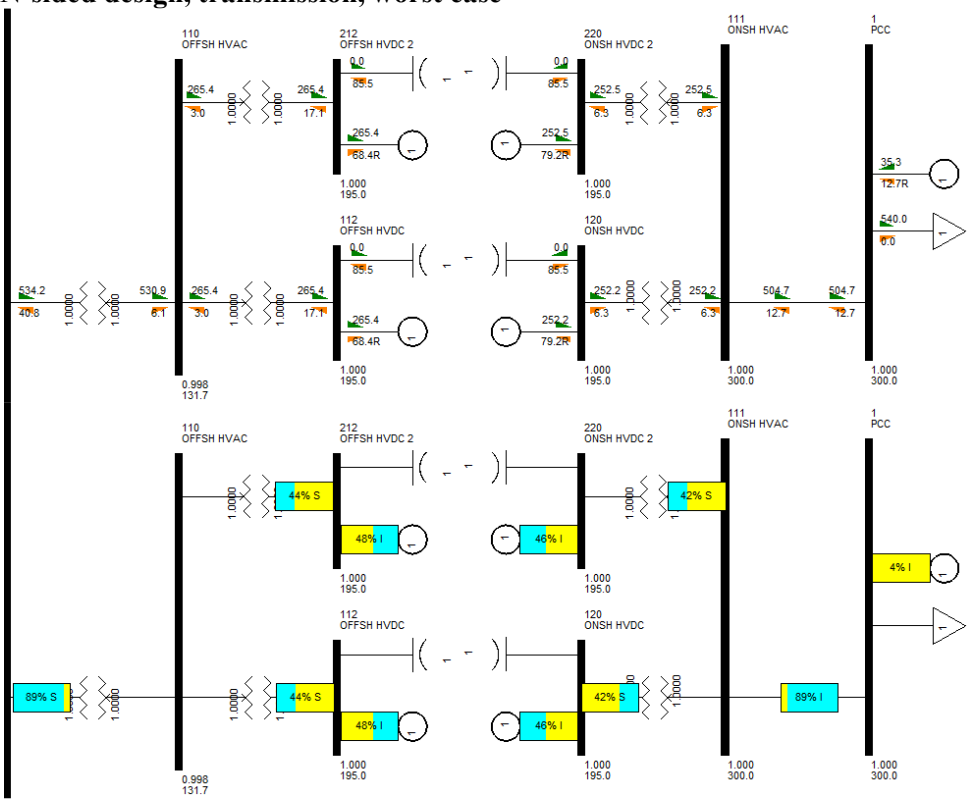

N-sided design, feeder, worst case

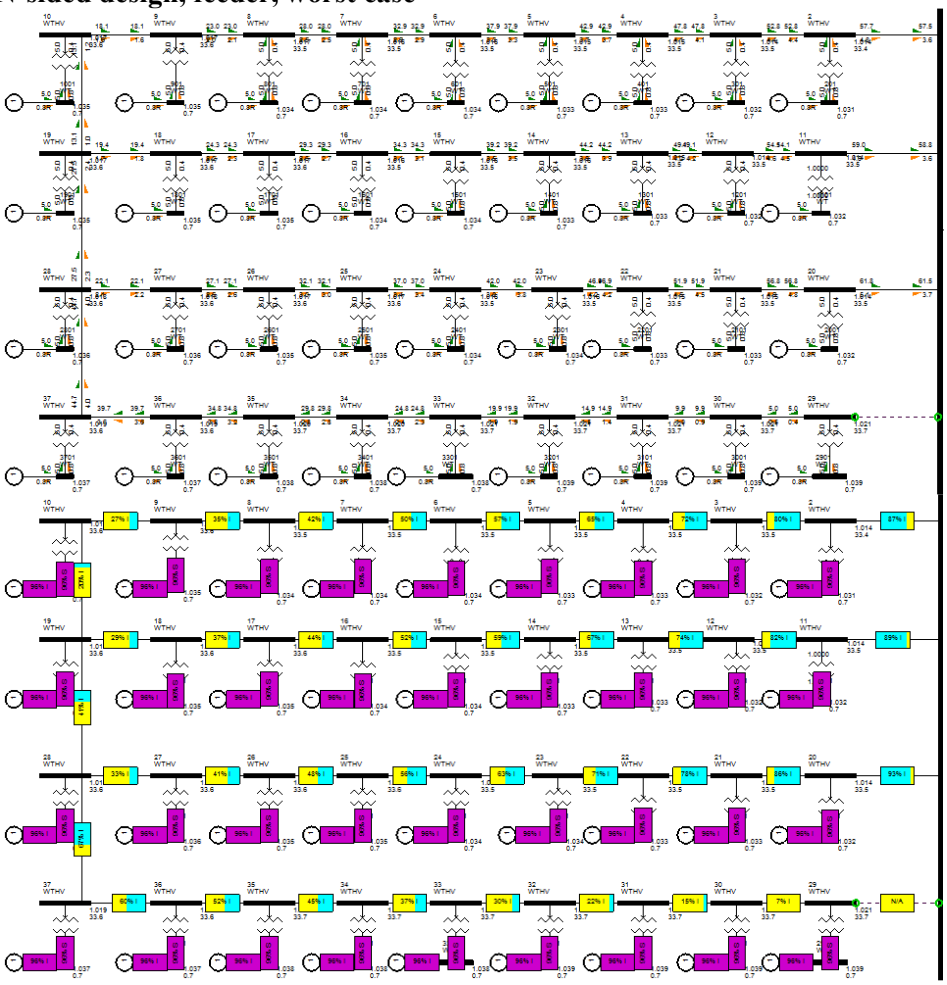

Star design, entire system

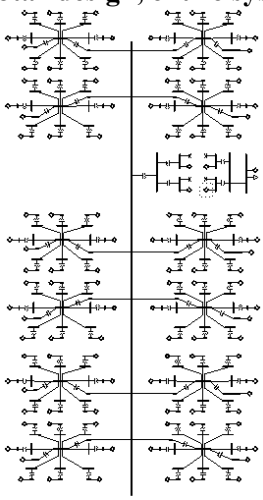

Star design, transmission, OK

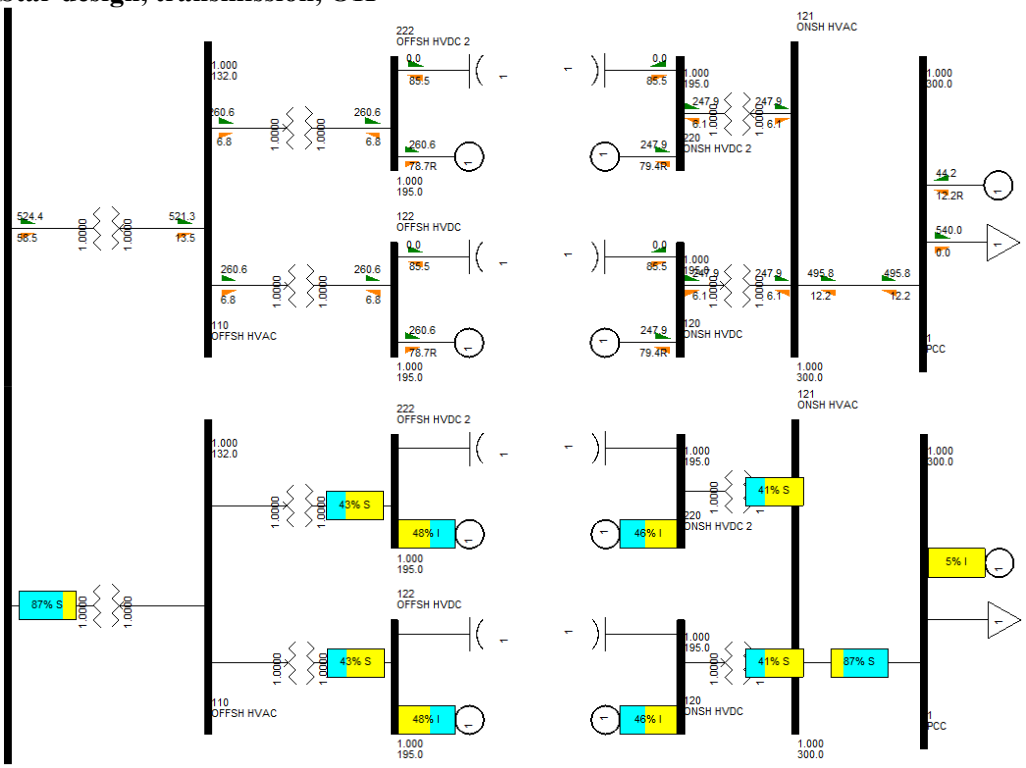

Star design, feeder OK

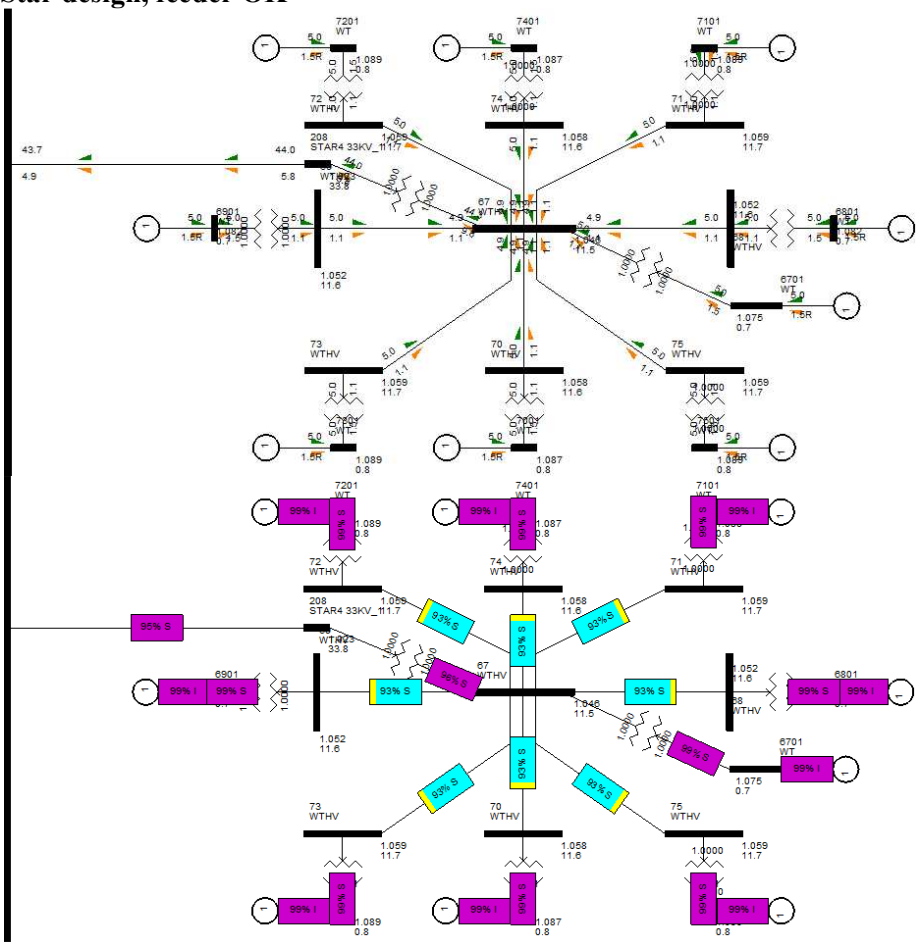

Star design, transmission, worst case

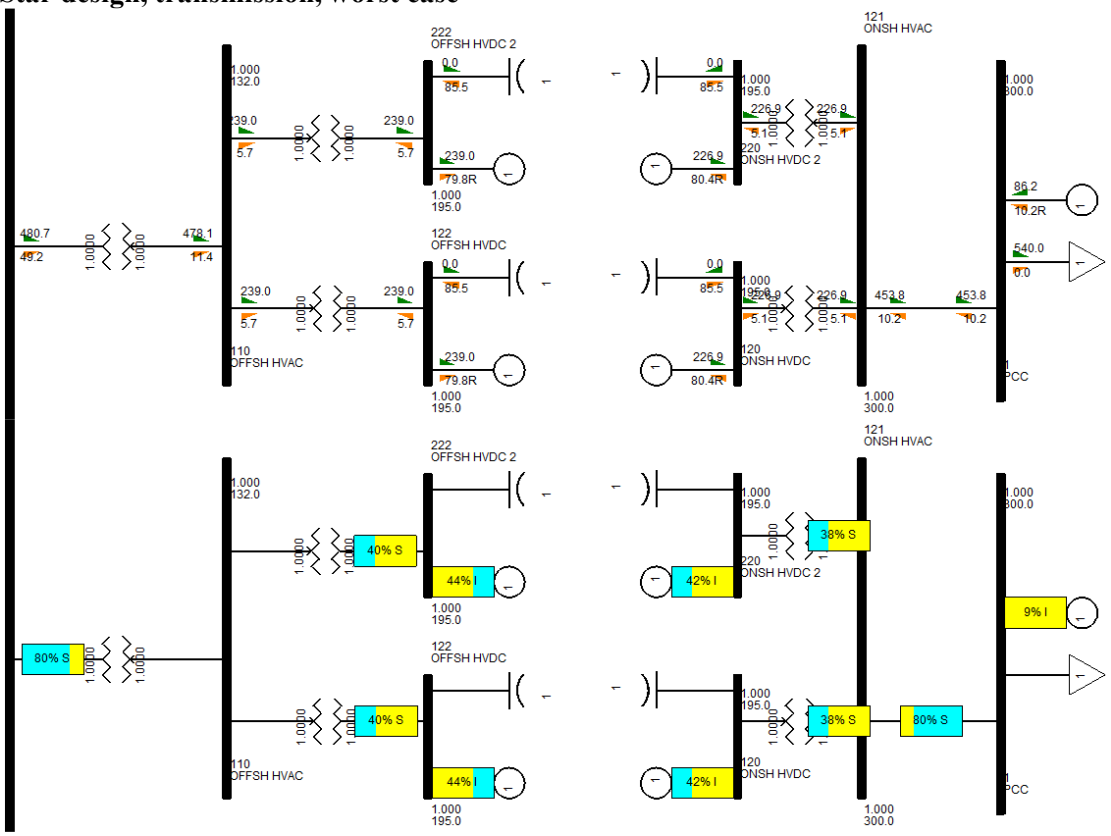

Star design, feeder, worst case

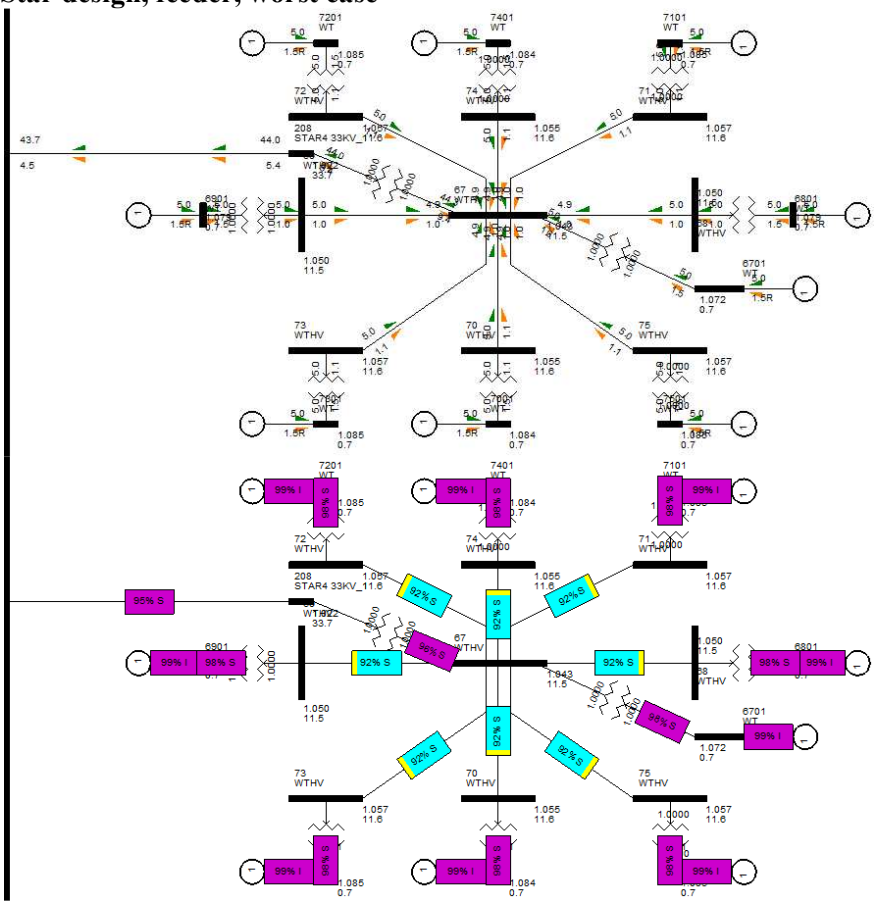

Appendix 3: Automatic sequence short circuit reports

Appplying a fault to the offshore substation bus, these are the ASCC-reports from PSS/E for the AC/AC systems, showing the fault current contributions from wind turbines and the transmission to shore:

Radial design

```
PSS/E SHORT CIRCUIT OUTPUT
WED, JUL 15 2009  11:46 .
HOME BUS IS   1000.  OFFSH SUB   33.000.

 .              *** FAULTED BUS IS:   1000 [OFFSH SUB   33.000] ***              .   0 LEVELS AWAY

 AT BUS   1000 [OFFSH SUB   33.000] AREA    1      (PU) V+: / 0.0000/    0.00

 THEV. R, X, X/R: POSITIVE  0.00272  0.03262   11.999
```

X--------- FROM ----------X	AREA	CKT	I/Z	THREE PHASE FAULT /I+/	AN(I+)	/Z+/	AN(Z+)	APP X/R
2 [WTHV 33.000]	1	1	PU/PU	0.6274	-39.60	0.0799	77.72	4.594
11 [WTHV 33.000]	1	1	PU/PU	0.6274	-39.60	0.0799	77.72	4.594
20 [WTHV 33.000]	1	1	PU/PU	0.6274	-39.60	0.0799	77.72	4.594
29 [WTHV 33.000]	1	1	PU/PU	0.6274	-39.60	0.0799	77.72	4.594
38 [WTHV 33.000]	1	1	PU/PU	0.6274	-39.60	0.0799	77.72	4.594
47 [WTHV 33.000]	1	1	PU/PU	0.6274	-39.60	0.0799	77.72	4.594
56 [WTHV 33.000]	1	1	PU/PU	0.6274	-39.60	0.0799	77.72	4.594
65 [WTHV 33.000]	1	1	PU/PU	0.6274	-39.60	0.0799	77.72	4.594
74 [WTHV 33.000]	1	1	PU/PU	0.6274	-39.60	0.0799	77.72	4.594
83 [WTHV 33.000]	1	1	PU/PU	0.6274	-39.60	0.0799	77.72	4.594
92 [WTHV 33.000]	1	1	PU/PU	0.6274	-39.60	0.0799	77.72	4.594
101 [WTHV 33.000]	1	1	PU/PU	0.6274	-39.60	0.0799	77.72	4.594
110 [TRANS OFFSH 400.00]	1	1	PU/PU	25.9139	-90.52	0.0158	86.00	14.286
TOTAL FAULT CURRENT (P.U.)				31.2126	-79.73			

Single sided design

```
PSS/E SHORT CIRCUIT OUTPUT                WED, JUL 15 2009  11:50 .HOME BUS IS   1000.OFFSH SUB   33.000.
 .              *** FAULTED BUS IS:   1000 [OFFSH SUB   33.000] ***              .   0 LEVELS AWAY  .
 AT BUS   1000 [OFFSH SUB   33.000] AREA    1      (PU) V+: / 0.0000/    0.00
 THEV. R, X, X/R: POSITIVE  0.00301  0.03283   10.899
```

X--------- FROM ----------X	AREA	CKT	I/Z	THREE PHASE FAULT /I+/	AN(I+)	/Z+/	AN(Z+)	APP X/R
2 [WTHV 33.000]	1	1	PU/PU	0.3760	-39.82	0.0799	77.72	4.594
10 [WTHV 33.000]	1	1	PU/PU	0.2507	-39.20	0.1358	76.97	4.321
11 [WTHV 33.000]	1	1	PU/PU	0.3760	-39.82	0.0799	77.72	4.594
19 [WTHV 33.000]	1	1	PU/PU	0.2507	-39.20	0.1358	76.97	4.321
20 [WTHV 33.000]	1	1	PU/PU	0.3760	-39.82	0.0799	77.72	4.594
28 [WTHV 33.000]	1	1	PU/PU	0.2507	-39.20	0.1358	76.97	4.321
29 [WTHV 33.000]	1	1	PU/PU	0.3760	-39.82	0.0799	77.72	4.594
37 [WTHV 33.000]	1	1	PU/PU	0.2507	-39.20	0.1358	76.97	4.321
38 [WTHV 33.000]	1	1	PU/PU	0.3760	-39.82	0.0799	77.72	4.594
46 [WTHV 33.000]	1	1	PU/PU	0.2507	-39.20	0.1358	76.97	4.321
47 [WTHV 33.000]	1	1	PU/PU	0.3760	-39.82	0.0799	77.72	4.594
55 [WTHV 33.000]	1	1	PU/PU	0.2507	-39.20	0.1358	76.97	4.321
56 [WTHV 33.000]	1	1	PU/PU	0.3760	-39.82	0.0799	77.72	4.594
64 [WTHV 33.000]	1	1	PU/PU	0.2507	-39.20	0.1358	76.97	4.321
65 [WTHV 33.000]	1	1	PU/PU	0.3760	-39.82	0.0799	77.72	4.594
73 [WTHV 33.000]	1	1	PU/PU	0.2507	-39.20	0.1358	76.97	4.321
74 [WTHV 33.000]	1	1	PU/PU	0.3762	-39.56	0.0799	77.72	4.594
82 [WTHV 33.000]	1	1	PU/PU	0.2508	-38.92	0.1358	76.97	4.321
83 [WTHV 33.000]	1	1	PU/PU	0.3760	-39.82	0.0799	77.72	4.594
91 [WTHV 33.000]	1	1	PU/PU	0.2507	-39.20	0.1358	76.97	4.321
92 [WTHV 33.000]	1	1	PU/PU	0.3760	-39.82	0.0799	77.72	4.594
100 [WTHV 33.000]	1	1	PU/PU	0.2507	-39.20	0.1358	76.97	4.321
101 [WTHV 33.000]	1	1	PU/PU	0.3760	-39.82	0.0799	77.72	4.594

```
   109 [WTHV        33.000]    1 1   PU/PU    0.2507   -39.20   0.1358    76.97    4.321
   110 [TRANS OFFSH 400.00]    1 1   PU/PU   25.6420   -90.01   0.0158    86.00   14.286
             TOTAL  FAULT  CURRENT  (P.U.)  30.9779   -79.22
```

Double sided design

```
.              PSS/E SHORT CIRCUIT OUTPUT               WED, JUL 15 2009  11:52 .HOME BUS IS   1000.
 .                                                                                .OFFSH SUB   48.000.
 .                                                                                .                  .
 .               *** FAULTED BUS IS:   1000 [OFFSH SUB   48.000] ***              .   0 LEVELS AWAY  .

 AT BUS   1000 [OFFSH SUB   48.000] AREA    1      (PU) V+: / 0.0000/    0.00

 THEV. R, X, X/R: POSITIVE  0.00299  0.03271   10.926

                                                  T H R E E   P H A S E   F A U L T
 X--------- FROM ----------X AREA CKT  I/Z      /I+/    AN(I+)    /Z+/    AN(Z+)  APP X/R
      2 [WTHV        48.000]    1 1   PU/PU    1.2286   -38.35   0.0422    78.32    4.838
     20 [WTHV        48.000]    1 1   PU/PU    0.6385   -40.62   0.0422    78.32    4.838
     29 [WTHV        48.000]    1 1   PU/PU    0.6385   -40.62   0.0422    78.32    4.838
     38 [WTHV        48.000]    1 1   PU/PU    0.6385   -40.62   0.0422    78.32    4.838
     47 [WTHV        48.000]    1 1   PU/PU    0.6385   -40.62   0.0422    78.32    4.838
     56 [WTHV        48.000]    1 1   PU/PU    0.6385   -40.62   0.0422    78.32    4.838
     65 [WTHV        48.000]    1 1   PU/PU    0.6385   -40.62   0.0422    78.32    4.838
     74 [WTHV        48.000]    1 1   PU/PU    0.6385   -40.62   0.0422    78.32    4.838
     83 [WTHV        48.000]    1 1   PU/PU    0.6385   -40.62   0.0422    78.32    4.838
     92 [WTHV        48.000]    1 1   PU/PU    0.6385   -40.62   0.0422    78.32    4.838
    101 [WTHV        48.000]    1 1   PU/PU    0.6385   -40.62   0.0422    78.32    4.838
    110 [TRANS OFFSH 400.00]    1 1   PU/PU   25.6419   -90.01   0.0158    86.00   14.286
              TOTAL  FAULT  CURRENT  (P.U.)  31.1076   -79.24
```

Shared ring system

```
.              PSS/E SHORT CIRCUIT OUTPUT               WED, JUL 15 2009  11:52 .HOME BUS IS   1000.
 .                                                                                .OFFSH SUB   33.000.
 .                                                                                .                  .
 .               *** FAULTED BUS IS:   1000 [OFFSH SUB   33.000] ***              .   0 LEVELS AWAY  .

 AT BUS   1000 [OFFSH SUB   33.000] AREA    1      (PU) V+: / 0.0000/    0.00

 THEV. R, X, X/R: POSITIVE  0.00302  0.03280   10.847

                                                  T H R E E   P H A S E   F A U L T
 X--------- FROM ----------X AREA CKT  I/Z      /I+/    AN(I+)    /Z+/    AN(Z+)  APP X/R
      2 [WTHV        33.000]    1 1   PU/PU    0.5312   -39.75   0.0799    77.72    4.594
     11 [WTHV        33.000]    1 1   PU/PU    0.5312   -39.75   0.0799    77.72    4.594
     20 [WTHV        33.000]    1 1   PU/PU    0.5312   -39.75   0.0799    77.72    4.594
     29 [WTHV        33.000]    1 1   PU/PU    0.5312   -39.75   0.0799    77.72    4.594
     38 [WTHV        33.000]    1 1   PU/PU    0.5312   -39.75   0.0799    77.72    4.594
     47 [WTHV        33.000]    1 1   PU/PU    0.5312   -39.75   0.0799    77.72    4.594
     56 [WTHV        33.000]    1 1   PU/PU    0.5312   -39.75   0.0799    77.72    4.594
     65 [WTHV        33.000]    1 1   PU/PU    0.5312   -39.75   0.0799    77.72    4.594
     74 [WTHV        33.000]    1 1   PU/PU    0.5312   -39.75   0.0799    77.72    4.594
     83 [WTHV        33.000]    1 1   PU/PU    0.5312   -39.75   0.0799    77.72    4.594
     92 [WTHV        33.000]    1 1   PU/PU    0.5312   -39.75   0.0799    77.72    4.594
    101 [WTHV        33.000]    1 1   PU/PU    0.5312   -39.75   0.0799    77.72    4.594
    110 [TRANS OFFSH 400.00]    1 1   PU/PU   25.6418   -90.00   0.0158    86.00   14.286
  22301 [          _2       ]    1 1   PU/PU    0.3911   -39.71   0.1439    77.71    4.592
  22801 [          _7       ]    1 1   PU/PU    0.3911   -39.71   0.1439    77.71    4.592
  23301 [          _<       ]    1 1   PU/PU    0.3911   -39.71   0.1439    77.71    4.592
              TOTAL  FAULT  CURRENT  (P.U.)  31.0150   -79.22
```

N-sided design (n=4)

```
.              PSS/E SHORT CIRCUIT OUTPUT                WED, JUL 15 2009  11:54 .HOME BUS IS   1000.
 .                                                                                  .OFFSH SUB   33.000.
 .                                                                                  .                  .
 .                *** FAULTED BUS IS:   1000 [OFFSH SUB   33.000] ***               .   0 LEVELS AWAY  .

 AT BUS   1000 [OFFSH SUB   33.000] AREA    1      (PU) V+: / 0.0000/    0.00

 THEV. R, X, X/R: POSITIVE  0.00302  0.03293   10.916

                                                    T H R E E   P H A S E   F A U L T
 X--------- FROM ----------X AREA CKT  I/Z      /I+/    AN(I+)    /Z+/    AN(Z+)  APP X/R
      2 [WTHV        33.000]    1 1   PU/PU    0.6219   -39.17   0.0647    83.88    9.331
     11 [WTHV        33.000]    1 1   PU/PU    0.6219   -39.17   0.0647    83.88    9.331
     20 [WTHV        33.000]    1 1   PU/PU    0.6219   -39.17   0.0647    83.88    9.331
     29 [WTHV        33.000]    1 1   PU/PU    0.6219   -39.17   0.0647    83.88    9.331
     38 [WTHV        33.000]    1 1   PU/PU    0.6219   -39.17   0.0647    83.88    9.331
     47 [WTHV        33.000]    1 1   PU/PU    0.6219   -39.17   0.0647    83.88    9.331
     56 [WTHV        33.000]    1 1   PU/PU    0.6219   -39.17   0.0647    83.88    9.331
     65 [WTHV        33.000]    1 1   PU/PU    0.6219   -39.17   0.0647    83.88    9.331
     74 [WTHV        33.000]    1 1   PU/PU    0.6219   -39.17   0.0647    83.88    9.331
     83 [WTHV        33.000]    1 1   PU/PU    0.6219   -39.17   0.0647    83.88    9.331
     92 [WTHV        33.000]    1 1   PU/PU    0.6219   -39.17   0.0647    83.88    9.331
    101 [WTHV        33.000]    1 1   PU/PU    0.6219   -39.17   0.0647    83.88    9.331
    110 [TRANS OFFSH 400.00]    1 1   PU/PU   25.6422   -90.02   0.0158    86.00   14.286
             TOTAL  FAULT  CURRENT  (P.U.)  30.9003   -79.23
```

Star design

```
.              PSS/E SHORT CIRCUIT OUTPUT                WED, JUL 15 2009  12:14 .HOME BUS IS   1000.
 .                                                                                  .COLLECTOR   33.000.
 .                                                                                  .                  .
 .                *** FAULTED BUS IS:   1000 [COLLECTOR   33.000] ***               .   0 LEVELS AWAY  .

 AT BUS   1000 [COLLECTOR   33.000] AREA    1      (PU) V+: / 0.0000/    0.00

 THEV. R, X, X/R: POSITIVE  0.00289  0.03320   11.496

                                                    T H R E E   P H A S E   F A U L T
 X--------- FROM ----------X AREA CKT  I/Z      /I+/    AN(I+)    /Z+/    AN(Z+)  APP X/R
    110 [TRANS OFFSH 400.00]    1 1   PU/PU   25.9115   -90.44   0.0158    86.00   14.286
    205 [STAR1 33KV_133.000]    1 1   PU/PU    0.5944   -36.48   0.0799    77.72    4.594
    206 [STAR2 33KV_133.000]    1 1   PU/PU    0.5944   -36.48   0.0799    77.72    4.594
    207 [STAR3 33KV_133.000]    1 1   PU/PU    0.5944   -36.48   0.0799    77.72    4.594
    208 [STAR4 33KV_133.000]    1 1   PU/PU    0.5944   -36.48   0.0799    77.72    4.594
    305 [STAR1 33KV_233.000]    1 1   PU/PU    0.5944   -36.48   0.0799    77.72    4.594
    306 [STAR2 33KV_233.000]    1 1   PU/PU    0.5944   -36.48   0.0799    77.72    4.594
    307 [STAR3 33KV_233.000]    1 1   PU/PU    0.5944   -36.48   0.0799    77.72    4.594
    308 [STAR4 33KV_233.000]    1 1   PU/PU    0.5944   -36.48   0.0799    77.72    4.594
    405 [STAR1 33KV  33.000]    1 1   PU/PU    0.5944   -36.48   0.0799    77.72    4.594
    406 [STAR2 33KV  33.000]    1 1   PU/PU    0.5944   -36.48   0.0799    77.72    4.594
    407 [STAR3 33KV  33.000]    1 1   PU/PU    0.5944   -36.48   0.0799    77.72    4.594
    408 [STAR4 33KV  33.000]    1 1   PU/PU    0.5944   -36.48   0.0799    77.72    4.594
             TOTAL  FAULT  CURRENT  (P.U.)  30.6559   -79.60
```

Appendix 4: Dynamic models

This appendix describes all the dynamic models used in this thesis. Block diagrams and parameters are given for all models, except from the ABB HVDC Light user model.

Wind turbine model

The figure underneath shows the principal scheme of the WT3 generic wind model in PSS/E.

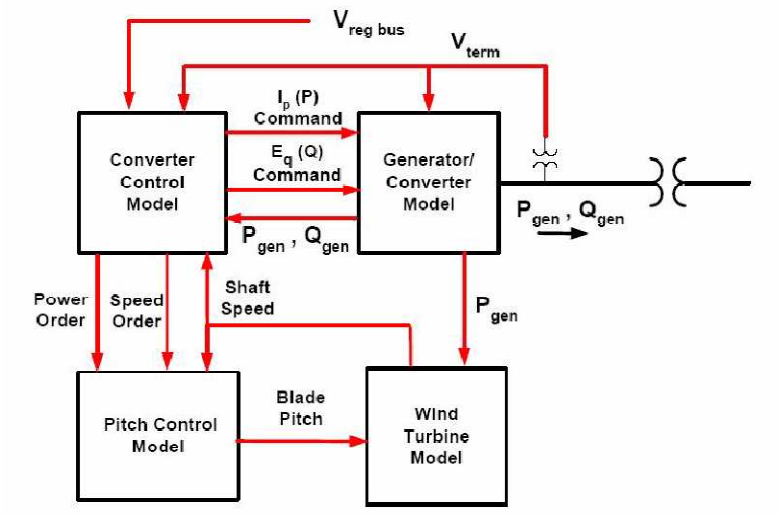

All issues of making an equivalent of a wind farm to be modeled are up to the user. The model provides the possibility to lump several turbines into one equivalent representation. The user should make a decision on how many original units that can be lumped into one equivalent machine presented in the load flow case. For *n* lumped machines, the machine rating M_{BASE} of the original machine must be multiplied by *n*. It is also up to the user to take care of the adequate equivalent of the wind farm feeders, collectors, and step up transformers.

Generator/converter model (WTRG1)

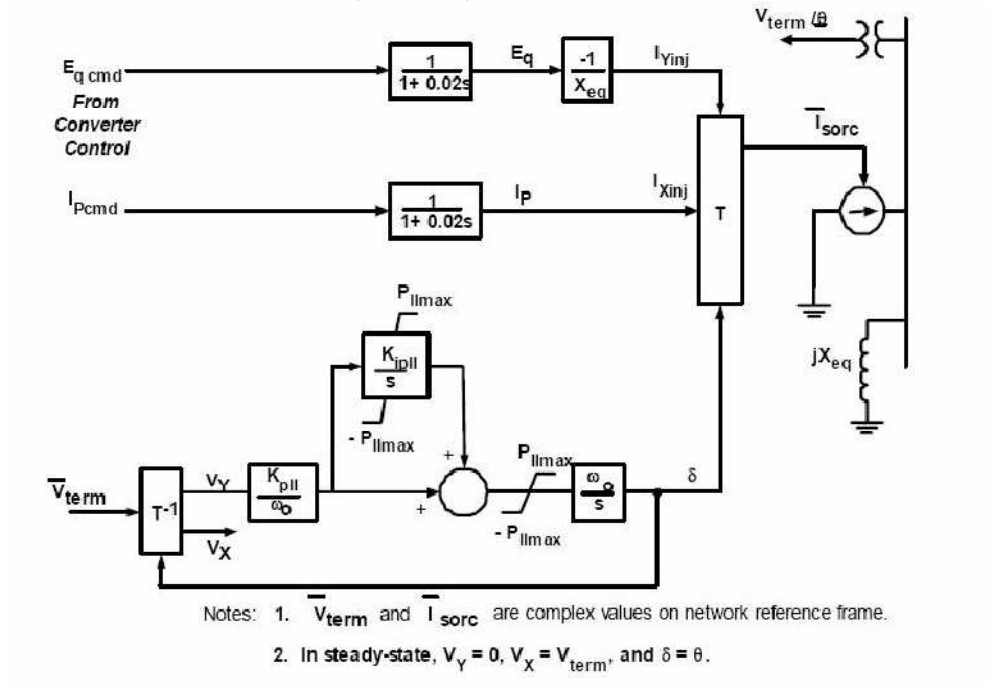

Notes: 1. $\overline{V}_{term}$ and $\overline{I}_{sorc}$ are complex values on network reference frame.

2. In steady-state, $V_Y = 0$, $V_X = V_{term}$, and $\delta = \theta$.

Parameters:

CONs		ICONs	
Xeq	0.8000	No of lumped turbines	1
PLL gain	30.0000		
PLL integrator gain	0.0000		
PLL min limit	0.1000		
Turbine MW rating	5.0000		

Electrical control model(WT3E1)

Reactive power control system:

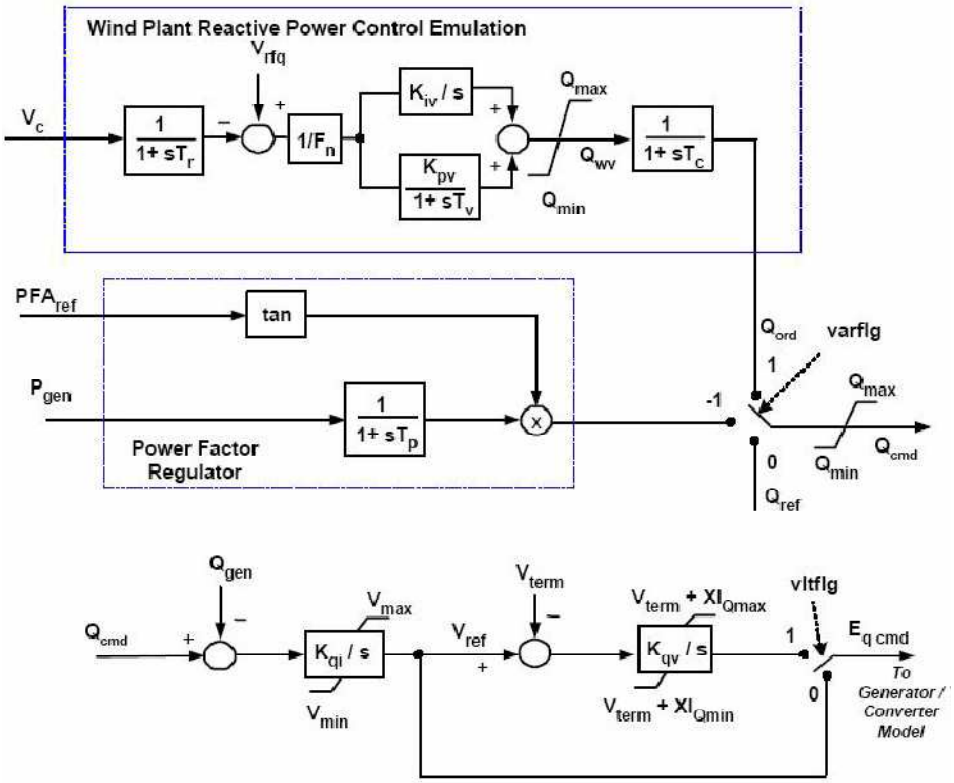

Torque/current control:

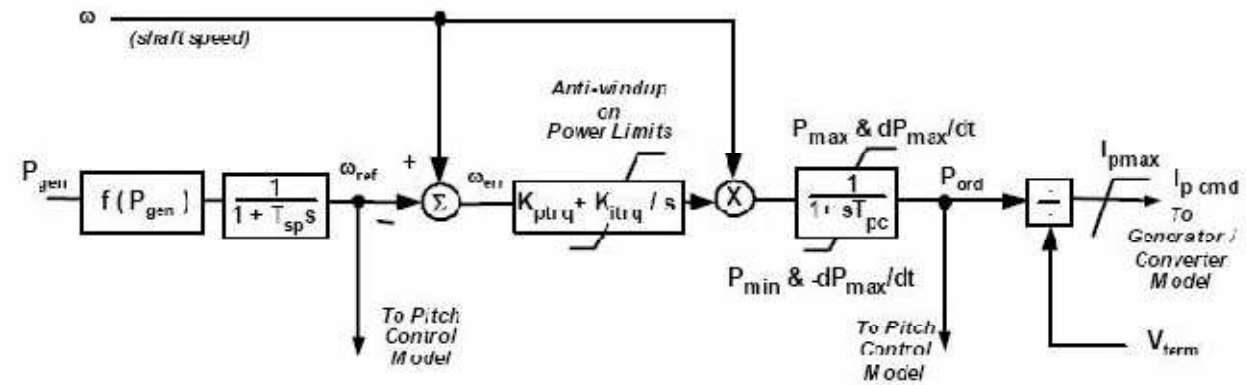

Parameters:

CONs		ICONs	
Tfv - V-regulator filter	0.150	Remote bus #	110
Kpv - V-regulator proportional gain	18.00	VARFLG: =0 Const. Q ctrl, =1 reactive power ctrl, = -1 const. pf ctrl	1
Kiv - V-regulator integrator gain	5.000	VLTFLG: =1 Closed loop terminal voltage control	AC: 0 DC: 1
Xc - line drop compensation reactance	0.050	From bus - interconnection transformer	301
Tfp - T-regulator filter	0.050	To bus - interconnection transformer	3
Kpp - T-regulator proportional gain	3.000	Id - interconnection transformer	'1'
Kip - T-regulator integrator gain	0.600		
PMX - T-regulator max limit	1.120		
PMN - T-regulator min limit	0.100		
QMX - V-regulator max limit	0.350		
QMN - V-regulator min limit	-0.436		
IPMAX - Max active current limit	1.100		
TRV - V-sensor	0.050		
RPMX - maximum Pordr derivative	0.450		
RPMN - minimum Pordr derivative	0.450		
T_POWER - Power filter time constant	5.000		
KQi - MVAR/Volt gain	0.050		
VMINCL	0.900		
VMAXCL	1.200		
Kqv - Volt/MVAR gain	40.00		
XIQmin - min. limit of (Vterm - Eq'cmd)	0.5000		
XIQmax - max. limit of (Vterm - Eq'cmd)	0.4000		
Tv - Lag time constant in WindVar controller	0.0500		
Tp - Pelec filter in fast PF controller	0.0500		
Fn - A portion of on-line wind turbines	1.0000		
Shaft speed at Pmin, pu	0.6900		
Shaft speed at 20% rated power, pu	0.7800		
Shaft speed at 40% rated power, pu	0.9800		
Shaft speed at 60% rated power, pu	1.1200		
Shaft speed at 80% rated power, pu	0.7400		
Shaft speed at 100% rated power, pu	1.2000		

Wind turbine model (WT3T1)

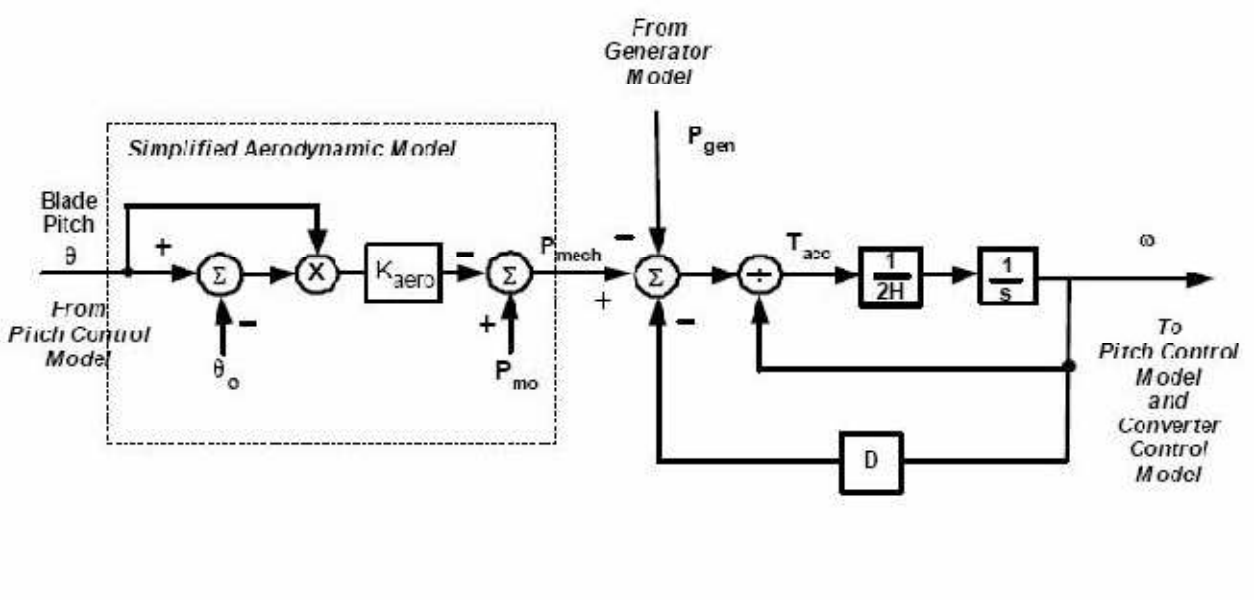

$H_t = H_{tfrac} * H$

$H_g = H - H_t$

$K = 2 * (2\pi \text{ Freq1 })^2 * H_t * H_g / H$

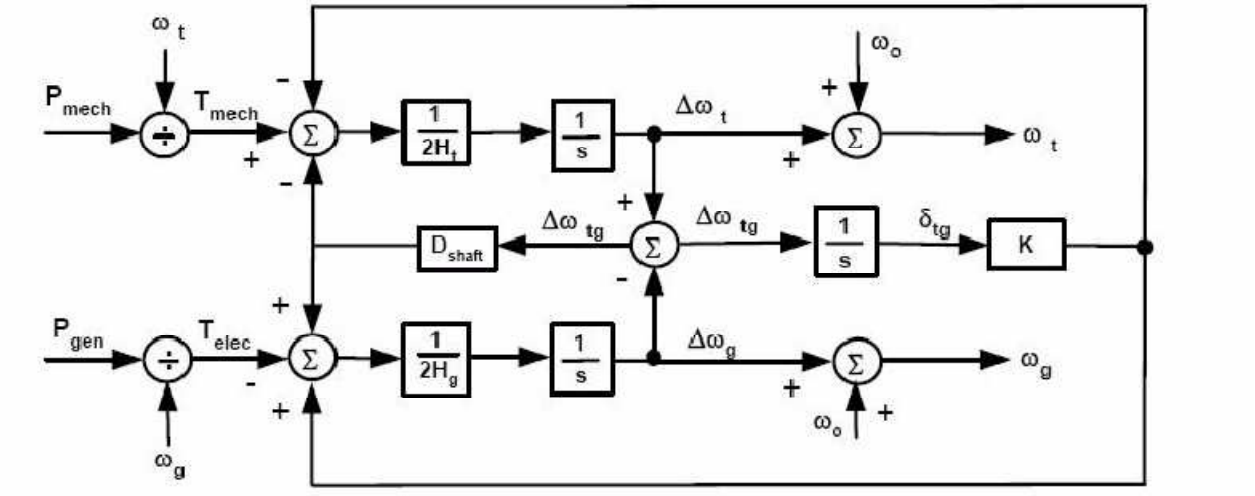

Parameters:

CONs		ICONs	
Vw - Initial wind speed, pu of rated wind speed	1.2500		
H - Total inertia constant, MW*sec/MVA	4.9500		
DAMP - Machine damping factor, pu P/pu speed	0.0000		
Kaero - Aerodynamic gain factor	0.0070		
Theta2 - Blade pitch at twice rated wind speed, deg.	21.9800		
Htfac - Turbine inertia fraction (Hturb/H)	0.8750		
Freq1 - First shaft torsional resonant frequency, Hz	1.8000		
DSHAFT - Shaft Damping factor, pu P/pu speed	1.5000		

Pitch control model (WT3P1)

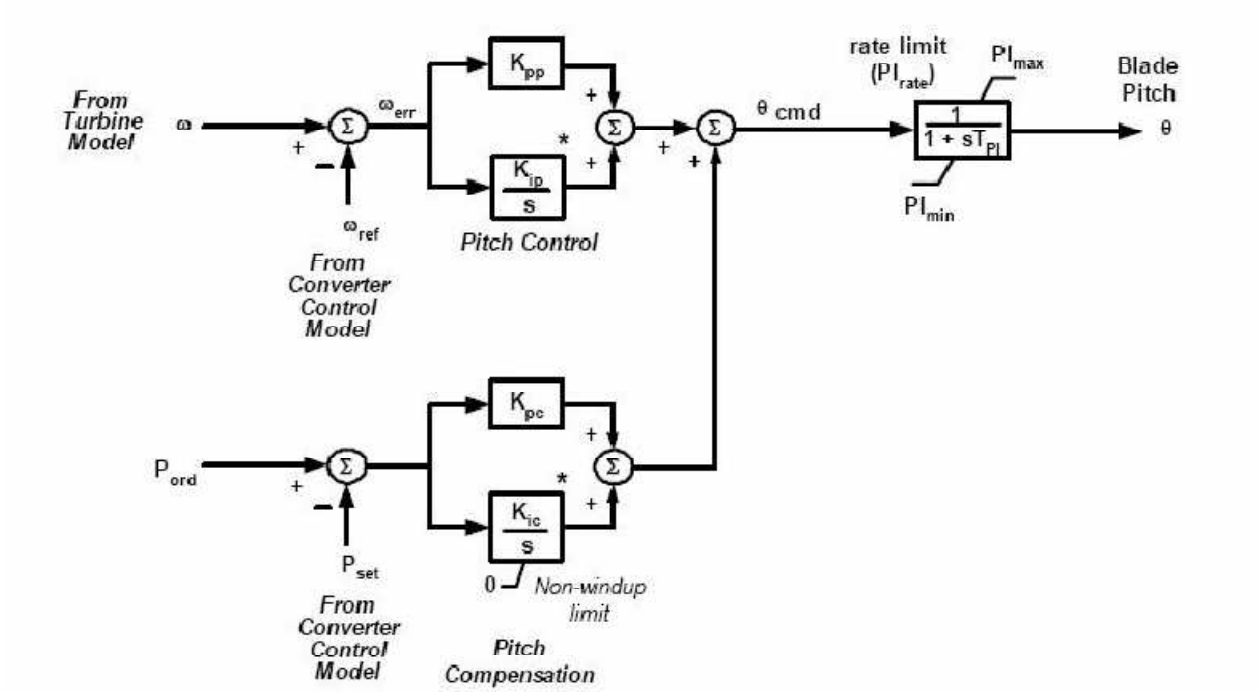

* The Pitch Control and Pitch Compensation integrators are non-windup integrators as a function of the pitch, i.e., the inputs of these integrators are set to zero when the pitch is in limits (Pimax or Pimin) and the integrator input tends to force the pitch command further against its limit. The outputs of these integrators are not limited except by the lower (zero) limit on the Pitch Compensation integrator.

Parameters:

CONs		ICONs	
Tp - Time constant of the output lag (sec)	0.3000		
Kpp - Proportional gain of PI regulator(pu)	150.0000		
Kip - Integrator gain of PI regulator (pu)	25.0000		
Kpc - Proportional gain of the compensator(pu)	3.0000		
Kic - Integrator gain of the compensator (pu)	30.0000		
TetaMin - Lower pitch angle limit (degrees)	0.0000		
TetaMax - Upper pitch angle limit (degrees)	27.0000		
RTetaMax - Upper pitch angle rate limit (deg/sec)	10.0000		
PMX - Power reference (pu)	1.0000		

SVC-model (CSVGN5)

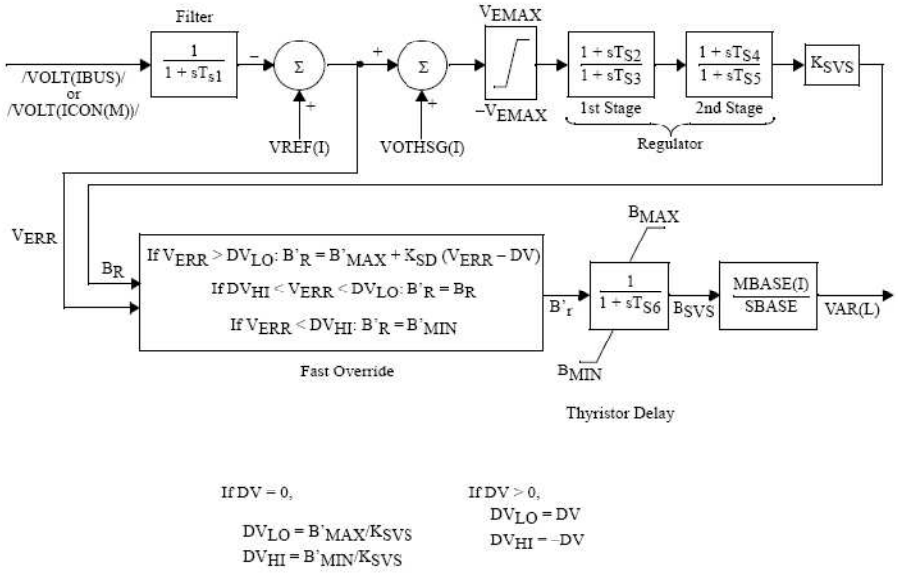

If DV = 0,
$DV_{LO} = B'_{MAX}/K_{SVS}$
$DV_{HI} = B'_{MIN}/K_{SVS}$

If DV > 0,
$DV_{LO} = DV$
$DV_{HI} = -DV$

Parameters:

CONs		ICONs	
TS1	0.0000	IB, remote bus number	0
VE MAX	0.1500		
TS2	0.1000		
TS3 (>0)	5.0000		
TS4	0.0000		
TS5	0.0000		
KSVS	400.0		
KSD	0.0000		
BMAX	1.0000		
B'MAX	1.0000		
B'MIN	-0.5000		
B MIN	-0.5000		
TS6 (>0)	0.0500		
DV	0.1500		

Onshore generator model

Salient pole generator model (GENSAL):

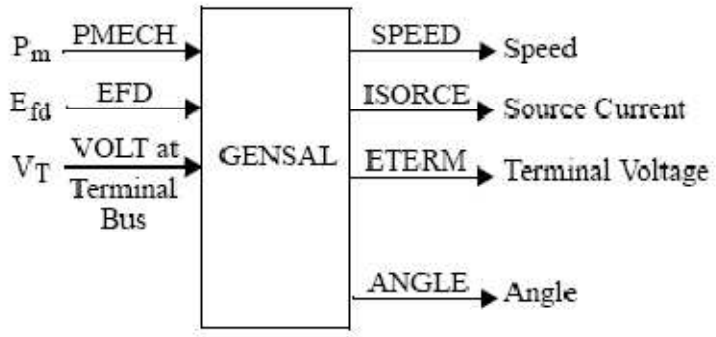

Parameters:

CONs		ICONs	
T'do (> 0)	7.0000		
T"do (> 0)	0.0400		
T"qo (> 0)	0.2500		
Inertia H	20.0000		
Speed Damping D	0.0000		
Xd	2.3000		
Xq	1.4000		
X'd	0.2768		
X"d = X"q	0.2000		
X1	0.1200		
S(1.0)	0.1000		
S(1.2)	0.3000		

Generator exciter model (SCRX):

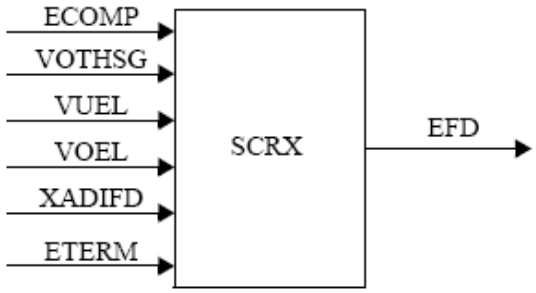

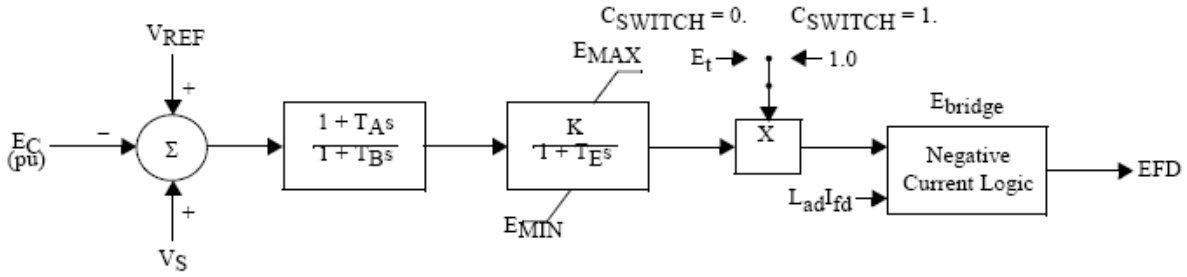

V_S = VOTHSG + VUEL + VOEL

Parameters:

CONs		ICONs	
TA/TB	0.1000		
TB (> 0)	10.0000		
K	200.0000		
TE	0.0500		
EMIN	0.0000		
EMAX	4.0000		
CSWITCH (0=bus fed, 1=solid fed)	0.0000		
rc/rfd	0.0000		

Generator governor model (HYGOV)

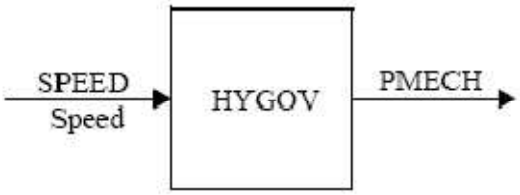

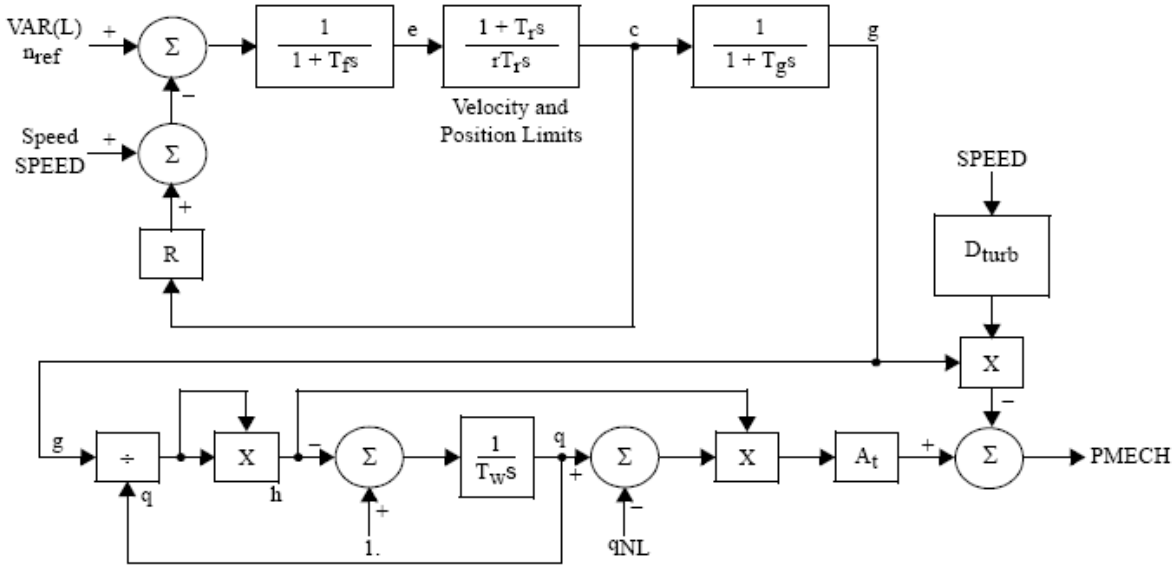

Parameters:

CONs		ICONs	
R, Permanent Droop	0.0500		
r, Temporary Droop	0.4000		
Tr (> 0) Governor Time Constant	8.0000		
Tf (> 0) Filter Time Constant	0.0500		
Tg (> 0) Servo Time Constant	0.2000		
VELM, Gate Velocity Limit	0.1000		
GMAX, Maximum Gate Limit	2.0000		
GMIN, Minimum Gate Limit	-2.0000		
TW (> 0) Water Time Constant	2.0000		
At, Turbine Gain	1.1000		
Dturb, Turbine Damping	1.7500		
qNL, No Load Flow	0.1000		

Appendix 5: Dynamic plots

This appendix shows all plots of P,Q, ω and U at the investigated buses in this thesis. Bus 201 (6701 for the AC/DC star design) is the first bus of the feeder where no fault occurs. Bus 3801 (5601 for the star design) is the first bus of the feeder where the fault occurs. Bus 4501 (5601 for the star designs) is the second outermost bus in the feeder where the fault occurs. Bus 4601 (6501 for the star designs) is the outermost bus in the feeder where the fault occurs. For all plots, the color code is as follows:

Green:	Active power	[*pu on system base*]
Blue:	Reactive power	[*pu on system base*]
Light blue:	Generator speed	[*pu on system base*]
Purple:	Voltage	[*pu on system base*]

RADIAL DESIGN

AC/AC TRANSMISSION

FAULT TYPE 1: TRANSMISSION FAULT

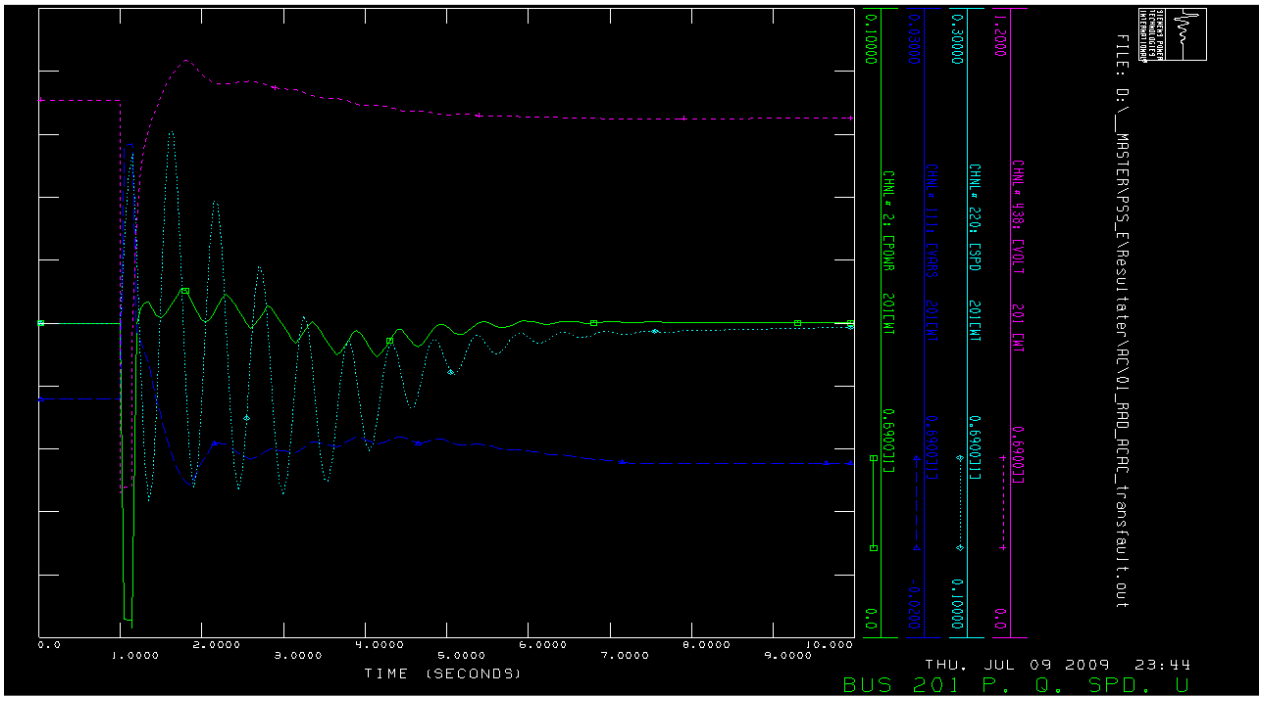

FAULT TYPE 2: FAULT BETWEEN INNERMOST TURBINE OF FEEDER AND SUBSTATION

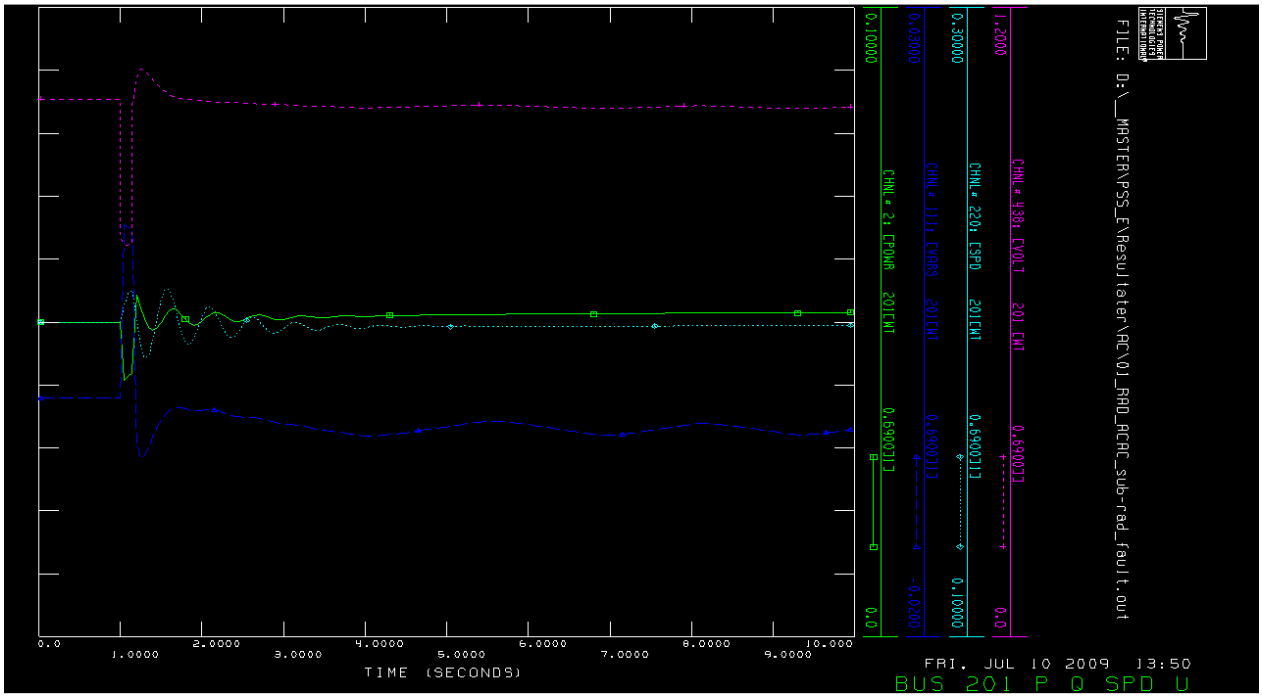

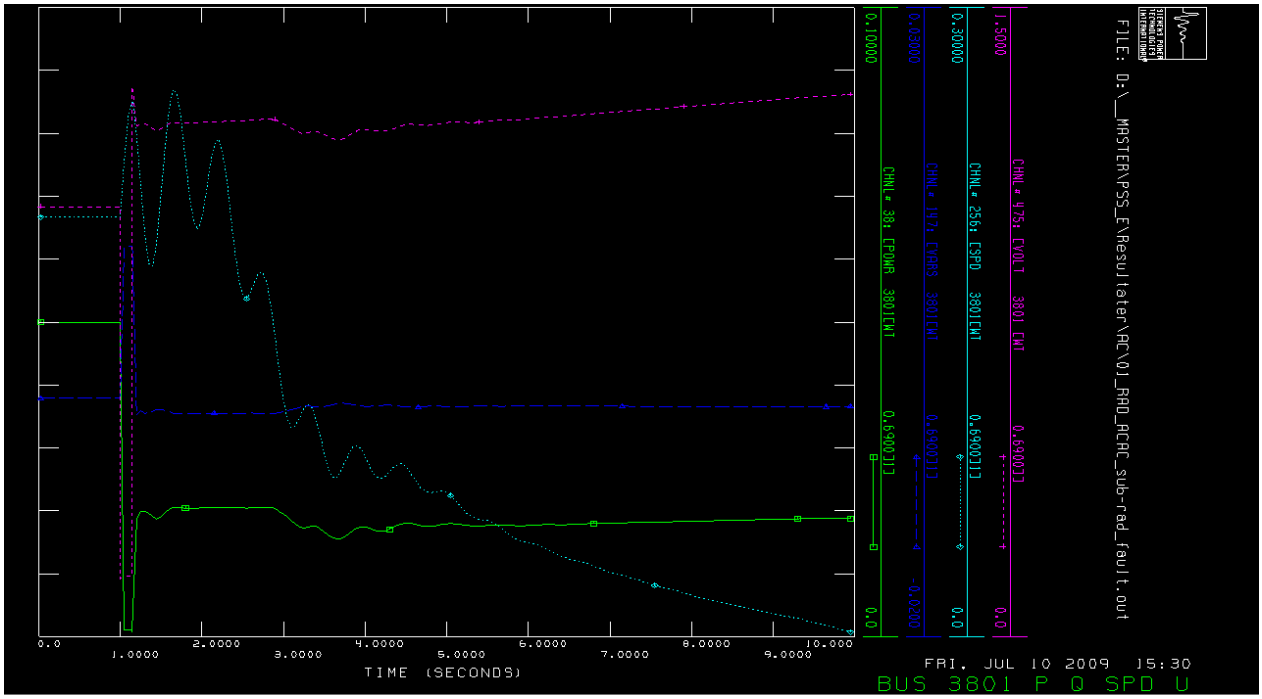

FAULT TYPE 3: FAULT IN THE OUTERMOST CABLE IN THE FEEDER

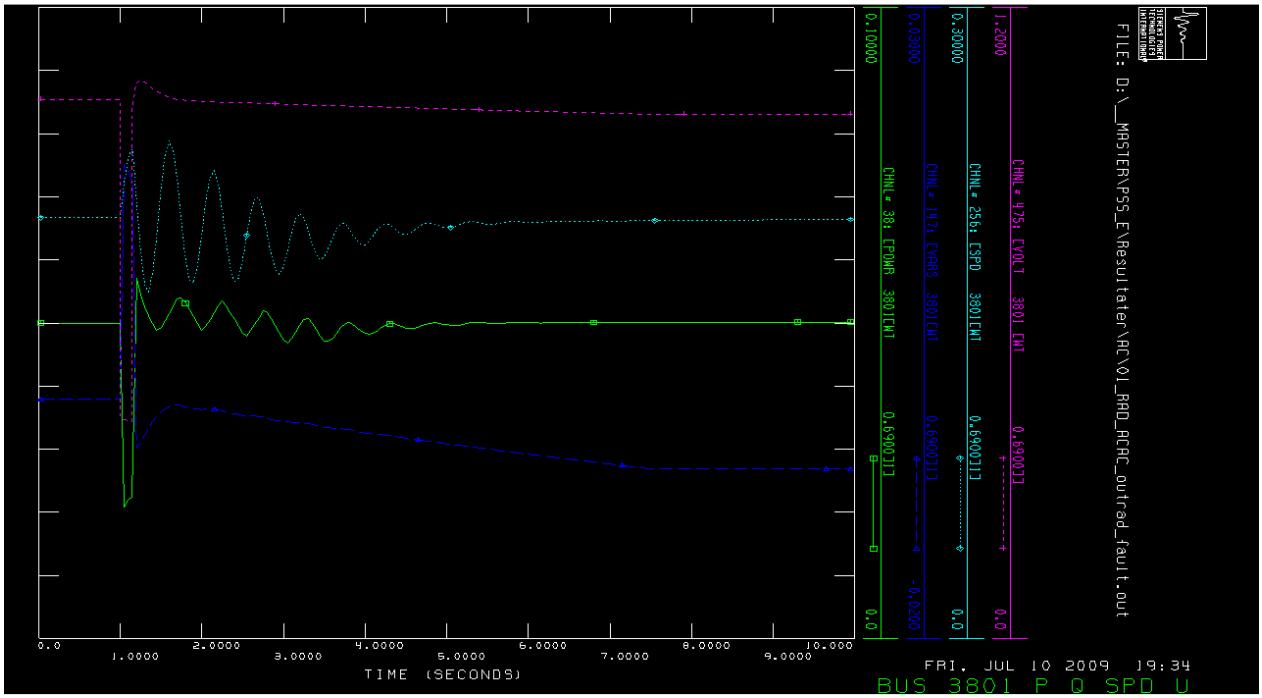

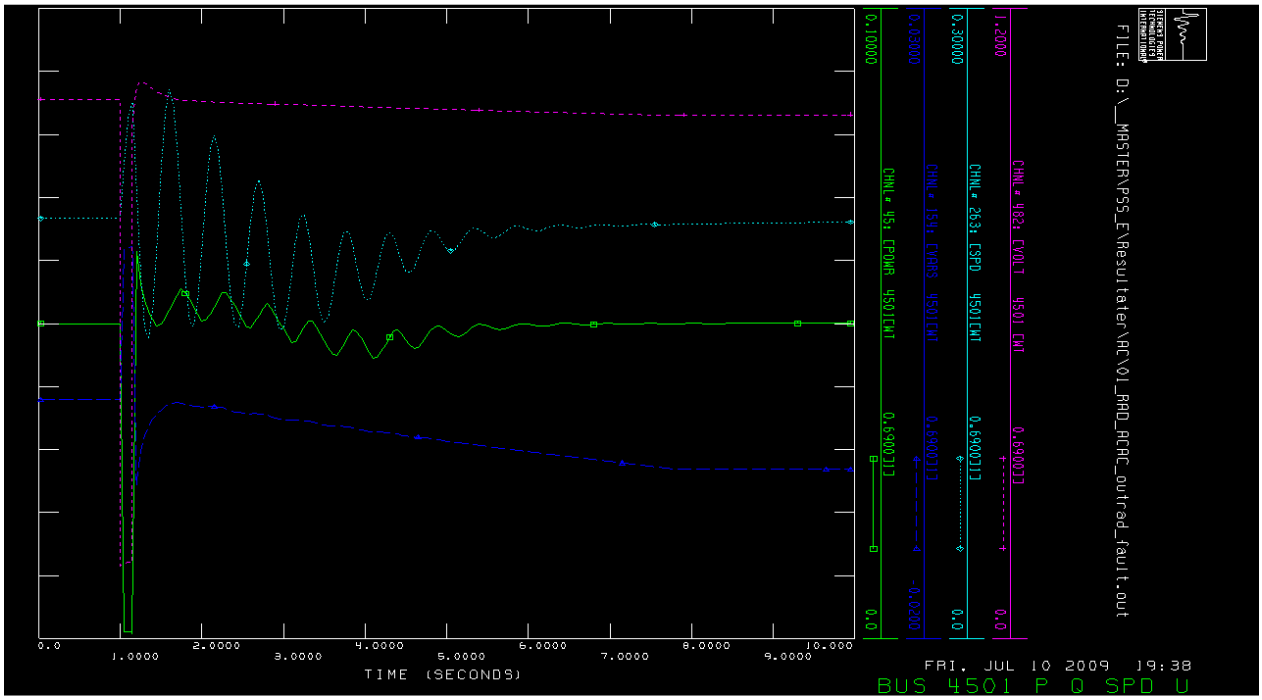

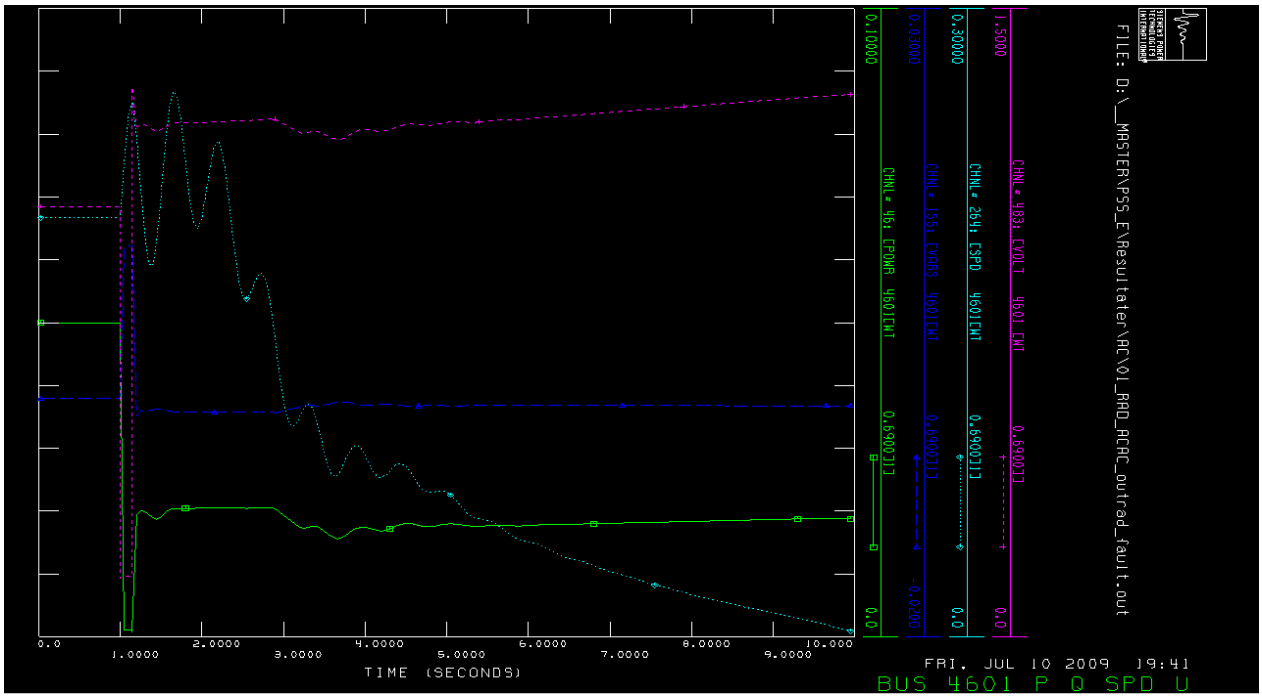
FILE: D:__MASTER\PSS_E\Resultater\AC\01_RAD_AC\AC_outrad_fault.out
CHNL = 483: [VOLT 4601 'CNT
CHNL = 264: [SPD 4601'CNT
CHNL = 46: [POWR 4601'CNT
TIME (SECONDS)
FRI, JUL 10 2009 19:41
BUS 4601 P Q SPD U

AC/DC TRANSMISSION

FAULT TYPE 1: TRANSMISSION FAULT

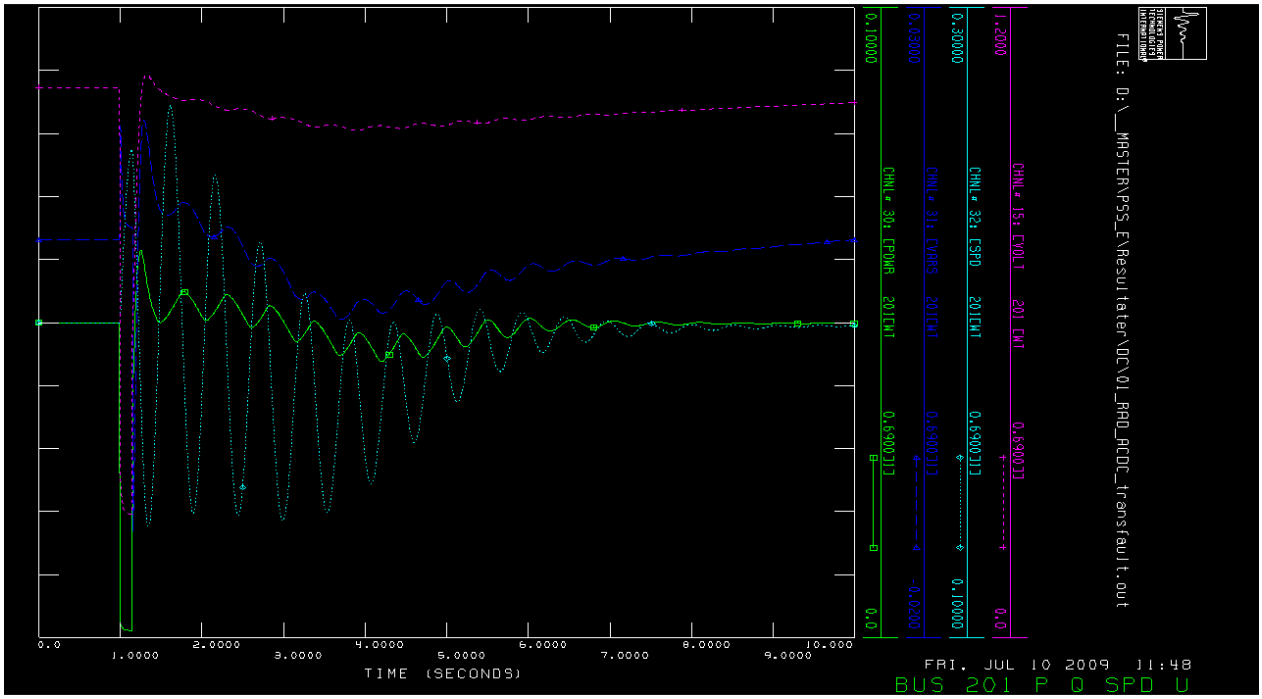

FAULT TYPE 2: FAULT BETWEEN INNERMOST TURBINE OF FEEDER AND SUBSTATION

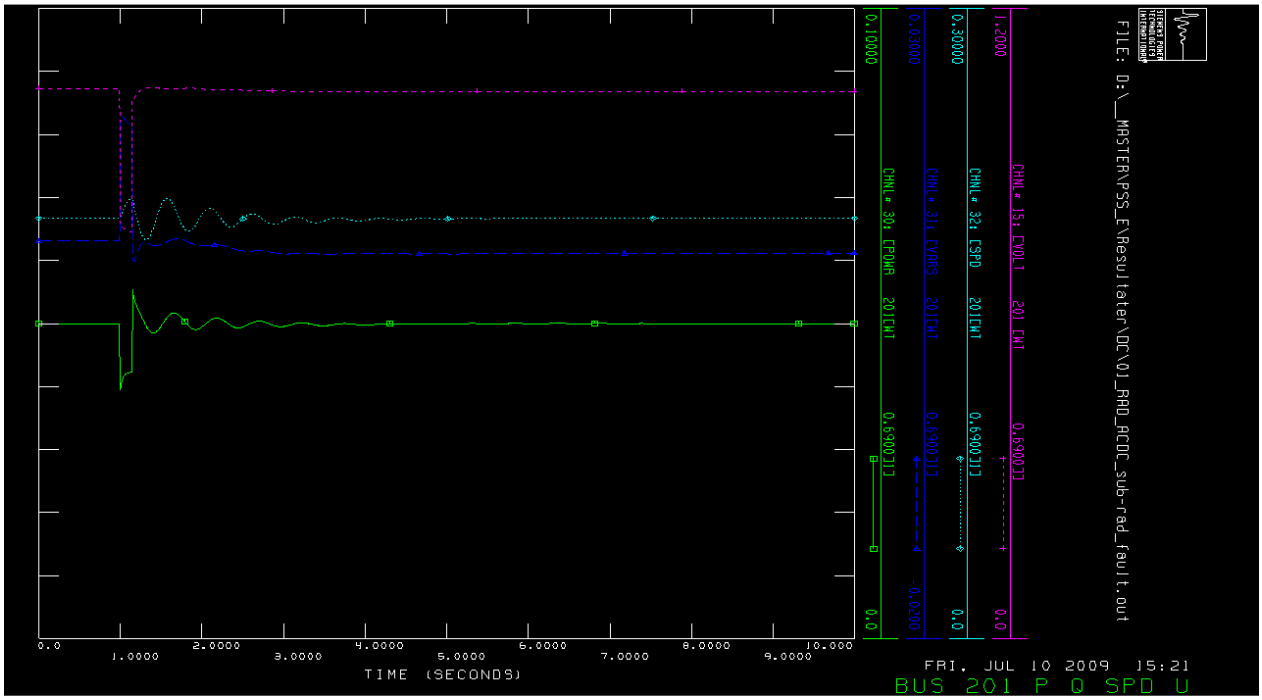

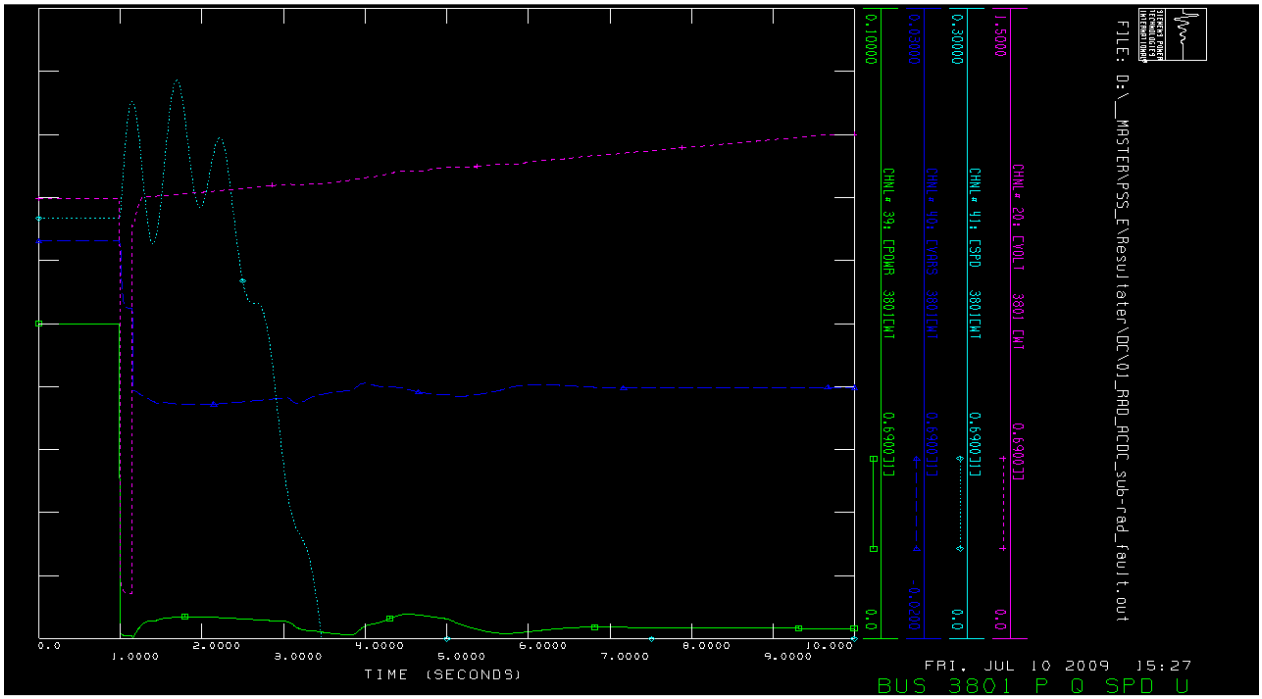

FAULT TYPE 3: FAULT IN THE OUTERMOST CABLE IN THE FEEDER

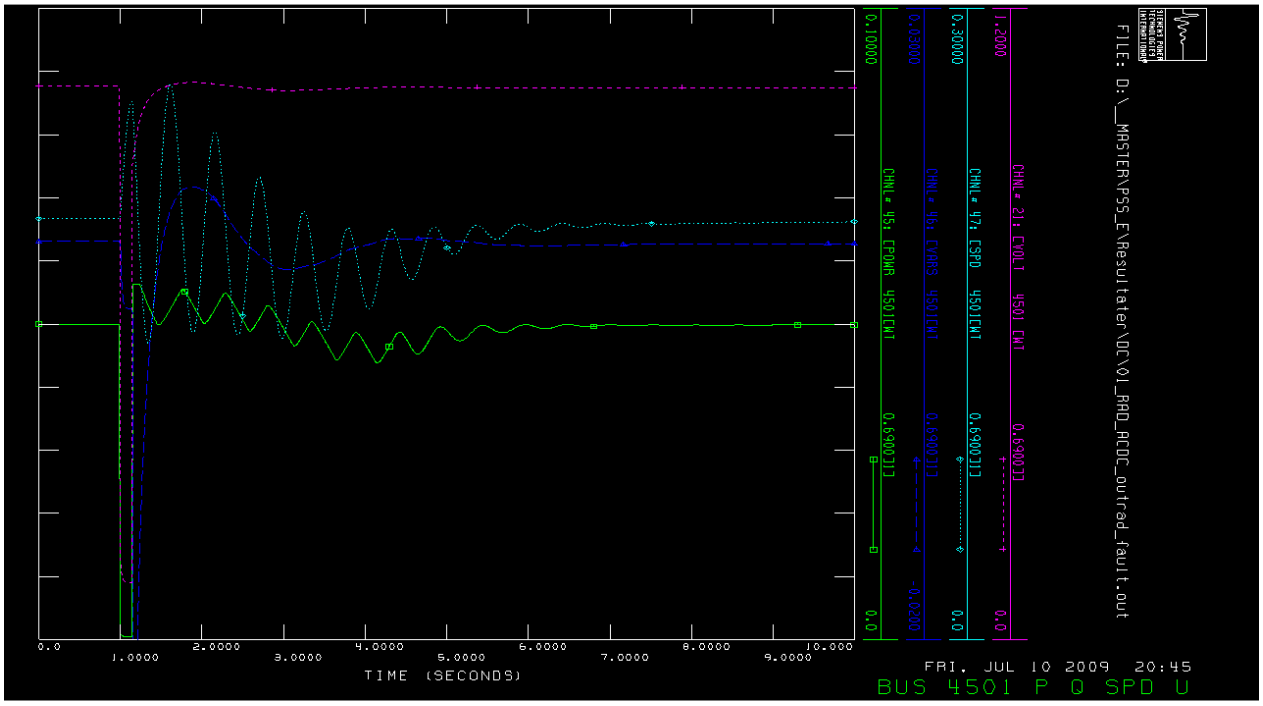

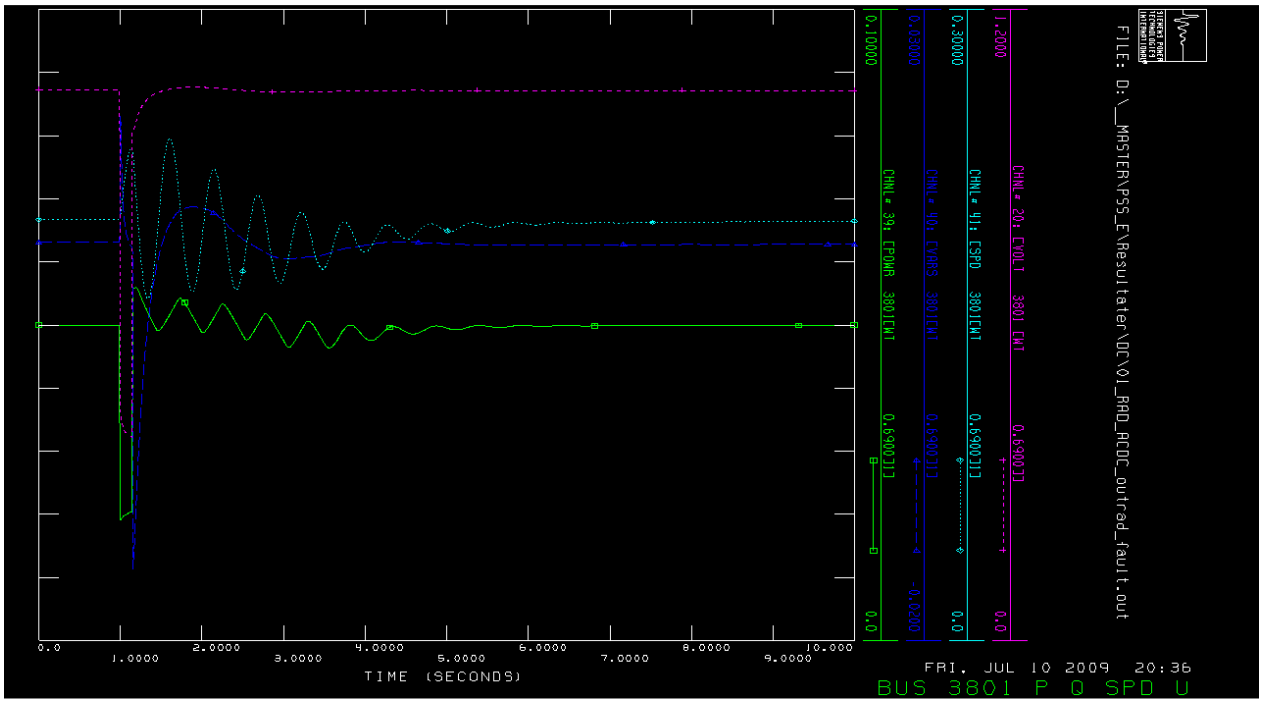

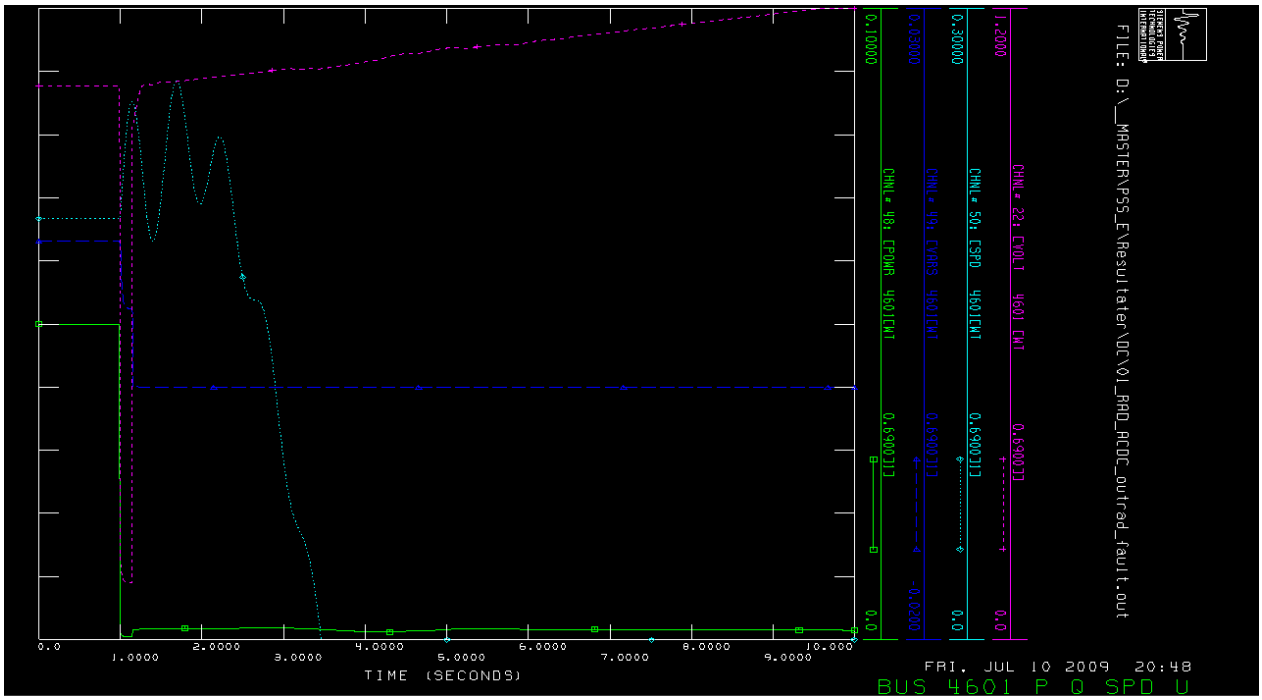
FILE: D:__MASTER\PSS_E\Resultater\DC\01_RAD_ACDC_outrad_fault.out
TIME (SECONDS)
FRI, JUL 10 2009 20:48
BUS 4601 P Q SPD U

SINGLE SIDED DESIGN

AC/AC TRANSMISSION

FAULT TYPE 1: TRANSMISSION FAULT

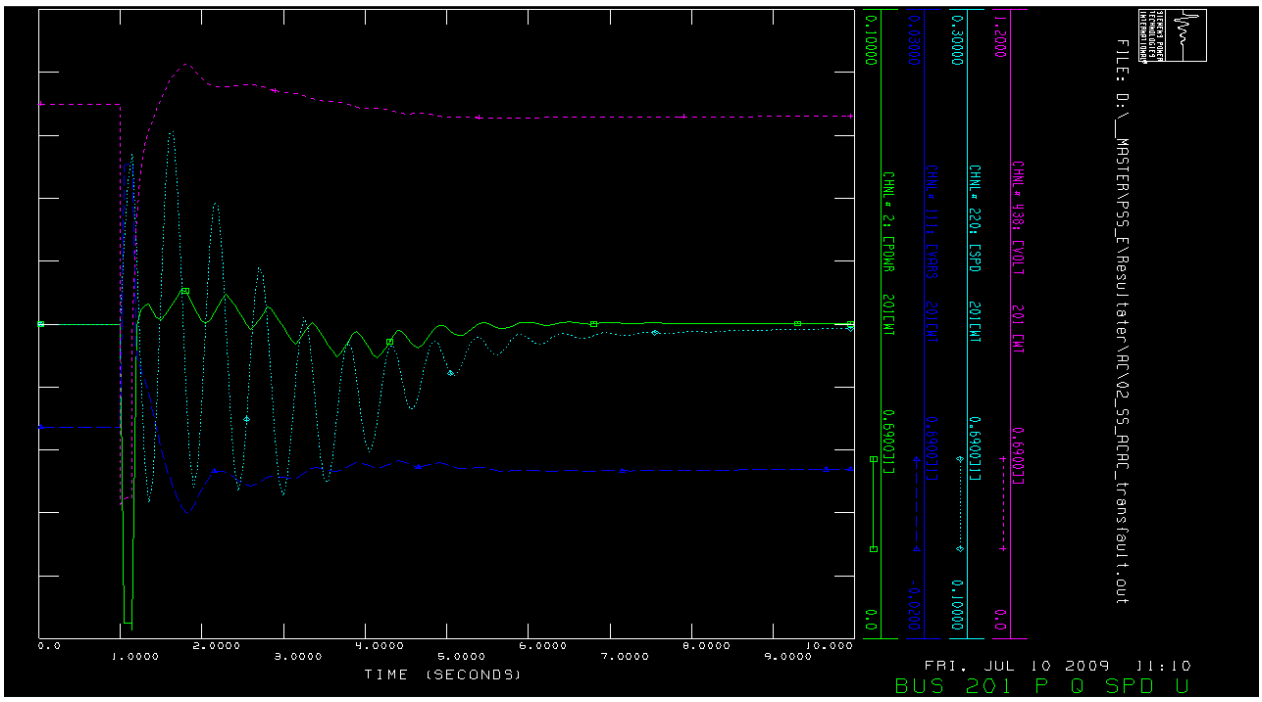

FAULT TYPE 2: FAULT BETWEEN INNERMOST TURBINE OF FEEDER AND SUBSTATION

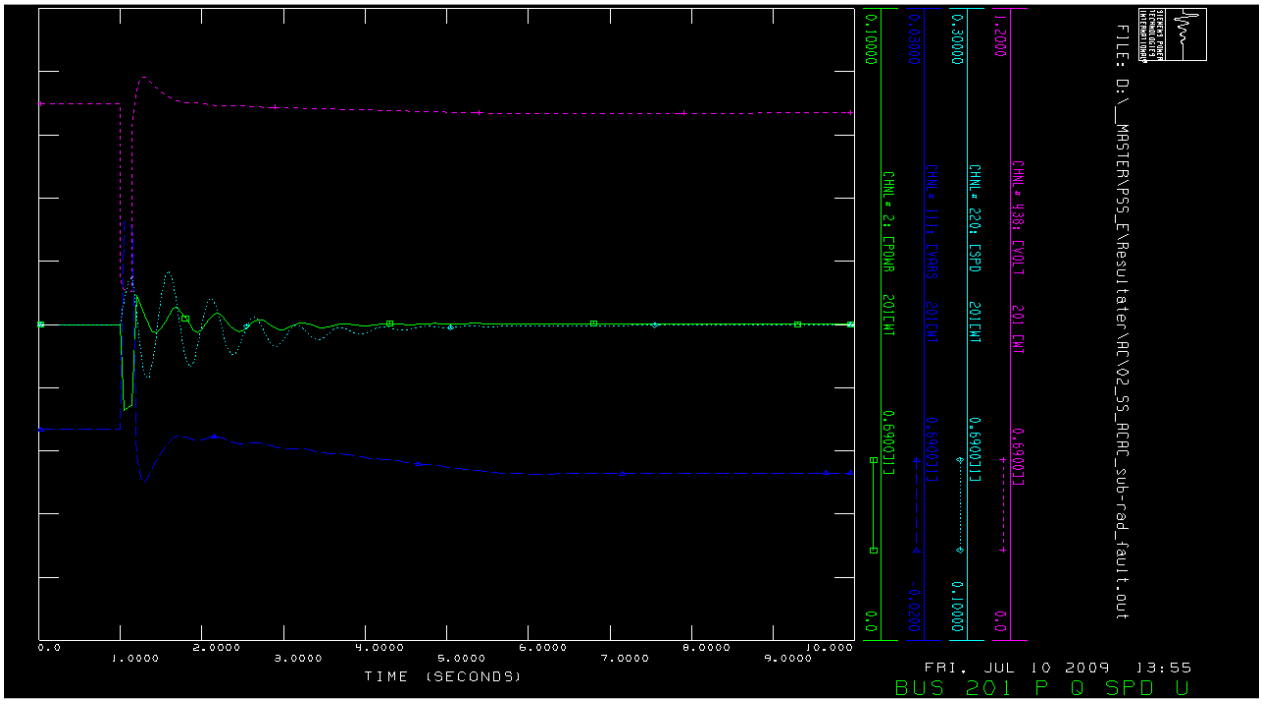

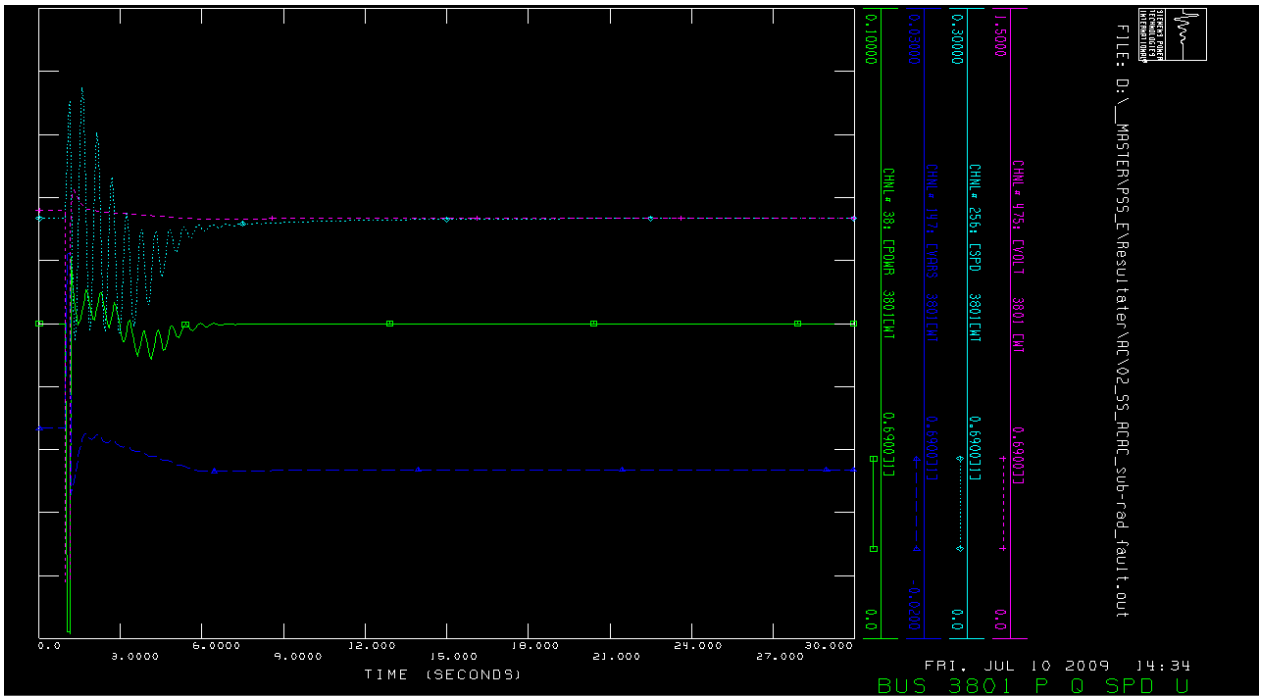

FAULT TYPE 3: FAULT IN THE OUTERMOST CABLE IN THE FEEDER

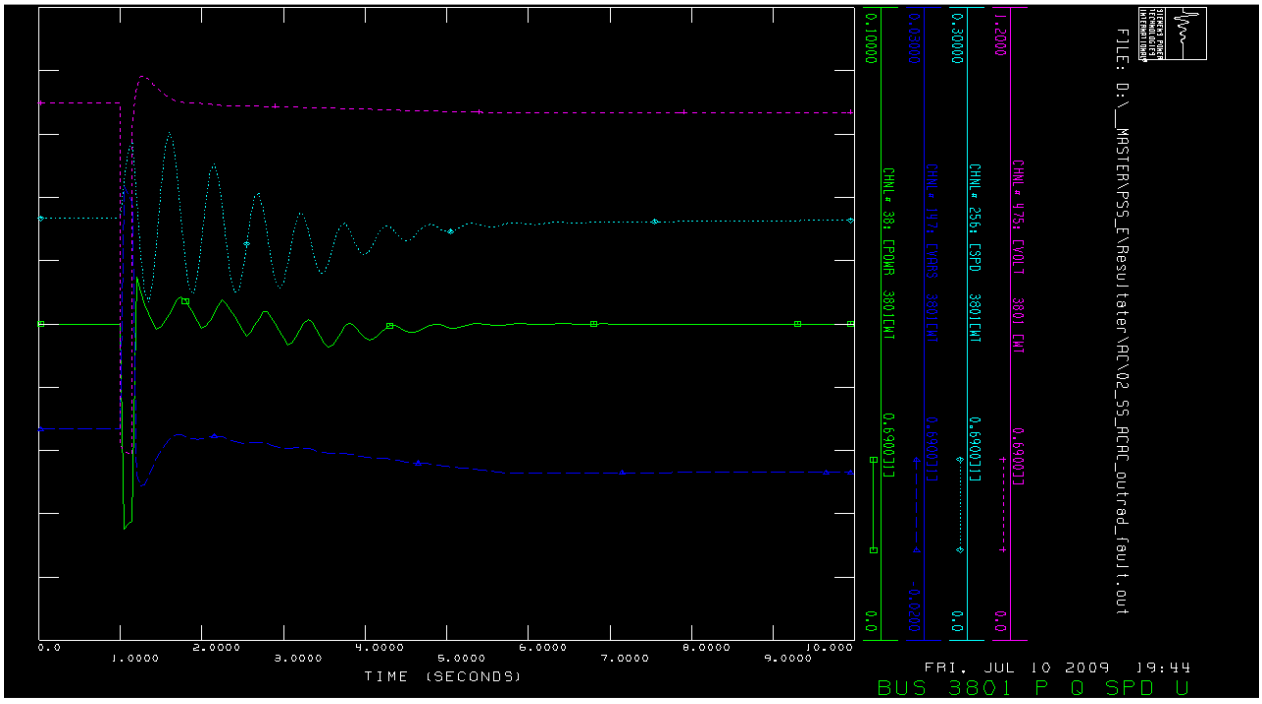

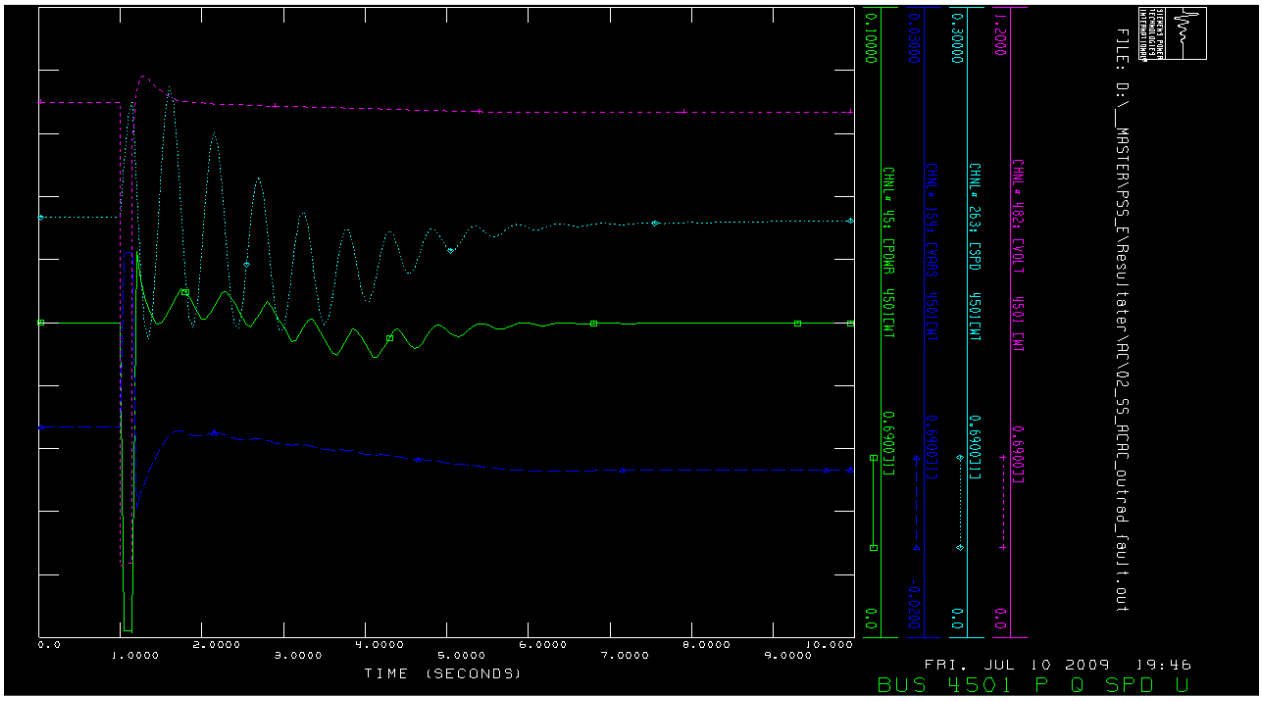

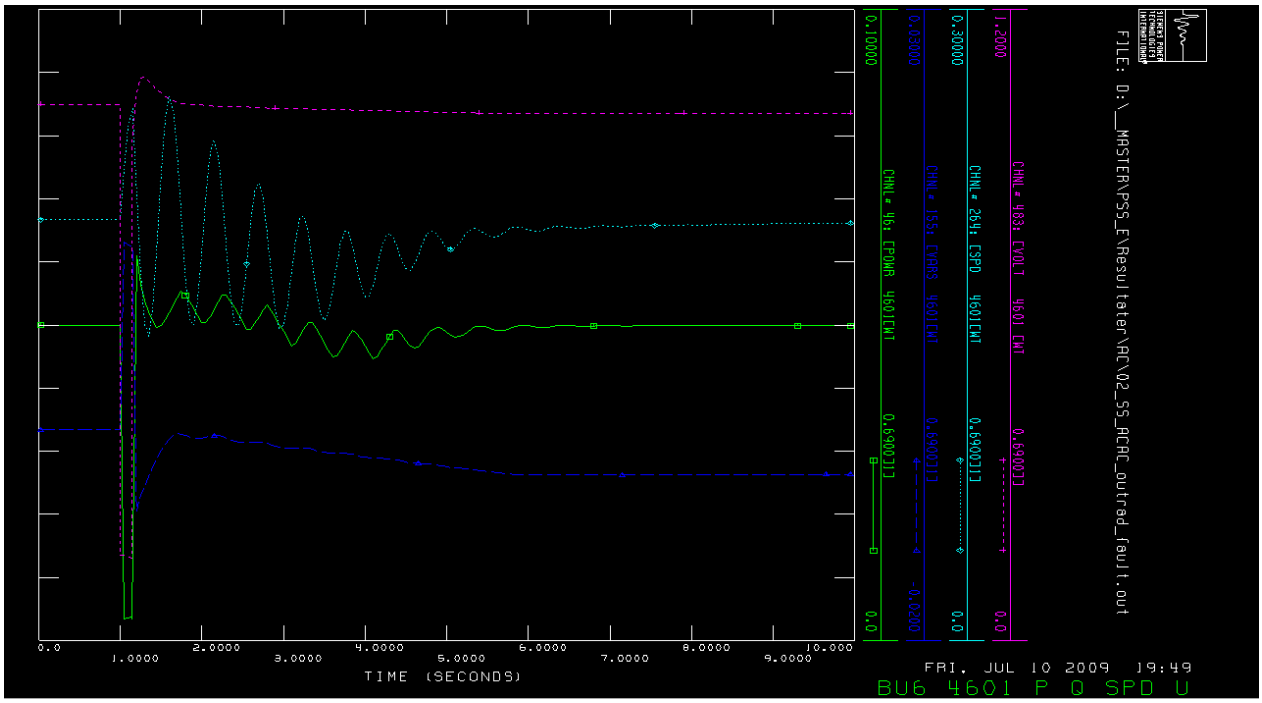
FILE: D:__MASTER\PSS_E\Resultater\AC\02_SS_ACAC_outrad_fault.out
CHNL # 46: EPOWR 4601CKT
CHNL # 154: EVARS 4601CKT
CHNL # 264: ESPD 4601CKT
CHNL # 483: EVOLT 4601 CKT
0.10000
0.0
0.30000
0.0
1.2000
0.0
0.69001
0.69001
0.69001
0.69001
0.0000
-0.0200
0.0
0.0
0.0
0.0
0.0
1.0000
2.0000
3.0000
4.0000
5.0000
6.0000
7.0000
8.0000
9.0000
10.000
TIME (SECONDS)
FRI, JUL 10 2009 19:49
BU6 4601 P Q SPD U

AC/DC TRANSMISSION

FAULT TYPE 1: TRANSMISSION FAULT

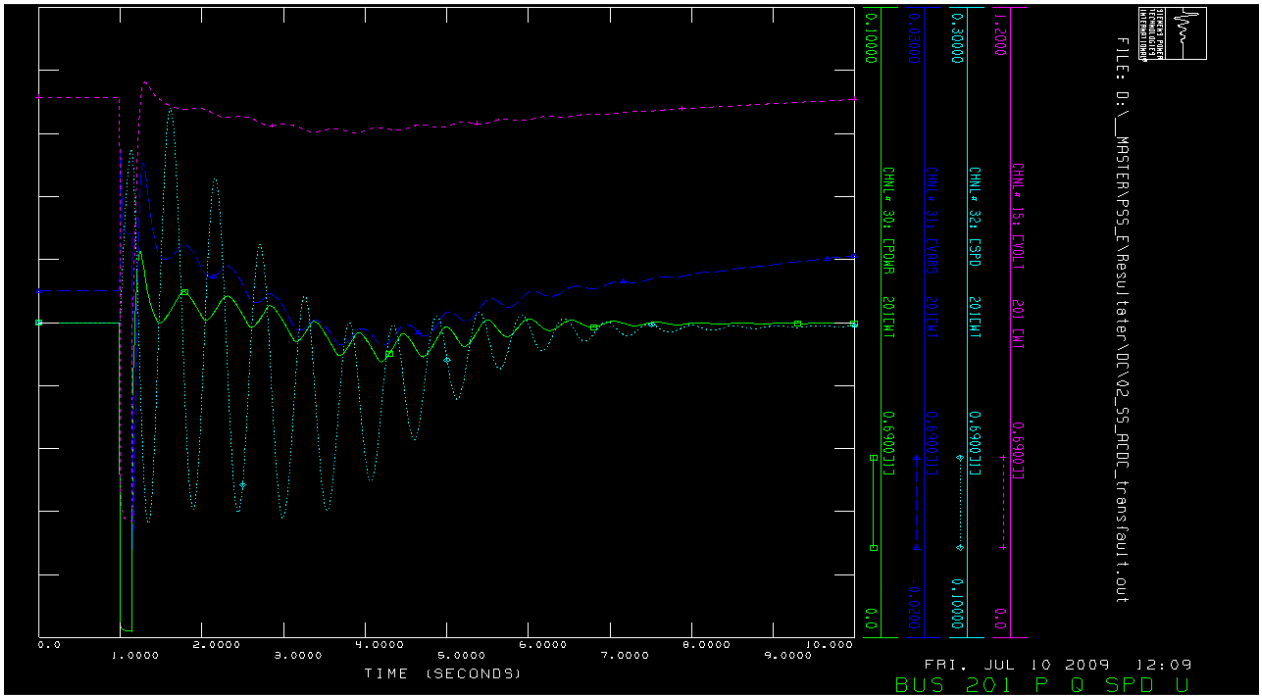

FAULT TYPE 2: FAULT BETWEEN INNERMOST TURBINE OF FEEDER AND SUBSTATION

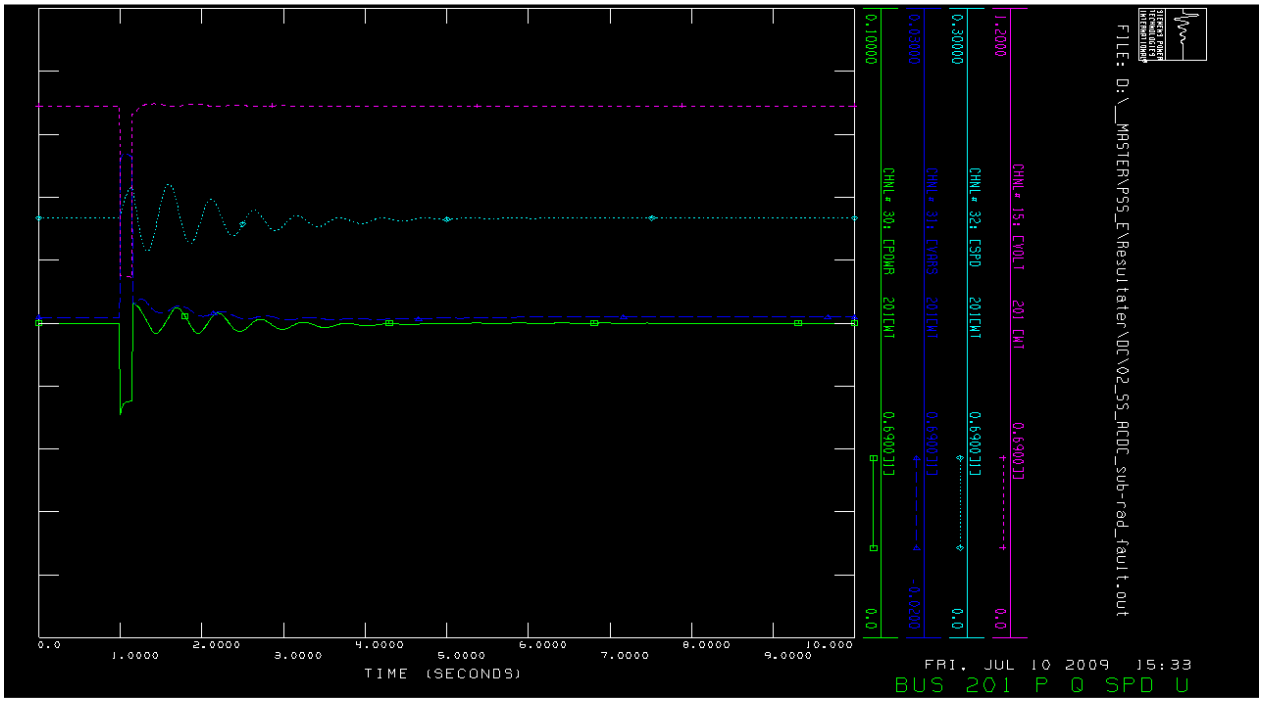

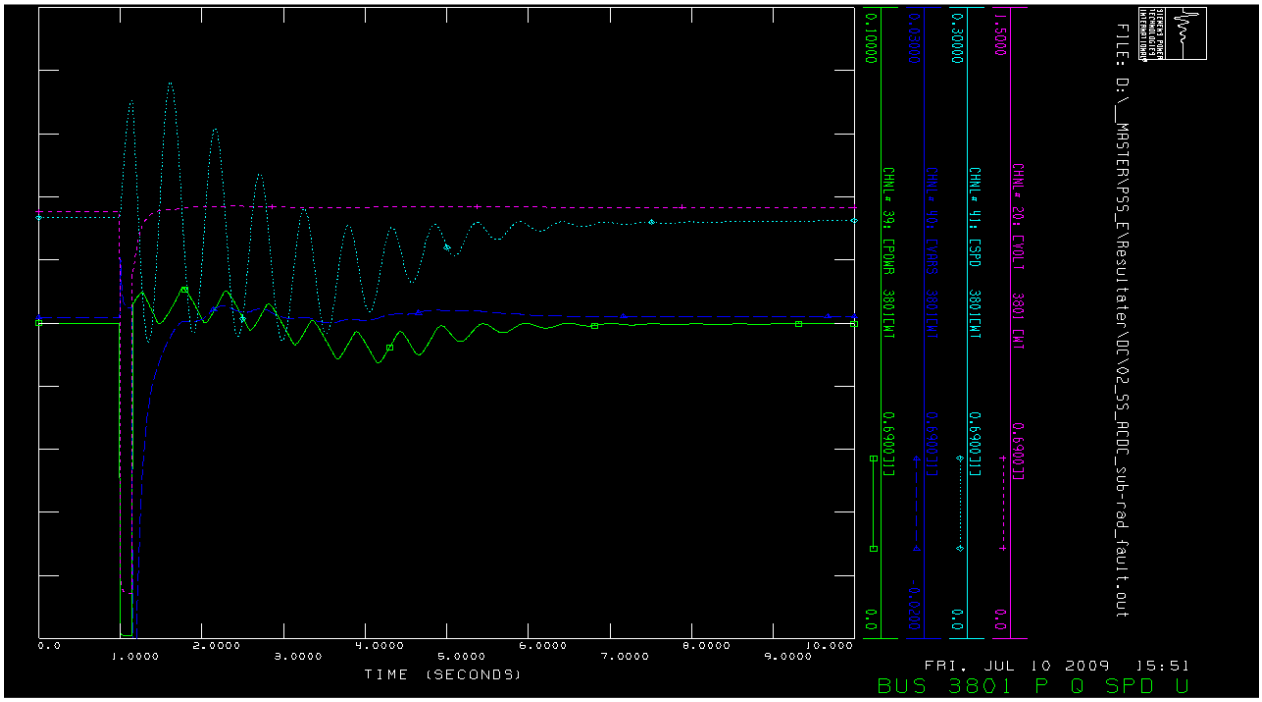

FAULT TYPE 3: FAULT IN THE OUTERMOST CABLE IN THE FEEDER

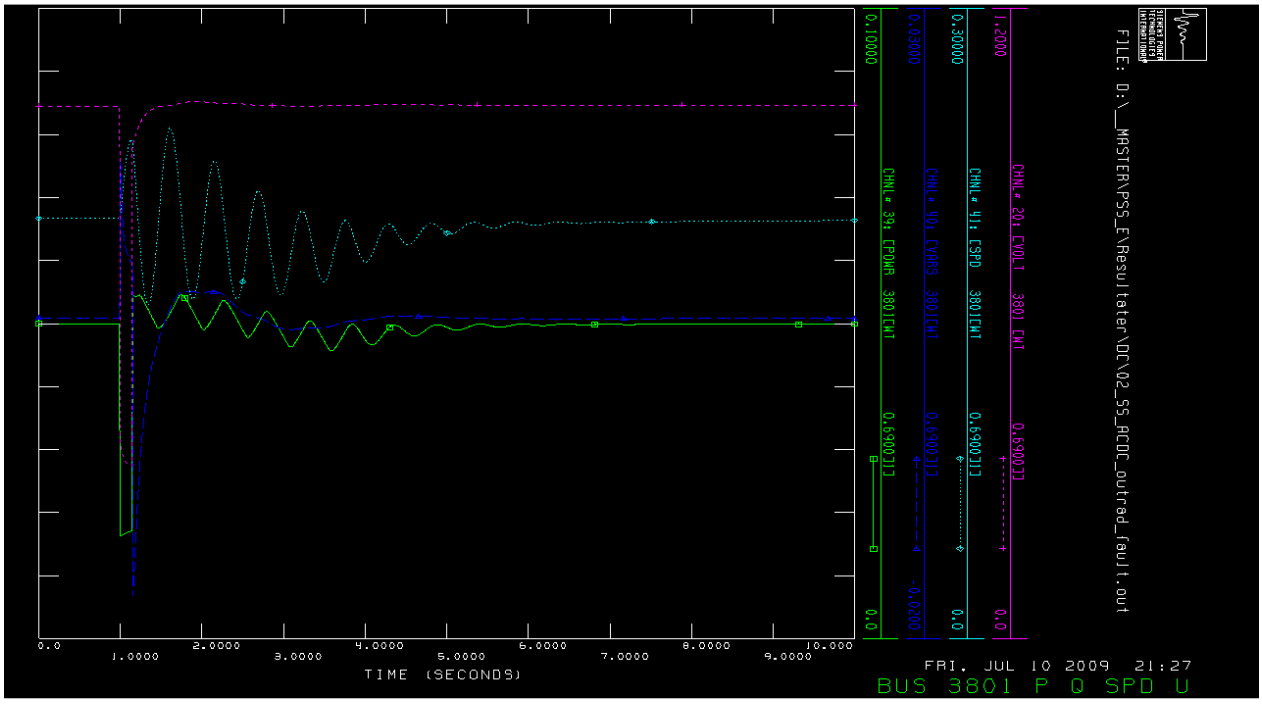

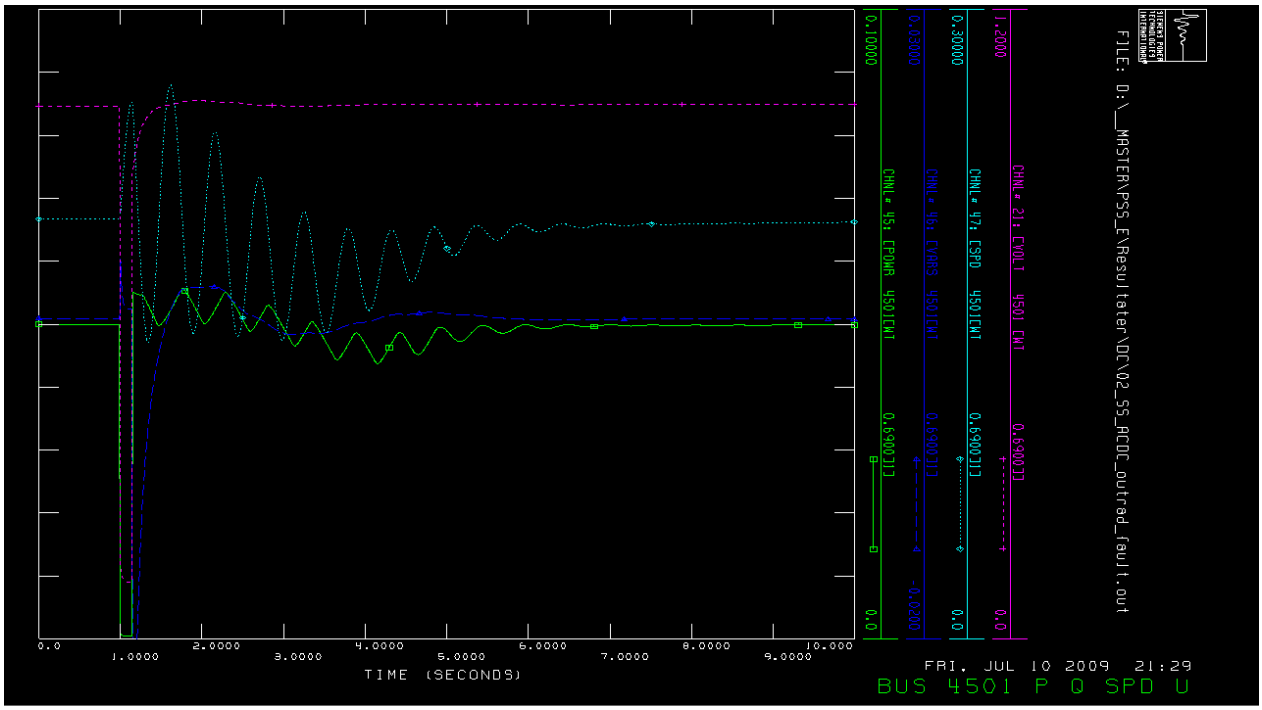

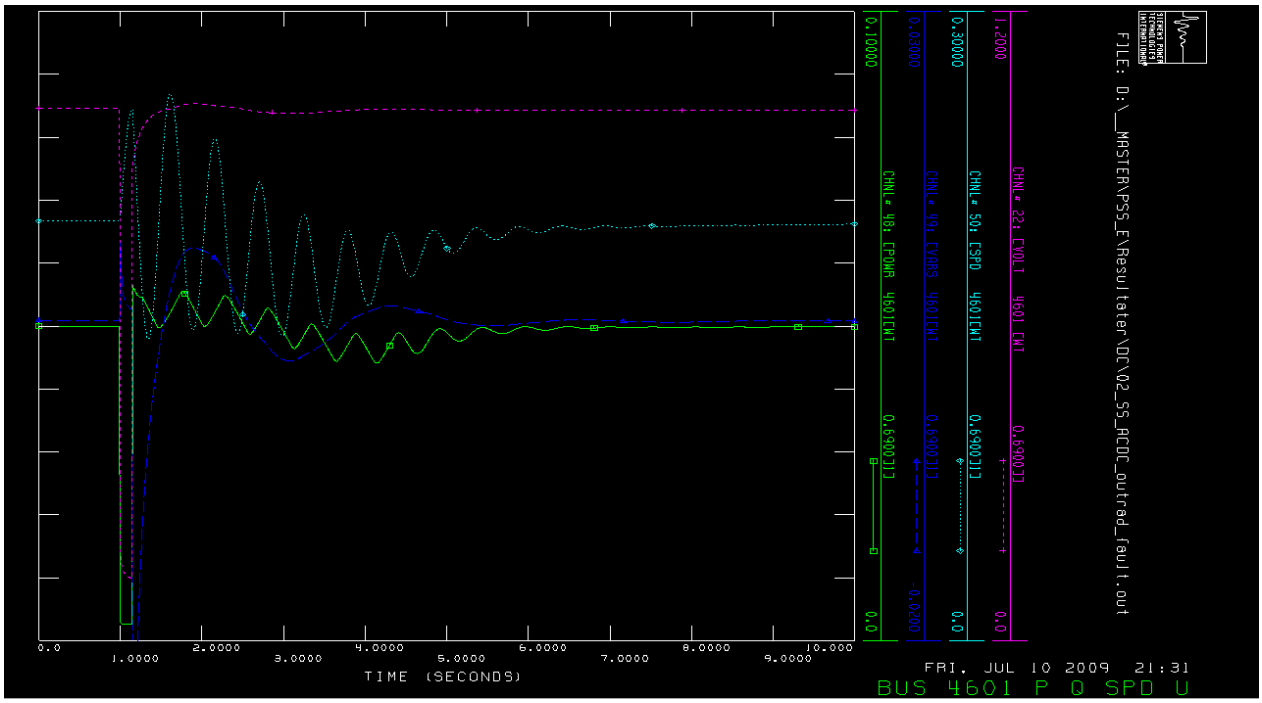
FILE: D:__MASTER\PSS_E\Resultater\DC\02_SS_ACDC_outrad_fault.out
CHNL # 48: [PWR 4601[KT
CHNL # 49: [VARS 4601[KT
CHNL # 50: [SPD 4601[KT
CHNL # 22: [VOLT 4601 [KT
0.10000
0.30000
1.2000
0.6900[]
0.0
TIME (SECONDS)
0.0
1.0000
2.0000
3.0000
4.0000
5.0000
6.0000
7.0000
8.0000
9.0000
10.000
FRI, JUL 10 2009 21:31
BUS 4601 P Q SPD U

DOUBLE SIDED DESIGN

AC/AC TRANSMISSION

FAULT TYPE 1: TRANSMISSION FAULT

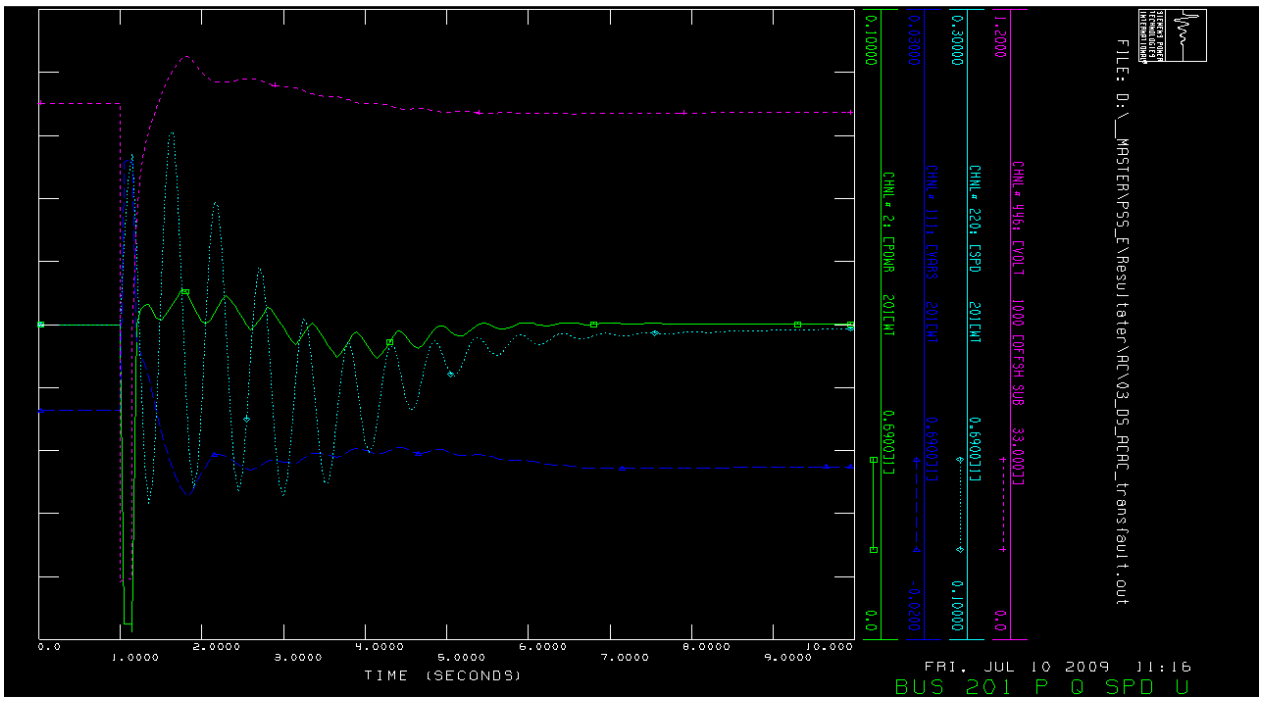

FAULT TYPE 2: FAULT BETWEEN INNERMOST TURBINE OF FEEDER AND SUBSTATION

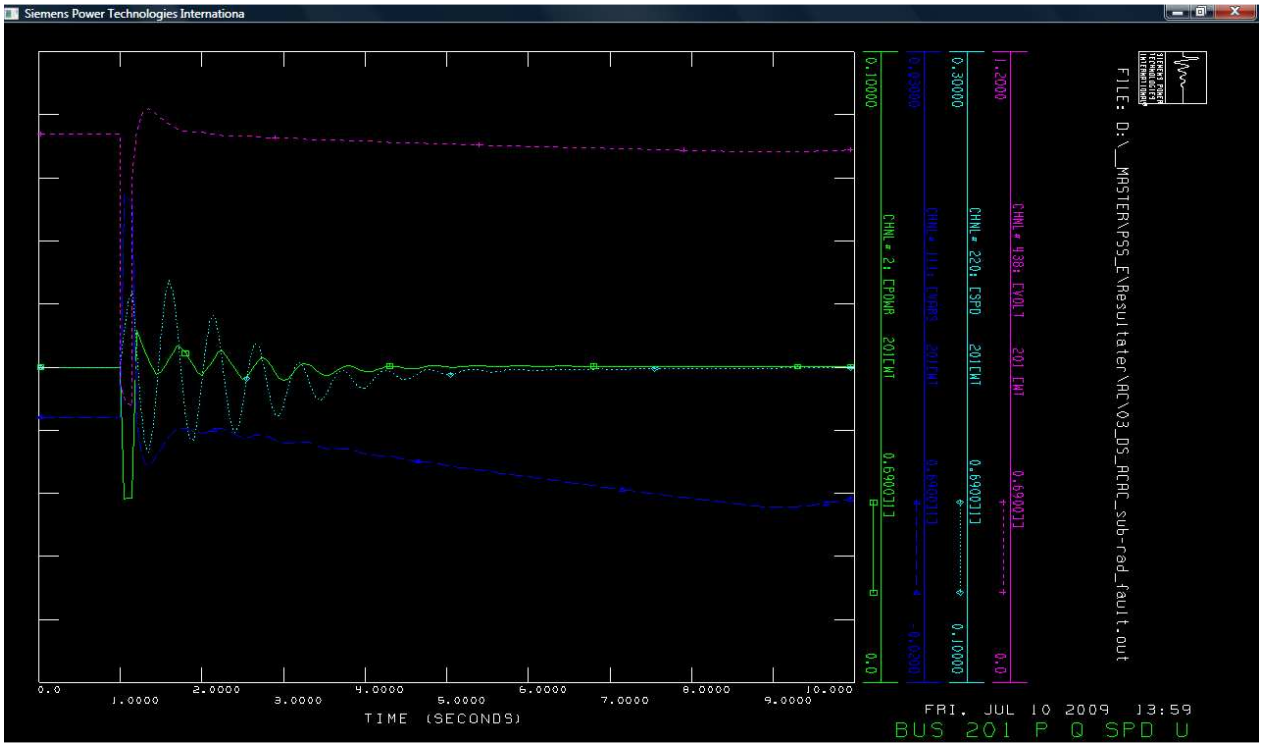

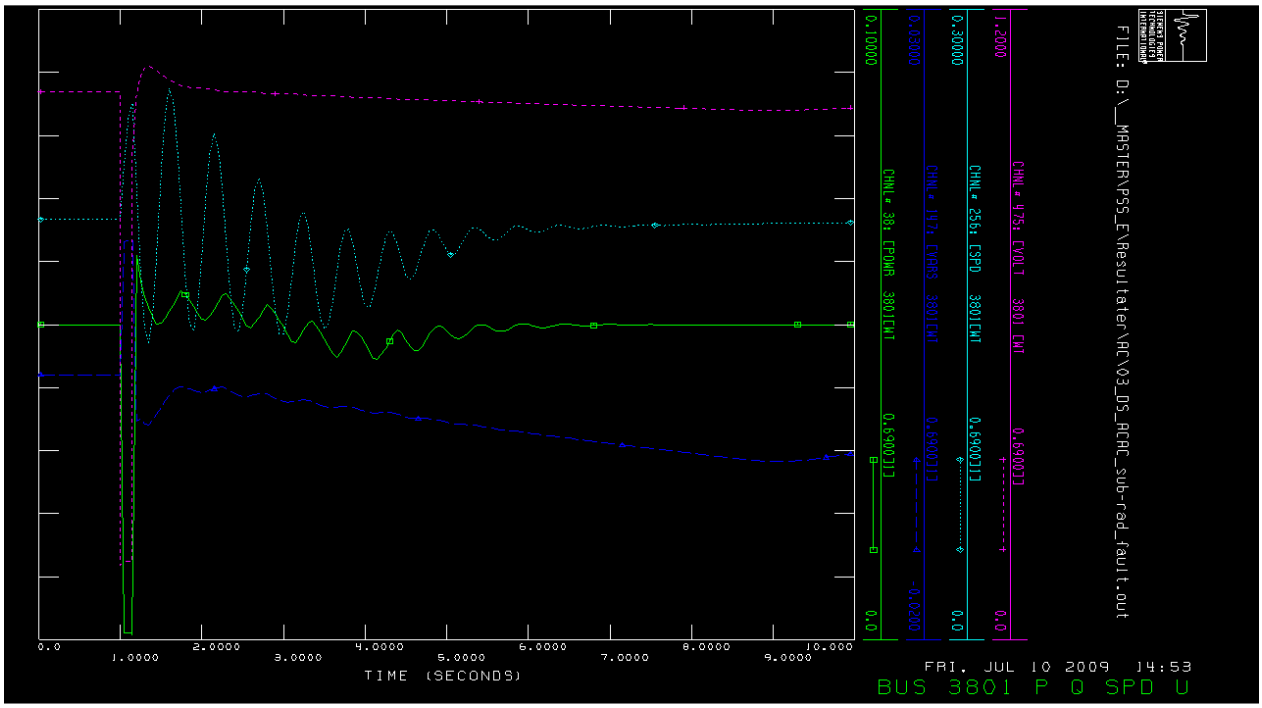

FAULT TYPE 3: FAULT IN THE OUTERMOST CABLE IN THE FEEDER

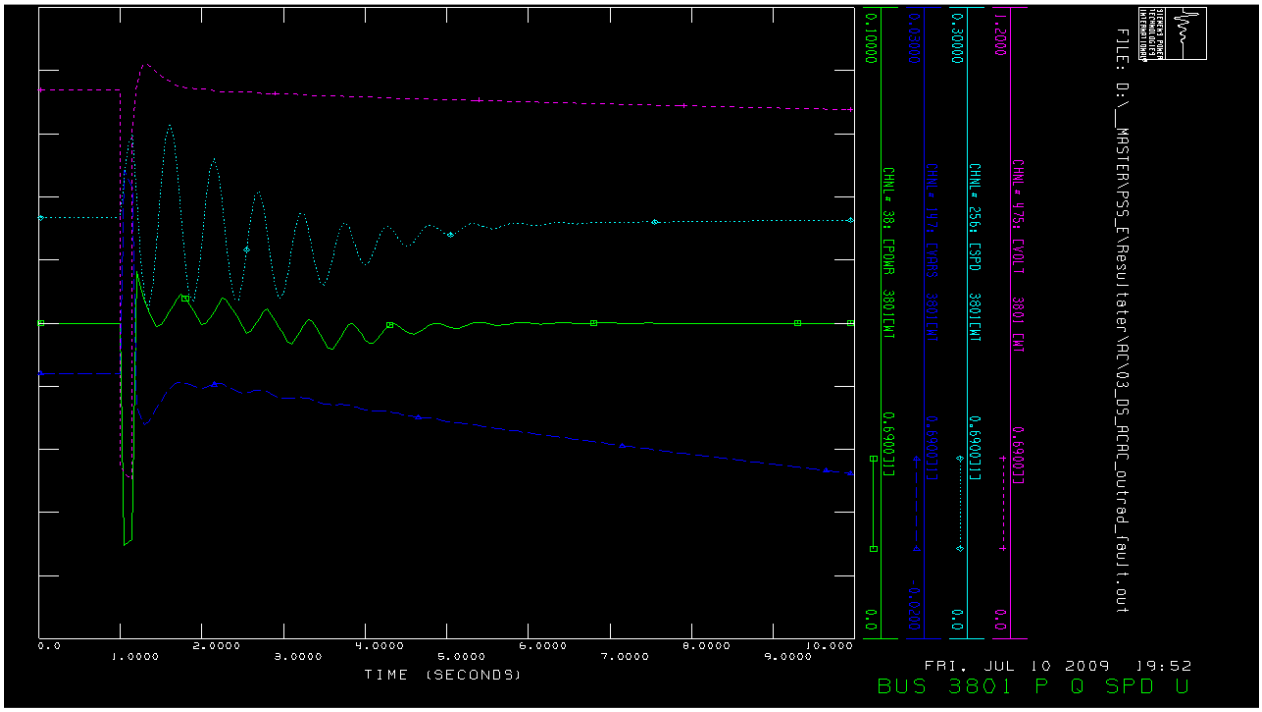

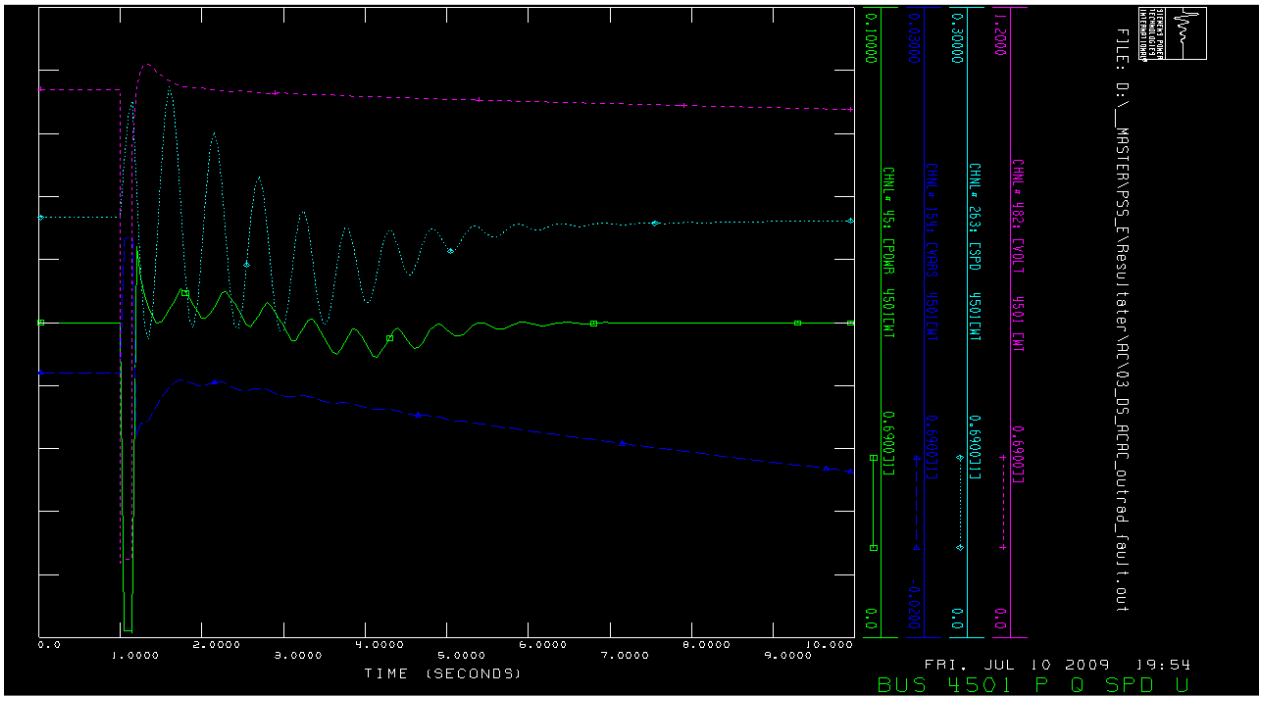

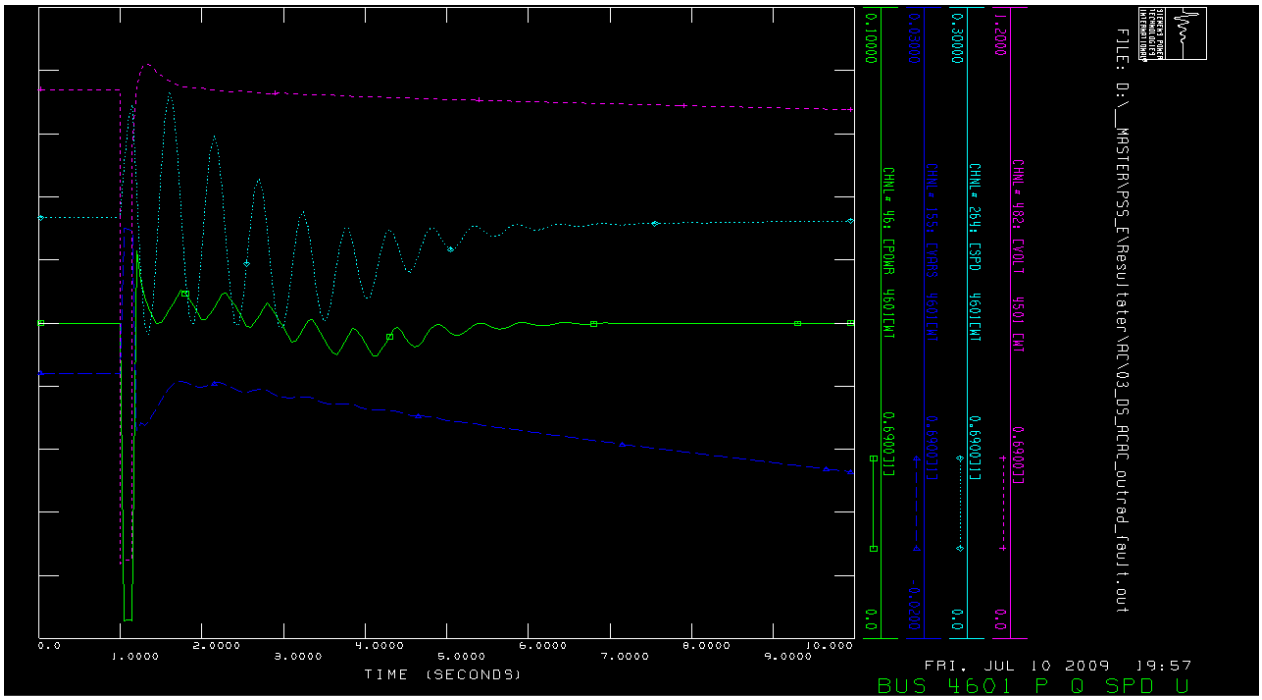
TIME (SECONDS)
0.0
1.0000
2.0000
3.0000
4.0000
5.0000
6.0000
7.0000
8.0000
9.0000
10.000
FRI, JUL 10 2009 19:57
BUS 4601 P Q SPD U
FILE: D:_MASTER\PSS_E\Resultater\AC\03_05_ACAC_outrad_fault.out

AC/DC TRANSMISSION

FAULT TYPE 1: TRANSMISSION FAULT

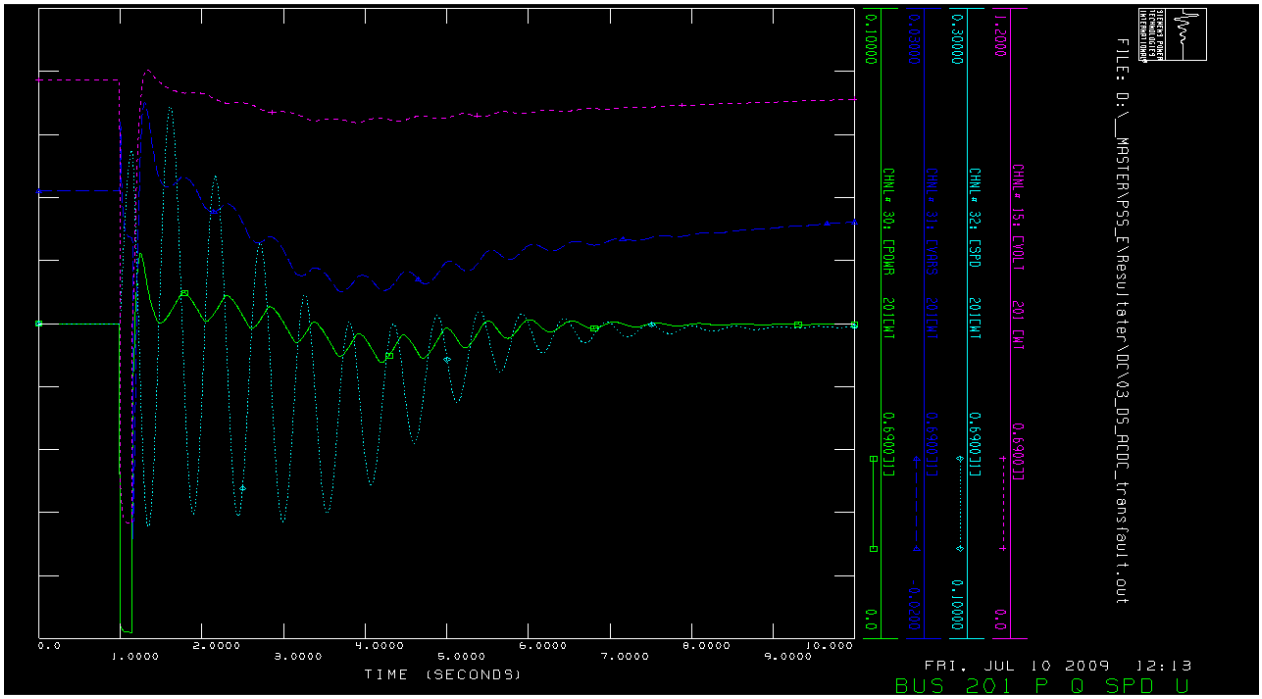

FAULT TYPE 2: FAULT BETWEEN INNERMOST TURBINE OF FEEDER AND SUBSTATION

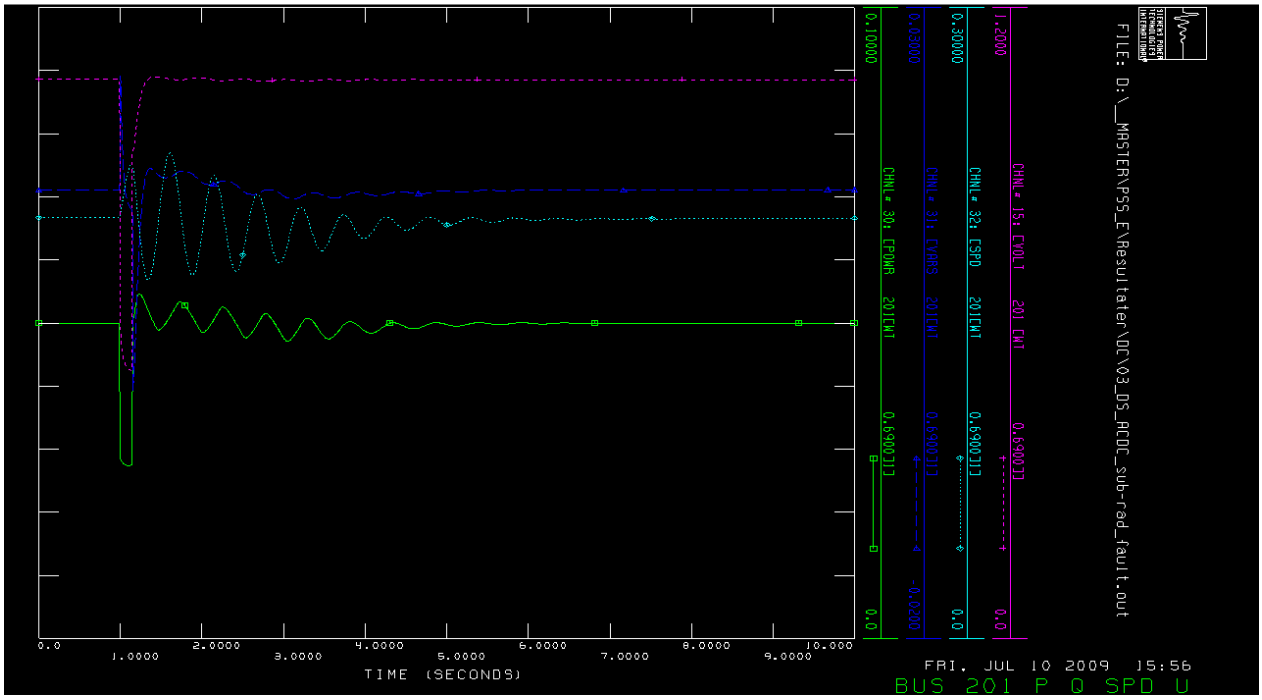

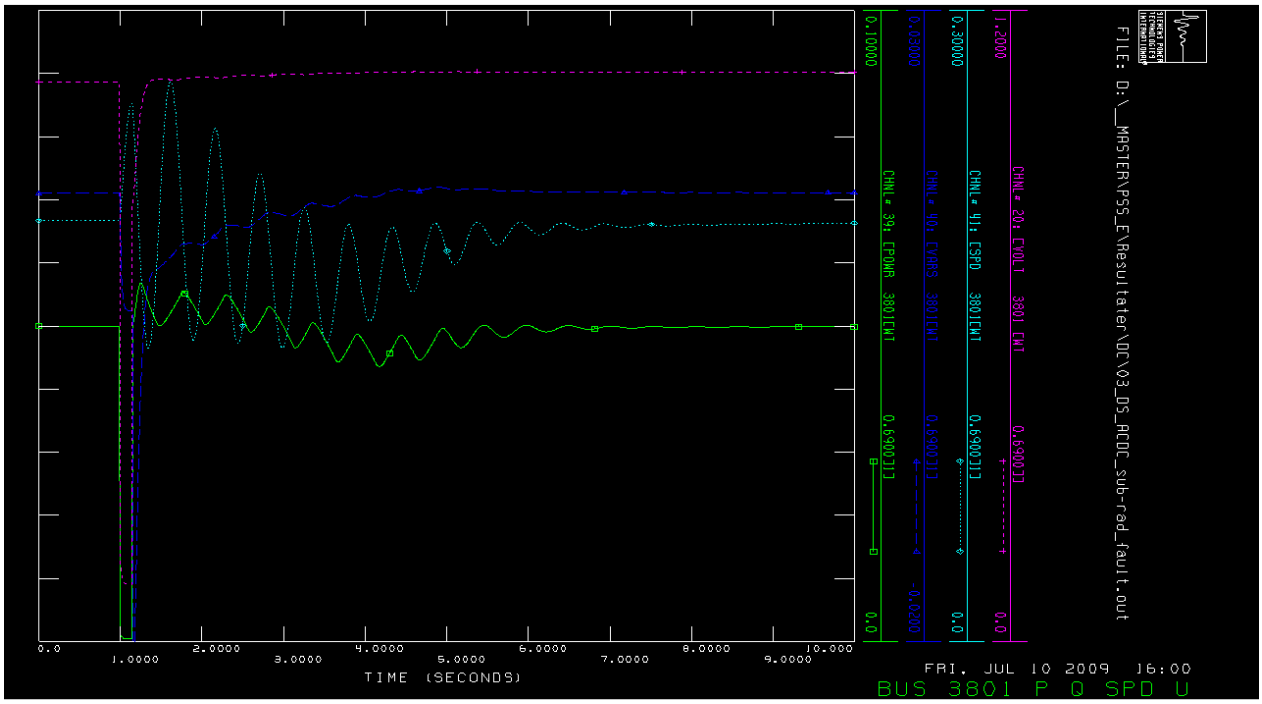

FAULT TYPE 3: FAULT IN THE OUTERMOST CABLE IN THE FEEDER

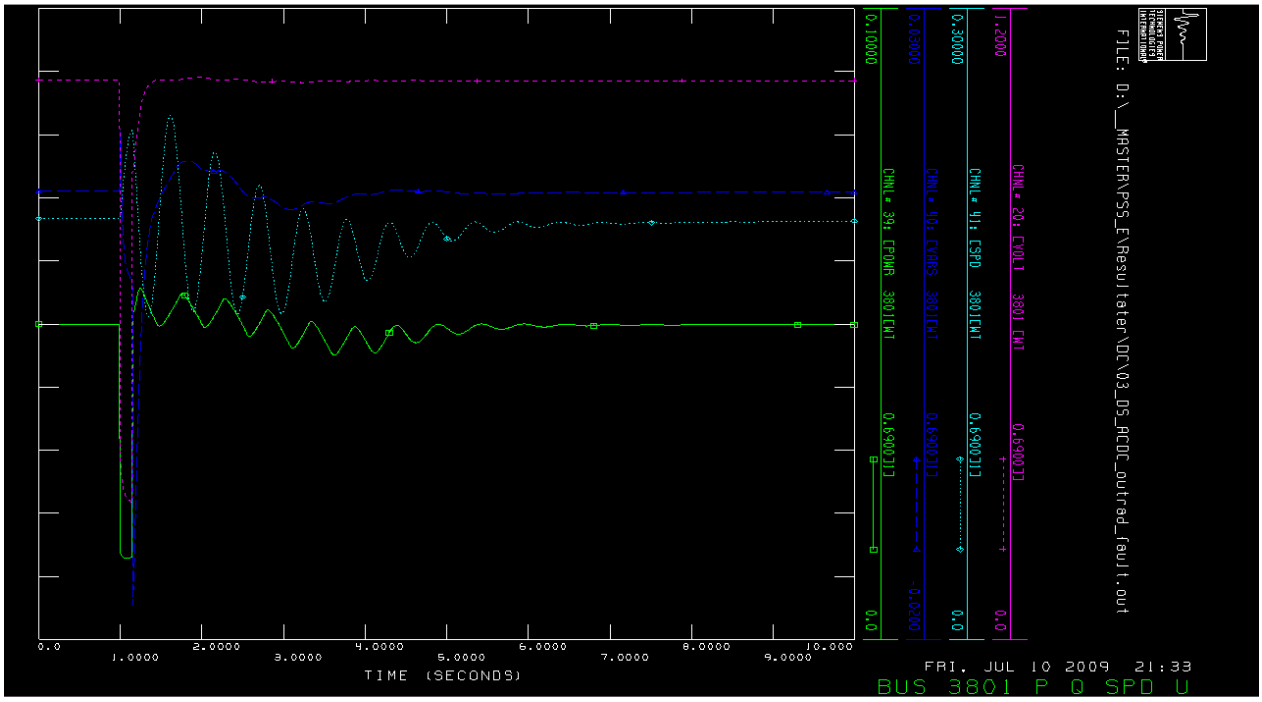

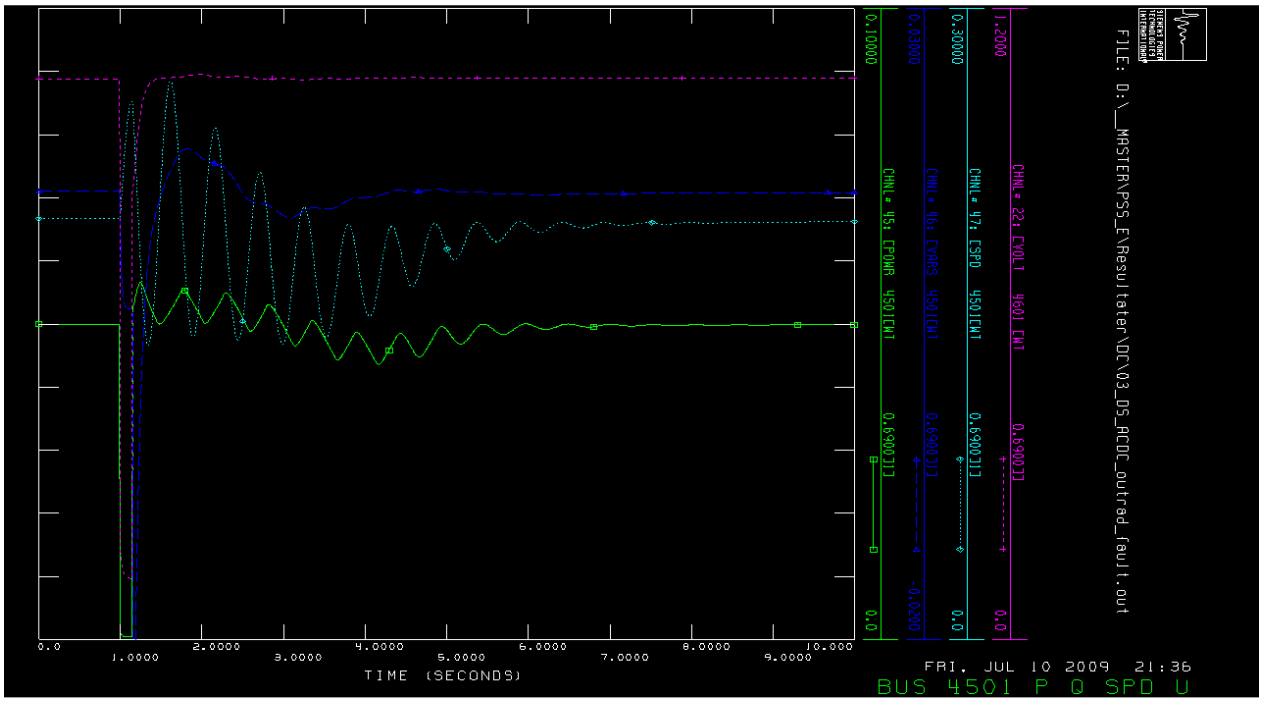

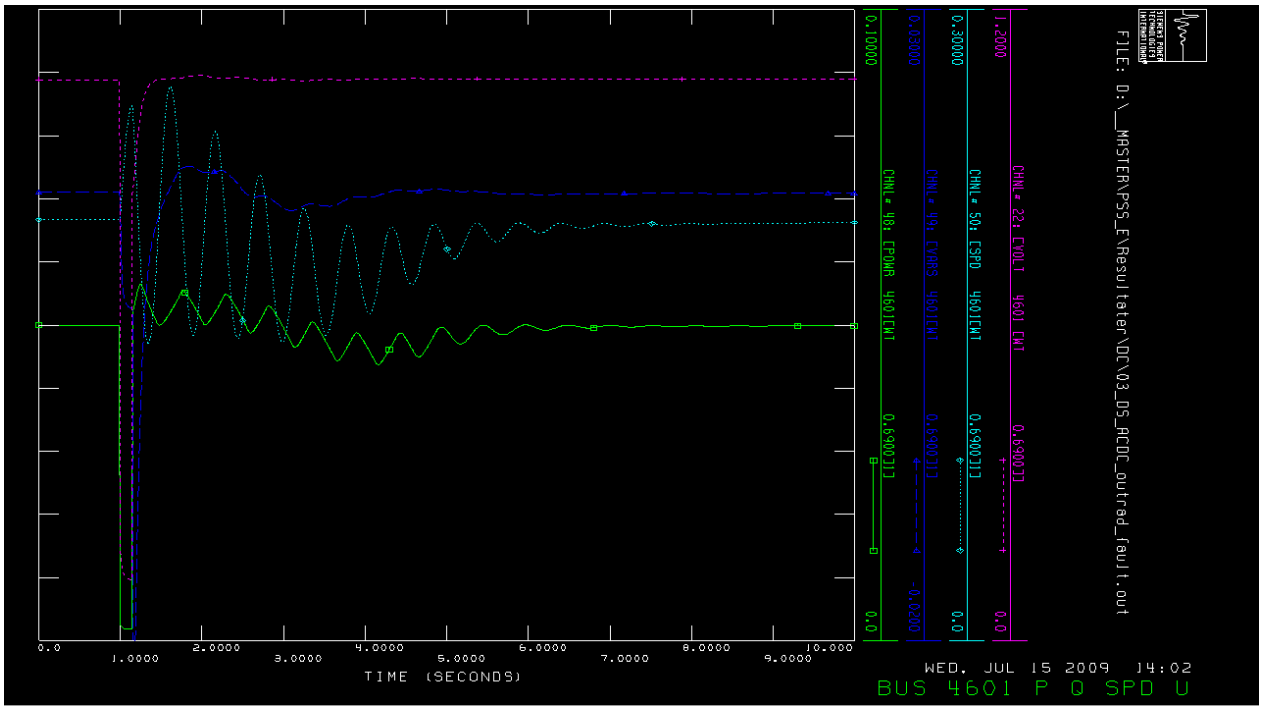
FILE: D:__MASTER\PSS_E\Resultater\DC\03_05_ACDC_outrad_fault.out
CHNL # 48: [PGNR 4601CKT
CHNL # 49: [VARS 4601CKT
CHNL # 50: [SPD 4601CKT
CHNL # 221: [VOLT 4601 CKT
0.10000
0.0
0.30000
0.0200
0.0
1.2000
0.0
0.6900
TIME (SECONDS)
0.0
1.0000
2.0000
3.0000
4.0000
5.0000
6.0000
7.0000
8.0000
9.0000
10.000
WED. JUL 15 2009 14:02
BUS 4601 P Q SPD U

SHARED RING DESIGN

AC/AC TRANSMISSION

FAULT TYPE 1: TRANSMISSION FAULT

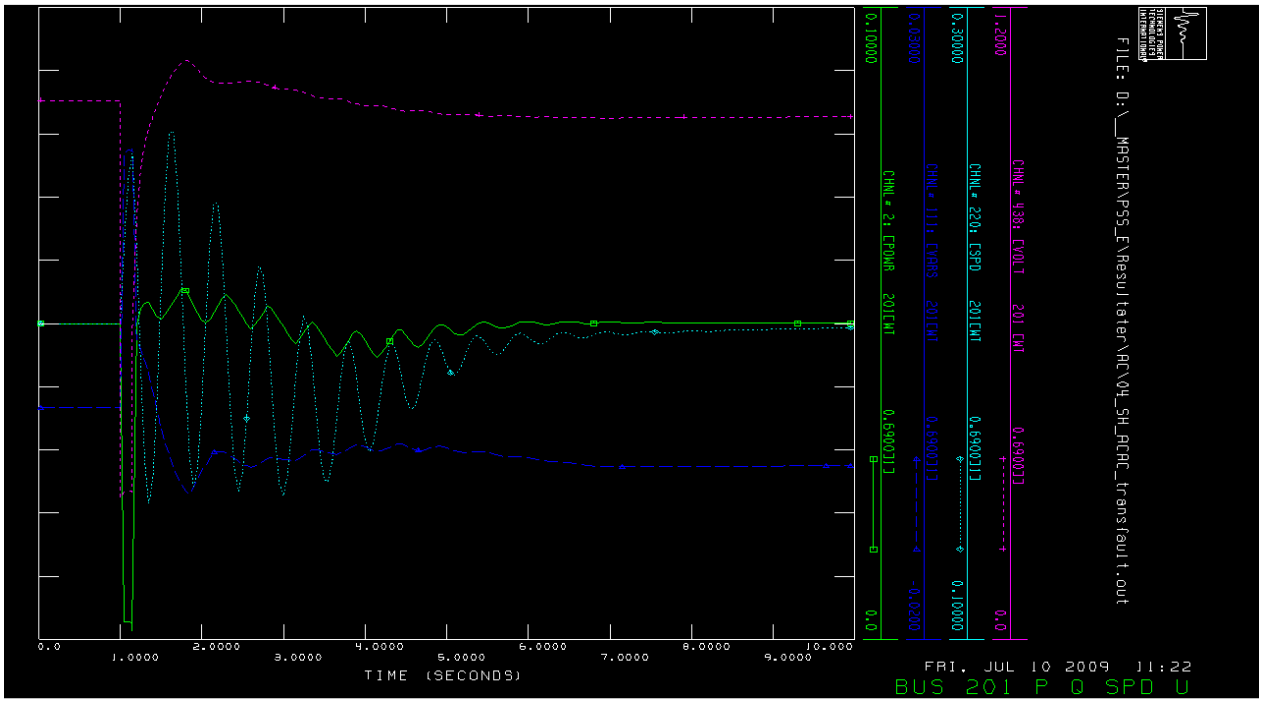

FAULT TYPE 2: FAULT BETWEEN INNERMOST TURBINE OF FEEDER AND SUBSTATION

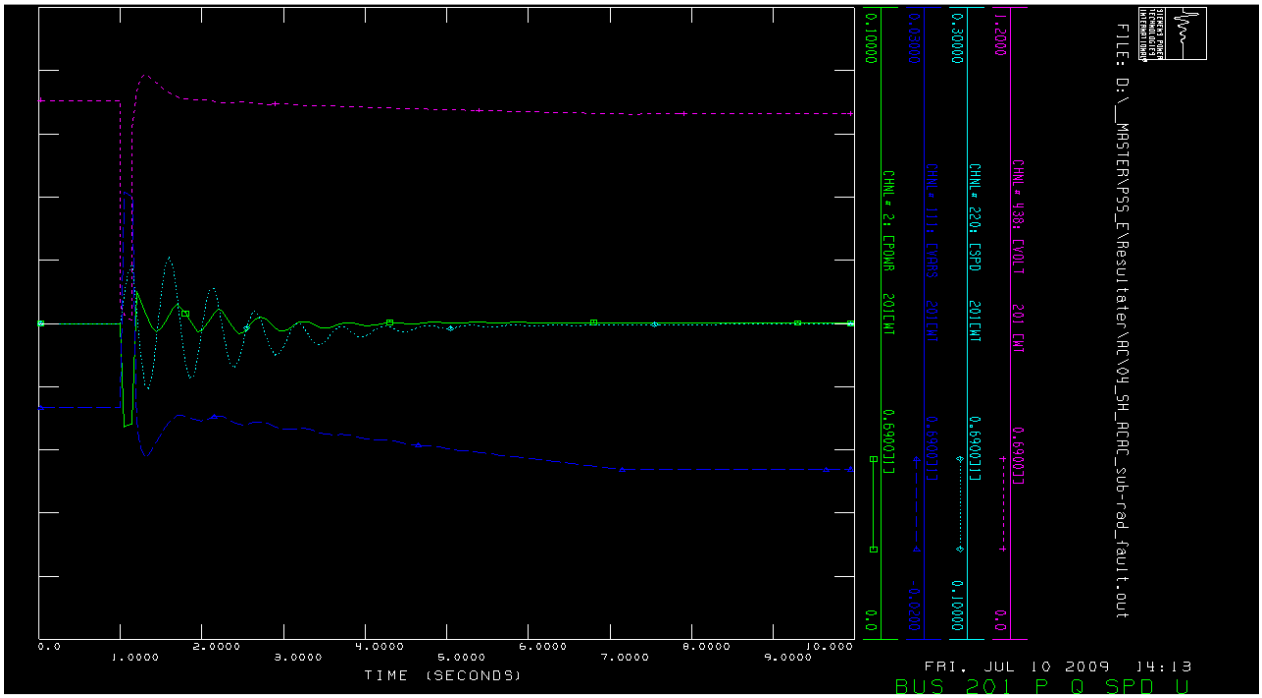

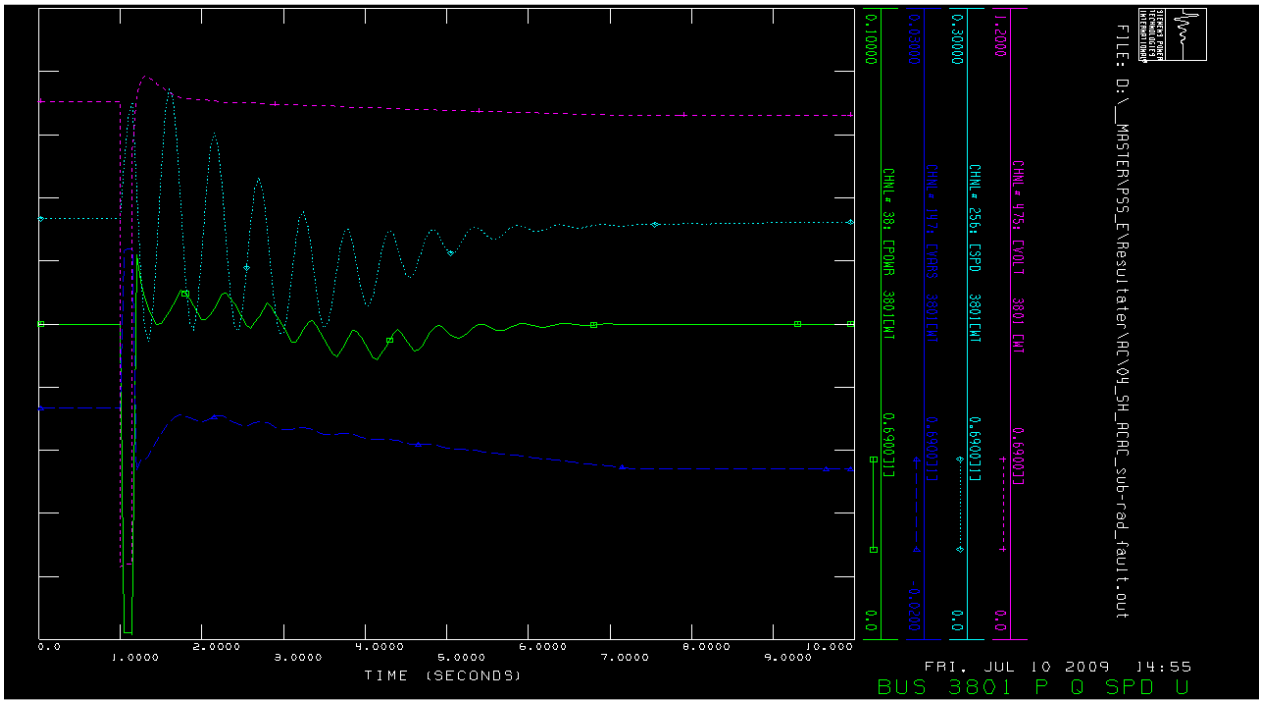

FAULT TYPE 3: FAULT IN THE OUTERMOST CABLE IN THE FEEDER

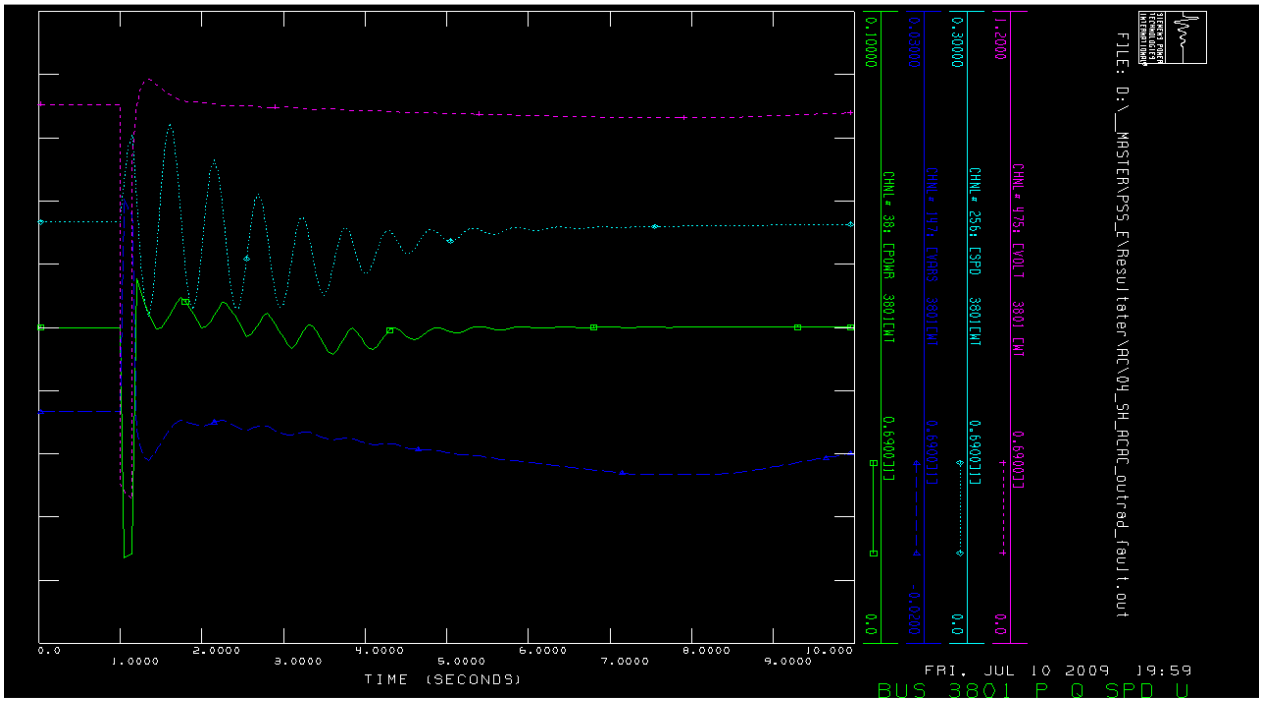

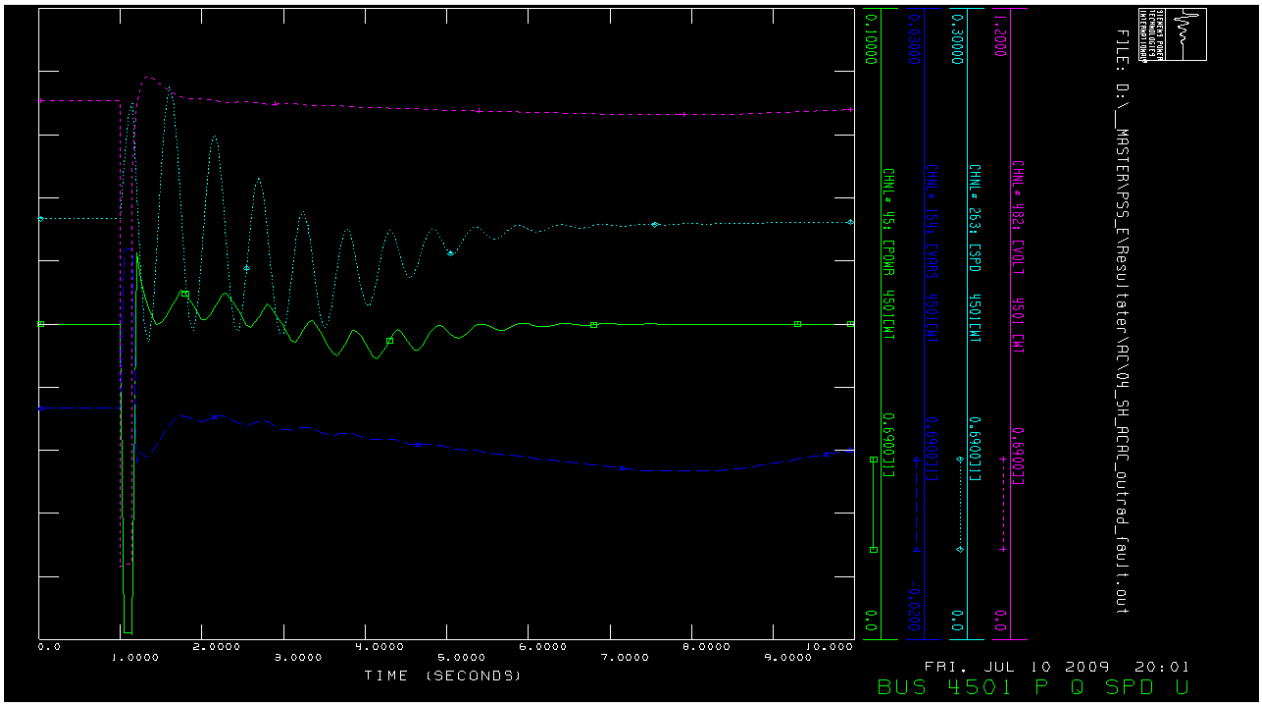

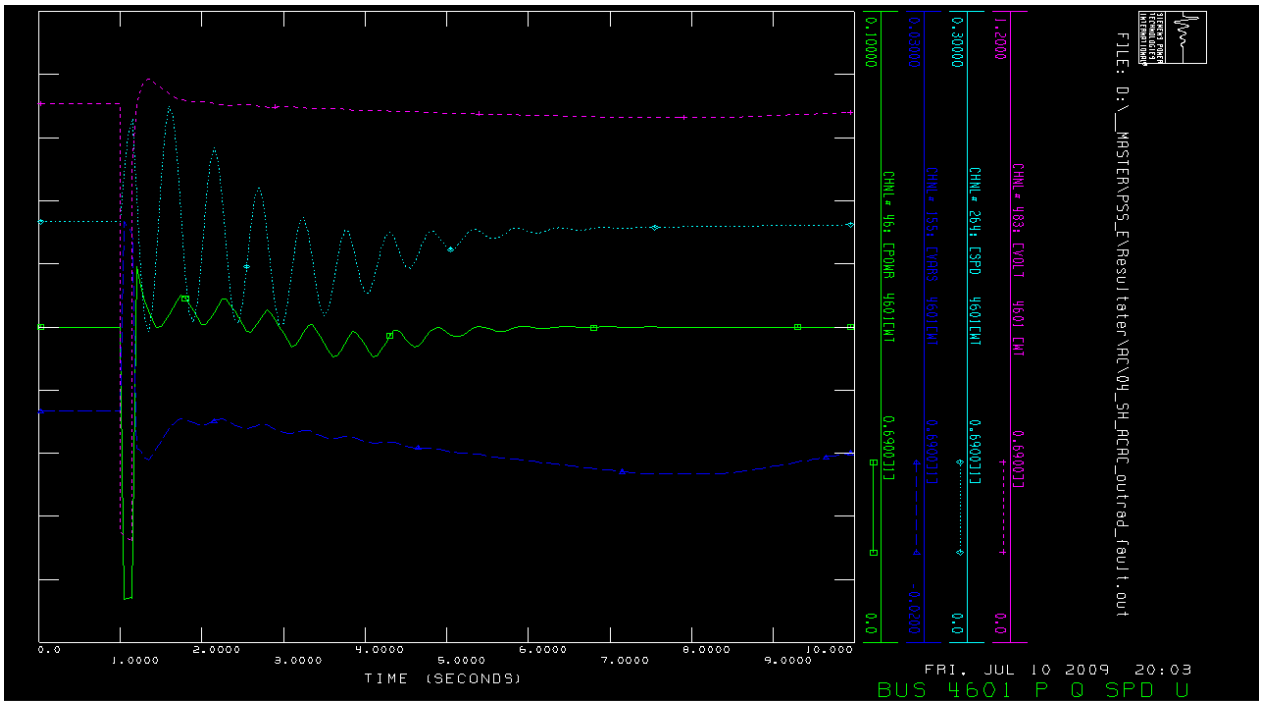
FILE: D:__MASTER\PSS_E\Resultater\AC\OV_SH_ACAC_outrad_fault.out
CHNL # 46: [POWR 4601[MT
CHNL # 155: CVARS 4601[MT
CHNL # 264: ESPD 4601[MT
CHNL # 483: CVOLT 4601 [MT
0.0
1.0000
2.0000
3.0000
4.0000
5.0000
6.0000
7.0000
8.0000
9.0000
10.000
TIME (SECONDS)
FRI, JUL 10 2009 20:03
BUS 4601 P Q SPD U

AC/DC TRANSMISSION

FAULT TYPE 1: TRANSMISSION FAULT

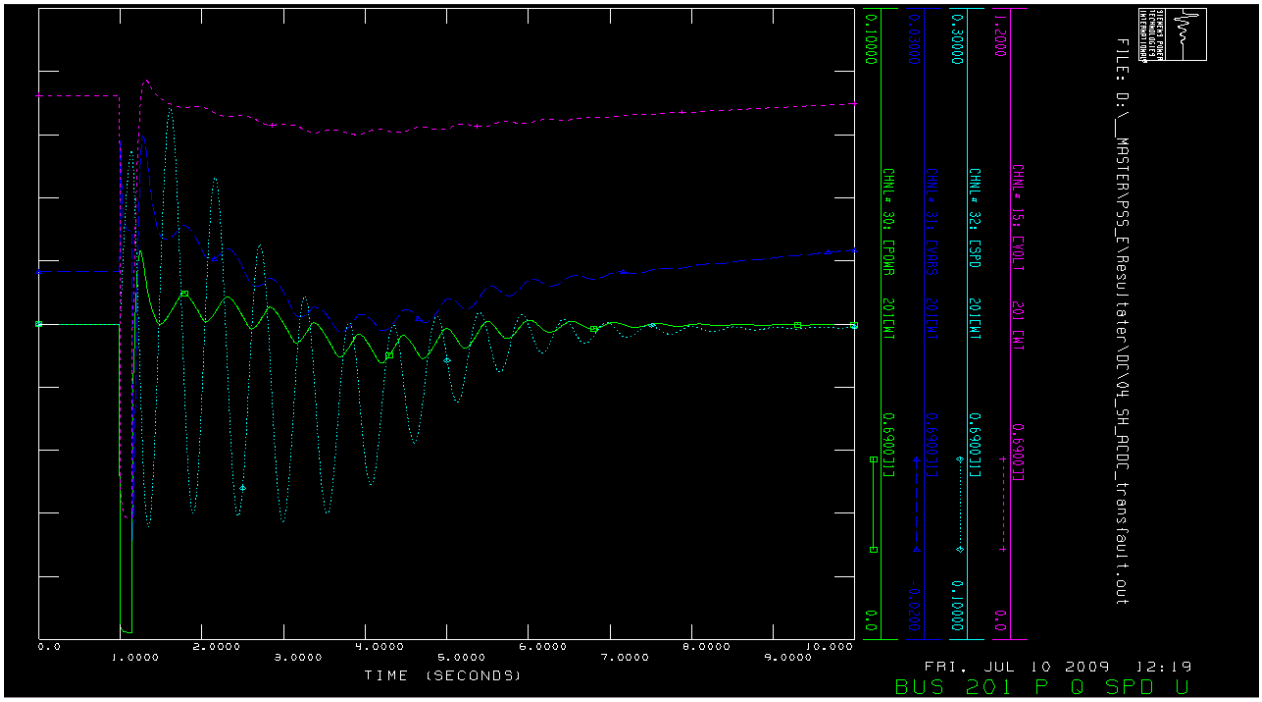

FAULT TYPE 2: FAULT BETWEEN INNERMOST TURBINE OF FEEDER AND SUBSTATION

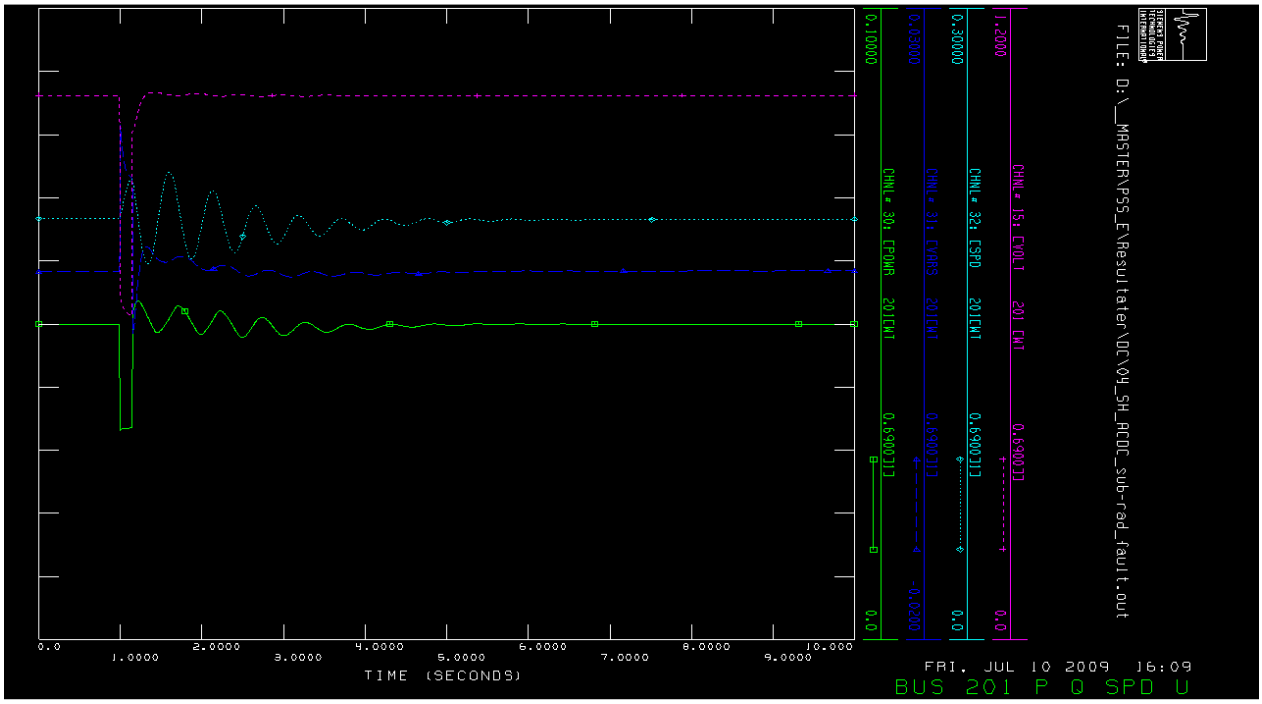

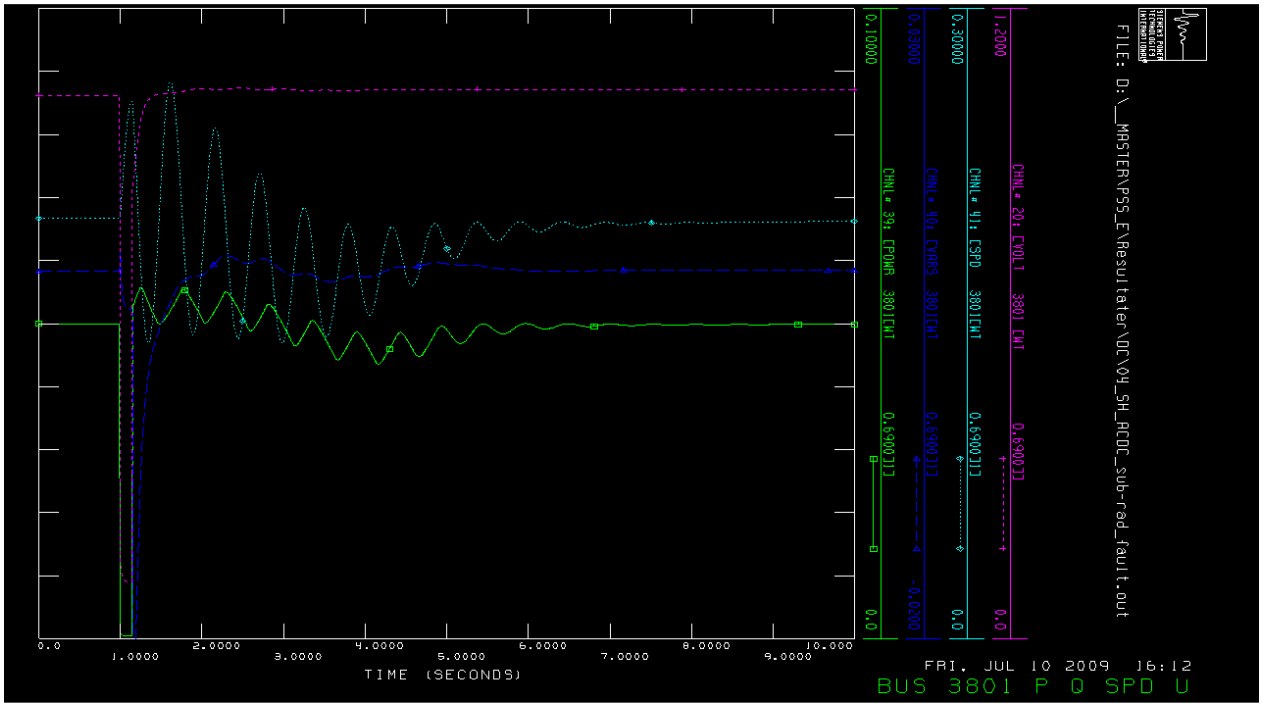

FAULT TYPE 3: FAULT IN THE OUTERMOST CABLE IN THE FEEDER

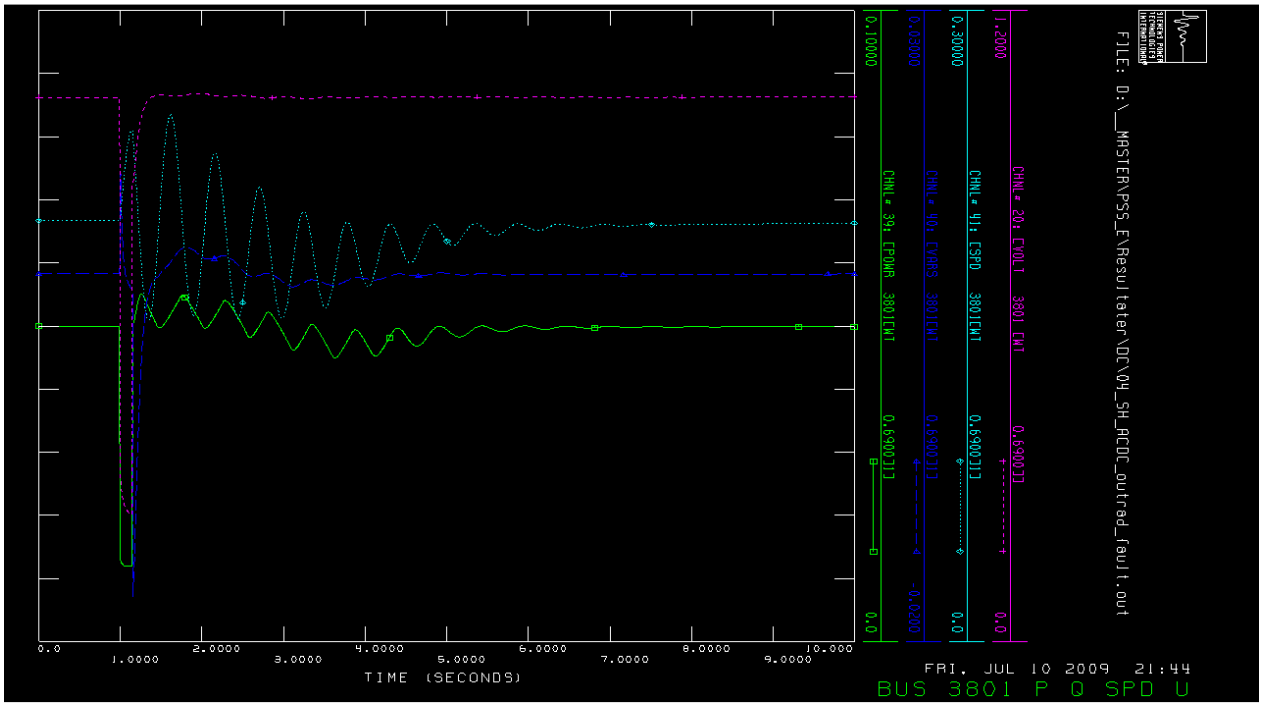

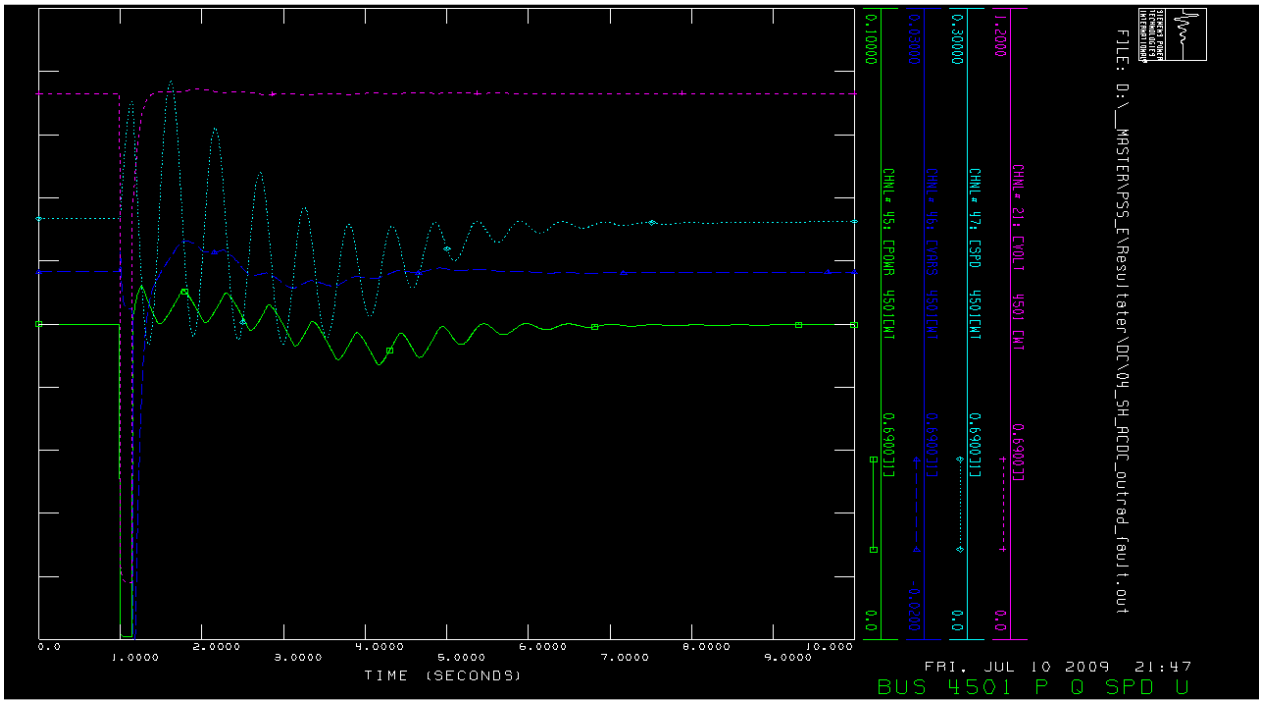

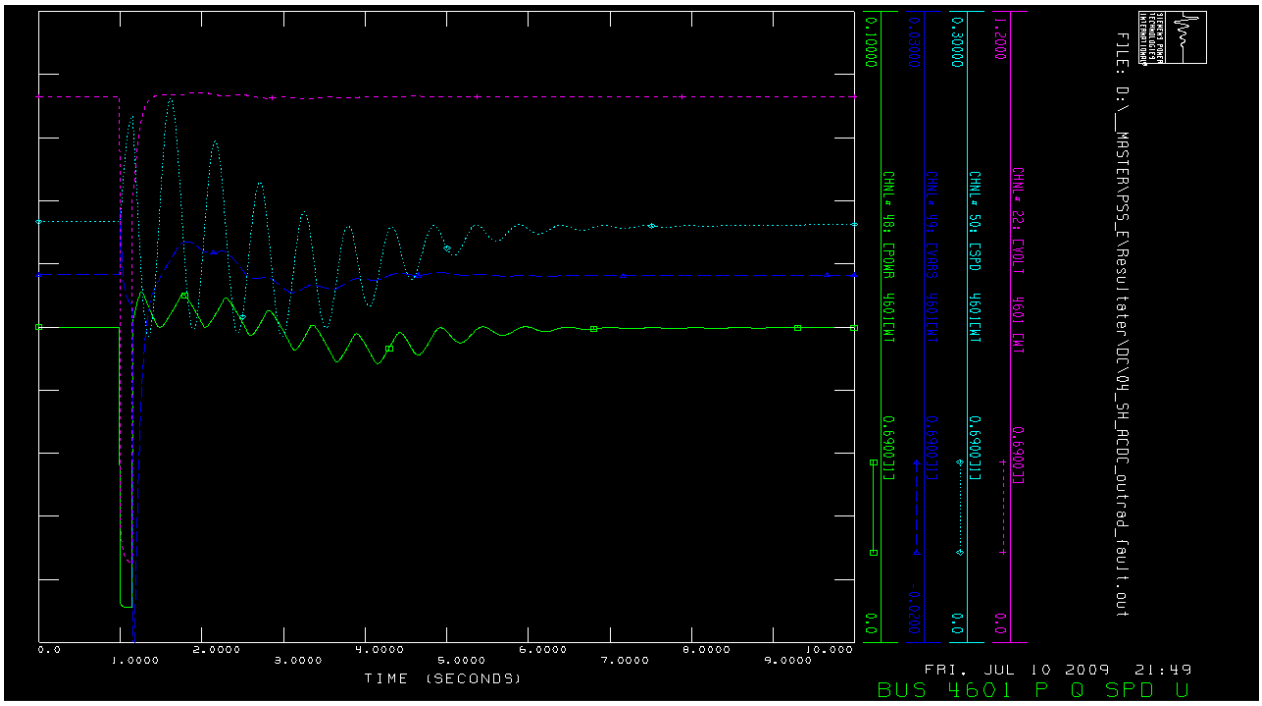
FILE: D:__MASTER\PSS_E\Resultater\DC\04_SH_ACDC_outrad_fault.out
CHNL# 48: [POWR 4601CKT
CHNL# 50: [SPD 4601CKT
CHNL# 22: [VOLT 4601 CKT
0.10000
0.0
0.30000
0.0
1.2000
0.0
0.6900 [
TIME (SECONDS)
0.0
1.0000
2.0000
3.0000
4.0000
5.0000
6.0000
7.0000
8.0000
9.0000
10.000
FRI, JUL 10 2009 21:49
BUS 4601 P Q SPD U

N-SIDED RING DESIGN

AC/AC TRANSMISSION

FAULT TYPE 1: TRANSMISSION FAULT

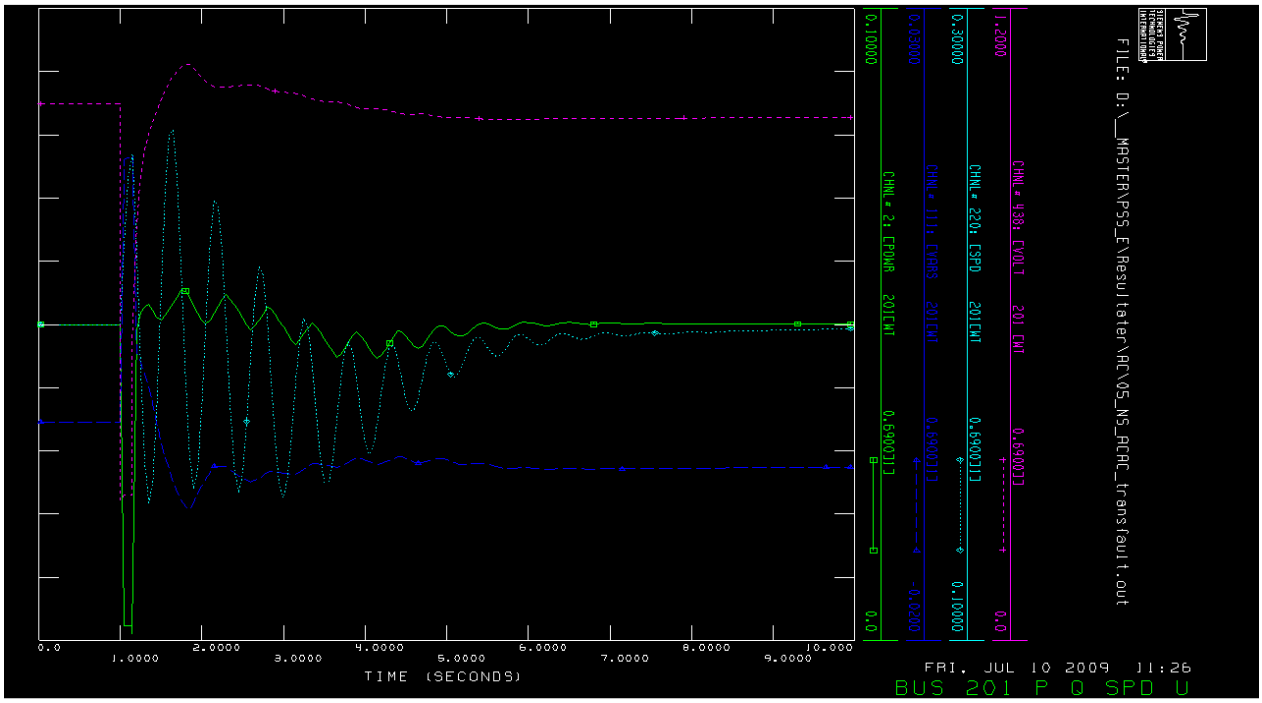

FAULT TYPE 2: FAULT BETWEEN INNERMOST TURBINE OF FEEDER AND SUBSTATION

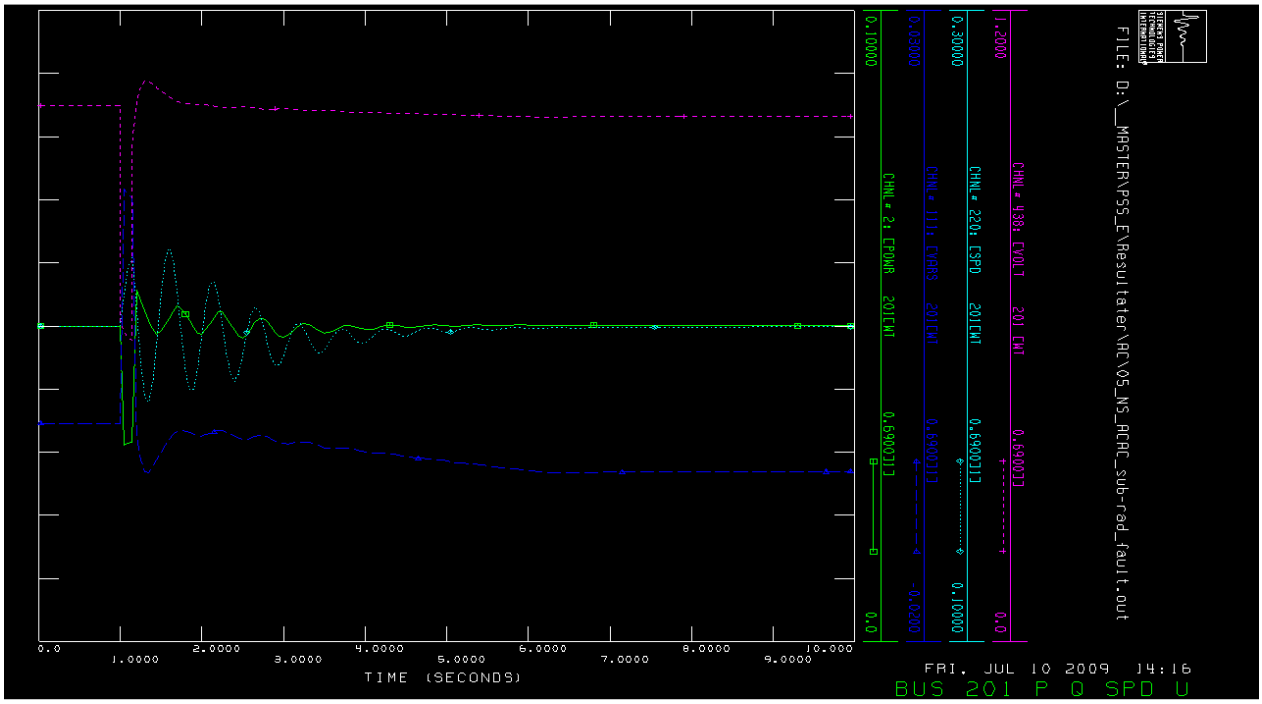

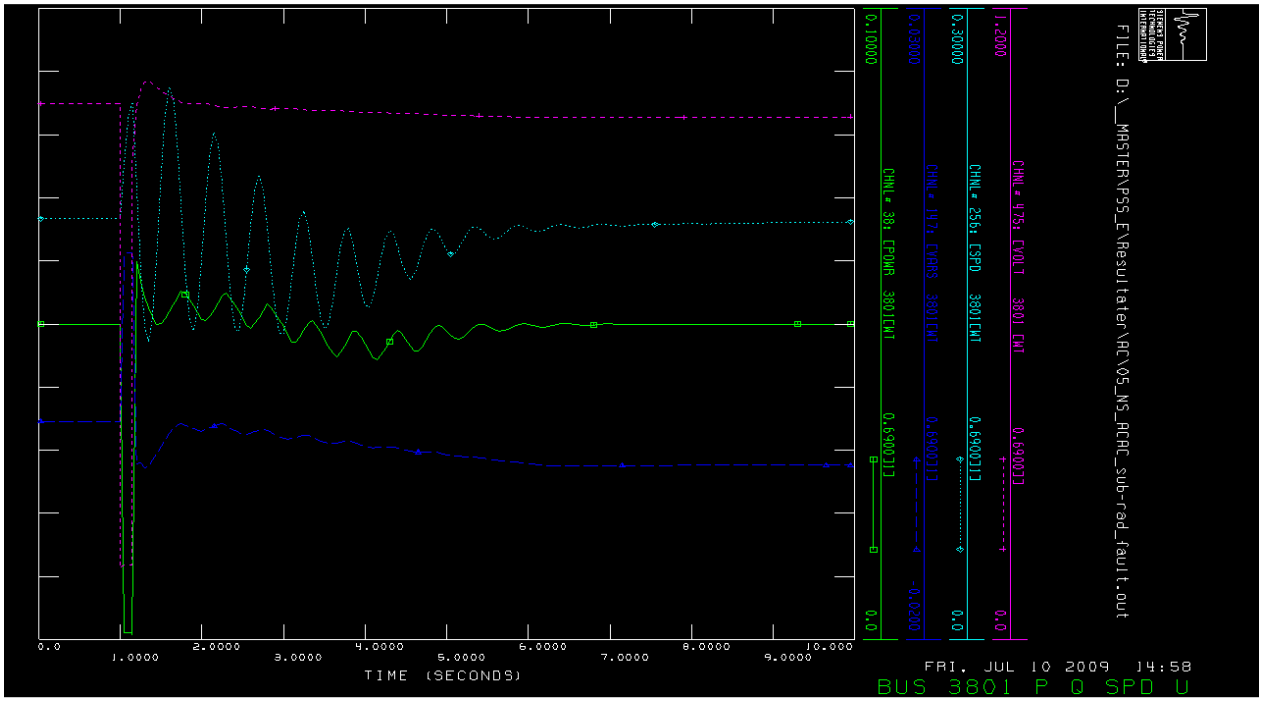

FAULT TYPE 3: FAULT IN THE OUTERMOST CABLE IN THE FEEDER

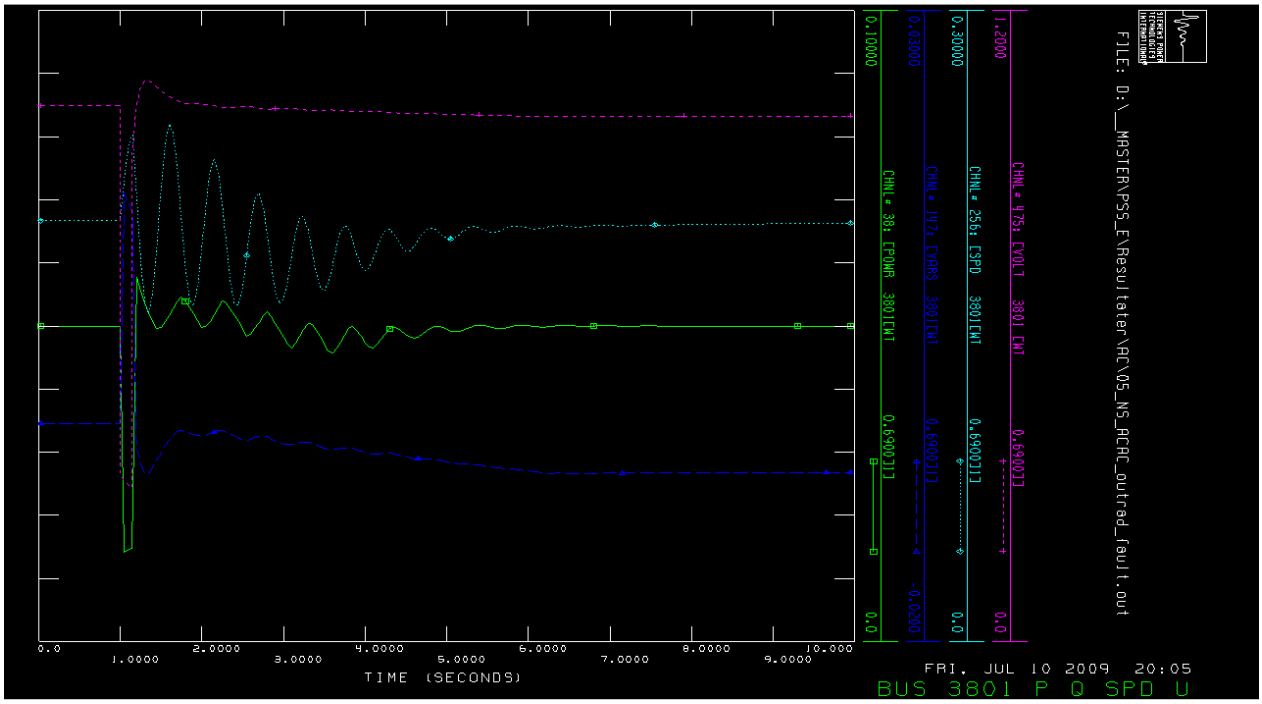

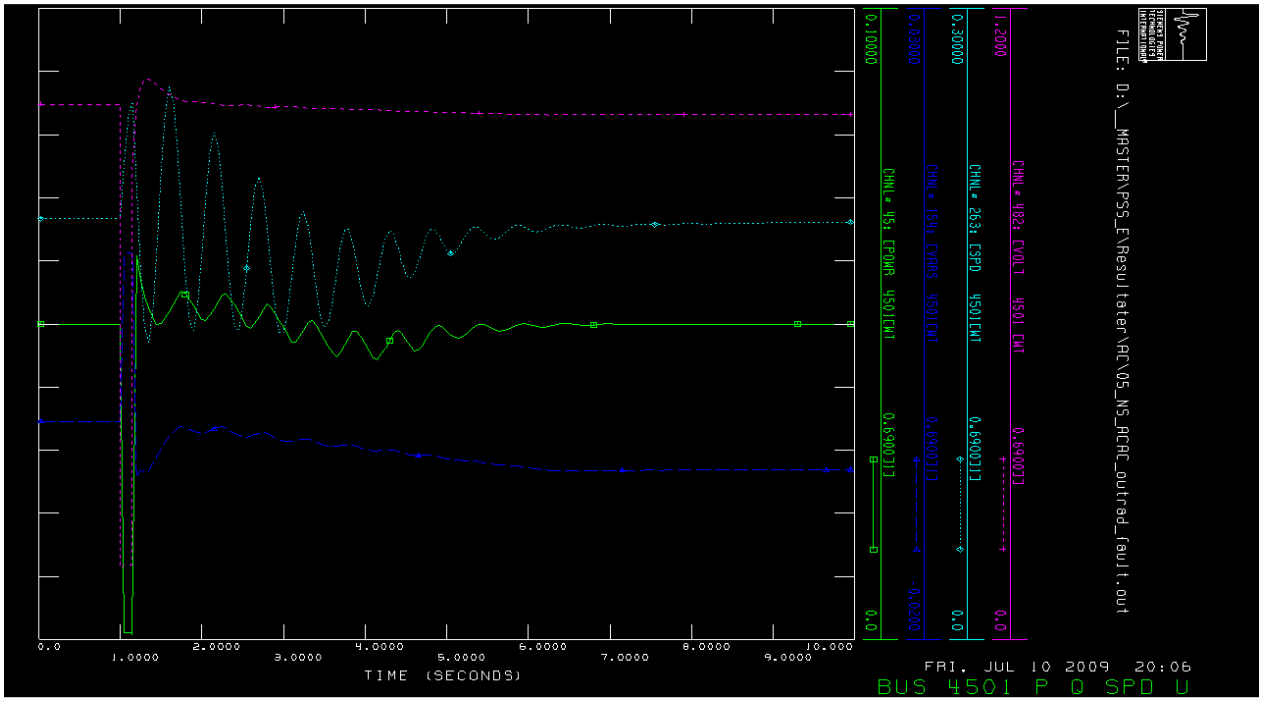

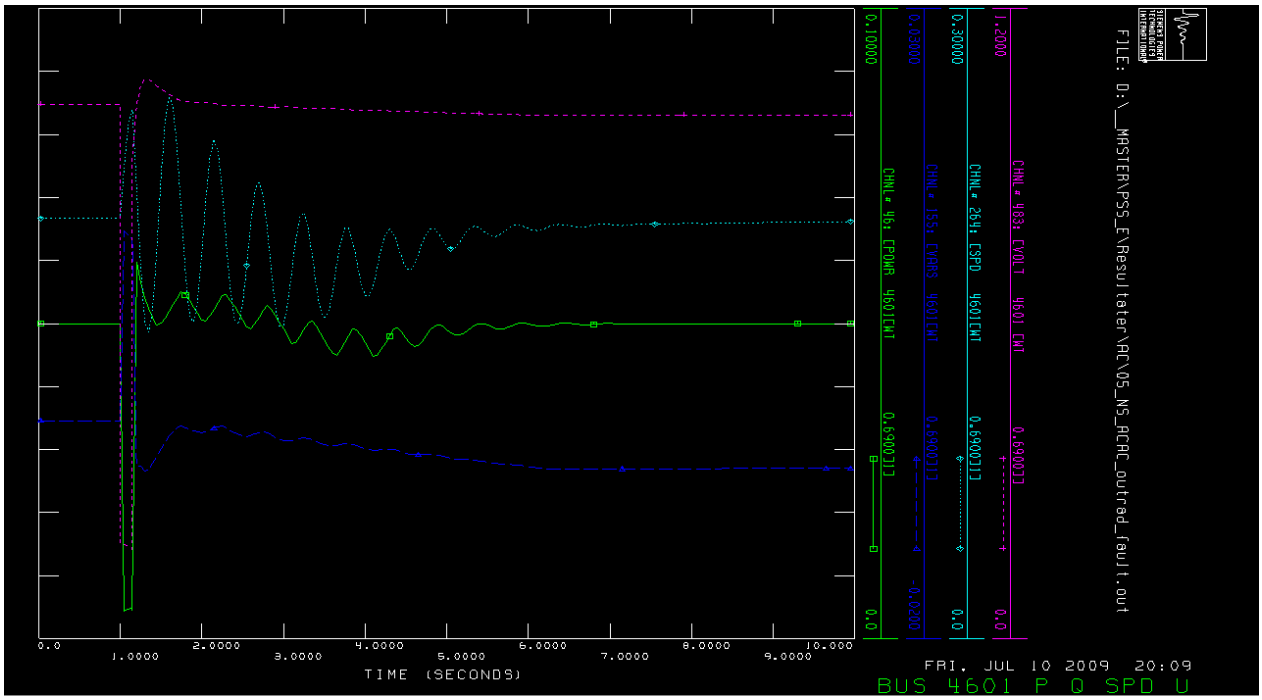
TIME (SECONDS)
FRI, JUL 10 2009 20:09
BUS 4601 P Q SPD U
FILE: D:_MASTER\PSS_E\Resultater\AC\05_NS_ACAC_outrad_fault.out

AC/DC TRANSMISSION

FAULT TYPE 1: TRANSMISSION FAULT

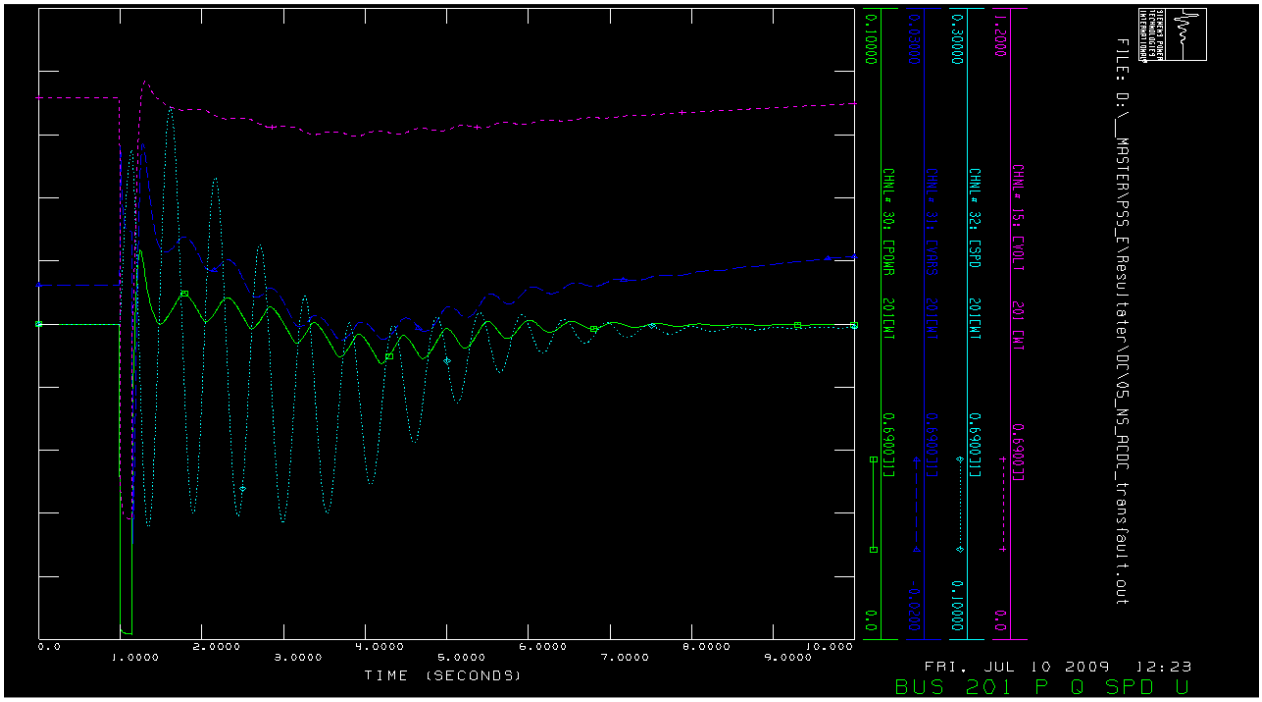

FAULT TYPE 2: FAULT BETWEEN INNERMOST TURBINE OF FEEDER AND SUBSTATION

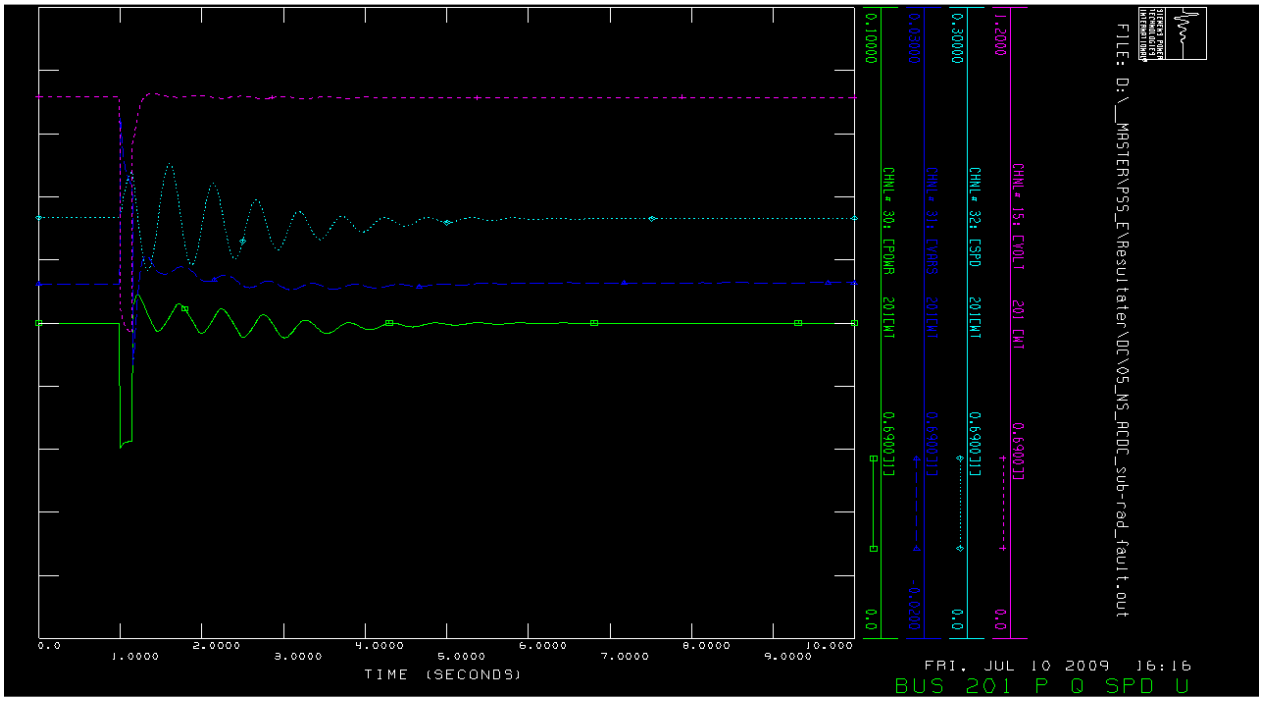

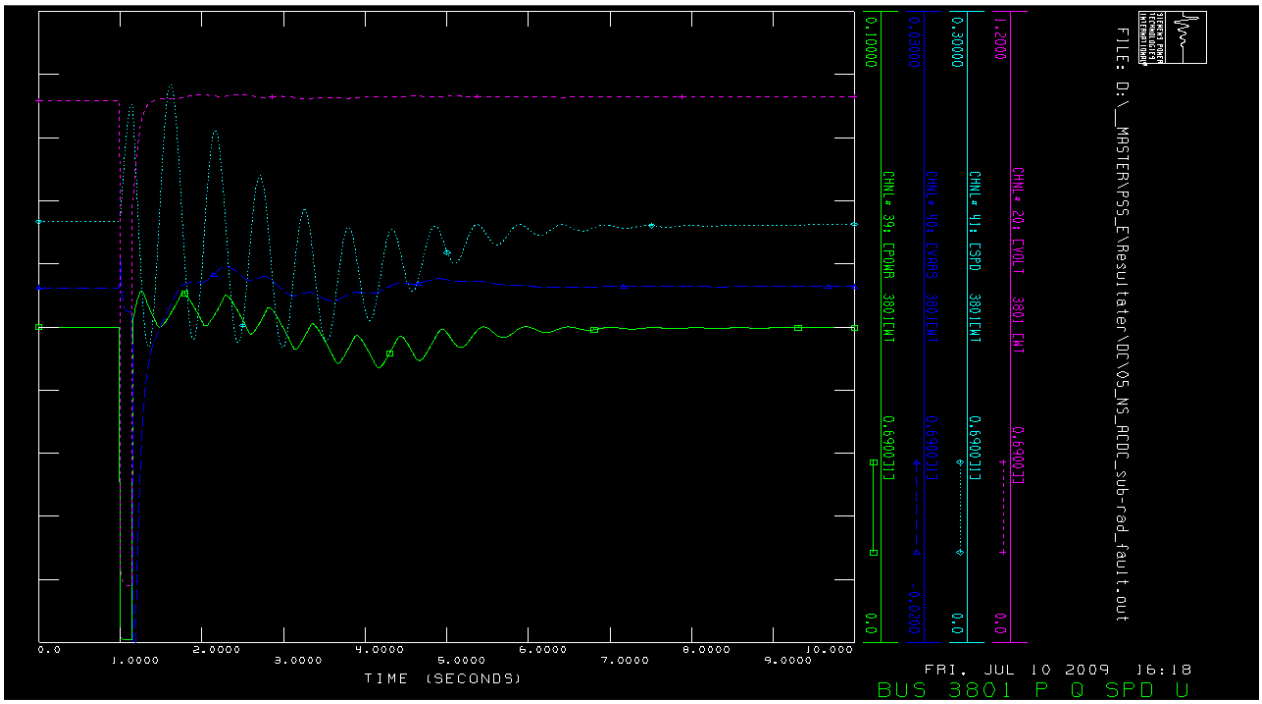

FAULT TYPE 3: FAULT IN THE OUTERMOST CABLE IN THE FEEDER

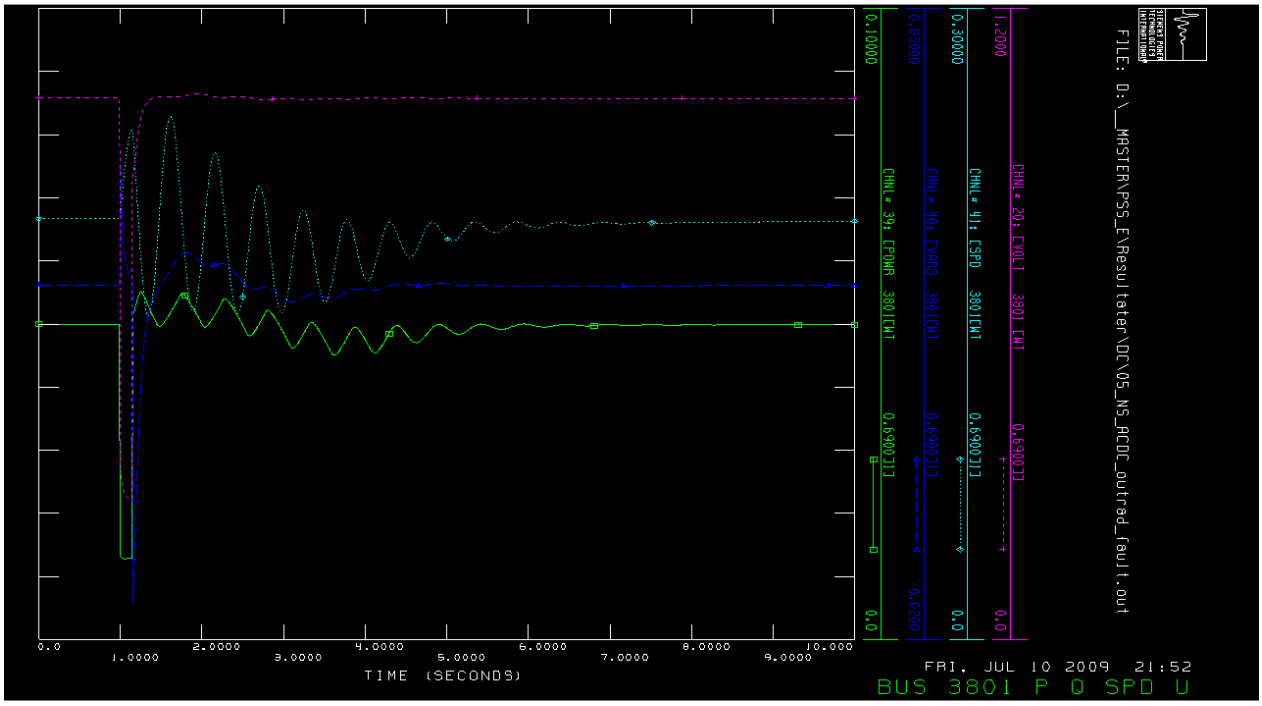

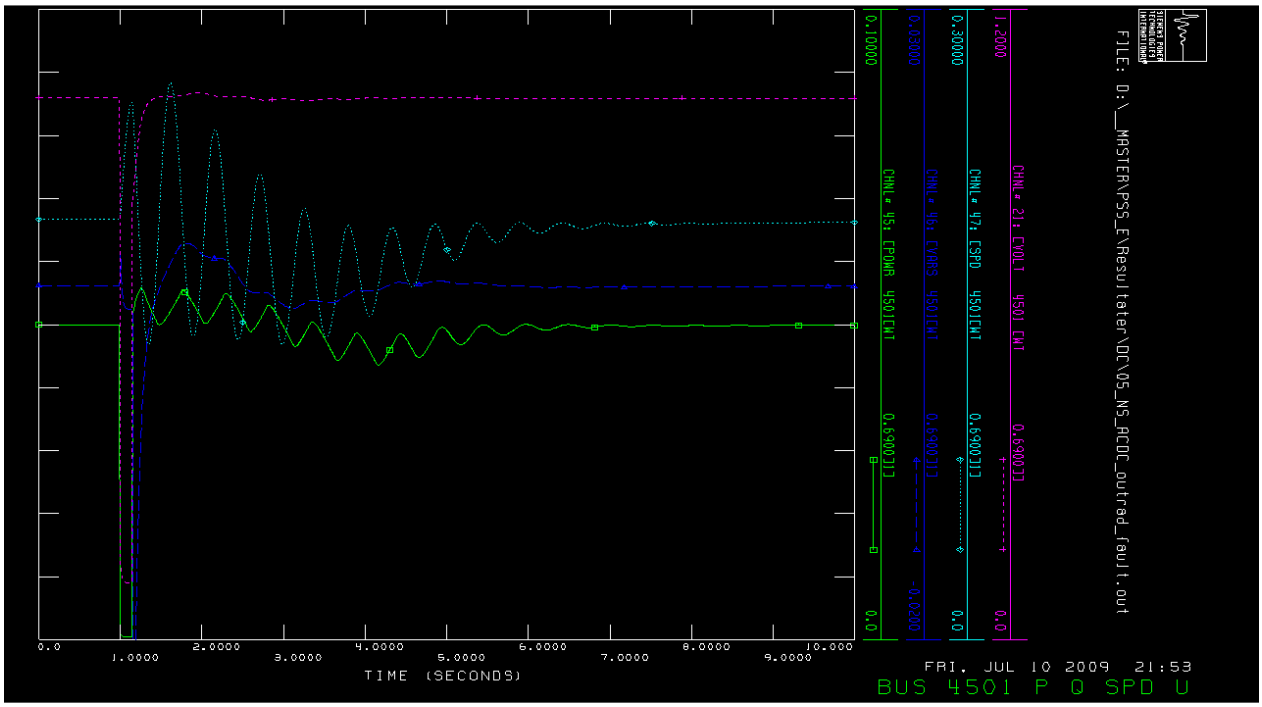

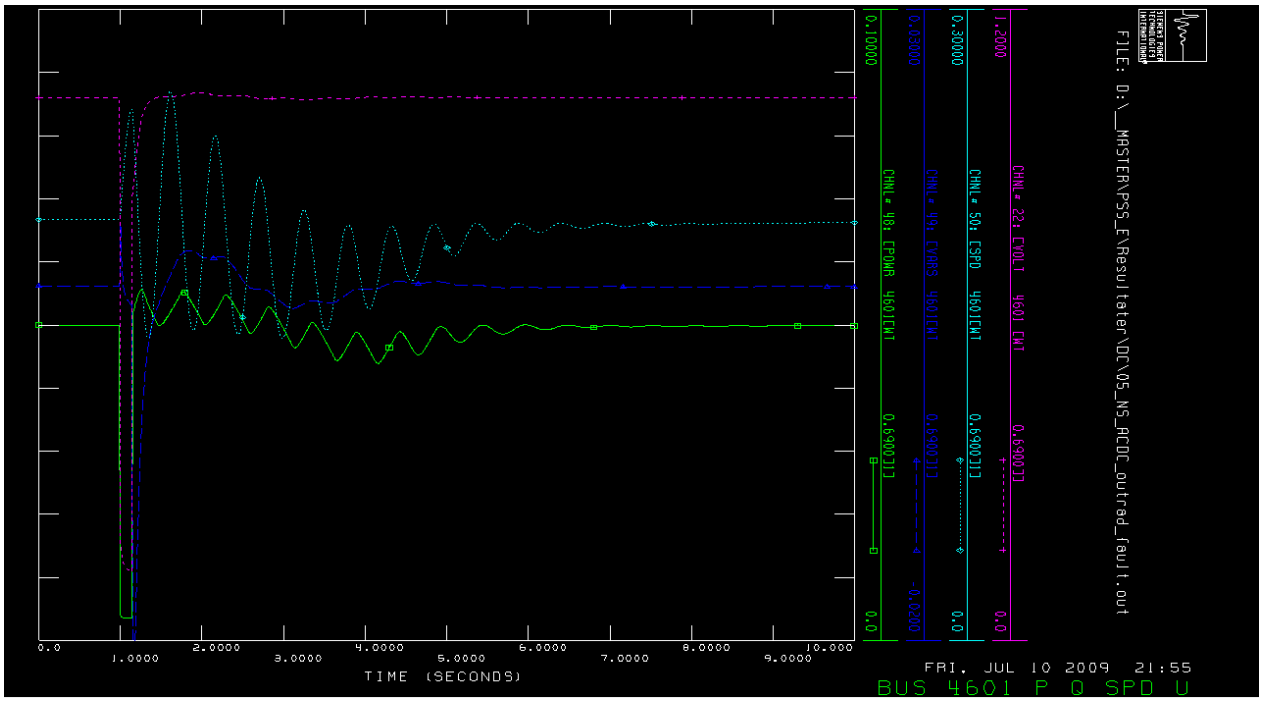
FILE: D:__MASTER\PSS_E\Resultater\DC\05_NS_ACDC_outrad_fault.out
CHNL # 48: [PGNR 4601CKT
CHNL # 50: [SPD 4601CKT
CHNL # 221: [VOLT 4601 CKT
TIME (SECONDS)
FRI, JUL 10 2009 21:55
BUS 4601 P Q SPD U

STAR DESIGN

AC/AC TRANSMISSION

FAULT TYPE 1: TRANSMISSION FAULT

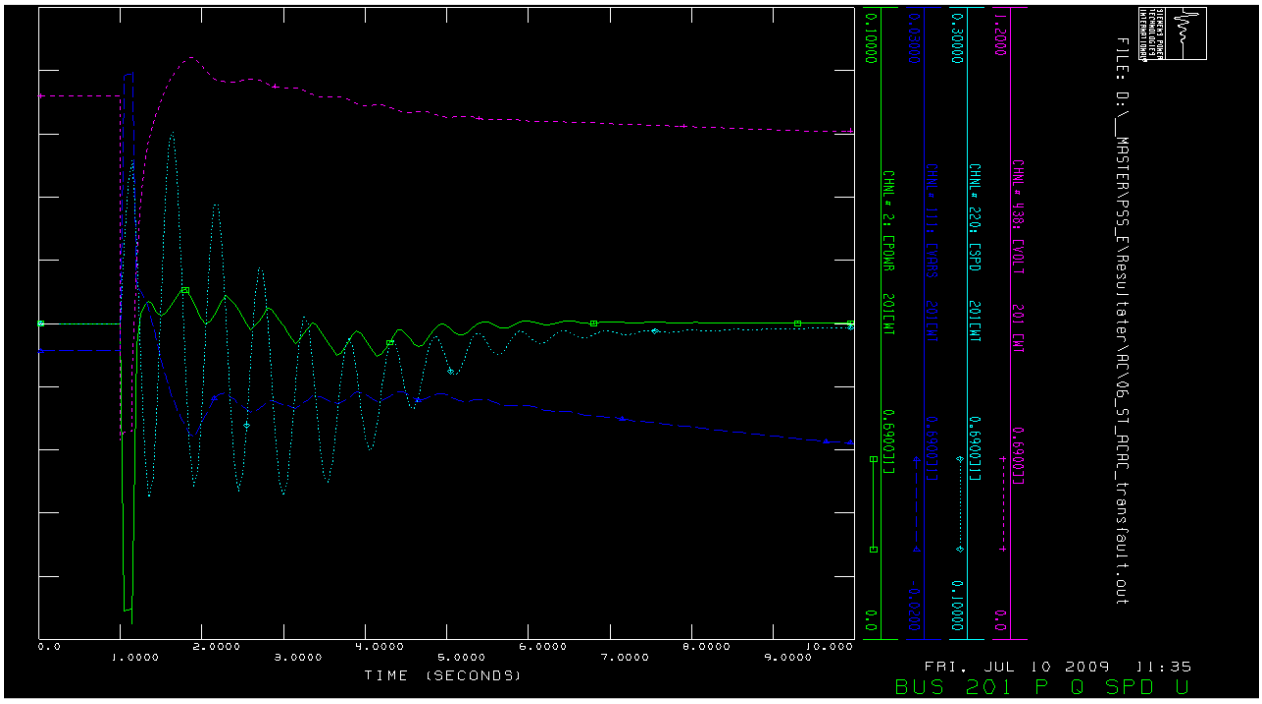

FAULT TYPE 2: FAULT BETWEEN INNERMOST TURBINE OF FEEDER AND SUBSTATION

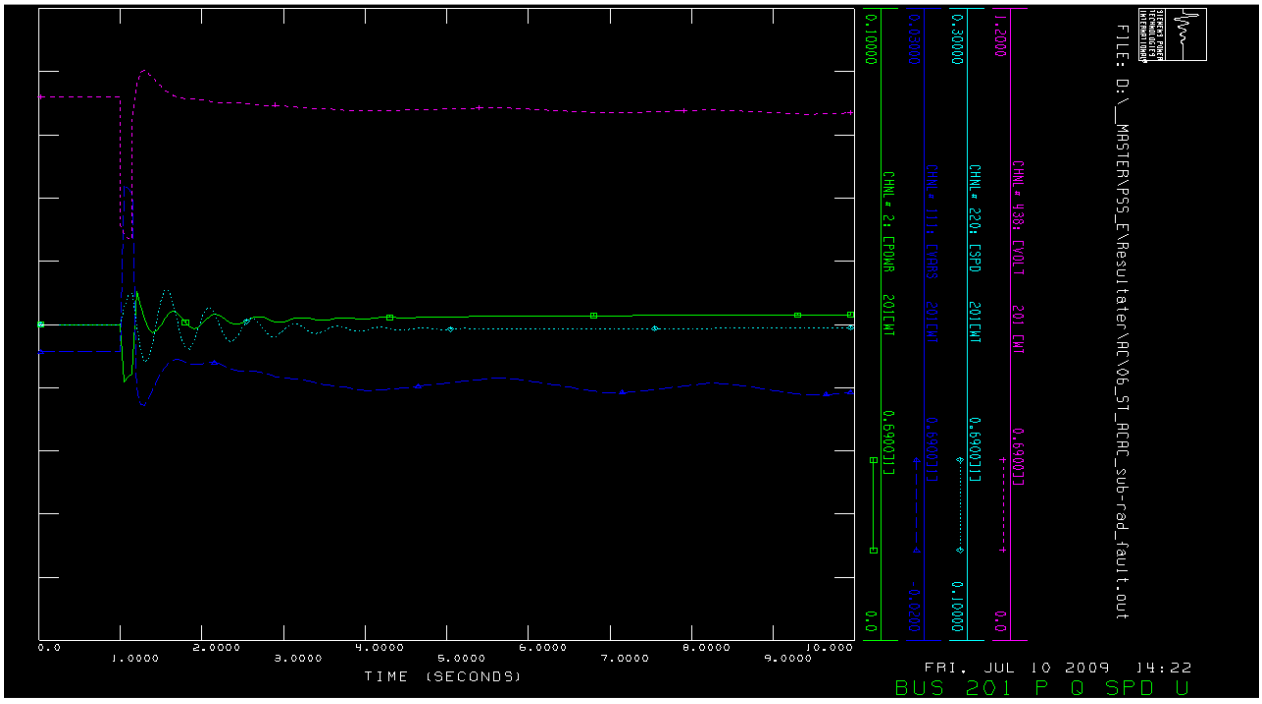

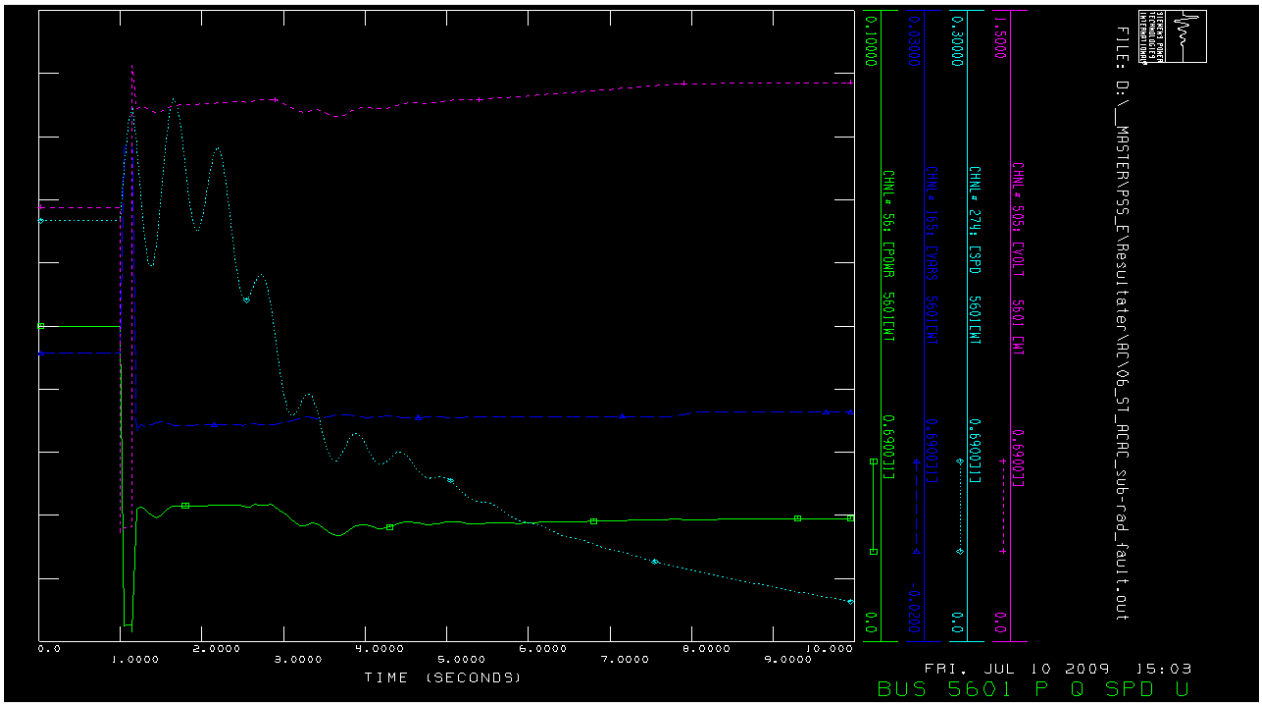

FAULT TYPE 3: FAULT IN THE OUTERMOST CABLE IN THE FEEDER

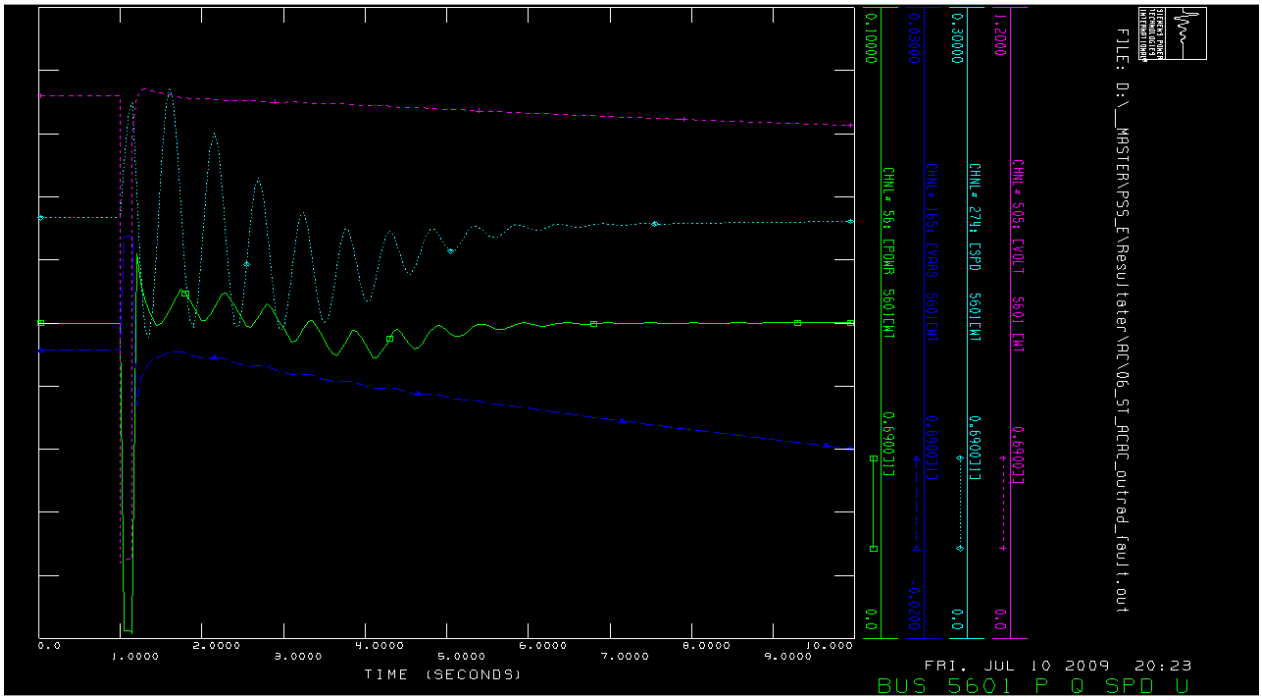

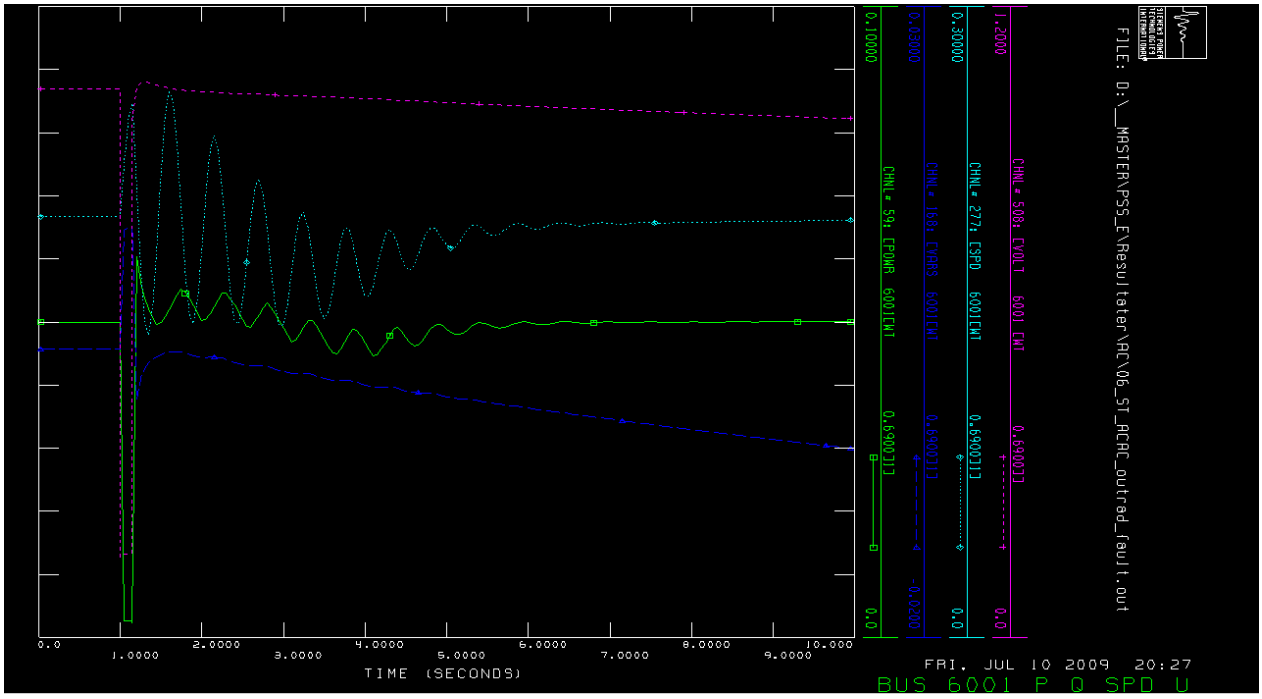

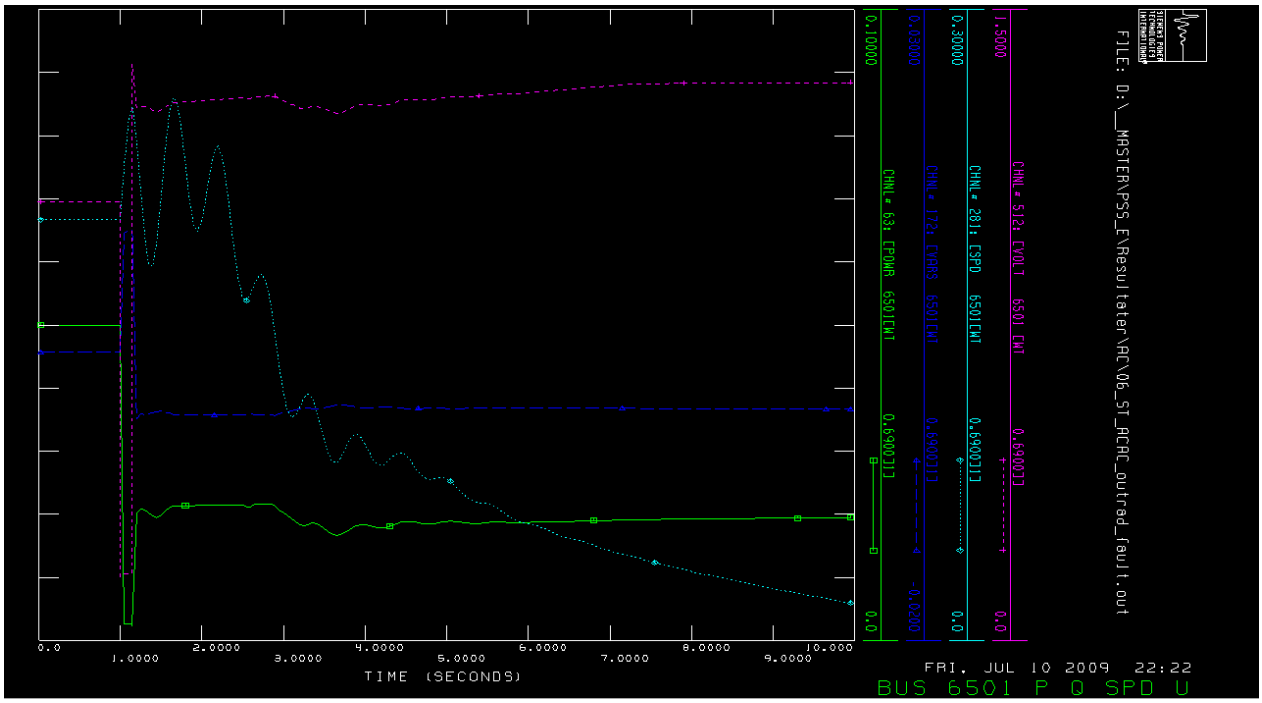
FILE: D:__MASTER\PSS_E\Resultater\AC\06_ST_ACAC_outrad_fault.out
TIME (SECONDS)
FRI, JUL 10 2009 22:22
BUS 6501 P Q SPD U

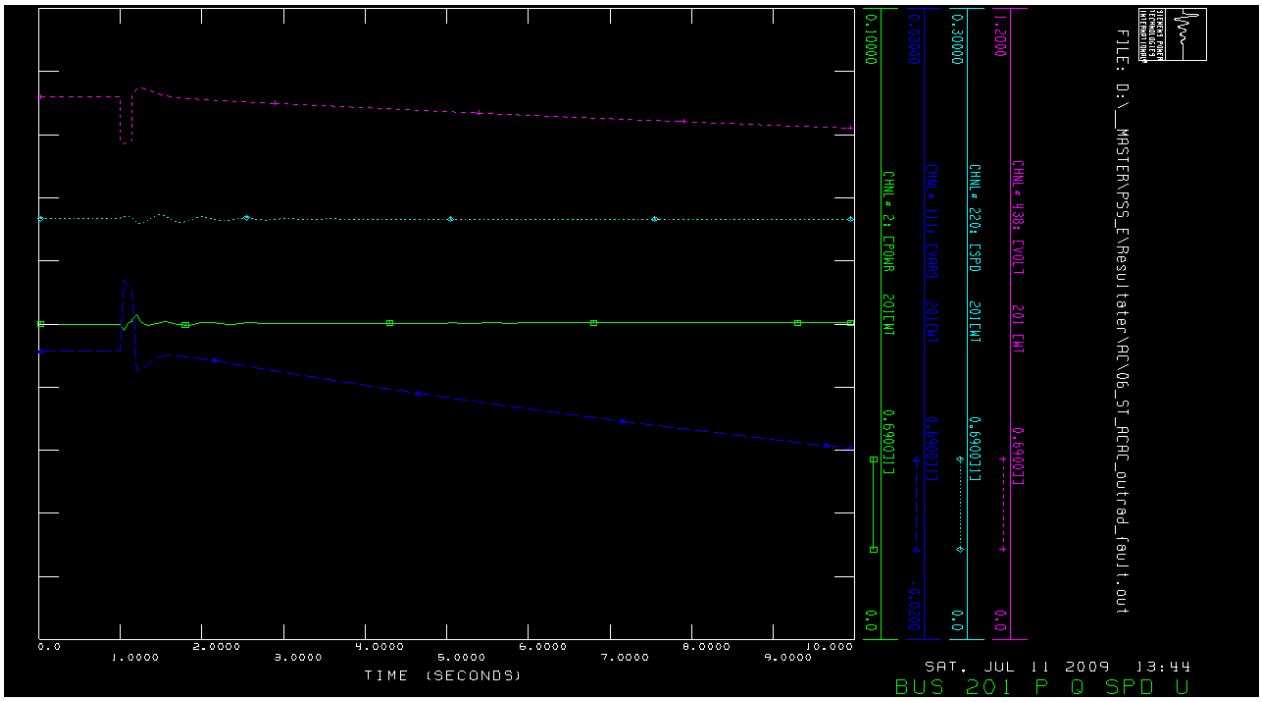
FILE: D:__MASTER\PSS_E\Resultater\AC\06_ST_ACAC_outrad_fault.out
TIME (SECONDS)
SAT, JUL 11 2009 13:44
BUS 201 P Q SPD U

AC/DC TRANSMISSION

FAULT TYPE 1: TRANSMISSION FAULT

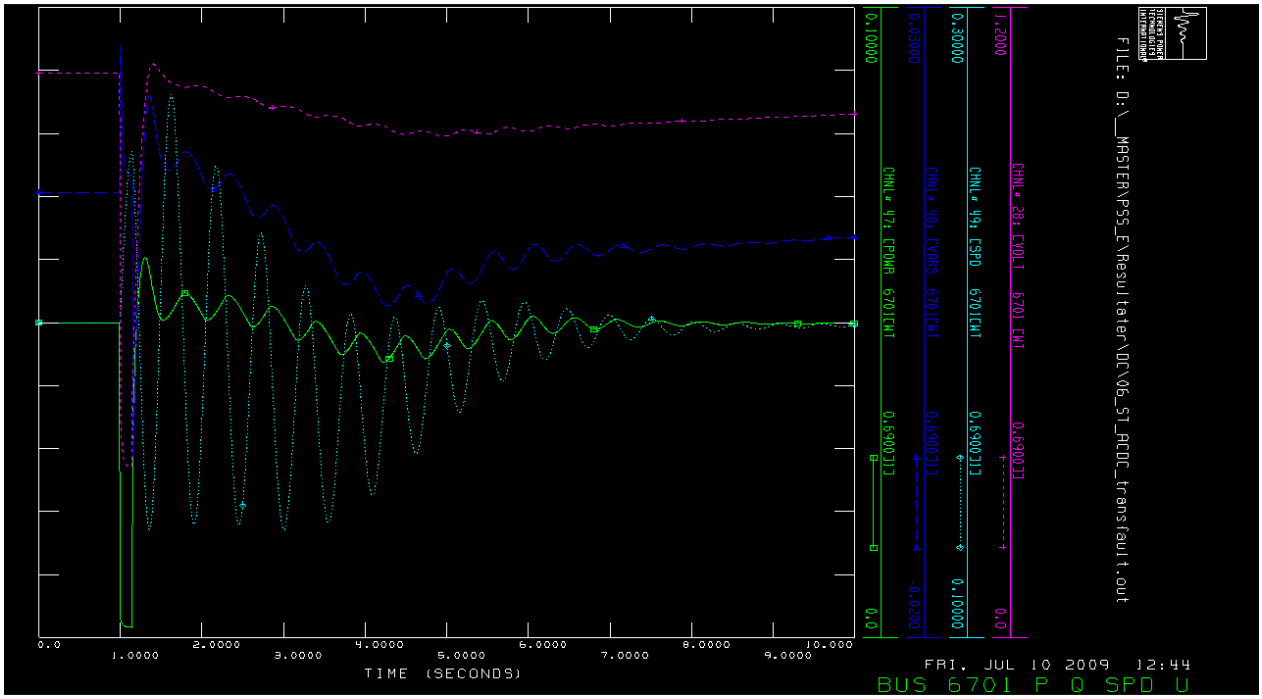

FAULT TYPE 2: FAULT BETWEEN INNERMOST TURBINE OF FEEDER AND SUBSTATION

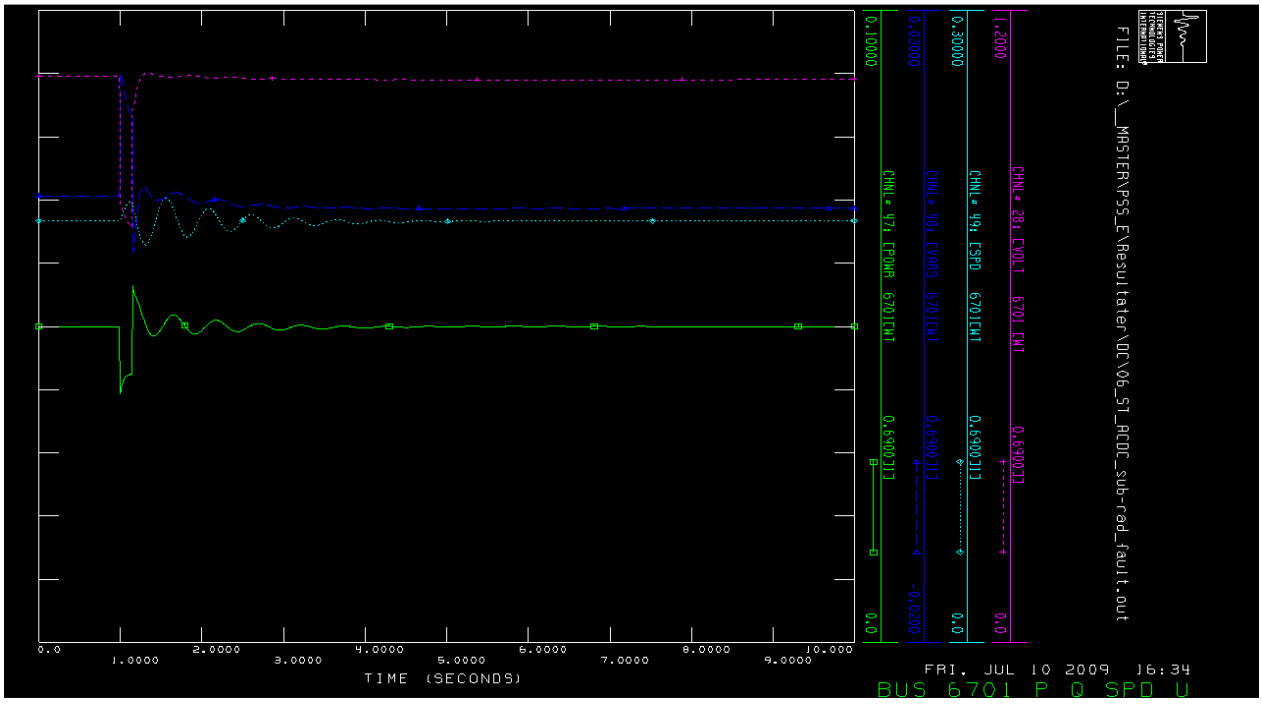

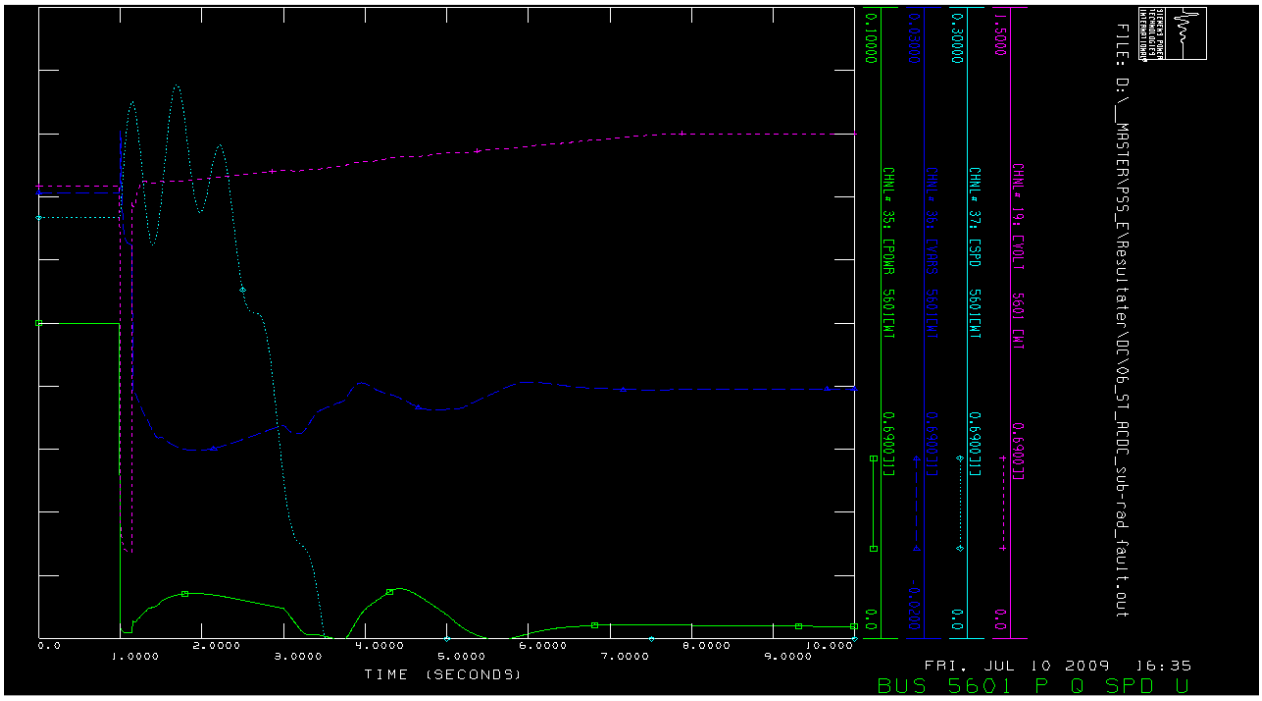

FAULT TYPE 3: FAULT IN THE OUTERMOST CABLE IN THE FEEDER

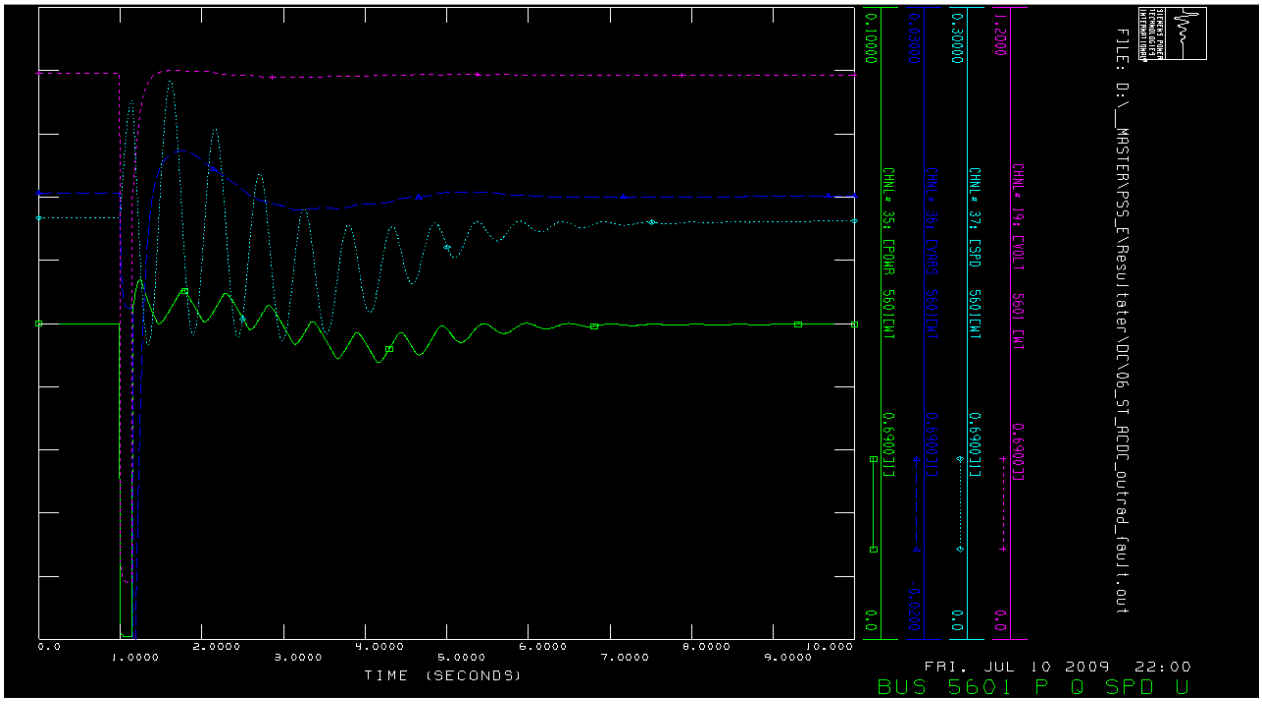

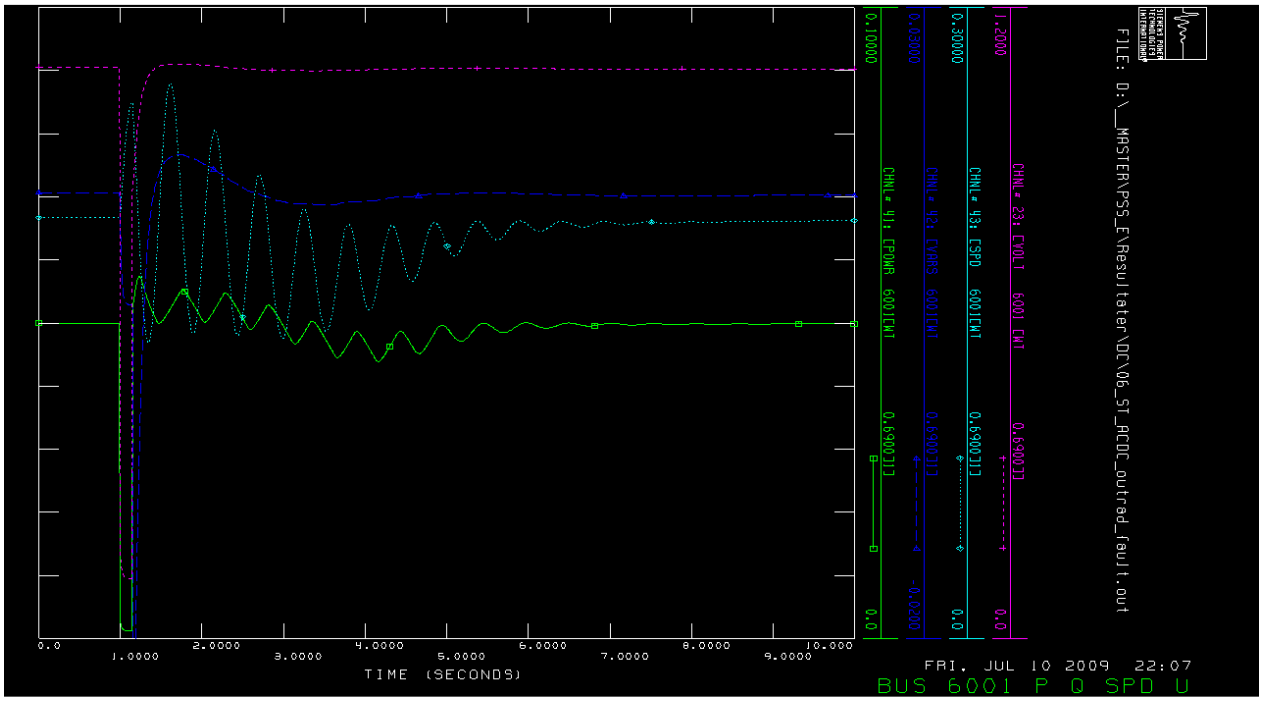

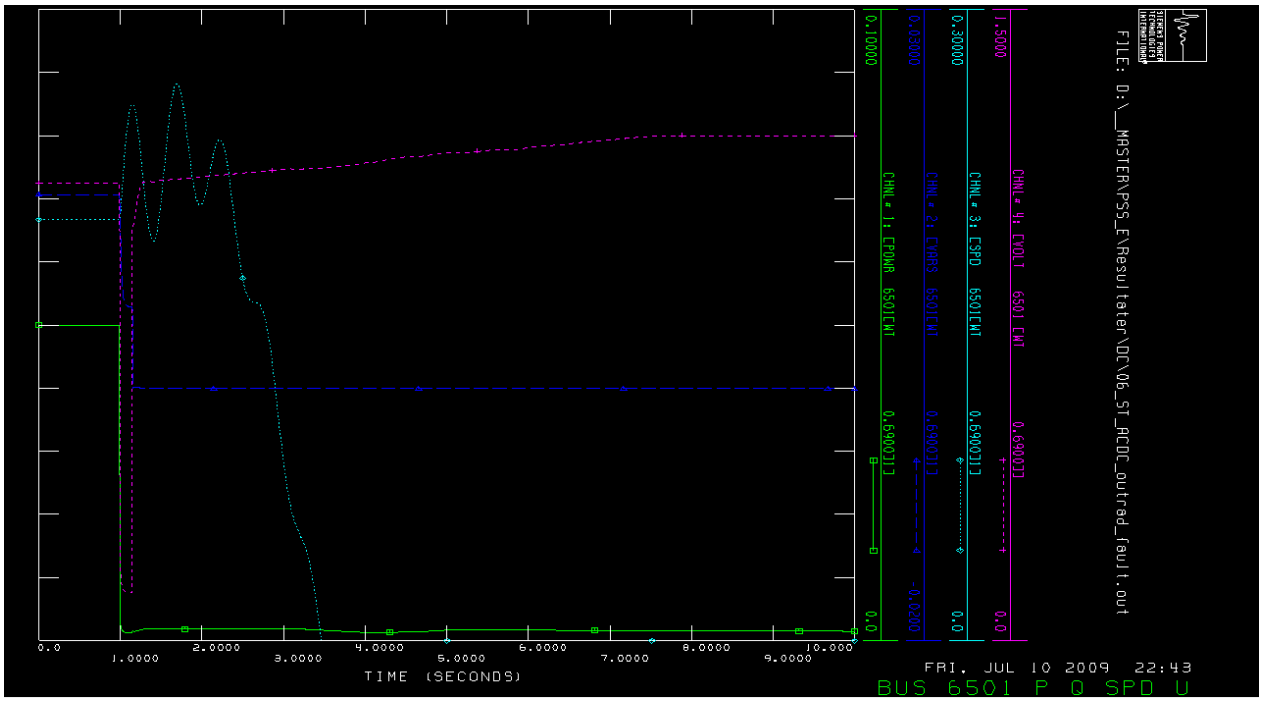
FILE: D:__MASTER\PSS_E\Resultater\DC\06_ST_ACDC_outrad_fault.out
TIME (SECONDS)
FRI, JUL 10 2009 22:43
BUS 6501 P Q SPD U

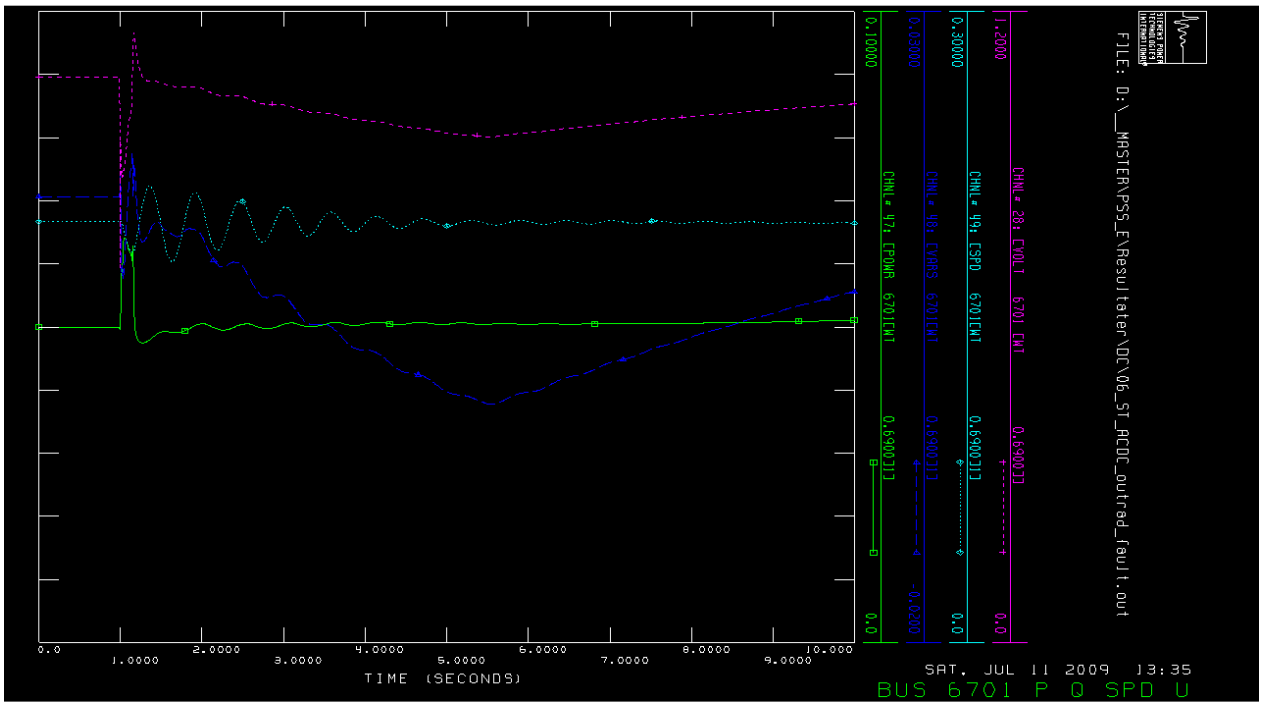
FILE: D:__MASTER\PSS_E\Resultater\DC\06_ST_ACDC_outrad_fault.out
TIME (SECONDS)
SAT, JUL 11 2009 13:35
BUS 6701 P Q SPD U

COMPARISON, MINIMUM AND MAXIMUM VALUES

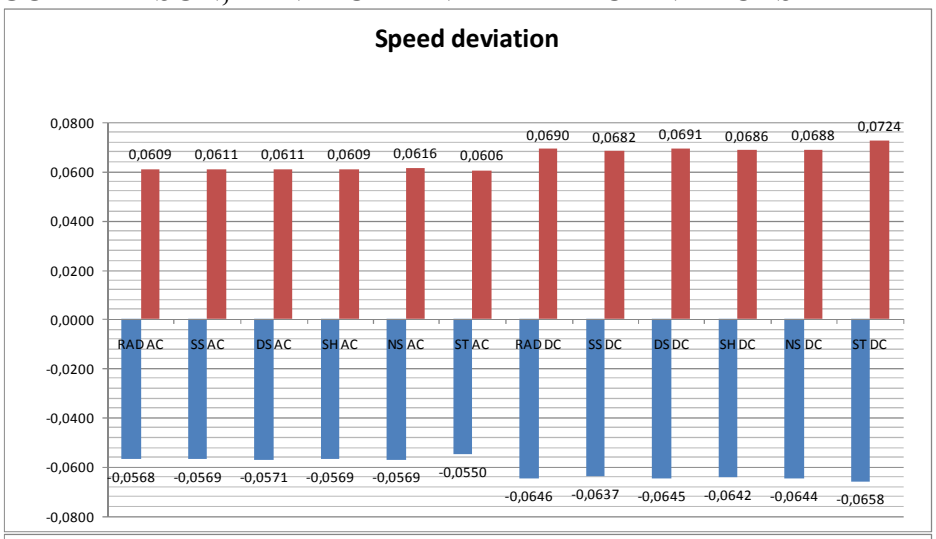

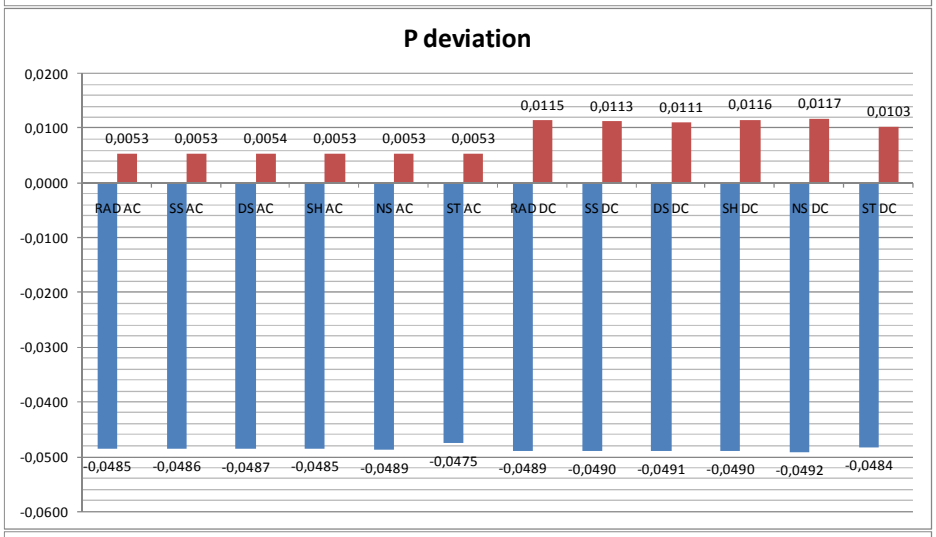

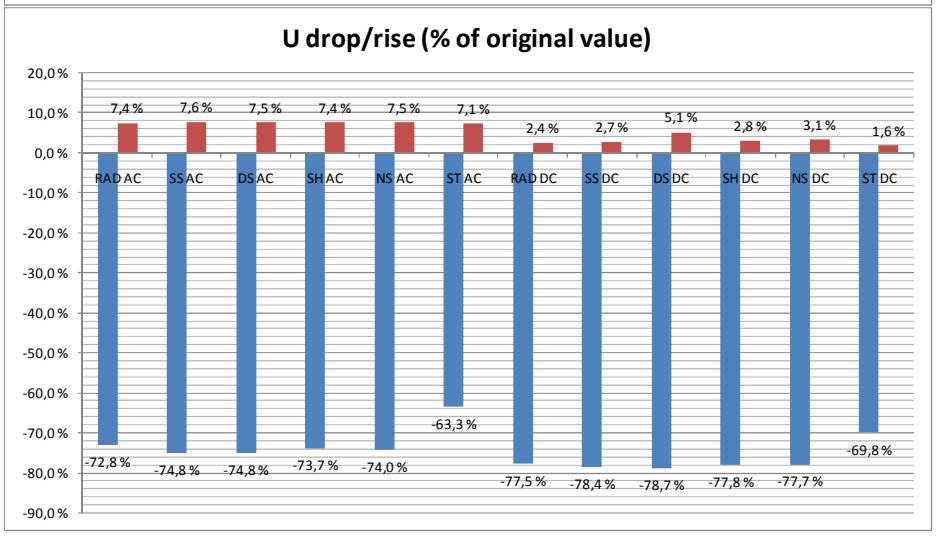

Fault 1. Bus 201. Ω, P, U minimum and maximum values

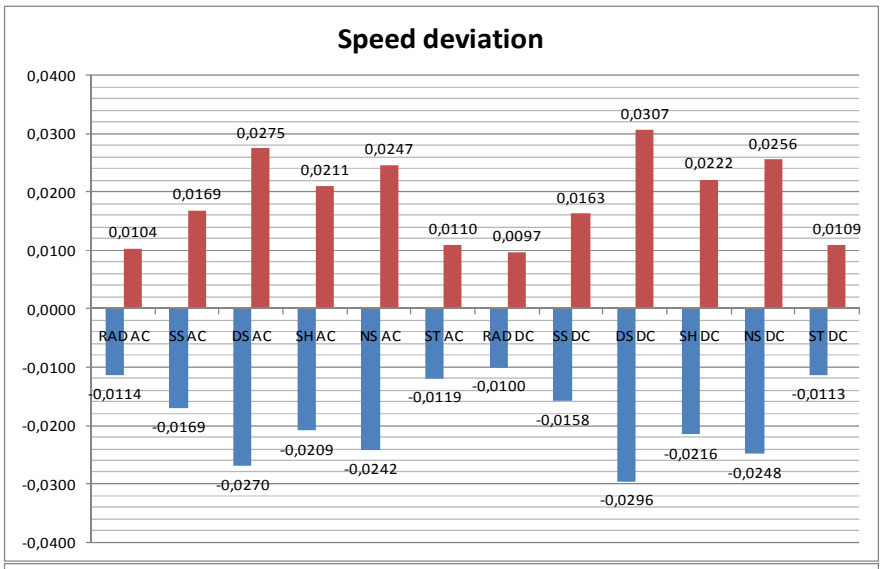

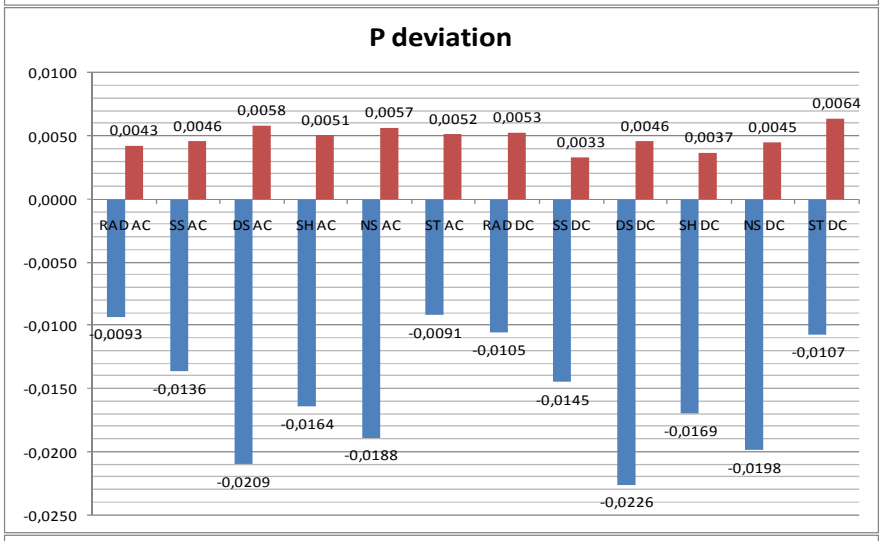

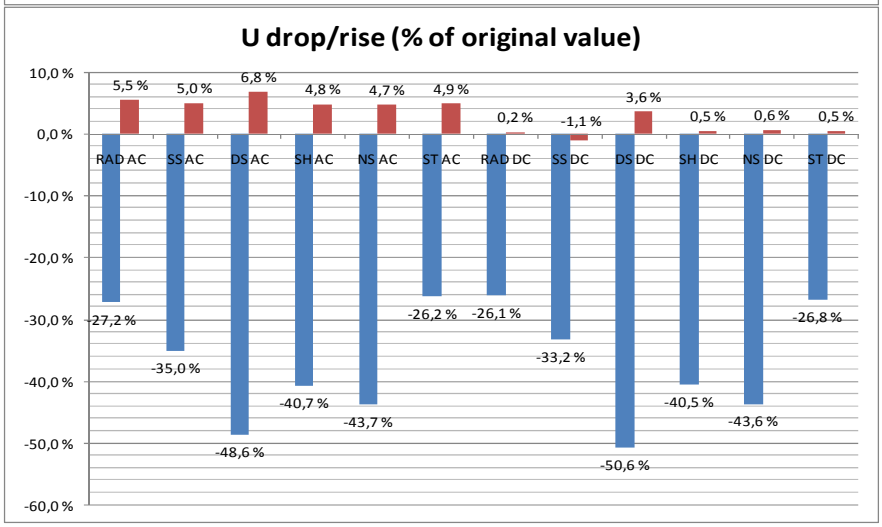

Fault 2. Bus 201 Ω, P, U minimum and maximum values

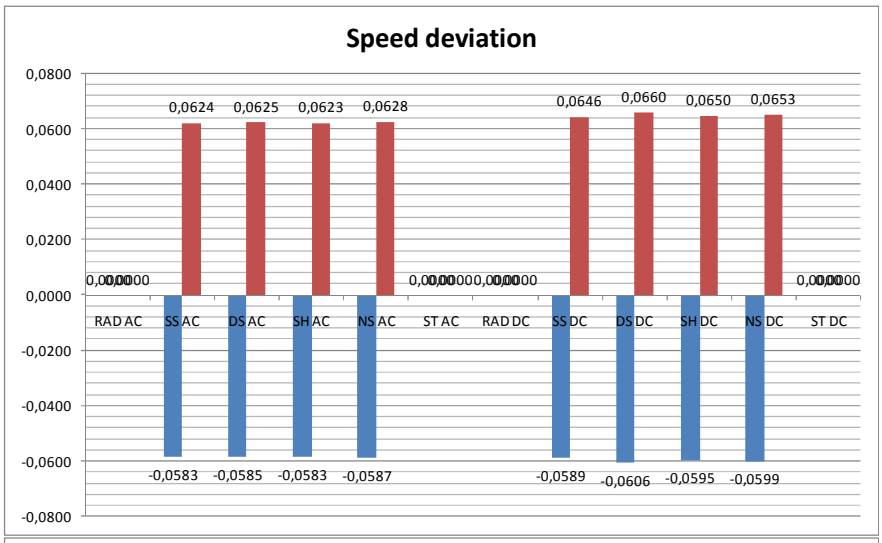

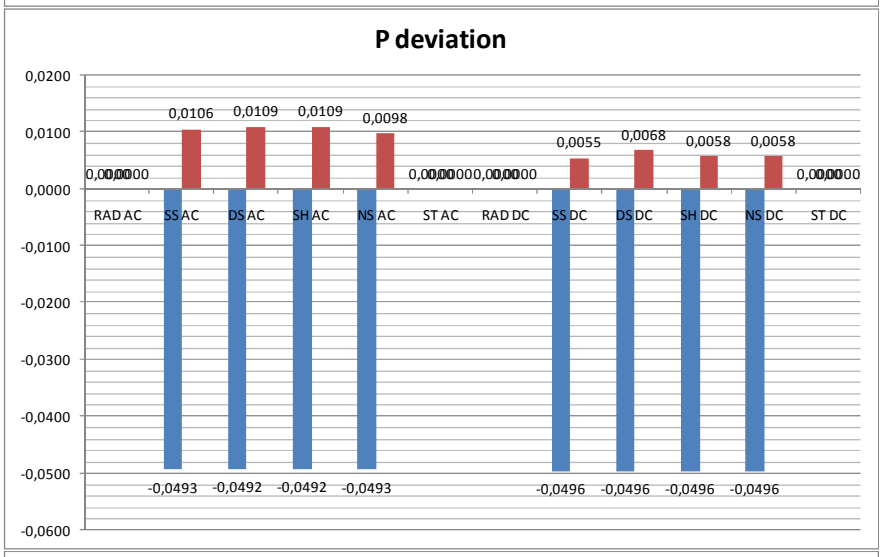

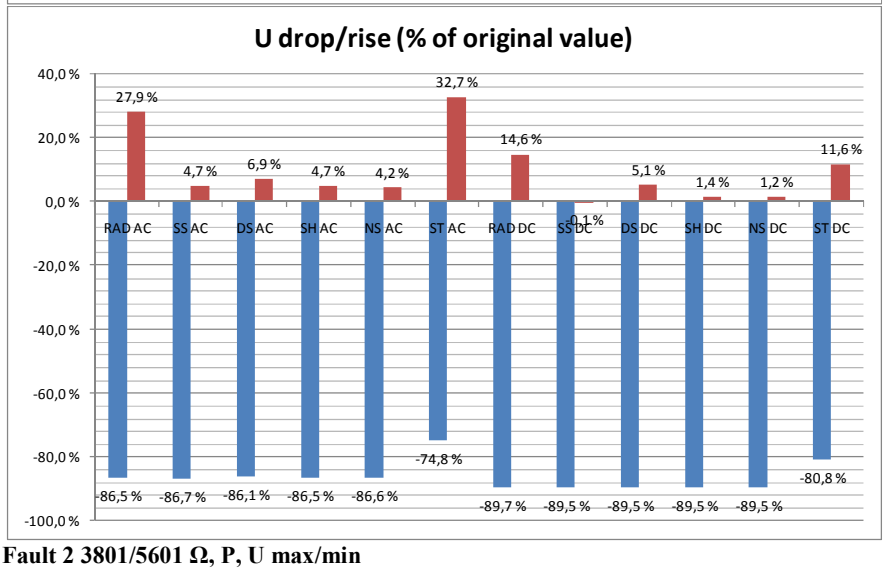

Fault 2 3801/5601 Ω, P, U max/min

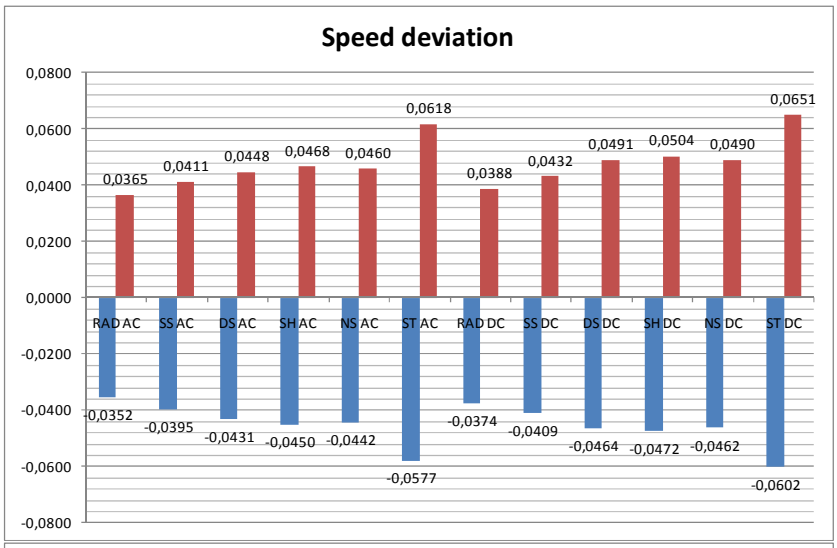

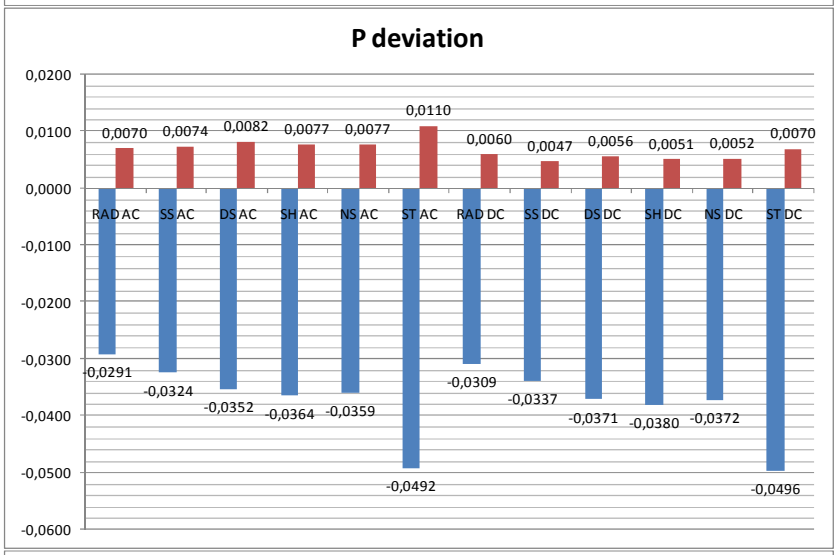

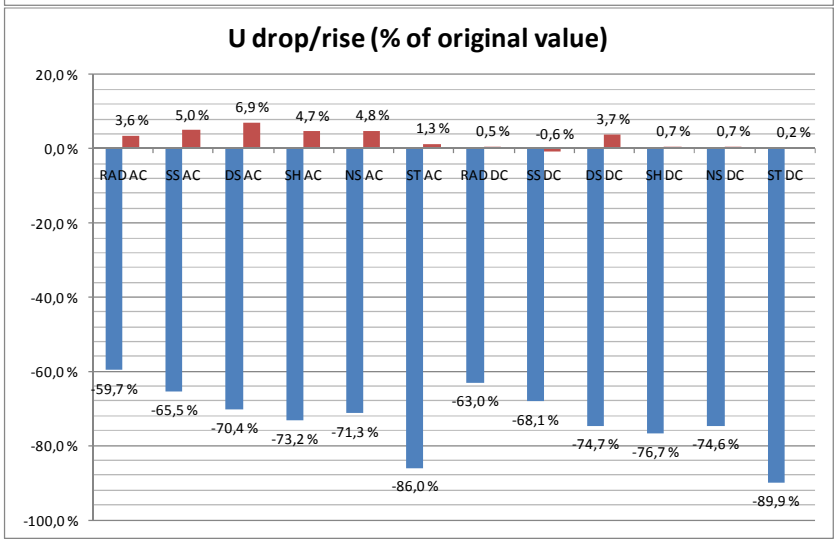

Fault 3. Bus 3801/5601 Ω, P, U minimum and maximum values

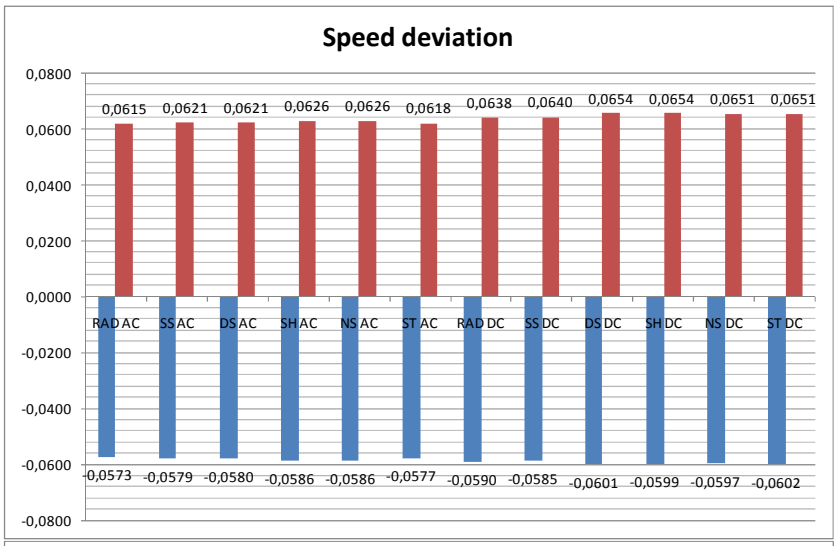

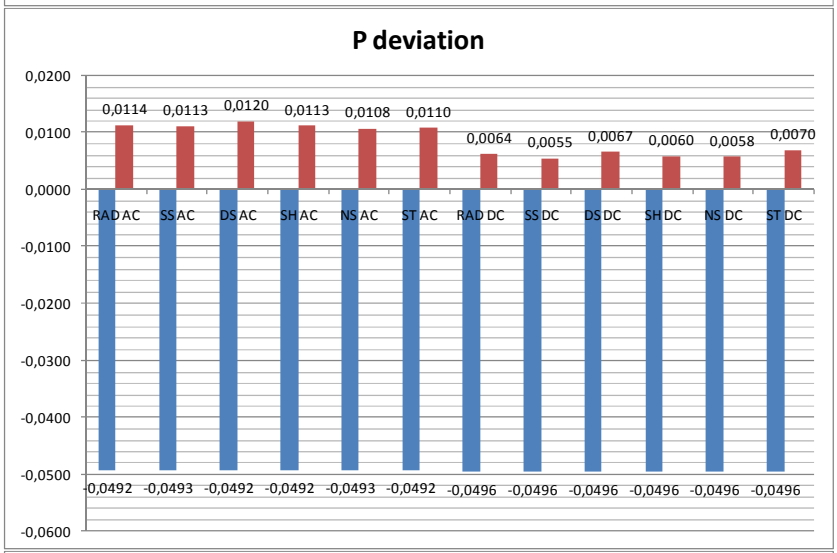

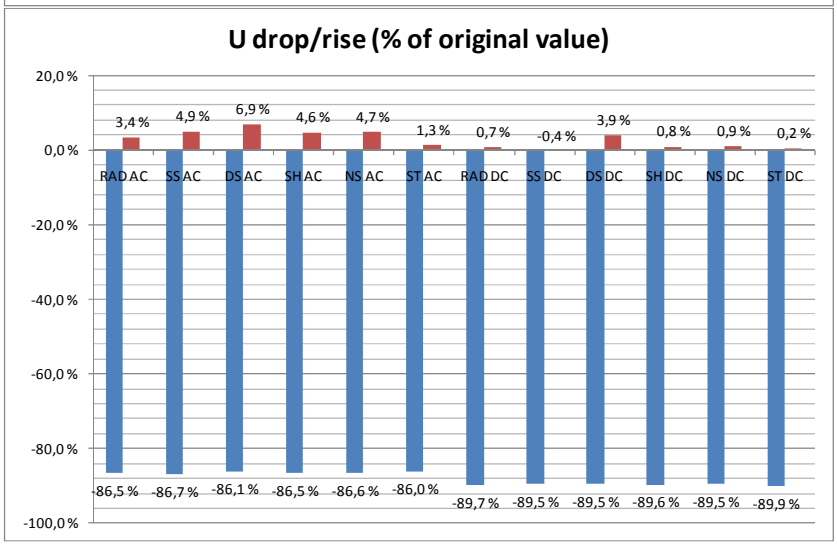

Fault 3. Bus 4501/5601. ω, P, U minimum and maximum values

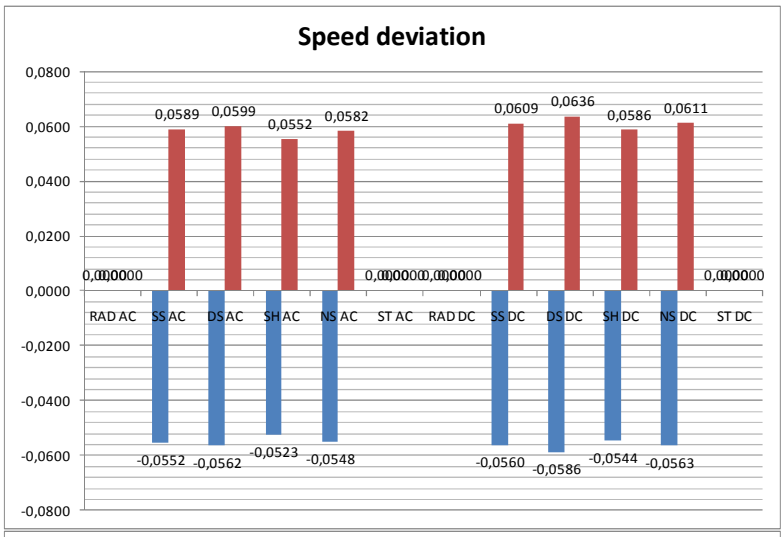

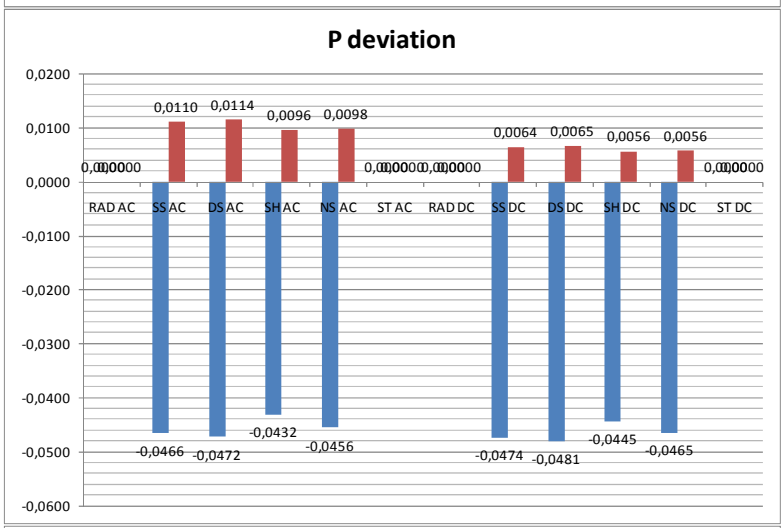

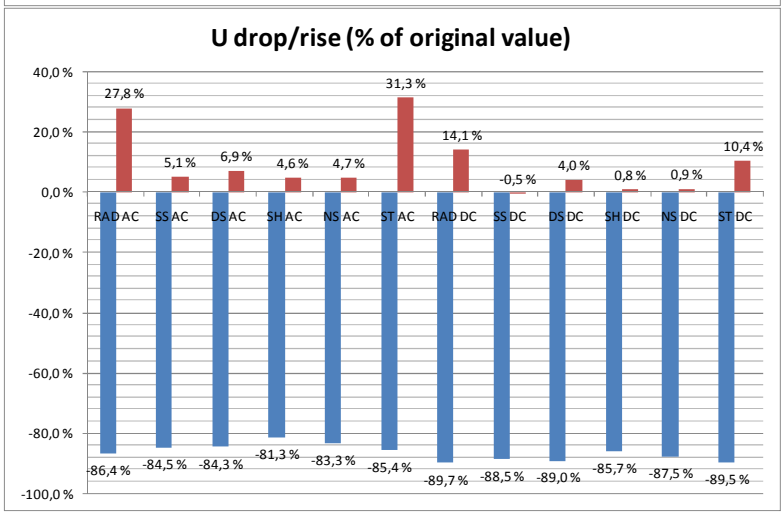

Fault 3. Bus 4601/6501. ω, P, U minimum and maximum values